

Stony Brook University



OFFICIAL COPY

The official electronic file of this thesis or dissertation is maintained by the University Libraries on behalf of The Graduate School at Stony Brook University.

© All Rights Reserved by Author.

**The Effects of Mineral Association and Aggregation on Particulate
Organic Matter Composition in the Water Column**

A Dissertation Presented

by

Lynn Abramson

to

The Graduate School
in Partial Fulfillment of the
Requirements
for the Degree of

Doctor of Philosophy

in

Marine and Atmospheric Science

Stony Brook University

December 2007

Stony Brook University
The Graduate School

Lynn Abramson

We, the dissertation committee for the above candidate for the Doctor of Philosophy degree, hereby recommend acceptance of this dissertation.

Cindy Lee, Dissertation Advisor
Distinguished Professor, School of Marine and Atmospheric Sciences

Robert C. Aller, Dissertation Advisor
Distinguished Professor, School of Marine and Atmospheric Sciences

Bruce J. Brownawell, Chairperson of Defense
Associate Professor, School of Marine and Atmospheric Sciences

Richard J. Reeder
Professor, Department of Geosciences

Ronald Benner
Professor, Department of Biological Sciences, University of South Carolina

This dissertation is accepted by the Graduate School.

Lawrence Martin
Dean of the Graduate School

Abstract of the Dissertation

**The Effects of Mineral Association and Aggregation on Particulate Organic Matter
Composition in the Water Column**

by

Lynn Abramson

Doctor of Philosophy

in

Marine and Atmospheric Science

Stony Brook University

2007

This thesis examines two important factors influencing POC export in the water column: mineral association and aggregation. Specifically, it focuses on 1) the occlusion of organic matter within biominerals, which may be the most permanent form of organic matter protection by minerals, and 2) the occlusion and transport of organic matter within aggregates, which may be the most quantitatively important form of organic-mineral association.

To assess the effects of organic matter occlusion within biominerals, scanning transmission X-ray microscopy (STXM) and carbon X-ray absorption near-edge structure (XANES) spectroscopy were used in combination to characterize the distribution and composition of organic matter in frustules of the diatom *Cylindrotheca closterium* and a biomimetic silica gel. Organic carbon, most likely protein, was distributed throughout the frustules and was not completely removed by extensive chemical treatment, suggesting that frustule-bound organic carbon is protected from decomposition until the frustule dissolves. The physical structure of the frustules appeared to be related to the chemical composition of this organic matter, with aromatic or unsaturated carbon concentrated in areas resembling the thin, perforated silica roofs that often cover pores in the frustule. A similar physical and chemical structure was observed in a biomimetic silica gel precipitated with poly-lysine. These results are consistent with the theory that organic constituents of diatom frustules direct silica precipitation and become incorporated within the silica matrix as it forms.

The fate of organic matter within water column aggregates was assessed by comparing the organic compositions of sinking (sediment trap) and suspended (*in situ* pump) particles collected in 2003 and 2005 in the northwest Mediterranean Sea. Sinking particles were enriched in fecal pellet and silicifying algae indicators, whereas suspended particles were enriched in fresh phytoplankton and calcifying algae indicators. Mass balance calculations indicate that the observed composition of suspended particles is best explained by extensive disaggregation of phytoplankton aggregates. Fecal pellets do not appear to undergo extensive disaggregation and exchange with suspended material, suggesting they are a more efficient mode of POC export to the deep sea than phytoplankton aggregates. In the summer of 2003, suspended and sinking particles were both enriched in microbial alteration products rather than algal or fecal pellet material, indicating greater exchange during periods of low flux when fecal pellets are not abundant.

To experimentally verify the field results, suspended and sinking particles were collected at two depths (20 m and 200 m) in the Mediterranean Sea in 2006. These particles were incubated independently in rotating tanks to assess exchange between sinking and suspended particles. Particles collected at 20 m were primarily composed of phytoplankton, and particles collected at 200 m were composed of both phytoplankton and fecal pellets. During the course of incubation, sinking phytoplankton aggregates underwent extensive exchange with suspended particles, as evidenced by repeated mass transfers and relative homogeneity in composition. Fecal pellets collected at 200 m by Net Trap underwent less exchange, with some transfer of suspended phytoplankton material into the sinking phase, but no apparent disaggregation. Unlike phytoplankton aggregates, fecal pellets appear to undergo little exchange with surrounding material and are more likely to remain intact during transit from the surface to deep ocean.

The results of this thesis highlight the importance of biogenic minerals and fecal pellets in contributing to the vertical flux of particulate organic carbon from surface waters to the deep sea. Better understanding of the factors controlling the formation and robustness of different particle types is critical for quantitative prediction of particle fluxes and the drawdown of carbon dioxide from the atmosphere.

DEDICATION

To my parents, who helped me become both a realist and an idealist

and to my husband Eric, who has helped me stay that way.

TABLE OF CONTENTS

LIST OF TABLES	ix
LIST OF FIGURES	xi
ACKNOWLEDGEMENTS	xviii
CHAPTER 1: Introduction	1
1. The Role of Sinking Particles in the Marine Carbon Cycle.....	1
2. Associations between Organic Matter and Minerals.....	1
2.1. Occlusion of Organic Matter within the Mineral Structure.....	2
2.2. Sorption onto Mineral Surfaces.....	3
2.3. Sorption within Mesopores.....	4
2.4. Occlusion of Organic Matter within Aggregates.....	5
3. Aggregation Processes.....	6
4. Thesis Objectives and Organization.....	7
References.....	9
CHAPTER 2: The Use of Soft X-ray Spectromicroscopy to Investigate the Distribution and Composition of Organic Matter in a Diatom Frustule and a Biomimetic Analog	14
Abstract.....	14
1. Introduction.....	15
2. Methods.....	17
2.1. Sample Preparation.....	17
2.2. X-ray Spectromicroscopy.....	18
2.3. Multivariate Statistical Analyses.....	20
3. Results and Discussion.....	21
3.1. Distribution of Organic Carbon.....	21
3.2. Overall Composition of Organic Carbon.....	23
3.3. Spatial Variations in Organic Carbon Composition.....	23
3.3.1. Relationship with Morphological Structures.....	25
3.3.2. Alternative Explanations.....	26
3.4. Comparison between Diatom Frustules and Biomimetic Silica Gel.....	28
4. Conclusions.....	28
References.....	30
Figures.....	34
CHAPTER 3: Organic Composition of <i>In Situ</i> Pump and Sediment Trap Samples: Implications for the Exchange of Material between Suspended and Sinking Particles	45
Abstract.....	45
1. Introduction.....	46
2. Methods.....	49
2.1. Sampling Location.....	49

2.2. Sediment Trap Sampling.....	49
2.3. <i>In Situ</i> Pump Sampling.....	51
2.4. Organic Analyses.....	52
2.5. Statistical Analyses.....	53
3. Results.....	54
3.1. Comparison of Suspended (1-70 μm Pump) and Sinking (TS Trap) Particles: 2003.....	54
3.1.1. Quantity.....	54
3.1.2. Composition.....	55
3.1.3. Principal Component Analysis.....	57
3.2. Comparison of Suspended (1-70 μm Pump) and Sinking (>70 μm Pump and TS Trap) Particles: 2005.....	58
3.2.1. Quantity.....	58
3.2.2. Composition.....	58
3.2.3. Principal Component Analysis.....	61
3.3. Comparison of Suspended (1-70 μm Pump) and Sinking (SV Trap) Particles: 2003.....	61
3.4. Comparison of Suspended (1-70 μm Pump) and Sinking (SV Trap) Particles: 2005.....	63
3.5. Comparison of All Suspended and Sinking Particles.....	64
3.5.1. Composition (Mole %) of All Samples below the Mixed Layer.....	64
3.5.2. Pigment Ratios for All Pump and TS Trap Samples.....	65
4. Discussion.....	66
4.1. Sources and Alteration of Suspended and Sinking Particles.....	66
4.1.1. Sinking Particles.....	66
4.1.2. Suspended Particles.....	69
4.1.3. Mechanisms of Sinking Particle Formation.....	70
4.2. Exchange between Suspended and Sinking Particles.....	74
4.2.1. Possible Differences between Sinking Fecal Pellets and Phytoplankton Aggregates.....	74
4.2.2. Mass Balance Calculations: Phytoplankton-Derived Material.....	75
4.2.3. Mass Balance Calculations: Microbially-Degraded Material and Fecal Pellets.....	80
4.2.4. Summary of Mass Balance Calculations: Differences between Phytoplankton Aggregates and Fecal Pellets.....	83
5. Conclusions.....	85
References.....	87
Tables.....	96
Figures.....	100
Appendix.....	115

CHAPTER 4: Fecal Pellets and Phytoplankton Aggregates: Differences in the Extent of Exchange between Suspended and Sinking Particles.....	127
Abstract.....	127
1. Introduction.....	127
2. Methods.....	129
2.1. Particle Collection and Incubation.....	129

2.2. Sampling of Incubation Chambers.....	130
2.3. Chemical Analyses.....	131
2.4. Statistical Analyses.....	133
3. Results and Discussion.....	133
3.1. Exchange between Suspended and Sinking Particles in the 20 m Plankton Tow Incubation.....	133
3.1.1. Visual and Microscopic Observations.....	133
3.1.2. Particulate Mass, Organic Carbon, Nitrogen, Silica, and Inorganic Carbon.....	133
3.1.3. Pigments and Amino Acids.....	136
3.1.4. Particular Pigment Biomarkers.....	137
3.1.5. Particular Amino Acid Biomarkers.....	139
3.1.6. Principal Component Analysis.....	140
3.2. Exchange between Suspended and Sinking Particles in the 200 m NetTrap Incubation.....	141
3.2.1. Visual and Microscopic Observations.....	141
3.2.2. Particulate Mass, Organic Carbon, Nitrogen, Silica, and Inorganic Carbon.....	141
3.2.3. Pigments and Amino Acids.....	145
3.2.4. Particular Pigment Biomarkers.....	146
3.2.5. Particular Amino Acid Biomarkers.....	147
3.2.6. Principal Component Analysis.....	147
3.3. Fecal Pellets and Phytoplankton Aggregates: Differences in the Extent of Exchange with Suspended Particles.....	148
4. Conclusions.....	151
References.....	152
Figures.....	157
 CHAPTER 5: Conclusions	 172
1. Summary and Implications of Major Findings.....	172
2. Directions for Future Research.....	175
References.....	178

LIST OF TABLES

Table 3.1. Dates and depths at which time-series trap (TS), settling velocity trap (SV), >70 μm pump (LP), and 1-70 μm pump (SP) samples were collected.....	97
Table 3.2. Pearson's correlation coefficients for changes in composition with settling velocity (for SV traps) and depth (for pumps) for all seasons in 2003 and 2005. Strong positive or negative correlations ($r=0.50$ to 1.00 or -0.50 to -1.00) are shown in bold, moderate positive or negative correlations ($r=0.30$ to 0.49 or -0.30 to -0.49) in regular text, and results that were not significant are labeled 'ns.'.....	98
Table 3.3. Minimum change in sinking particle fluxes with depth ($\partial J_{\text{sink}}/\partial z$) and settling velocities (ω) required to balance the decay of chl <i>a</i> in the suspended phase.....	99
Table 3.4. Minimum change in sinking particle fluxes with depth ($\partial J_{\text{sink}}/\partial z$) and settling velocities (ω) required to balance the decay and production of phytin and phide+pyropheide in the suspended phase.....	100
Table 3.A1. Concentration ($\mu\text{mol C l}^{-1}$) or flux ($\mu\text{mol C m}^{-2}\text{d}^{-1}$) and composition of pigments (mol %) during three sampling periods in spring-summer, 2003. Most data shown are for 1-70 μm particles collected by in situ pump, thought to represent suspended or very slowly sinking particles. Data for time series trap (TS) samples, assumed to represent sinking particles, are shown where available. The time series trap data shown are for those cups which most closely overlapped with the pump casts. Fig. 3.4 graphically depicts this data.....	117
Table 3.A2. Concentration ($\mu\text{mol C l}^{-1}$) or flux ($\mu\text{mol C m}^{-2}\text{d}^{-1}$) and composition of amino acids (mol %) during three sampling periods in spring-summer, 2003. The caption for Table 3.A1 describes the samples in more detail.....	119
Table 3.A3. Concentration ($\mu\text{mol C l}^{-1}$) or flux ($\mu\text{mol C m}^{-2}\text{d}^{-1}$) and composition of pigments (mol %) during three sampling periods in the spring of 2005. Most data shown are for 1-70 μm particles collected by in situ pump, thought to represent suspended or very slowly sinking particles. Data for larger (>70 μm) pump (LP) and time series trap (TS) samples, assumed to represent sinking particles, are shown where available. The time series trap data shown are for those cups which most closely overlapped with the pump casts. Fig. 3.5 graphically depicts this data.....	120
Table 3.A4. Concentration ($\mu\text{mol C l}^{-1}$) or flux ($\mu\text{mol C m}^{-2}\text{d}^{-1}$) and composition of amino acids (mol %) during three sampling periods in the spring of 2005. The caption for Table 3.A3 describes the samples in more detail.....	122
Table 3.A5. Composition of pigments (mol %) with settling velocity for spring-summer, 2003. Most data shown are for the settling velocity trap (collected in duplicate and averaged). Also shown are data for the 1-70 μm pumps (small pump, or SP) collected at approximately	

the same depth. As the data for each settling velocity class are integrated over the entire deployment period, we have averaged the pump data collected at the beginning and end of each trap deployment for comparison.....124

Table 3.A6. Composition of amino acids (mol %) with settling velocity for spring-summer, 2003. The caption for Table 3.A5 describes the samples in more detail.....125

Table 3.A7. Composition of pigments (mol %) with settling velocity for the spring of 2005. Most data shown are for the settling velocity traps (collected in duplicate and averaged). Also shown are data for the 1-70 μm pumps (small pump, or SP) and $>70 \mu\text{m}$ pumps (large pump, or LP) collected at approximately the same depths. As the data for each settling velocity class are integrated over the entire deployment period, we have averaged the pump data from all three pump casts to the extent possible.....126

Table 3.A8. Composition of amino acids (mol %) with settling velocity for the spring of 2005. The caption for Table 3.A7 describes the samples in more detail.....127

LIST OF FIGURES

Figure 2.1. Image of untreated *C. closterium* cells observed under 1000X magnification using light microscopy. The diatoms were $\sim 15 \mu\text{m}$ pennate cells with long spines on either end, resulting in a total length of $\sim 40 \mu\text{m}$. Valvar (looking down on one valve, or “lid” of the frustule) and apical (looking down on one side of the frustule, where the two valves intersect) planes of view are indicated by crossbars.....34

Figure 2.2. Carbon maps of *Cylindrotheca closterium* frustules. The left panels are images of the samples observed under STXM and the right panels are carbon maps. In the carbon maps, the distribution of organic carbon (shown in white) was obtained by taking the ratio of images acquired at different energies (280-283 vs. 293-296 eV) and mapping out the areas that exhibited the greatest change in absorbance just below the carbon absorption edge (290 eV). a: Whole frustule boiled in 10% SDS followed by 2:1 $(\text{CH}_2\text{Cl}_2:\text{MeOH})$. Carbon loadings (indicated by brightness in carbon map) appear to be proportional to sample thickness. b: Fragment produced by freeze-lysing diatoms and then cleaning them with 2:1 $(\text{CH}_2\text{Cl}_2:\text{MeOH})$ followed by 30% H_2O_2 . The elongated, curved appearance of this fragment suggests that it may have originally been located at the intersection of the valvar (surface, or looking down on one valve) and apical (side) planes of view of the frustule (see box in Fig. 2.1). Lines are provided to indicate alignment of features. Thin, patterned regions (pointed out by lines) appear to have high carbon content. c: Fragments prepared as in sample b and then hydrolyzed in 6N HCl. As in a, carbon loadings appear to be proportional to sample thickness.....35

Figure 2.3. XANES carbon spectrum of *C. closterium* frustule (cleaned with 2:1 $(\text{CH}_2\text{Cl}_2:\text{MeOH})$ and H_2O_2) compared with that of a pure polylysine standard. Presence of carbonyl peak (denoted by C=O) in both samples suggests chemical similarity between polylysine and the organic matter present in the diatom frustule. The x-axis is X-ray energy (eV) and the y-axis is $-\ln$ of the ratio in absorbance of the sample (I) and background (IO).....36

Figure 2.4. Results of cluster analysis on fragment of *C. closterium* frustule. Sample was freeze-lysed and cleaned with 2:1 $(\text{CH}_2\text{Cl}_2:\text{MeOH})$ followed by 30% H_2O_2 . The top left panel (a) is an image of the sample observed under STXM. The top right panel (b) depicts the clusters detected by cluster analysis. Five clusters were apparent. Images of each cluster are provided (c-g) with XANES spectra to right. The background (c) contained no carbon. The thick, solid regions of the frustule (d) contained carbonyl material (denoted by C=O). The thin, highly patterned regions (e) contained unsaturated or aromatic carbon (denoted by C=C) as well as carbonyl material. An additional cluster was present containing organic material, possibly with a small amount of potassium (f). A fifth cluster was present containing organic material and a larger amount of potassium (g). The x-axis is X-ray energy (eV) and the y-axis is $-\ln$ of the ratio in absorbance of the sample (I) and background (IO).....37

Figure 2.5. Results of cluster analysis on fragments of *C. closterium* frustule. The flat appearance of the fragments suggest that they may have originally part of one of the valves of the frustule (see box in Fig. 2.1). Sample was freeze-lysed, cleaned with 2:1(CH₂)₂Cl₂:MeOH, with 30% H₂O₂, and finally, hydrolyzed in 6N HCl at 110°C for 20 h. Panels (a-g) are as described in Fig. 2.4.....38

Figure 2.6. Results of cluster analysis on fragments of *C. closterium* frustule. Sample was freeze-lysed, cleaned with 2:1(CH₂)₂Cl₂:MeOH, with 30% H₂O₂, and finally, hydrolyzed in 6N HCl at 110°C for 20 h. Panels (a-g) are as described in Fig. 2.4.....39

Figure 2.7. Results of cluster analysis on fragment of *C. closterium* frustule. Sample was freeze-lysed, cleaned with 2:1(CH₂)₂Cl₂:MeOH, with 30% H₂O₂, and finally, hydrolyzed in 6N HCl at 110°C for 20 h. Panels (a-f) are as described in Fig. 2.4.....40

Figure 2.8. SEM images of *C. closterium*. a) Overview of a cell taken at 5000x magnification. b) Image taken at 50,000x magnification showing small pores located along fibrulae (heavy silicified “buttons” at top and bottom of image and raphe (slit in center of frustule), indicated with boxes. Criss-cross pattern throughout the lower portion of the frustule may also be due to presence of pores. c) Image taken at 100,000x magnification showing pores along raphe. d) Image taken at 50,000x showing pores at the end of the spine. Pores were present throughout both spines.....41

Figure 2.9. Beam damage test on fragment of *C. closterium* frustules. Sample was freeze-lysed and then cleaned with 2:1(CH₂)₂Cl₂:MeOH followed by 30% H₂O₂. Top left panel (a) depicts an image of the sample observed under STXM. Boxes indicate regions subjected to beam damage (area where shutter was opened, allowing full exposure to beam). Top right panel (b) depicts clusters detected by cluster analysis. Three clusters were apparent. Images of each cluster are provided (c-f) with XANES spectra to right. The background (c) contained no carbon. Two clusters (d and e) were very similar, primarily containing carbonyl carbon with some unsaturated or aromatic carbon. X-axis depicts X-ray energy (eV) and y-axis depicts -ln of the ratio in absorbance of the image (I) and background (IO).....43

Figure 2.10. Results of cluster analysis on synthetic silica gel prepared by adding polylysine to a buffered solution of silicic acid. Following preparation, the sample was cleaned with 30% H₂O₂ and then hydrolyzed in 6N HCl. The top left panel (a) is an image of the sample observed under STXM and the top right (b) depicts the clusters detected by cluster analysis. Two clusters were apparent. Images of each cluster are provided (c-d) with XANES spectra to right. The background (c) contained no carbon. The gel (d) contained carbonyl material and possibly a small amount of unsaturated or aromatic carbon. The x-axis is X-ray energy (eV) and the y-axis is -ln of the ratio in absorbance of the sample (I) and background (IO).....44

Figure 3.1. Vertical profiles of pigments and amino acids in the 1-70 µm particulate fraction (collected on the 1 µm filter of in situ pumps) for three sampling periods in spring and summer of 2003 and 2005. Samples collected at the same depth within about a week were averaged for comparison with corresponding time series trap samples. a) During all sampling periods in 2003, pigments and amino acids reached a subsurface maximum at about 25-75 m and then decreased to nearly 0 µmol C l⁻¹ within the upper 200-400 m. As of

March 4-10, 2003, the pigment and amino acid maxima occurred at 50 m depth, where concentrations were 0.11 and 1.7 $\mu\text{mol C l}^{-1}$, respectively. From May 7-12, the maxima remained at 50 m depth, where concentrations increased to 0.31 and 4.0 $\mu\text{mol C l}^{-1}$, respectively. By June 30, the pigment maximum was at 75 m and had decreased in concentration to 0.07 $\mu\text{mol C l}^{-1}$; the amino acid maximum remained at 50 m and had decreased to 1.9 $\mu\text{mol C l}^{-1}$. b) On March 2, 2005, pigments were about 0.003 $\mu\text{mol C l}^{-1}$ throughout the upper 300 m, thereafter decreasing to about 0.001 $\mu\text{mol C l}^{-1}$. The amino acid maximum occurred at the surface (1.0 $\mu\text{mol C l}^{-1}$). As of March 9-14, 2005, the pigment and amino acid maxima again occurred at the surface, where concentrations were 0.01 and 0.82 $\mu\text{mol C l}^{-1}$, respectively. By April 29-30, maximum concentrations had increased to 0.03 $\mu\text{mol C l}^{-1}$ pigments at 35 m and 4.8 $\mu\text{mol C l}^{-1}$ amino acids at the surface.....100

Figure 3.2. Vertical profiles of pigments and amino acids in the $>70 \mu\text{m}$ particulate fraction (collected on the $70 \mu\text{m}$ Teflon screen of in situ pumps) for three sampling periods in the spring of 2005. On Mar. 2, data markers for amino acids and pigments overlap at surface, so amino acid point is not visible. Concentrations were several orders of magnitude lower in this size class than in the $1-70 \mu\text{m}$ fraction, possibly because larger particles are generally rarer than smaller particles. Many samples were below detection limits, partly due to these low concentrations as well as the small size of the punches and possible artifacts from drying the samples. Pigment and amino acid maxima were generally deeper in the $> 70 \mu\text{m}$ fraction, probably since they represent organic matter export, rather than production. On March 2, concentrations of pigments and amino acids at the surface were about 0.002 nmol C l^{-1} and 0.002 $\mu\text{mol C l}^{-1}$, respectively (data markers overlap on figure), and increased to 0.005 nmol C l^{-1} and 0.007 $\mu\text{mol C l}^{-1}$ by 300-400 m depth. Since no data were available between 0-200 m depth, it is possible the actual maxima occurred higher in the water column. As of March 9-14, the amino acid maximum occurred at about 25 m depth (0.023 $\mu\text{mol C l}^{-1}$) and the pigment maximum at 100 m depth (0.026 nmol C l^{-1}). On April 29-30, the pigment and amino acid maxima occurred at 150 m depth (0.024 nmol C l^{-1} and 0.029 $\mu\text{mol C l}^{-1}$, respectively).....102

Figure 3.3. Temporal changes in pigment and amino acid fluxes from March 6-June 30, 2003 (a) and March 4-April 28, 2005 (b) measured using IRS sediment traps operated in time series mode. Each data point represents the median of a 5-7 day sampling interval. a) Time series data for 2003 are described by Lee et al. (submitted) and Wakeham et al. (submitted); data for pigments and amino acids are presented again here after conversion to $\mu\text{mol C m}^{-2}\text{d}^{-1}$ to facilitate comparison with the pumps. Fluxes of pigments and amino acids at 238 m peaked around March 13, reaching 33 and 1685 $\mu\text{mol C m}^{-2}\text{d}^{-1}$, respectively (synchronous with elevated satellite chlorophyll), then decreasing substantially to 4 and 255 $\mu\text{mol C m}^{-2}\text{d}^{-1}$, respectively, by the beginning of April. A small, secondary bloom occurred in early May, with fluxes increasing again to 11 and 652 $\mu\text{mol C m}^{-2}\text{d}^{-1}$, respectively, by about May 20, then decreasing to below 1 and 189 $\mu\text{mol C m}^{-2}\text{d}^{-1}$ throughout June. Fluxes at 771 and 1918 m were temporally offset by ~ 10 d and generally ranged from 20-80% of those at 238 or 117 m. Fluxes of total mass and organic carbon (Lee et al., submitted; Wakeham et al., submitted) followed similar temporal patterns (peaking at 910 and 71 $\text{mg m}^{-2}\text{d}^{-1}$, respectively, in early March, then decreasing to 138 and 11 $\text{mg m}^{-2}\text{d}^{-1}$ by early April, increasing again slightly to 165 and 16 $\text{mg m}^{-2}\text{d}^{-1}$ in the first two weeks of May, and finally decreasing to below 25 and 5 $\text{mg m}^{-2}\text{d}^{-1}$ throughout June). B) In 2005, maximum fluxes of pigments and amino acids at 313 m occurred around March 25, peaking at 17 and 438 $\mu\text{mol C m}^{-2}\text{d}^{-1}$,

respectively. Smaller peaks occurred earlier in March and again around April 15, reaching 6-7 and 237-315 $\mu\text{mol C m}^{-2}\text{d}^{-1}$, respectively. By the end of April, pigment and amino acid fluxes decreased to 0.4 and 53 $\mu\text{mol C m}^{-2}\text{d}^{-1}$, respectively. Fluxes at 924 m were temporally offset by ~ 10 d and generally ranged from 20-90% of those at 313 m. Fluxes of total mass and organic carbon followed similar temporal variations, which appeared to be related to dust events (Lee et al., submitted), reaching 906 and 26 $\text{mg m}^{-2}\text{d}^{-1}$, respectively, in early March and 880 and 25 $\text{mg m}^{-2}\text{d}^{-1}$, respectively, at the end of March, then declining by the end of April to about 26 and 4 $\text{mg m}^{-2}\text{d}^{-1}$, respectively.....103

Figure 3.4. Depth profiles of pigment and amino acid composition of particles during three sampling periods in spring-summer, 2003. Most data shown are for 1-70 μm particles collected by in situ pump, thought to represent suspended or very slowly sinking particles. Data for time series trap (TR) samples, assumed to represent sinking particles, are shown where available. The time series trap data shown are for those cups which most closely overlapped with the pump casts. The March 4-10 pump casts are compared with the March 6-11 trap sample (1st deployment, 1st cup), the May 7-12 pump casts with the April 30 – May 6 trap sample (1st deployment, last cup), and the June 30 pump cast with the June 25-30 trap sample (2nd deployment, last cup).....105

Figure 3.5. Principal component analysis on the 2003 pump and TS trap data. Variable loadings are scaled up 10X and plotted on the same axes as sample site scores. Numbers represent depth (in m) for the 1-70 μm pump samples and the date of the midpoint of each sampling interval for the TS samples.....107

Figure 3.6. Depth profiles of pigment and amino acid composition of particles during three sampling periods in the spring of 2005. Most data shown are for 1-70 μm particles collected by in situ pump, thought to represent suspended or very slowly sinking particles. Data for larger (>70 μm) pump (LP) and time series trap (TS) samples, assumed to represent sinking particles, are shown where available. The time series trap data shown are for those cups which most closely overlapped with the pump casts. The March 2 pump cast is compared with the March 4-9 trap sample (1st cup), the March 9-14 pump casts with the March 9-14 trap sample (2nd cup), and the April 29-30 pump cast with the April 23-28 trap sample (last cup)....108

Figure 3.7. Principal component analysis on the 2005 pump and TS trap data. Variable loadings are scaled up 10X and plotted on the same axes as sample site scores. Numbers represent depth (in m) for the 1-70 μm pump samples and >70 μm pump samples, and the date of the midpoint of each sampling interval for the TS samples.....110

Figure 3.8. Changes in pigment and amino acid composition of particles with settling velocity for spring-summer, 2003. Most data shown are for the settling velocity trap (collected in duplicate and averaged. Also shown are data for the 1-70 μm pumps (small pump, or SP) collected at approximately the same depth. As the data for each settling velocity class are integrated over the entire deployment period, we have averaged the pump data collected at the beginning and end of each trap deployment for comparison. The 238 m SV trap deployment from March 6-May 6 is compared with the 200 m pump casts averaged over March 4-10 and May 7-12. The 117 m trap deployment from May 14-June 30 is compared with the 100 m pump casts averaged over May 7-12 and June 25-30.....111

Figure 3.9. Changes in pigment and amino acid composition of particles with settling velocity for the spring of 2005. Most data shown are for the settling velocity traps (collected in duplicate and averaged) at 313, 524, and 1918 m. Also shown are data for the 1-70 μm pumps (small pump, or SP) and $>70 \mu\text{m}$ pumps (large pump, or LP) collected at 300, 500, and 1800 m. As the data for each settling velocity class are integrated over the entire deployment period (March 4-May 1), wherever possible we have averaged the data from all three sets of pump casts (March 2, March 9-14, and April 29-30) for comparison. At 300 m, data for LP were available for March 2 and Apr. 29-30, but not March 9-14; data for SP were available for all 3 time periods. At 500 m, data for LP were available only from April 29-30; data for SP were available for all 3 time periods. At 1818 m, data for both LP and SP were available only from March 9-14.....112

Figure 3.10. Average mole % of the pigment and amino acid biomarkers in all samples collected from > 200 m depth. Bar depicts the mean, and error bars the maximum and minimum contributions of each biomarker observed. SP: small particles (1-70 μm) collected by *in situ* pump in 2003 (200-800 m from March 5-10, 200-1100 m from May 7-12, and 200-1800 m on June 30) and 2005 (200-500 m on March 2, 200-1800 m from March 9-14, and 200-750 m from April 29-30). LP: large particles ($>70 \mu\text{m}$) collected by *in situ* pump in 2005 200-500 m on March 2, 200-1800 m from March 9-14, and 200-750 m from April 29-30). TS: time-series trap samples collected in 2003 (238 and 771 m from March 6-May 6; 117 and 1918 m from May 14-June 30) and 2005 (313 and 924 m from March 4-April 28). SV: settling-velocity trap samples collected in 2003 (238 m from March 6-May 6; 117 m from May 14-June 30) and 2005 (313, 524, and 1918 m from March 4-May 1).....113

Figure 3.11. The relationship between chl *a* and its microbial degradation product phytin (a) or zooplankton alteration products phide + pyrophide (b) for all 1-70 μm pump (SP), $>70 \mu\text{m}$ pump (LP), and TS trap samples (TS). Chl *a*, phytin, and phide + pyrophide are normalized to total pigments (i.e., as in the mol % calculations) to eliminate differences in total pigment concentrations. Data from all depths and time periods sampled are shown.....114

Figure 4.1. Changes in particulate mass, organic carbon (POC), inorganic carbon (PIC), nitrogen (PN), biogenic silica (BSi), and lithogenic silica (LSi) in suspended and sinking particles during incubation of the 20 m plankton tow material.....157

Figure 4.2. Changes in particulate pigments and amino acids (PAAs) in suspended and sinking particles during the 20 m plankton tow incubation.....158

Figure 4.3. Changes in the pigments chlorophyll *a* (chl *a*), fucoxanthin (fuco), pheophorbide (phide), pyropheophorbide (pyrophide), and pheophytin (phytin) in suspended and sinking particles during the 20 m plankton tow incubation.....159

Figure 4.4. Changes in the amino acids serine (SER), threonine (THR), glycine (GLY), aspartic acid (ASP), glutamic acid (GLU), β -alanine (BALA), and γ -aminobutyric acid (GABA) in suspended and sinking particles during the 20 m plankton tow incubation.....160

Figure 4.5. Composition of total particulate mass and organic carbon in suspended and sinking particles in the 200 m NetTrap incubation. Top panel shows the % contribution of particulate nitrogen (N), organic carbon (OC), inorganic carbon (IC), biogenic silica (BSi) as SiO₂, lithogenic material (litho) calculated from lithogenic silica measurements assuming crustal ratios, and uncharacterized components (other) to total mass. Bottom panel shows the contribution of pigments (pig) and amino acids (AA), and uncharacterized components to particulate organic carbon.....161

Figure 4.6. Percent composition (in mol % of total pigments and amino acids) of selected pigments and amino acids in suspended and sinking particles during the 20 m plankton tow incubation. Pigments shown are chlorophyll *a* (chl *a*), fucoxanthin (fuco), pheophorbide (phide), pyropheophorbide (pyrophide), and pheophytin (phytin). Amino acids shown are (SER), threonine (THR), glycine (GLY), aspartic acid (ASP), glutamic acid (GLU), β-alanine (BALA), and γ-aminobutyric acid (GABA).....162

Figure 4.7. Principal component analysis performed on the data from the 20 m plankton tow incubation. Suspended and sinking particles are circled.....163

Figure 4.8. Changes in particulate mass, organic carbon (POC), inorganic carbon (PIC), nitrogen (PN), biogenic silica (BSi), and lithogenic silica (LSi) in suspended and sinking particles during the 200 m NetTrap incubation.....164

Figure 4.9. Changes in particulate pigments and amino acids (PAAs) in suspended and sinking particles during the 200 m NetTrap incubation.....165

Figure 4.10. Changes in the pigments chlorophyll *a* (chl *a*), fucoxanthin (fuco), pheophorbide (phide), pyropheophorbide (pyrophide), and pheophytin (phytin) in suspended and sinking particles during the 200 m NetTrap incubation.....166

Figure 4.11. Changes in the amino acids serine (SER), threonine (THR), glycine (GLY), aspartic acid (ASP), glutamic acid (GLU), β-alanine (BALA), and γ-aminobutyric acid (GABA) in suspended and sinking particles during the 200 m NetTrap incubation.....167

Figure 4.12. Composition of total particulate mass and organic carbon in suspended and sinking particles in the 200 m NetTrap incubation. Top panel shows the % contribution of particulate nitrogen (N), organic carbon (OC), inorganic carbon (IC), biogenic silica (BSi) as SiO₂, lithogenic material (litho) calculated from lithogenic silica measurements assuming crustal ratios, and uncharacterized components (other) to total mass. Bottom panel shows the contribution of pigments (pig) and amino acids (AA), and uncharacterized components to total particulate organic carbon.....168

Figure 4.13. Percent composition (in mol % of total pigments and amino acids) of selected pigments and amino acids in suspended and sinking particles during the 200 m NetTrap incubation. Pigments shown are chlorophyll *a* (chl *a*), fucoxanthin (fuco), pheophorbide (phide), pyropheophorbide (pyrophide), and pheophytin (phytin). Amino acids shown are (SER), threonine (THR), glycine (GLY), aspartic acid (ASP), glutamic acid (GLU), β-alanine (BALA), and γ-aminobutyric acid (GABA).....169

Figure 4.14. Principal component analysis performed on the data from the 200 m NetTrap incubation. Suspended and sinking particles are circled.....170

Figure 4.15. Principal component analysis performed on the combined data from the 20 m plankton tow and 200 m NetTrap incubations. Suspended and sinking particles from both incubations are circled.....171

ACKNOWLEDGEMENTS

Many individuals contributed to the development, execution, and interpretation of this work. Foremost, my advisors Cindy Lee and Robert Aller generously contributed their ideas, time, and funding to help me carry out my research. More importantly, they provided constant support and guidance and were instrumental in my development as a scientist and as a person. I feel so fortunate to have had two advisors who are both so talented and at the same time so down-to-earth, friendly, and caring.

Cindy, you have been both my toughest critic and biggest supporter, raising the bar very high but doing everything you could to help me meet it. You are an inspiration to me, having overcome so many personal struggles to become a successful scientist and wonderful person. I am always amazed by your constant wonder and excitement about exploring new ideas and your capacity for seeing the big picture. Your positive attitude has helped me get through setbacks in my research and difficult times in my personal life. You have not only been a great mentor to me, but also everything from a friend to therapist to adoptive mother, filling whatever role was required at the time. You are always warm, caring, and full of concern for your students, and maintain a great sense of humor even in the toughest times.

Bob, I have always appreciated your rare ability to approach even the most complex problems with brilliant simplicity. It is a pleasure discussing my research with you, because you understand and explain everything with such clarity. You have helped me countless times in working out challenges in experimental design and data interpretation, and I especially appreciate your help approaching my mass balance calculations in a clear, methodical way. On a personal level, I have always enjoyed your great sense of humor, and have loved our cheerful banter about everything from my obsession with moisturizers to your copious sweating during a run (quite opposite problems, when you think about it!). I am inspired by your ability to remain in a good mood no matter what the circumstances, and admire the respect and objectivity with which you treat everyone from a first year student to a distinguished scientist.

Many other individuals have contributed to my scientific development and dissertation research. I would particularly like to thank my committee members, Bruce Brownawell, Rich Reeder, and Ron Benner. I appreciate all of your helpful comments during both the proposal and defense stages. Bruce provided extremely insightful comments on my dissertation and particularly helped me strengthen Chapters 3 and 4. Rich provided particularly helpful guidance with Chapter 2, helping me work out experimental challenges and providing valuable comments on the completed manuscript. Ron was especially helpful in the initial design of my incubations, in improving my understanding of the biological implications of my research, and in identifying areas of the dissertation in need of clarification.

I would also like to thank all of my co-authors for the work presented in Chapter 2. Chris Jacobsen helped with the development and interpretation of this research. Sue Wirick spent countless hours helping me obtain the XANES spectra and images. Finally, Jay Brandes provided invaluable assistance with the data interpretation and manuscript preparation. Several other individuals contributed to this work. The statistical tools used in evaluating the XANES spectra were largely developed by Mirna Lerotic, who provided considerable assistance with the data analysis. Anitra Ingalls paved the way for my research with her research on the preservation of biomineral-bound proteins. Shelagh Palma, Bassem Allam, Sue Pawagi, Klaus Kemp, and Jim Quinn provided assistance with sample preparation and examination.

All of our MedFlux collaborators contributed to Chapters 3 and 4 in some way, whether through sample collection, laboratory analyses, or the development of ideas. I would particularly like to thank Rob Armstrong, Kirk Cochran, David Hirschberg, Stuart (“Stewie”) Wakeham, Michael Peterson, Madeleine Goutx, Juan-Carlos Miquel, Beat Gassler, and Scott Fowler. All of these individuals provided many ideas, answered many questions, and above all always made MedFlux cruises enjoyable and memorable. The dedicated crews of the R/V Seward Johnson II and Endeavor, as well as our funding from the NSF Chemical Oceanography program, also made this work possible.

I have shared the Lee and Aller labs with many wonderful labmates over the past six years. In particular, Jenni Szlosek and Zhanfei Liu have been the best of friends. My graduate school experience is inextricably linked with memories of us deploying *in situ* pumps on a freezing, windy day in November, making movies about the “groovy” sediment

trap, grinding mud from Flax Pond, endlessly shaking 20 liter cubiconainers of seawater, running through the streets of Monaco, fighting with the HPLC, and just enjoying a meal together. Thank you for being such fun, supportive “academic siblings” to me. Many other students and staff in our research group have been wonderful friends and colleagues, especially Jianhong Xue, Joan Fabres, Tina Schoolmeester, Brivaela Moriceau, Anja Engel, Caterina Panzeca, Bessy Alexandratos, and Christina Heilbrun. I have really enjoyed getting to know my newest labmates, Tiantian Tang and Fabian Batista. Tiantian, thank you in particular for all of your help finishing up my lab work- you were an incredibly helpful, careful, and enthusiastic assistant!

In addition to my labmates, I have made so many good friends here at Stony Brook, especially Ann Zulkosky, Lora Clarke, Teresa Mathews, Patrice Argant, Zosia Turek, Gillian Stewart, Catherine Vogel, and Sandy Lucas. I have so many memories of laughing and crying with you, hanging out at the Velvet Lounge or John Harvard’s, being confused with the other “tall girls”, eventful moving experiences involving abundant firewood, couches, and Goldendoodles, dressing up in ridiculous political costumes, dancing wildly, and talking to the refrigerator. I am so happy that a few of us will now be graduating together, so we can share that experience as well!

Many other friends and family have provided me with love and support over the years. Jasmin Roohi, Kristin Fitzsimmons, Allison Strype, and Liz Matthews have been there for me since the days of surprise birthday cakes on the Staten Island Ferry, and I have enjoyed growing up with all of you. My aunts, uncles, and cousins, Carol, Mich, Mike, and Ryan Landron and Denise, Jim, and Kim Thompson, have given me so much love and support over the years. My in-laws, Isaac Abramson, Rita Timmer, Karen, Lloyd, Mikela, and Hayden Becker, and Alon Abramson have also given me so much love and support and have become my own family.

Finally, I want to thank the three most important people in my life: my parents, Theodore and Maryalice Kowalchuk, and my husband, Ariel (Eric) Abramson. My parents were always incredibly loving and supportive of me. They made me the biggest priority in their lives, and spent countless hours helping me with science fair projects and homework assignments, driving me to speech and debate tournaments, music lessons, and sports practices, and organizing walkathons, dances, and PTA meetings at my school. They led their own lives with passion and determination, and by their example, I developed a sense of

purpose and passion for living. They supported and encouraged me through all my successes and failures, and in doing so gave me the confidence and persistence to pursue my goals. My parents taught me to dream big and to go after those dreams.

Where my parents left off in raising me, my husband has definitely taken over in supporting me and helping me achieve my goals. Eric, I have so much respect and appreciation for you. I always love being with you, enjoy your great sense of humor and fun attitude, and admire your level-headedness and ambition. Thank you for in turn loving me for who I am, for appreciating my good qualities while accepting my bad qualities. Thank you for making sacrifices for me and for always being willing to compromise and work together as a team. Whatever life has in store for us, I know we can get through it together.

CHAPTER 1

Introduction

1. The Role of Sinking Particles in the Marine Carbon Cycle

Sinking particles transport organic matter produced in surface waters to the deep ocean, driving the drawdown of carbon dioxide from the atmosphere. During transit, >90% of particulate organic carbon (POC) is heterotrophically remineralized (Hedges, 1992), resulting in a rapid decrease in particle fluxes with depth (Suess, 1980; Martin et al., 1987, Antia et al., 2001) and the replacement of phytoplankton products with refractory compounds or decomposition products (Wakeham et al., 1997). In spite of this efficient remineralization, a small fraction of the organic carbon produced in surface waters survives transit to the deep ocean (Lee and Wakeham, 1988), supplying energy to the benthos and remaining out of contact with the atmosphere for ~1000 years.

Labile organic matter can escape decomposition in the water column if it is exposed to environmental conditions that retard decomposition or if it is rapidly exported to the seafloor. Understanding how such mechanisms of protection operate is crucial for quantitative prediction of POC fluxes in different environments. This thesis addresses two important factors influencing POC decomposition: chemical or physical protection by associated minerals, and aggregation processes.

2. Associations between Organic Matter and Minerals

Attempts to quantitatively predict POC fluxes often relate export to primary or new production; however, deep fluxes of POC (below 1000 m) can be highly variable and not well predicted by production. Armstrong et al. (2002) demonstrated that deep POC fluxes are consistently about 5% of total mass fluxes in the open ocean, indicating that the export of POC below 1000 m is quantitatively related to the simultaneous export of minerals. They suggested that this relationship may indicate that the export of minerals depends on a threshold concentration of organic “glue” needed to aggregate small mineral particles together (e.g., Golchin et al., 1998; Mayer, 1999; Arnarson and Keil, 2001; Klaas and Archer, 2002). They also suggested that ballast minerals may prevent the degradation of associated

organic matter by increasing the density, and therefore, sinking rate of POC (e.g., Ittekkot and Haake, 1990; Honjo, 1966), or by physically or chemically protecting it from microbial attack (e.g., Christensen and Blackburn, 1982; Gordon and Millero, 1985; Bartlett and Doner, 1988; Ingalls et al., 2003).

Theoretically, minerals could protect organic matter from decomposition via two general mechanisms: physical protection, in which minerals physically obstruct organic matter, making it inaccessible to enzymatic attack, and chemical protection, in which the chemical interactions between organic matter and minerals cause enzymatic hydrolysis to become energetically unfavorable. Within these two general classes, there might be numerous different types of associations, each offering varying degrees of protection against decomposition. Organic-mineral interactions have been discussed extensively in soil and sedimentary research, but have only recently begun to receive attention in water column research (e.g., Lee et al., 2000; Hedges et al., 2001).

2.1. Occlusion of Organic Matter within the Mineral Structure

Organic matter can be a component of mineral matrices. There is not much evidence for covalent bonding between minerals and organic molecules (Kinrade et al., 2002; Sahai, 2004); however, there is evidence for the occurrence of weaker electrostatic interactions (Hecky et al., 1973; Volcani, 1981; Mitzutani et al., 1998; Kröger et al., 1999, 2000; Noll et al., 2002), which may impede microbial hydrolysis. It is even more likely that mineral-bound organic matter is physically protected at the molecular level by its occlusion within the mineral structure. X-ray diffraction and ¹³C-nuclear magnetic resonance spectroscopy have provided evidence that organic matter can be located within clays in terrestrial soils, particularly those rich in smectite or montmorillonite (Theng, 1974; Theng et al., 1986; Curry et al., 2007).

The occlusion of organic matter within biominerals appears to be particularly common. The silica and calcium carbonate biominerals that comprise the tests of marine plankton precipitate on a glycoprotein scaffold that can constitute 0.2 weight% of the shell, or 28 weight% of the entire cell wall (Hecky et al., 1973; Weiner and Erez, 1984; Swift and Wheeler, 1991). Much of this organic matter remains even after harsh extraction procedures and is released only upon dissolution of the mineral, suggesting that it is tightly and irreversibly bound within the mineral structure (Ingalls et al., 2003). The ratio of mineral-

bound to non-mineral-bound amino acids tends to increase with depth in the water column and sediments, suggesting that biominerals do, in fact, protect mineral-bound organic matter from decomposition (Ingalls et al., 2003).

This type of organic-mineral association probably offers the most permanent protection of all types of associations. However, it is likely the least significant on a mass basis since such a small fraction of organic matter is associated with minerals in this manner (Hecky et al., 1973; Weiner and Erez, 1984).

2.2. Sorption onto Mineral Surfaces

Some organic matter may be also be protected by sorption onto mineral surfaces. Although this organic matter would be physically exposed to the external environment, its decomposition might be retarded by chemical interactions with the mineral surface. Organic matter can be bound to mineral surfaces via cation bridging (particularly in Ca, Fe, and Al-rich minerals), ligand exchange, electrostatic attraction, or H-bonding (Theng, 1974; Oades, 1988; Hur and Schlautman, 2003). Numerous studies (e.g., Christensen and Blackburn, 1982; Gordon and Millero, 1985; Baldock and Skjemstad, 2000) have documented suppressed decomposition of organic matter sorbed onto terrestrial soils and marine sediments. Sorption onto mineral surfaces may also alter the inherent reactivity of organic matter by bringing organic molecules into closer contact with each other. This may increase the likelihood of condensation reactions, producing high molecular weight, refractory organic complexes (Collins et al., 1995).

Quantitative relationships between mineral surface area and organic matter protection have been observed in marine sediments. In continental shelf environments from varying locations and of different mineralogies, organic carbon concentrations are linearly related to surface area, extrapolating to an intercept of 0.86 mg OC m⁻² SA (Mayer, 1994). This background fraction of organic matter may be protected from degradation by its sorption onto sediments. However, such a correlation does not necessarily imply protection, but possibly just the continuous sorption of fresh organic matter onto mineral surfaces. Keil et al. (1997) noted that although the concentration of organic matter per unit surface area remains constant as sediments move from rivers out onto shelves (~0.7-0.8 mg-OC m⁻²), significant changes in the $\delta^{13}\text{C}$ of the sorbed organic matter (indicative of whether its source is terrestrial or marine) occur. The isotopic values of $\sum\text{CO}_2$ produced during

remineralization are consistent with a terrestrial signature (Aller, 1998), indicating that at concentrations approaching the “monolayer equivalent,” most marine organic matter produced *in situ* on the shelves replaces almost all of the terrestrial organic matter initially sorbed on riverine sediments.

2.3. Sorption within Mesopores

Some surface-bound organic matter may also be protected within tiny mesopores (generally <10 nm) on mineral surfaces (Mayer, 1994). Since most of the surface area of these sediments is comprised of tiny mesopores 2-8 nm in diameter, most organic matter sorbed on the surface must be enclosed within these pores. Decomposing organisms or their exoenzymes may be physically excluded from these mesopores, resulting in physical protection (on scales of several nm) of the organic matter.

Zimmerman et al. (2004) provided experimental evidence in support of this possibility by comparing the sorption of amino acid monomers and polymers onto synthetic mesoporous and nonporous alumina and silica. All compounds smaller than about one-half the mean pore diameter (8.2 nm for alumina and 3.4 nm for silica) demonstrated significantly greater sorption (normalized to surface-area) and less desorption on mesoporous materials than nonporous materials. Curry et al. (2007) also found the retention of organic matter within clay mesopores after enzymatic digestion. This suggests that once sorbed within mesopores, organic matter may be protected from decomposition.

Other studies on the size fractionation of organic compounds by sorption (e.g., Gu et al., 1995; Hur and Schlautman, 2003) have found that higher molecular weight or longer chain length molecules sometimes exhibit increased sorption onto minerals. Possible reasons for this include more multi-site adsorption and greater van der Waals forces for larger molecules (Theng, 1974). However, these studies focused on complex mixtures of organic matter or on relatively high molecular weight compounds that would be too large to adsorb within mesopores, and therefore do not necessarily contradict the findings of Zimmerman et al. (2004).

2.4. Occlusion of Organic Matter within Aggregates

Organic matter can also be located inside an aggregate of inorganic particles, perhaps gluing the individual particles together. This intra-aggregate pool might be physically protected (on scales of several μm to mm) against decomposition.

Contrary to what Mayer (1994) first postulated, subsequent studies (e.g., Ransom et al., 1998; Mayer, 1999; Bock and Mayer, 2001; Arnarson and Keil, 2001) found that organic matter is most likely not sorbed as a monolayer, but in localized patches that amount to <15 % of the surface area of grains. This finding was the basis for the “glue hypothesis”, which proposed that patches of organic “glue” might adhere individual grains together, allowing protection within inter-granular, rather than intra-granular pores (Mayer, 1999; Arnarson and Keil, 2001).

Numerous studies have found that aggregation inhibits the decomposition of various organic compounds in terrestrial soils (e.g., Bartlett and Doner, 1988; Killham et al., 1993). Some organic matter persists in ancient shales (e.g., Salmon et al., 2000), indicating that mineral flocs can preserve organic matter for long time periods. At small scales (in interstitial pores about 0.1 - 10 μm in diameter), aggregation may place a physical barrier between organic substrates and decomposing organisms or their extracellular enzymes (Baldock and Skjemstad, 2000). Previous studies have found that bacteria can exist in soil aggregates only when the interstitial pore spaces are at least three times their own diameter (Oades, 1988; Baldock and Skjemstad, 2000). Consequently, over 90% of the pore space in soils should be inaccessible to bacteria or their exoenzymes (Oades, 1988; Van Veen and Kuikman, 1990). Even those pores large enough to accommodate bacteria may be inaccessible to protozoan grazers (Killham et al., 1993). Protozoan grazing on bacteria enhances substrate decomposition by increasing the turnover of bacterial biomass and regenerating nutrients (Taylor, 1982; Caron, 1994). Therefore, the exclusion of protozoans from aggregates could very well retard decomposition (Lee, 1992).

Even on larger scales (in interstitial pores that are tens of microns to centimeters in diameter) the depletion of oxygen within aggregates might also retard decomposition (Baldock and Skjemstad, 2000; Salmon et al., 2000). This theory may or may not be applicable to aggregates in marine environments. In the ocean, oxygen depletion does not always retard bacterial decomposition; rather, its effect varies among organic compounds (Lee, 1992). However, anoxia could make interstitial spaces an unsuitable habitat for many

protozoans, thereby hindering decomposition in a manner similar to that proposed by Lee (1992) and Killham et al. (1993).

3. Aggregation Processes

The relatively large concentration of POC associated with minerals (5 weight %) indicates that occlusion within the mineral structure or sorption as a monolayer or within mesopores are probably not the dominant mechanisms driving quantitative relationships between POC and mass fluxes. Rather, the idea that organic matter adheres mineral particles together, and in turn is either physically protected against decomposition or more rapidly exported through the water column, seems the most viable explanation.

Most individual (non-aggregated) particles in the water column are less than 2 μm in diameter and have very low settling velocities, so their export to the deep ocean is largely controlled by aggregation processes (McCave, 1975). Aggregate formation can occur via abiotic flocculation mechanisms (McCave, 1975; Alldredge and Silver, 1988), or via biological aggregation, such as the production of fecal pellets by zooplankton (Pilska and Honjo, 1987). Aggregates of organic matter and minerals can be present as amorphous marine snow (typically several mm in diameter), zooplankton fecal pellets (hundreds of μm to several mm in diameter), phytoplankton aggregates (several μm to hundreds of μm in diameter), and aggregates of clay and silt particles (several μm to tens of μm in diameter) (McCave, 1975; Alldredge and Silver, 1988).

Minerals have been shown to promote the aggregation of organic matter in marine systems (Hamm, 2002). In Engel et al. (submitted a, b), we found that they may enhance organic matter preservation as well. We compared the aggregation and decomposition of calcifying and non-calcifying cultures of *Emiliana huxleyi* incubated independently in rotating tanks over a period of 30 days. Calcifying cells aggregated faster and produced smaller aggregates with higher settling velocities, excess densities, and mass compared with those produced by non-calcifying cells (Engel et al., submitted a). Over the 30-day incubation, the decomposition of particulate organic carbon and nitrogen were twice as high in non-calcifying cells, and biomarkers indicative of decomposition (e.g., pheopigments and the amino acid β -alanine) became enriched in non-calcified coccolithophorids relative to calcified cells (Engel et al., submitted b). Furthermore, after initial aggregation, organic matter concentrations remained constant in aggregates of both cells, indicating that

aggregation can retard the decomposition of organic matter. These results highlight the importance of aggregates, particularly those containing minerals, in the flux of organic carbon to the deep sea.

However, the magnitude of particulate organic matter transport and preservation in aggregates depends on the extent to which aggregates remain intact during transit through the water column. Hill (1998) suggested that the consistency of settling velocity measurements in the ocean implies that particles undergo continual aggregation and disaggregation to adjust to changes in size and density. According to Stokes' Law, settling velocity is proportional to the square of the particle's radius and its excess density over seawater (McCave, 1975); therefore, as particles become larger or accumulate more minerals, they should sink increasingly faster. However, Hill (1988) concluded that as aggregates become larger or denser, shear eventually increases to a point where it causes disruption. In addition, inertial drag also increases with size, resulting in a large Reynolds number, so that Stokes Law may no longer apply (Khelifa and Hill, 2006). Aggregates have settling velocities that are 1-5 orders of magnitude greater than those for individual plankton cells or inorganic particles (Shanks and Trent, 1980; Alldredge and Gottschalk, 1988; Gibbs, 1985), so the extent to which particles aggregate or disaggregate in the water column is extremely important in determining the vertical flux of organic and inorganic material (Fowler and Knauer, 1986; Asper et al., 1992).

Even if aggregates provide no physical protection against decomposition, the extent of particle disaggregation and resulting changes in settling velocity would affect the residence time of POC in the water column, and therefore the efficiency of remineralization. Evaluating factors influencing the extent of particle disaggregation is therefore important in quantitatively predicting organic matter fluxes.

4. Thesis Objectives and Organization

This thesis examines two important factors influencing POC export in the water column: physical or chemical protection by minerals, and aggregation. Specifically, it focuses on 1) the occlusion of organic matter within biominerals, which may be the most permanent form of organic matter protection by minerals, and 2) the occlusion and transport of organic matter within aggregates, which may be the most quantitatively important form of organic-mineral association. The objectives of this research were to:

1. Determine what fraction of the organic matter bound within diatom frustules is protected against chemical attack, and what mechanisms (i.e., chemical interaction, physical occlusion) might be responsible for this protection.
2. Evaluate the extent to which sinking particles undergo disaggregation and exchange with surrounding material during transit through the water column, in turn influencing their residence time in the water column and the remineralization of their organic components.
3. Determine some of the factors influencing the robustness of different types of sinking particles and consequently, the extent to which they disaggregate and exchange with surrounding material.

Chapter 2 addresses how organic constituents are distributed throughout the frustule of one diatom species and how this distribution is affected by progressively more stringent levels of chemical attack. This was investigated using chemical oxidation and hydrolysis techniques and X-ray near-edge spectromicroscopy (XANES) at the carbon edge, which simultaneously provided information on the physical structure of diatom frustules as well as the distribution and molecular composition of the organic matter within.

Chapter 3 addresses the extent of exchange between sinking and suspended particles by evaluating compositional differences between sediment trap and *in situ* pump samples collected in the northwest Mediterranean Sea. Differences in the extent of exchange for different sinking particle types (zooplankton fecal pellets and phytoplankton aggregates) and seasons (spring and summer) were evaluated.

Chapter 4 experimentally compares the extent of exchange between suspended and sinking particles within the mixed layer and at the base of the mixed layer in the northwest Mediterranean Sea to determine how the most robust, physically protective aggregates are formed. This chapter further discusses the differences between fecal pellets and phytoplankton aggregates introduced in the previous chapter.

Chapter 5 summarizes the major findings of this work and suggests future research directions.

References

- Allredge, A.L., Gotschalk, C.C., 1988. *In situ* settling behavior of marine snow. *Limnology and Oceanography* 33, 339-351.
- Allredge, A.L., Silver, M., 1988. Characteristics, dynamics and significance of marine snow. *Progress in Oceanography* 20, 41-82.
- Aller, R.C., 1998. Mobile deltaic and continental shelf muds as suboxic, fluidized bed reactors. *Marine Chemistry* 61, 143-155.
- Antia, A.N., Koeve, W., Fischer, G., Blanz, T., Schulz-Bull, D., Scholten, J., Neuer, S., Kremling, K., Kuss, J., Peinert, R., Hebbeln, D., Bathmann, U., Conte, M., Fehner, U., Zeizschel, B., 2001. Basin-wide particulate carbon flux in the Atlantic Ocean: Regional export patterns and potential for atmospheric CO₂ sequestration. *Global Biogeochemical Cycles* 15(4), 845-862.
- Armstrong, R.A., Lee, C., Hedges, J.I., Honjo, S., Wakeham, S.G., 2002. A new, mechanistic model for organic carbon fluxes in the ocean based on the quantitative association of POC with ballast minerals. *Deep-Sea Research II* 49, 219-236.
- Arnarson, T.S., Keil, R.G., 2001. Organic-mineral interactions in marine sediments studied using density fractionation and X-ray photoelectron spectroscopy. *Organic Geochemistry* 32, 1401-1415.
- Asper, V.L., Deuser, W.G., Knauer, G.A., Lohrenz, S.E., 1992. Rapid coupling of sinking particle fluxes between surface and deep ocean waters. *Nature* 357, 670-672.
- Baldock, J.A., Skjemstad, J.O., 2000. Role of the soil matrix and minerals in protecting natural organic materials against biological attack. *Organic Geochemistry* 31, 697-710.
- Bartlett, J.R., Doner H.E., 1988. Decomposition of lysine and leucine in soil aggregates: sorption and compartmentalization. *Soil Biology and Biochemistry* 20, 755-759.
- Bock, M.J., Mayer, L.M., 2000. Mesodensity organo-clay associations in a near-shore sediment. *Marine Geology* 163, 65-75.
- Caron, D.A., 1994. Inorganic nutrients, bacteria, and the microbial loop. *Microbial Ecology* 28, 295-298.
- Christensen, D., Blackburn, T.H., 1982. Turnover of ¹⁴C-labelled acetate in marine sediments. *Marine Biology* 71, 113-119.
- Collins, M.J., Bishop, A.N., Farrimond, P., 1995. Sorption by mineral surfaces: Rebirth of the classical condensation pathway for kerogen formation? *Geochimica et Cosmochimica Acta* 59, 2387-2391.

- Curry, K.J., Bennet, R.H., Mayer, L.M., Curry, A., Abril, M., Biesiot, P.M., Hulbert, M.H., 2007. Direct visualization of clay microfabric signatures driving organic matter preservation in fine-grained sediment. *Geochimica et Cosmochimica Acta* 71, 1709-1720.
- Engel, A., Abramson, L., Szlosek, J., Liu, Z., Stewart, G., Hirschberg, D., Lee, C. Investigating the effect of ballasting by CaCO₃ in *Emiliana huxleyi*: II. Decomposition of particulate organic matter. Submitted to Deep-Sea Research II (a).
- Engel, A., Szlosek, J., Abramson, L., Liu, Z., and Lee, C. Decomposition of calcifying and non-calcifying *Emiliana huxleyi* (Prymnesiophyceae): II. Formation, settling velocities and physical properties of aggregates. Submitted to Deep-Sea Research II (b).
- Fowler, S.W., Knauer, G.A., 1986. Role of large particles in the transport of elements and organic compounds through the oceanic water column. *Progress in Oceanography* 16,147-194.
- Gibbs, R.J., 1985. Estuarine flocs: Their size, settling velocity and density. *Journal of Geophysical Research* 90, 3249-3251.
- Golchin, A., Baldock, J.A., Oades, J.M., 1998. A model linking organic matter decomposition, chemistry, and aggregate dynamics. In: Lal, R., J.M. Kimble, R.F. Follett, and B.A. Stewart (Eds.), *Soil Processes and the Carbon Cycle*. CRC Press, Boca Raton, Florida, pp. 245-266.
- Gordon, A.S., Millero, F.J., 1985. Sorption mediated decrease in the biodegradation rate of organic compounds. *Microbial Ecology* 11, 289-298.
- Gu, B., Schmitt, J., Chen, C., Liang, L., McCarthy, J.F., 1995. Sorption and desorption of different organic matter fractions on iron oxide. *Geochimica et Cosmochimica Acta* 59, 219-229.
- Hamm, C.E., 2002. Interactive aggregation and sedimentation of diatoms and clay-sized lithogenic material. *Limnology and Oceanography* 47, 1790-1795.
- Hecky, R.E., Mopper, K., Kilham, P., Degens, E.T., 1973. The amino acid and sugar composition of diatom cell-walls. *Marine Biology* 19, 323-331.
- Hedges, J.I., 1992. Global biogeochemical cycles: progress and problems. *Marine Chemistry* 39, 67-93.
- Hedges, J.I., Baldock, J.A., G elinas, Y., Lee, C., Peterson, M., Wakeham, S., 2001. Evidence for the non-selective preservation of organic matter in sinking marine particles. *Nature* 409, 801-804.
- Hill, P.S., 1998. Controls on floc size in the sea. *Oceanography* 11, 13-18.

- Honjo, S., 1996. Fluxes of particles to the interior of the open oceans. In: Ittekkot, V., Schäfer, P., Honjo, S., Depetris, P.J. (Eds.), *Particle Flux in the Ocean*, SCOPE, Vol. 57. Wiley, New York, pp. 91–254.
- Hur, J., Schlautman, M.A., 2003. Molecular weight fractionation of humic substances by sorption onto minerals. *Journal of Colloid Interface Science* 264, 313-321.
- Ingalls, A.E., Lee, C., Wakeham, S.G. Hedges, J.I., 2003. The role of biominerals in the sinking flux and preservation of amino acids in the Southern Ocean along 170°W. *Deep-Sea Research II* 50, 709-734.
- Ittekkot, V., Haake, B., 1990. The terrestrial link in the removal of organic carbon. In: Ittekkot, V., Kempe, S., Michaelis, M., Spitzzy, A. (Eds.) *Facets of Modern Biogeochemistry*, Springer, Berlin, pp. 319-325.
- Keil, R.G., Mayer, L.M., Quay, P.D., Richey, J.E., Hedges, J.I., 1997. Loss of organic matter from riverine particles in deltas. *Geochimica et Cosmochimica Acta* 61,1507-1511.
- Khelifa, A., Hill, P.S., 2006. Models for effective density and settling velocity of flocs. *Journal of Hydraulic Research* 44, 390–401.
- Killham, K., Amato, M., Ladd, J.N., 1993. Effect of substrate location in soil and soil pore-water regime on carbon turnover. *Soil Biology and Biochemistry* 25(1), 57-62.
- Kinrade, S.D., Gillson, A.M.E., Knight, C.T.G., 2002. Silicon-29 NMR evidence of a transient hexavalent silicon complex in the diatom *Navicula pelliculosa*. *Journal of the Chemical Society – Dalton Transactions* 3, 307-309.
- Klaas, C., Archer, D. E., 2002. Association of sinking organic matter with various types of mineral ballast in the deep sea: Implications for the rain ratio. *Global Biogeochemical Cycles* 16, 1116, doi:10.1029/2001GB001765.
- Kröger, N., Deutzmann, R., Bergdorf, C. Sumper, M., 2000. *Proceedings of the National Academy of Sciences* 97, 14133-14138.
- Kröger, N., Deutzmann, R., Sumper, M., 1999. Polycationic peptides from diatom biosilica that direct silica nanosphere formation. *Science* 286, 1129-1132.
- Lee, C., 1992. Controls on organic carbon preservation: The use of stratified water bodies to compare intrinsic rates of decomposition in oxic and anoxic systems. *Geochimica et Cosmochimica Acta* 56, 3323-3335.
- Lee, C., Wakeham, S.G., 1988. Organic matter in seawater: Biogeochemical processes. In: Riley, J.P. (Ed.), *Chemical Oceanography* 9, Academic Press. pp. 1-51.

- Lee, C, Wakeham, S.G., Hedges, J.I., 2000. Composition and flux of particulate amino acids and chloropigments in equatorial Pacific seawater and sediments. *Deep-Sea Research I* 47, 1535–1568.
- Martin, J.H., Knauer, G.A., Karl, D.M., Broenkow, W.W., 1987. VERTEX: Carbon cycling in the Northeast Pacific. *Deep-Sea Research Part A* 34, 2A, 267-285.
- Mayer, L.M., 1994. Surface area control of organic carbon accumulation in continental shelf sediments. *Geochimica et Cosmochimica Acta* 58, 1271-1284.
- Mayer, L.M., 1999. Extent of coverage of mineral surfaces by organic matter in marine sediments. *Geochimica et Cosmochimica Acta* 63, 207-215.
- McCave, I.N. 1984. Size spectra and aggregation of suspended particles in the deep ocean. *Deep-Sea Research* 31, 329-252.
- Mizutani, T., Nagase, H., Fujiwara, N., Ogoshi, H., 1998. Silicic acid polymerization catalyzed by amines and polyamines. *Bulletin of the Chemical Society of Japan* 71, 2017-2022.
- Noll, F., Sumper, M., Hampp, N., 2002. Nanostructure of diatom silica surfaces and of biomimetic analogs. *Nano Letters* 2, 91-95.
- Oades, J.M., 1988. The retention of organic matter in soils. *Biogeochemistry* 5, 35-70.
- Pilskaln, C.H. and Honjo, S., 1987. The fecal pellet fraction of biogeochemical particle fluxes to the deep sea. *Global Biogeochemical Cycles*, 1, 31-48.
- Ransom, B., Kim, D., Kastner, M., Wainwright, S., 1998. Organic matter preservation on continental slopes: importance of mineralogy and surface area. *Geochimica et Cosmochimica Acta* 62, 1329-1345.
- Sahai, N., 2004. Calculation of ²⁹Si NMR shifts of silicate complexes with carbohydrates, amino acids, and MuHicarboxylic acids: Potential role in biological silica utilization. *Geochimica et Cosmochimica Acta* 68, 227-237.
- Salmon, V., Derenne, S., Lallier-Vergès, E., Largeau, C., Beaudoin, B., 2000. Protection of organic matter by mineral matrix in a Cenomanian black shale. *Organic Geochemistry* 31, 463-474.
- Shanks A.L. and Trent, J.D., 1980. Marine snow: sinking rates and potential role in vertical flux. *Deep-Sea Research* 27, 137-143.
- Suess, E., 1980. Particulate organic carbon flux in the oceans- surface productivity and oxygen utilization. *Nature* 288, 260-263.
- Swift, D.M. and Wheeler, A.P., 1992. Evidence of an organic matrix from diatom biosilica. *Journal of Phycology* 28, 202-209.

- Taylor, G.T., 1982. The role of pelagic heterotrophic protozoa in nutrient cycling: a review. *Annales de l'Institut Océanographique* 58, 227-241.
- Theng, B.K.G., 1974. *Chemistry of Clay-Organic Reactions*. Wiley, New York, 343 pp.
- Theng, B.K.G., Churchman, G.J., Newman, R.H., 1986. The occurrence of interlayer clay-organic complexes in two New Zealand soils. *Soil Science* 142: 262-266.
- Van Veen, J.A., Kuikman, P.J., 1990. Soil structural aspects of decomposition of organic matter by microorganisms. *Biogeochemistry* 11, 213:233.
- Volcani, B.E., 1981. Cell wall formation in diatoms: morphogenesis and biochemistry. In: Simpson, T.L., Volcani, B.E. (Eds.), *Silicon and siliceous structures in biological systems*. Springer-Verlag, New York, pp. 157-200.
- Wakeham, S.G., Hedges, J.I., Lee, C., Peterson, M.L., Hernes, P.J., 1997. Compositions and transport of lipid biomarkers through the water column and surficial sediments of the equatorial Pacific Ocean. *Deep-Sea Research II* 44, 2131-2162.
- Weiner, S., Erez, J., 1984. Organic matrix of the shell of the foraminifer, *Heterostegina depressa*. *Journal of Foramineral Research* 14, 206-212.
- Zimmerman, A.R., Goyne, K.W., Chorover, J., Comarneni, S., Brantley, S.L., 2004. Mineral mesopore effects on nitrogenous organic matter adsorption. *Organic Geochemistry* 35, 355-375.

CHAPTER 2

The Use of Soft X-ray Spectromicroscopy to Investigate the Distribution and Composition of Organic Matter in a Diatom Frustule and a Biomimetic Analog

Abstract

Diatoms are common marine algae that play a significant role in the global carbon cycle through their role in biogenic silica production and the transport of organic matter to the seafloor. Recent work has shown that silicified cell walls, or frustules, of diatoms contain a significant amount of organic matter, and that the proportion of diatom-bound organic matter increases with depth in the water column and sediments. Here we investigate the association between organic matter and the mineral phase. We used a combination of scanning transmission X-ray microscopy (STXM) and carbon X-ray absorption near-edge structure (XANES) spectroscopy to characterize the distribution and composition of organic matter in frustules of the diatom *Cylindrotheca closterium* and a biomimetic silica gel. To our knowledge, this study represents the first successful attempt to simultaneously image and obtain chemical information about the organic matter within a diatom frustule using X-ray spectromicroscopy near the carbon edge. Organic carbon, most likely protein, was distributed throughout the frustules and was not removed by harsh chemical treatment. The physical structure of the frustules appeared to be related to the chemical composition of this organic matter, with aromatic or unsaturated carbon being concentrated in the most intricately patterned regions of the frustule. A similar physical and chemical structure was observed in a biomimetic silica gel precipitated spontaneously with polylysine. These results are consistent with the theory that organic constituents of diatom frustules direct silica precipitation and become incorporated within the silica matrix as it forms. The relationship between organic matter composition and silica morphology, the failure of harsh chemical treatments to remove this organic matter, and the spontaneous nature of the co-precipitation of silica and organic matter indicate some chemical interaction between the siliceous and organic components of diatom frustules. Frustule-bound organic matter should therefore be protected from decomposition in the water column or diagenetic alteration in sediments unless the frustule dissolves.

Keywords: diatom frustules, organic matter, degradation, minerals, preservation

1. Introduction

The ratio of particulate organic carbon to mineral ballast converges to a nearly constant value ($\sim 3\text{-}7$ wt% POC) in particles sinking below 1800 m depth in the ocean, implying a strong association between organic carbon and mineral material (Armstrong et al., 2002; Klaas and Archer, 2002). Diatoms are common marine algae that play a significant role in the global carbon cycle through their role in biogenic silica production and the transport of organic matter to the seafloor. They produce an intricately-patterned silicified cell wall known as a frustule, which itself contains organic constituents that contribute to the export of carbon from the surface ocean. In addition to organic coatings on the outer or inner surfaces of the frustule (Round et al., 1990), some organic matter appears to be bound within the mineral structure itself, comprising up to 0.2 weight% of the shell, or 28 weight% of the entire cell wall (Hecky et al., 1973; Weiner and Erez, 1984). This organic matter consists primarily of silaffins, or proteins with sulfated polysaccharide side-chains (Kröger et al., 1999) as well as some polyamines (Kröger et al., 2000) and sugars (Hecky et al., 1973). It remains even after hydrolysis with HCl or chemical oxidation and is released only upon HF-dissolution of frustules (Swift and Wheeler, 1991; Kröger et al., 1999; Ingalls et al., 2003). Therefore, a substantial fraction of this biomineral-bound organic carbon may be protected from decomposition in the water column and sediments (King, 1974; Robbins and Brew, 1990; Ingalls et al., 2003). Even though this material represents only a small fraction of the total organic carbon in the ocean, it can represent a significant fraction of carbon in siliceous sediments.

Although organic components are known to be present within diatom frustules, their precise location and type of association with the silica frustule have not been characterized. It is not clear whether the organic constituents exist as a layer on the exterior or interior surface of the frustule, or if they are located internally within the frustule itself, dispersed among the silica molecules. Also, the level of chemical interaction between the organic and siliceous components is unknown.

The extent to which organic components of the frustule are protected from decomposition likely depends on the nature of their association with silica. Consequently, understanding this association is important in predicting the contribution of frustule-bound

organic matter to the biological carbon pump. In addition, this information is crucial for the interpretation of paleoceanographic tools such as the use of frustule-bound carbon to measure radiocarbon age in low-carbonate sediments (Ingalls et al. 2004) or the use of frustule-bound nitrogen isotopes as tracers of nutrient availability (Sigman et al. 1999). These techniques rely on the assumption that the organic matter within frustules undergoes no diagenetic alteration following its burial in sediments. Although some of the organic matter in frustules is clearly protected against such modification, it is still not certain how complete this protection is or what level of chemical association it requires.

Previous studies addressing the silicification mechanisms of diatoms provide some clues as to the nature of the association between organic matter and silica in frustules. In the diatom cell, solid deposits of silica are formed in organelles called silica deposition vesicles. As these silica deposits are arranged into the intricate patterning of the frustule, they remain intimately attached to the silicalemma, or membrane covering these vesicles (Li and Volcani, 1984). This suggests that the organic membrane acts as a template for silica deposition, possibly via hydrogen bonding or ionic interaction (Volcani, 1981), or condensation on the hydroxyl groups of serine and threonine (Hecky et al., 1973). Natural proteins and polyamines isolated from HF-dissolved frustules, as well as some synthetic polyamines, are capable of precipitating nanostructured silica when added to solutions of silicic acid, suggesting that the organic constituents of diatom frustules may direct patterns of silica deposition (Mitzutani et al., 1998; Kröger et al., 2000; Noll et al., 2002). This implies some degree of chemical interaction between the silica and organic matter in frustules. Recent studies using ^{29}Si -NMR (e.g., Kinrade et al., 2002; Sahai, 2004) attempted to determine if silicon forms ester or ether-like complexes with organic molecules, but found that the dominant form in diatoms is monosilicic acid.

The objectives of this study were to elucidate 1) how the organic scaffold might influence silica precipitation in diatom frustules and 2) what fraction of the frustule-bound organic matter is protected against chemical attack. Specifically, we examined how organic constituents are distributed throughout the frustule of one diatom species and how this was altered by progressively more stringent levels of chemical attack. The distribution of organic matter entrapped within a silica gel was also investigated to elucidate whether the co-precipitation of organic and inorganic components occurs spontaneously and survives chemical attack. These goals were accomplished using chemical oxidation and hydrolysis

techniques and soft X-ray spectromicroscopy, which simultaneously provided information on the physical structure of diatom frustules as well as the distribution and molecular composition of the organic matter within.

2. Methods

2.1. Sample Preparation

We investigated the distribution and composition of organic matter in diatom frustules and a synthetic silica gel. The diatom *Cylindrotheca closterium* (also known as *Nitzschia closterium*) was selected because it was found to have a thin, spectrally transparent frustule. Attempts were made with other species as well (including several *Coscinodiscus* species and diatomaceous earth samples); however, the thick silica in these diatoms absorbed X-rays too strongly to determine whether carbon was present. *C. closterium* was isolated from a natural seawater sample and identified according to Tomas (1997) and Round et al. (1990). Cells were grown in batch culture (f/2 media with salinity 35.1 psu) at 15°C with a light flux of 100 $\mu\text{mol m}^{-2}\text{s}^{-1}$ in a 16h:8h light:dark cycle. The silica gel was prepared by adding polylysine to a buffered solution of silicic acid and allowing the silica to precipitate overnight. Mizutani et al. (1998), Kröger et al. (1999, 2000, 2002), and Noll et al. (2002) have previously used a similar approach, precipitating silica by adding natural or commercially available silaffins and polyamines to silicic acid. The synthetic silica is referred to here as a “gel” out of convention with previous research; however, it is important to note that the silica gel had more of a solid than gel-like appearance and retained its physical appearance even after drying.

Untreated diatoms were examined by light microscopy (1000X magnification) to determine the general structure of cells. The samples were then subjected to progressively more stringent levels of treatment (a surfactant, mild oxidant, and finally, strong acid) to elucidate the strength of the association between the organic matter and silica. Intracellular and surficial organic matter was first removed from the fresh *C. closterium* cultures (since it would mask spectroscopic signals from the frustule-bound organic matter) by freeze-lysing the diatoms and sonicating them for 30 min in 2:1 (CH₂Cl₂:MeOH). Subsequent cleaning procedures (performed on both the diatoms and gel) included treatment with 30% H₂O₂ overnight and finally, with 6N HCl at 110°C for 20 h. Samples were rinsed three times with Milli-Q water following each cleaning procedure. Finally, each sample was resuspended in

deionized water and a small drop was placed on a Si_3N_4 window (a 100-nm thick transparent film used to mount samples) and allowed to air-dry. This caused the sample to be distributed in a thin layer over the window.

In the initial development of these cleaning procedures, we checked for unrecovered amino acids after the final step (HCl hydrolysis) by performing a second hydrolysis as in Ingalls et al. (2003). Using high-performance liquid chromatography, we did not detect any remaining amino acids, indicating that any material still present was likely bound within the frustule. Upon HF dissolution of diatom frustules (yielding the frustule-bound organic carbon), generally 0.02-0.05% of the total hydrolyzable amino acids associated with the diatoms remains (Ingalls et al., 2003).

Any treatment of the samples with solvents, freeze-lysing, or sonication, unavoidably fractured the thin frustules into small fragments. As discussed by Round et al. (1990), this species has an extremely delicate frustule that is often dissolved by standard cleaning procedures such as treatment in acid. Although it was difficult to determine how specific fragments corresponded to different parts of the intact frustule, this fracturing was an unavoidable necessity, since we needed to clean the frustules as thoroughly as possible. In addition, the fragments were thinner than intact frustules (consisting of part of only one valve, instead of both), providing fine-scale resolution of frustule morphology and organic matter distribution that could not be resolved otherwise. To preserve some intact frustules for examination, an additional sample was prepared by boiling cells in 10% sodium dodecyl sulfate (SDS) for 30 min. and then treating them with 2:1 $(\text{CH}_2\text{Cl}_2:\text{MeOH})$ for 30 min. without sonication. This did not remove organic matter as completely, but at least destroyed most surface coatings. In addition, intact diatoms were examined using scanning electron microscopy (SEM). Klaus Kemp of Microlife Services prepared this sample, and Jim Quinn of Stony Brook University operated the SEM.

2.2. X-ray Spectromicroscopy

“Soft” X-ray spectromicroscopy provides physical and chemical information based on the absorption of low-energy X-rays (100 – 1000 eV) by a sample. In this energy region, and in particular, between the binding energies of *K*-shell electrons in carbon (~290 eV) and oxygen (~560 eV), organic matter shows strong absorption and phase contrast, whereas water is relatively non-absorbing (Jacobsen, 1999). This enables the imaging and chemical

analysis of organic-rich materials. At X-ray photon energies about 10 eV below the absorption edge of carbon (290 eV), or the binding energy required to remove an inner-shell electron, electrons can be promoted to molecular π^* or σ^* orbitals. This produces absorption resonances that depend on the chemical binding state of the atom. X-ray spectromicroscopy is inferior in resolution compared with scanning and transmission electron microscopy, and in chemical specificity compared with high-performance liquid chromatography and nuclear magnetic resonance spectroscopy (Myneni, 2002; Brandes et al., 2004). Nevertheless, its advantage over many other microscopic and chemical analysis techniques is that it provides combined physical and chemical data (Myneni, 2002; Brandes et al., 2004).

The use of soft X-ray spectromicroscopy to investigate the distribution and composition of organic carbon in environmental samples is relatively new. Recent applications have focused on terrestrial or atmospheric materials such as fulvic and humic acids (Myneni, 2002), interplanetary dust (Flynn et al., 2004), and fossil plant cell walls (Boyce et al., 2002). Brandes et al. (2004) applied X-ray spectromicroscopy to organic carbon in marine samples, comparing the distributions of proteins, carbohydrates, lipids, algaenans, acidic compounds, and black carbon in sediment trap samples from the Arabian Sea. Improved statistical techniques have made such spatial and compositional comparisons possible (Lerotic et al. 2004, 2005). Imaging the organic carbon within diatom frustules is extremely difficult, since the organic constituents are so dilute and the oxygen atoms in silica are strongly absorbing of X-rays at low energies, creating a very low signal over the background absorption. To our knowledge, this study represents the first successful attempt to simultaneously image and obtain chemical information about the organic matter within a diatom frustule using X-ray spectromicroscopy near the carbon edge.

The samples were examined by transmission soft X-ray spectromicroscopy at the X-1A beamline (outboard branch) of the National Synchrotron Light Source (NSLS) facility at Brookhaven National Laboratory. At the NSLS, an undulator produces the X-ray beam, which passes through a monochromator and is focused to a spot using Fresnel zone plates at the X-1A beamline (Feser et al., 2001; Flynn et al., 2004). Samples and all microscope components are kept in a helium-filled chamber to prevent CO_2 , O_2 , or N_2 from absorbing X-ray photons (Feser et al., 2000). Further details on X-ray spectromicroscopy, and in

particular, on the operation of the X-1A beamline are provided by Jacobsen (1999), Feser et al. (2001) and Flynn et al. (2004).

Scanning transmission X-ray microscopy (STXM) was used to generate a high-resolution (~ 50 nm) image of each sample. Information on the chemical composition of each sample was obtained simultaneously through X-ray absorption near-edge structure (XANES) spectroscopy near the carbon edge (290 eV). Stacks (series of images taken at different energies) were generally conducted starting at a photon energy of about 280 eV and progressing to about 305 – 310 eV. The X-ray photon energy was increased by 0.1 eV increments in the vicinity of the C edge (from ~ 284 -290 eV) and by 0.2 – 0.5 eV at energies away from the edge to minimize the exposure of the samples to the potentially damaging X-ray beam. Each stack of images was digitally aligned, and XANES spectra were generated by calculating the natural logarithm of the ratio in optical density (absorbance) of the sample and background areas. In addition, the distribution of organic carbon in each sample was determined by calculating a ratio of the optical density of images taken below and at the absorption edge for C. This produced a carbon map highlighting areas showing the greatest change in absorbance near the absorption edge.

STXM images were acquired for 44 *C. closterium* samples (usually above and below the C edge for comparison) and 10 silica gel samples. XANES spectroscopy and carbon mapping were performed on 11 of the diatom samples and 3 of the silica gel samples. Results were consistent among samples; most interesting images are depicted here. A spectrum was also collected for pure sodium silicate to determine if silica could produce any peaks mimicking organic matter. The silica produced a constant absorbance over the energy range used to examine the samples.

2.3. Multivariate Statistical Analyses

The stack data were evaluated using multivariate statistical techniques to roughly assess how the composition of organic matter varied spatially in the samples. These techniques are described in detail by Lerotic et al. (2004, 2005) and will only be summarized here. Each pixel within a sample image can have a slightly unique chemical composition and corresponding XANES spectrum. Principal components analysis (a type of regression analysis) was first used to detect the most common spectral signatures in a sample (e.g., peaks in X-ray absorption at 285 or 288 eV, broad plateaus in absorption after 290 eV, etc.).

Cluster analysis was then used to find natural groupings of similar pixels within the sample image according to the relative weights of the principal components (i.e., spectra) they contained (Brandes et al., 2004; Lerotic et al., 2004). When pixels are grouped according to the absolute amount of each principal component they contain, this can create artifacts arising from variations in sample thickness (i.e., thicker regions have more of each component). To eliminate this problem, the cluster analysis was performed using the angle distance measure technique (Lerotic et al., 2005). This technique groups pixels according to their ratios of the principal components (i.e., relative contribution of each spectrum), irrespective of absolute absorbance (which would depend on thickness).

3. Results and Discussion

3.1. Distribution of Organic Carbon

Observation of untreated *C. closterium* cells by light microscopy revealed fairly uniform pennate cells with long spines on both ends and a total length of $\sim 40 \mu\text{m}$ (Fig. 2.1). Carbon maps of the untreated and cleaned *C. closterium* frustules indicated that carbon was distributed throughout most or all of each frustule fragment, rather than in discrete patches (Fig. 2.2). This observation is consistent with the theory that the organic template is a requirement for silica precipitation and an integral component of the silica matrix. In the SDS-cleaned (Fig. 2.2a) sample, only large-scale patterning could be observed (looking through the two valves of the frustule simultaneously obscured the fine-scale patterning of the sample). In this sample, carbon seemed to be evenly distributed in proportion to thickness, which is indicated by absorbance below the C edge. Thicker (darker) regions in the STXM image corresponded with more C-rich (brighter) regions in the carbon map. Treatment with H_2O_2 revealed the finer-scale patterning of the frustule (Fig. 2.2b). At this scale, carbon mostly appeared to be concentrated in thin, highly patterned regions. In the acid-cleaned (Fig. 2.2c) sample, however, carbon again seemed to be evenly distributed in proportion to thickness. Most likely, hydrolysis of the sample in HCl removed some organic coating that was resistant to H_2O_2 oxidation (and which may have been concentrated in the highly patterned regions with high surface area). This indicates that there were different portions of organic matter (with varying susceptibilities to chemical attack) associated with the frustules. Some organic matter was associated with the internal or external surfaces of the frustule (e.g., as an organic coating or cell wall), but a portion remained even after

chemical oxidation and hydrolysis, suggesting it was present internally within the silica matrix itself.

It is still not clear precisely how organic matter and silica are associated in the frustule, but our results are most consistent with the idea that molecules of organic matter and silica are interspersed throughout the frustule. This is suggested by our observations that organic matter was evenly distributed throughout the frustule, was not completely removed by harsh chemical treatments, and that partial removal of this organic matter resulted in partial dissolution and fracturing of the frustule. If organic matter were present as a discrete layer on the external or internal surface of the frustule, it would probably be more vulnerable to chemical attack, and its removal would not disrupt the structural integrity of the frustule as extensively. As suggested by Li and Volcani (1984), the silicium may be permanently incorporated within the frustule during silica precipitation and become an integral structural component. Since a portion of this organic matter was resistant to chemical attack, it is also likely protected from decomposition in nature. Conversely, silica may be protected from dissolution by the associated organic matter, as previously suggested by Bidle and Azam (1999) and Bidle et al. (2002).

The extent to which silica and organic matter in frustules protect each other from dissolution or decomposition likely depends on other components of the frustule, such as mineral impurities. Previous research (e.g., van Beusekom and Weber, 1995; van Bennekom et al., 1989; van Cappellen and Qiu, 1997) has demonstrated that diatoms sometimes substitute Al for Si in frustules, and that high Al/Si ratios retard frustule dissolution. Consequently, organic matter in frustules with a high Al content may also be protected from decomposition over longer timescales.

The different portions of organic matter associated with the frustule are not necessarily discrete, but may instead be characterized by a continuum of different associations with silica. Rather than having a distinct boundary between the organic portion of the cell wall and silicified frustule, the cell wall may consist of a gradual transition from a less silicified region to a more silicified region. Some of this cell wall material may be vulnerable to chemical attack (e.g., the surface coating that was removed by HCl), whereas some of it may be protected by its association with silica.

3.2. Overall Composition of Organic Carbon

XANES spectra were collected from each sample as a whole to assess the overall composition of biomineral-bound carbon. These spectra displayed resonance peaks near 285 and 288 eV, corresponding to aromatic/ unsaturated and carbonyl structures, respectively, and a broad plateau from about 290-295 eV, which is present in the spectra of all organic compounds and corresponds to the C absorption edge and higher resonances (Fig. 2.3, top line; Müller et al., 1998; Brandes et al., 2004). The carbonyl peak most likely resulted from carboxylic acid in proteins in the frustules (Kaznatcheyev et al., 2002). Comparison of the frustule spectra with the spectrum for pure polylysine, which also displayed a peak at 288 eV, further supports this explanation (Fig. 2.3). Proteins usually exhibit carbonyl peaks between 288.0 and 288.3 eV; the presence of amide bonds shifts the carbonyl peak down in energy by 0.2-0.3 eV compared with pure carboxylic acids (Zubavichus et al., 2004; Brandes et al., 2004). Some samples, however, exhibited slightly higher-energy carbonyl peaks (288.4-288.5 eV) more consistent with free organic acids (Figs. 2.4, 2.5). These proteins may have been comprised mostly of short chains of amino acids with fewer amide bonds.

The unsaturated or aromatic peak at 285 eV may have been produced by the aromatic amino acids phenylalanine, tryptophan, tyrosine, or histidine (which have aromatic side chains) (Kaznatcheyev et al., 2002) or by aromatic polyamines or sugars. Hydrolysates of HF-dissolved diatom frustules are generally depleted in aromatic amino acids (Hecky et al., 1973; Ingalls et al., 2003); however, the presence of the aromatic peak only indicates that such compounds are present, even if in dilute concentrations.

3.3. Spatial Variations in Organic Carbon Composition

Cluster analysis was performed on each sample to detect any spatial heterogeneity in organic compounds within the frustules. Interestingly, different organic constituents appeared to be distributed throughout the frustules in a way that was related to their nanoscale morphology. Figures 2.4-2.7 depict the results of cluster analysis for four samples. The first sample depicted (Fig. 2.4) was freeze-lysed and cleaned with 2:1(CH₂)₂Cl₂:MeOH followed by 30% H₂O₂. The other three samples (Figs. 2.5-2.7) were treated in the same manner followed by hydrolysis in 6N HCl at 110°C for 20h. Each figure consists of a

STXM image of the sample (a), a composite image of all of the clusters detected (b), and an image and XANES spectrum for each cluster (c-g).

Each sample contained 4-5 different types of material, grouped into clusters by their relative proportions of each principal component. In each sample, the background (c) was free of carbon. The thick portion of the frustule (d) contained carbonyl material (indicated by the peak at about 288 eV) and exhibited a dip just before 285 eV. As described in section 3.2, the carbonyl material was most likely composed of protein. It is not clear what produced the dip; it may represent the trailing end of a lower-energy (< 280 eV) peak from another element. Manual integration of this portion of the frustule produced the same feature, indicating that it was not an artifact of cluster analysis.

The thin, highly patterned regions (e) contained unsaturated or aromatic carbon (indicated by the peak at about 285 eV) as well as carbonyl material. These regions are quite rich in unsaturated carbon, with XANES spectra resembling those of pure aromatic amino acids and other aromatic-rich organic compounds (Cody et al., 1998; Kaznatcheyev et al., 2002).

Several additional clusters were apparent. One cluster (f) contained organic material and occasionally (in Figs. 2.4-2.6) a small amount of potassium (indicated by the two peaks at 297.1 and 299.8 eV). Finally, three of the samples (Figs. 2.4-2.6) exhibited a cluster (g) containing organic material and a larger amount of potassium. It is unlikely that this potassium resulted from the incomplete removal of salts, since the samples were rinsed many times using several different solvents and distilled water. Any organic components of the cell not bound inside the frustule (e.g., potassium-rich ion channels or enzymes in the attached cell wall) would probably have been removed by the organic solvents. This material may have been present within some organic component of the frustule, and consequently survived the harsh sample treatments.

It is interesting that although the total distribution of organic matter may have changed slightly with each of the progressively more stringent sample treatments (as shown in the carbon maps), the bulk composition of this organic matter did not change. Both the H₂O₂ (Fig. 2.4) and HCl- cleaned samples (Figs. 2.5-2.7) contained protein and a similar distribution of saturated and unsaturated material, indicating the organic constituents of diatom frustules are protected from chemical attack by electrostatic interactions or physical occlusion in the silica. This is an important finding both for carbon preservation in the

ocean as well as future studies investigating the composition of organic carbon in diatom frustules.

3.3.1. Relationship with Morphological Structures

The relationship between the composition of organic matter and frustule morphology in the samples is consistent with the theory that an organic template (e.g., the silicalemma) directs the precipitation and patterning of silica. The reverse is also possible, that as silica precipitates in different morphological patterns, it entrains different organic compounds. However, since other studies (e.g., Mitzutani et al., 1998; Kröger et al., 2000; Noll et al., 2002) have found evidence that organic composition directs silica deposition, the former explanation appears more likely.

To describe how the chemical composition and morphology of the frustules might be related, the physical structure of diatom frustules must be explained. In addition to their larger scale (on the order of several μm) morphological features such as valves and spines, frustules also contain much smaller scale (on the order of several nm) structures that produce the intricate patterning we observed using STXM. In most diatoms, each valve (“lid”) of the silica frustule is perforated by numerous pores called areolae, which are thought to allow solute exchange across the cell membrane (Tomas, 1997). The complexity of these areolae differs among diatom species. In some species, the areolae are simple holes, while in others they are hollow chambers, with a roof, floor, and walls (Round et al., 1990). In many raphid diatoms (those with a longitudinal slit through the frustule), the pores are covered by a delicate layer of silica perforated by numerous smaller pores (Round et al., 1990). Since *C. closterium* is a raphid diatom, and the structures we observed are consistent with a layer of finely perforated silica covering a larger opening (this is particularly evident in Fig. 2.4), we suggest that the compositional differences we found were located within the areolae.

The thin, finely-patterned regions of the *C. closterium* frustules (Figs. 2.4-2.7e) resemble the perforated roofs covering the pores, whereas the opaque regions of the frustule (Figs. 2.4-2.7d) may correspond to the walls between neighboring pores. Our results suggest that aromatic compounds are located in the perforated roofs of these pores, perhaps directing the elaborate, fine-scale structure of the silica there. The scanning electron microscopy (SEM) image in Fig. 2.8 shows that these pores appear to be distributed

throughout the frustule, including along the raphe (slit in the center of the diatom shown in Fig. 2.8b and c), fibrillae (heavily silicified “buttons” at the top and bottom of Fig. 2.8b), and spine (Fig. 2.8d). In *C. closterium*, the pores are most prevalent between thin siliceous ribs, or costae, subtending the raphe (Round et al., 1990) (e.g., see the criss-cross pattern apparent in the lower half of Fig. 2.8b), indicating that most of the samples were likely from this region. In these images, the fine-scale surface structure of the pores (i.e., the finely-patterned lid) could not be resolved since they were obscured by the gold coating.

Assuming that organic constituents of diatom frustules do direct silica deposition, these findings suggest that variations in the composition of this organic matter control nanoscale variations in frustule morphology. This is consistent with the mechanism of silica deposition proposed by Kröger et al. (2000), who argued that interactions between species-specific polyamines and silica-precipitating proteins control the frustule morphologies of different diatom species. Furthermore, the results of this study suggest that these compositional variations not only control morphological differences among species of diatoms, but within the frustule of a single diatom.

If silica molecules are deposited on an organic template, they must do so through chemical interaction with these organic components. More likely, this occurs via electrostatic attraction, since little evidence has been found for the formation of covalent organo-silicon complexes (Kinrade et al., 2002; Sahai, 2004).

3.3.2. *Alternative Explanations*

The exposure of organic matter to high radiation doses can result in beam damage, or a loss of mass and change in the apparent composition of organic matter in a sample (Williams et al., 1993; Zhang et al., 1995; Müller et al., 1998; Beetz and Jacobsen, 2003). Beam damage is an unlikely explanation for the compositional variations observed, however, since the radiation doses to samples in this study were approximately 10^6 Gy, which is below the threshold for observable mass loss in dry biological specimens (Williams et al., 1993). Also, stacks were always conducted starting at lower energies and moving to higher energies to minimize radiation doses at the lower-energy end of the spectrum (280-290 eV). Using the same radiation doses on the same microscope, Kaznatcheyev et al. (1992) found no evidence of beam damage to amino acids, the dominant material in the samples investigated in this study. Also, when beam damage causes a shift towards lower energies, this normally

results in the production of several lower-energy peaks (most noticeably around 286.5 eV), as opposed to a single peak at 285 eV (Zhang et al., 1995). Nevertheless, beam damage tests were performed on 5 samples; the results of one of these are shown in Fig. 2.9. The beam was focused on small regions within a H₂O₂-cleaned sample and the shutter was opened, allowing full exposure to the X-ray beam. A short stack was then taken over a larger region of the sample. Finally, cluster analysis was used to determine if the composition of organic matter differed in the small areas exposed to the beam as compared with the surrounding region.

The samples contained two clusters (d and e) that were practically indistinguishable, each containing carbonyl carbon and possibly a small amount of unsaturated or aromatic carbon. The samples did not exhibit any variation in the vicinity of the area subjected to beam damage. This suggests that natural variations in organic matter concentrations, rather than beam damage, produced the observed variations in optical density. This sample was similar in structure to the image shown in Fig. 2.5, and had approximately the same baseline absorbance ($-\ln I/I_0 = 0.4$ eV) before correction to zero, indicating these two samples were of comparable thicknesses. Therefore, the sample used in the beam damage test is considered representative of the other samples.

Finally, it is also unlikely that contamination of the samples could have produced the apparent patterns in the presence of unsaturated or aromatic material. Contaminants would have adsorbed onto all regions to some extent (even if they were preferentially concentrated in some regions), but many regions did not contain any of this material. It is possible that the aromatic compounds observed in the pores were an artifact of treatment (e.g., hydrophobic compounds coalescing in a small space due to exposure to aqueous solvents). However, if these compounds were not bound within the silica, we would expect to see at least a small amount present in the background. We checked for any unrecovered amino acids following treatment, and are confident that the rigorous cleaning procedures performed (sonicating in 2:1 MeCl₂:MeOH, oxidation with H₂O₂, followed by hydrolysis in 6N HCl, rinsing 3X in distilled water after each step) removed any organic matter not bound within the silica.

3.4. Comparison between Diatom Frustules and Biomimetic Silica Gel

The morphological and chemical properties of the synthetic silica gel were similar to those of the diatom frustules (compare Fig. 2.10 with Figs. 2.4-2.7). Also, the fine-scale morphology of the frustules and gel appear to be consistent with the general nanostructure of biogenic silica observed under scanning electron and atomic force microscopy by previous researchers (Kröger et al., 2002; Noll et al., 2002; Sumper, 2002). XANES analysis of the gel indicated that it contained organic matter (primarily carboxyl carbon), consistent with lysine incorporation. A XANES spectrum of the pure silicic acid used to prepare the gel did not reveal any organic peaks, indicating that the peaks observed in the gel were produced by the polylysine added, and not by contamination. The morphological and chemical similarities between the gel and frustules support the hypothesis that organic compounds direct the precipitation of silica in diatom frustules.

Furthermore, since treatment of the gel with H₂O₂ and 6N HCl failed to remove at least part of this organic matter, it would appear that the polylysine did not merely catalyze silica precipitation, but became incorporated within the gel as it formed. This is a tentative conclusion, since the results of subsequent experiments (unpublished) suggest that a large fraction of polylysine eventually diffuses out of the gel or is released by dissolution of the silica (losses of ~60-75% after 3 days, and ~88-98% after 84 days were observed).

4. Conclusions

Soft X-ray spectromicroscopy is a promising technique with a variety of applications in environmental science. The use of this technique in conjunction with multivariate statistical analyses can help elucidate spatial variations in the composition of organic matter in natural samples.

The results of this study are consistent with the theory that the organic constituents of diatom frustules direct their nanoscale patterning, and that this organic matter is protected from chemical attack once incorporated in the shell. The relationship between organic matter composition and silica morphology, the failure of harsh chemical treatments to remove all of this organic matter, and the spontaneous nature of the co-precipitation of silica and organic matter indicate some level of chemical interaction between the siliceous and organic components of diatom frustules. Although some surface coatings or cell wall material may be subject to chemical attack, this biomineral-bound organic matter should be

protected against decomposition until the mineral dissolves. Furthermore, paleoceanographic techniques using diatom-bound organic matter as proxies of past environmental changes should be extremely reliable.

References

- Armstrong, R.A., Lee, C., Hedges, J.I., Honjo, S., Wakeham, S.G., 2002. A new, mechanistic model for organic carbon fluxes in the ocean based on the quantitative association of POC with ballast minerals. *Deep-Sea Research II* 49, 219-236.
- Beetz, T., Jacobsen, C., 2003. Soft X-ray radiation-damage studies in PMMA using a cryo-STXM. *Journal of Synchrotron Radiation* 10, 280-283.
- Bidle, K., Azam, F., 1999. Accelerated silica dissolution by marine bacterial assemblages. *Nature* 397, 508-512.
- Bidle, K., Manganello, M., Azam, F., 2002. Regulation of ocean silicon and carbon preservation by temperature control on bacteria. *Science* 298, 1980-1984.
- Boyce, C., Cody, G., Feser, M., Jacobsen, C., Knoll, A., Wirick, S., 2002. Organic chemical differentiation within fossil plant cell walls detected with X-ray spectromicroscopy. *Geology* 30, 1039-1042.
- Brandes, J.A., Lee, C., Wakeham, S., Peterson, M., Jacobsen, C., Wirick, S., Cody, G., 2004. Examining marine particulate organic matter at sub-micron scales using scanning transmission X-ray microscopy and carbon X-ray absorption near edge structure spectroscopy. *Marine Chemistry* 92, 107-121.
- Cha, J.N., Shimizu, K., Zhou, Y., Christiansen, S.C., Chmelka, B.F., Stucky, G.D., Morse, D.E., 1999. Silicatein filaments and subunits from a marine sponge direct the polymerization of silica and silicones in vitro. *Proceedings of the National Academy of Sciences* 96, 361-365.
- Cody, G.D., Ade, H., Wirick, S., Mitchell, G.D., Davis, A., 1998. Determination of chemical-structural changes in vitrinite accompanying luminescence alteration using C-NEXAFS analysis. *Organic Geochemistry* 28, 441-455.
- Feser, M., Beetz, T., Carlucci-Dayton, M., Jacobsen, C., 2000. Instrumentation advances and detector development with the Stony Brook scanning transmission X-ray microscope. In: *X-ray Microscopy: Proceedings of the Sixth International Conference* (eds. W. Meyer-Ilse, A. Warwick and D.T. Attwood). American Institute of Physics, Melville, New York. pp. 367-372. (Also available at <http://xray1.physics.sunysb.edu/research/publications.php>)
- Feser, M., Beetz, T., Carlucci-Dayton, M., Jacobsen, C., 2001. Scanning transmission soft X-ray microscopy at beamline X-1A at the NSLS - advances in instrumentation and selected applications. In: *Soft X-ray and EUV Imaging Systems II* (eds. D.A. Tichenor and J.A. Folta). Society of Photo-Optical Instrumentation Engineers, Bellingham, Washington. pp. 146-153. (Also available at <http://xray1.physics.sunysb.edu/research/publications.php>)

- Flynn, G.J., Keller, L.P., Jacobsen, C., Wirick, S., 2004. An assessment of the amount and types of organic matter contributed to the Earth by interplanetary dust. *Advances in Space Research* 33, 57-66.
- Hecky, R.E., Mopper, K., Kilham, P., Degens, E.T., 1973. The amino acid and sugar composition of diatom cell-walls. *Marine Biology* 19, 323-331.
- Ingalls, A.E., Lee, C., Wakeham, S.G., Hedges, J.I., 2003. The role of biominerals in the sinking flux and preservation of amino acids in the Southern Ocean along 170°W. *Deep-Sea Research II* 50, 709-734.
- Ingalls, A.E., Anderson, R.F., Pearson, A., 2004. Radiocarbon dating of diatom-bound organic compounds. *Marine Chemistry* 92, 91-105.
- Jacobson, C., 1999. Soft X-ray microscopy. *Trends in Cell Biology* 9, 44-47.
- Kaznacheyev, K., Osanna, A., Jacobsen, C., Plashkevych, O., Vahtras, O., Ågren, H., Carravetta, V., Hitchcock, A.P., 2002. Innershell absorption spectroscopy of amino acids. *Journal of Physical Chemistry A* 106, 3153-3168.
- King, K.J., 1974. Preserved amino acids from silicified protein in fossil Radiolaria. *Nature* 252, 690-692.
- Kinrade, S.D., Gillson, A.M.E., Knight, C.T.G., 2002. Silicon-29 NMR evidence of a transient hexavalent silicon complex in the diatom *Navicula pelliculosa*. *Journal of the Chemical Society – Dalton Transactions* 3, 307-309.
- Klaas, C., Archer, D. E., 2002. Association of sinking organic matter with various types of mineral ballast in the deep sea: Implications for the rain ratio. *Global Biogeochemical Cycles* 16, 1116, doi:10.1029/2001GB001765.
- Kröger, N., Deutzmann, R., Sumper, M., 1999. Polycationic peptides from diatom biosilica that direct silica nanosphere formation. *Science* 286, 1129-1132.
- Kröger, N., Deutzmann, R., Bergdorf, C., Sumper, M., 2000. *Proceedings of the National Academy of Sciences* 97, 14133-14138.
- Kröger, N., Lorenz, S., Brunner, E., Sumper, M., 2002. Self-assembly of highly phosphorylated silaffins and their function in biosilica morphogenesis. *Science* 298, 584-586.
- Lerotic, M., Jacobsen, C., Gillow, J.B., Francis, A.J., Wirick, S., Vogt, S., Maser, J., 2005. Cluster analysis of soft X-ray spectromicroscopy: finding the patterns in complex specimens. *Journal of Electron Spectroscopy and Related Phenomena* 144-147C, 1137-1143. (Also available at <http://xray1.physics.sunysb.edu/research/publications.php>)

- Lerotic, M., Jacobsen, C., Schäfer, T. Vogt, S., 2004. Cluster analysis of soft X-ray microscopy data. *Ultramicroscopy* 100, 35-57.
- Li, C.W., Volcani, B.E., 1984. Aspects of silicification in wall morphogenesis of diatoms. *Philosophical Transactions of the Royal Society of London B* 304, 519-528.
- Martin-Jézéquel, V., Hildebrand, M. Brzezinski, M.A., 2000. Silicon metabolism in diatoms: implications for growth. *Journal of Phycology* 36, 821-840.
- Mitzutani, T., Nagase, H., Fujiwara, N., Ogoshi, H., 1998. Silicic acid polymerization catalyzed by amines and polyamines. *Bulletin of the Chemical Society of Japan* 71, 2017-2022.
- Müller, H.U., Zharnikov, M., Völkel, B., Schertel, A., Harder, P., Grunze, M., 1998. Low-energy electron-induced damage in hexadecanethiolate monolayers. *Journal of Physical Chemistry B* 102, 7949-7959.
- Myneni, S.C.B., 2002. Soft X-ray spectroscopy and spectromicroscopy studies of organic molecules in the environment. In: Fenter, P., Rivers, M., Sturchio, N., Sutton, S (Eds.), *Reviews in Mineralogy and Geochemistry* 49, Applications of Synchrotron Radiation in Low-Temperature Geochemistry and Environmental Science, pp. 485-571.
- Noll, F., Sumper, M., Hampp, N., 2002. Nanostructure of diatom silica surfaces and of biomimetic analogs. *Nano Letters* 2, 91-95.
- Robbins, L.L., Brew, K., 1990. Proteins from the organic matrix of core-top and fossil planktonic foraminifera. *Geochimica et Cosmochimica Acta* 54, 2285-2292.
- Round, F.E., Crawford, R.M., Mann, D.G., 1990. *The Diatoms: Biology and Morphology of the Genera*. Cambridge University Press, Cambridge, England.
- Sahai, N., 2004. Calculation of ^{29}Si shifts of silicate complexes with carbohydrates, amino acids, and MuHicarboxylic acids: potential role in biological silica utilization. *Geochimica et Cosmochimica Acta* 68, 227-234.
- Sigman, D.M., Altabet, M.A., Francois, R., McCorkle, D.C., Gaillard, J.F., 1999. The isotopic composition of diatom-bound nitrogen in Southern Ocean sediments. *Paleoceanography* 14, 118-134.
- Sigman, D.M., Boyle, E.A., 2000. Glacial/interglacial variations in atmospheric carbon dioxide. *Nature* 407, 859-869.
- Sumper, M., 2002. A phase separation model for the nanopatterning of diatom biosilica. *Science* 295, 2430-2433.
- Swift, D.M. and Wheeler, A.P., 1992 Evidence of an organic matrix from diatom biosilica. *Journal of Phycology* 28, 202-209.

- Tomas, C.R. (ed.), 1997. Identifying Marine Phytoplankton. Academic Press, San Diego.
- van Bennekom, A.J., Jansen, J.H.F., van der Gaast, S.J., van Iperen, J.M., Pieters, J., 1989. Aluminum-rich opal: an intermediate in the preservation of biogenic silica in the Zaire (Congo) deep-sea fan. *Deep-Sea Research* 36, 173-190.
- van Beusekom, J.E.E., Weber, A., 1995. Der einfluß von aluminium auf das wachstum und die entwicklung von kieselalgen in der Nordsee. *Deutsche Hydrographische Zeitschrift (German Journal of Hydrography) Supplement* 5. Hamburg and Rostock, Germany, pp. 213-220.
- van Cappellen, P., Qiu, L., 1997. Biogenic silica dissolution in sediments of the Southern Ocean. I: Solubility. *Deep-Sea Research II* 44, 1109-1128.
- Volcani, B.E., 1981. Cell wall formation in diatoms: morphogenesis and biochemistry. In: Simpson, T.L., Volcani, B.E. (Eds.), *Silicon and siliceous structures in biological systems*. Springer-Verlag, New York, pp. 157-200.
- Weiner, S., Erez, J., 1984. Organic matrix of the shell of the foraminifer, *Heterostegina depressa*. *Journal of Foramineral Research* 14, 206-212.
- Williams, S., Zhang, X., Jacobsen, C., Kirz, J., Lindaas, S., Van't Hof, J., Lamm S.S., 1993. Measurements of wet metaphase chromosomes in the scanning transmission x-ray microscope. *Journal of Microscopy* 170, 155-165.
- Zhang, X., Jacobsen, C., Lindaas, S., Williams, S., 1995. Exposure strategies for polymethyl methacrylate from in situ x-ray absorption near edge structure spectroscopy. *Journal of Vacuum Science and Technology B* 13, 1477-1483.
- Zubavichus, Y., Fuchs, O., Weinhardt, L., Heske, C., Umbach, E., Denlinger, J.D., Grunze, M., 2004. Soft X-Ray-Induced Decomposition of Amino Acids: An XPS, Mass Spectrometry, and NEXAFS Study. *Radiation Research* 161, 346-358.



Figure 2.1. Image of untreated *C. closterium* cells observed under 1000X magnification using light microscopy. The diatoms were $\sim 15 \mu\text{m}$ pennate cells with long spines on either end, resulting in a total length of $\sim 40 \mu\text{m}$. Valvar (looking down on one valve, or “lid” of the frustule) and apical (looking down on one side of the frustule, where the two valves intersect) planes of view are indicated by crossbars.

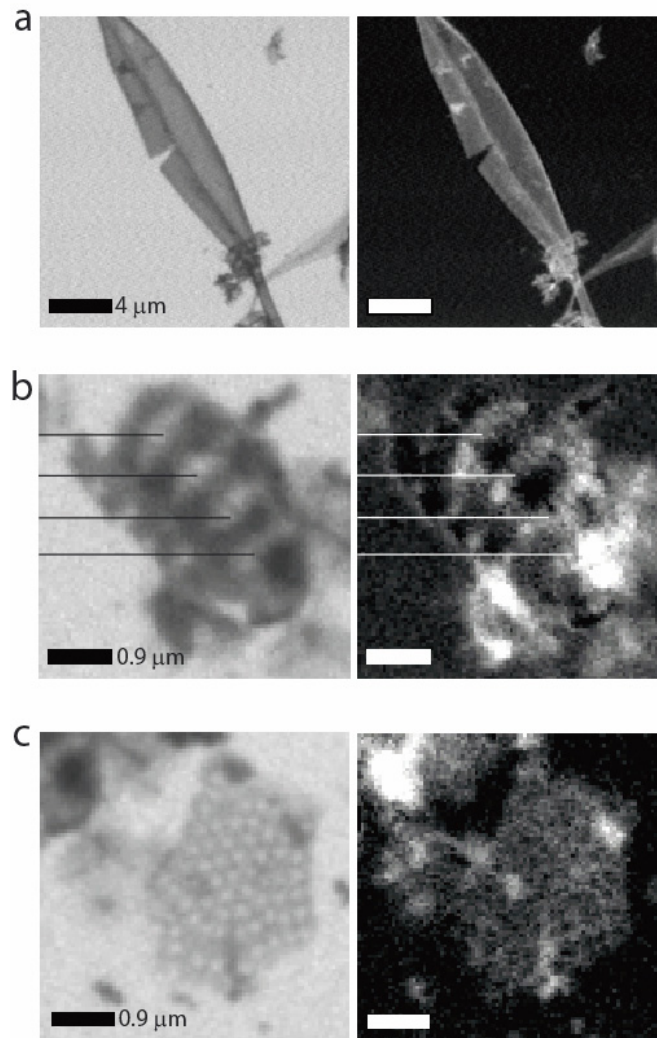


Figure 2.2. Carbon maps of *Cylandrotheca closterium* frustules. The left panels are images of the samples observed under STXM and the right panels are carbon maps. In the carbon maps, the distribution of organic carbon (shown in white) was obtained by taking the ratio of images acquired at different energies (280-283 vs. 293-296 eV) and mapping out the areas that exhibited the greatest change in absorbance just below the carbon absorption edge (290 eV). a: Whole frustule boiled in 10% SDS followed by 2:1 (CH)₂Cl₂:MeOH. Carbon loadings (indicated by brightness in carbon map) appear to be proportional to sample thickness. b: Fragment produced by freeze-lysing diatoms and then cleaning them with 2:1(CH)₂:MeOH followed by 30% H₂O₂. The elongated, curved appearance of this fragment suggests that it may have originally been located at the intersection of the valvar (surface, or looking down on one valve) and apical (side) planes of view of the frustule (see box in Fig. 2.1). Lines are provided to indicate alignment of features. Thin, patterned regions (pointed out by lines) appear to have high carbon content. c: Fragments prepared as in sample b and then hydrolyzed in 6N HCl. As in a, carbon loadings appear to be proportional to sample thickness.

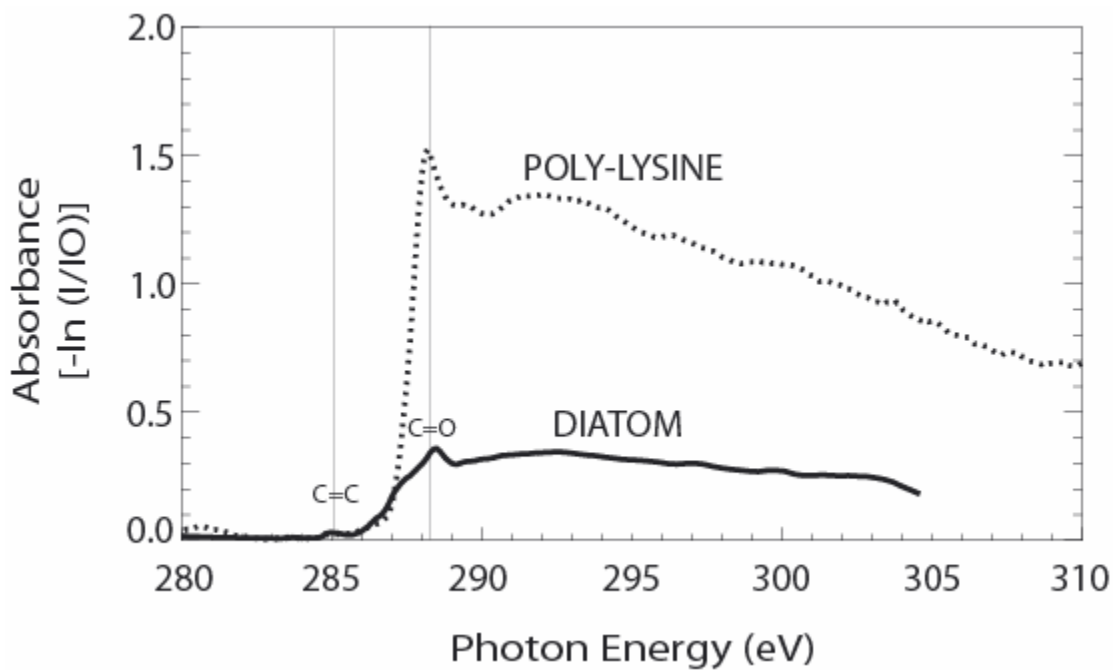


Figure 2.3. XANES carbon spectrum of *C. closterium* frustule (cleaned with 2:1(CH₂)₂Cl₂:MeOH and H₂O₂) compared with that of a pure polylysine standard. Presence of carbonyl peak (denoted by C=O) in both samples suggests chemical similarity between polylysine and the organic matter present in the diatom frustule. The x-axis is X-ray energy (eV) and the y-axis is -ln of the ratio in absorbance of the sample (I) and background (IO).

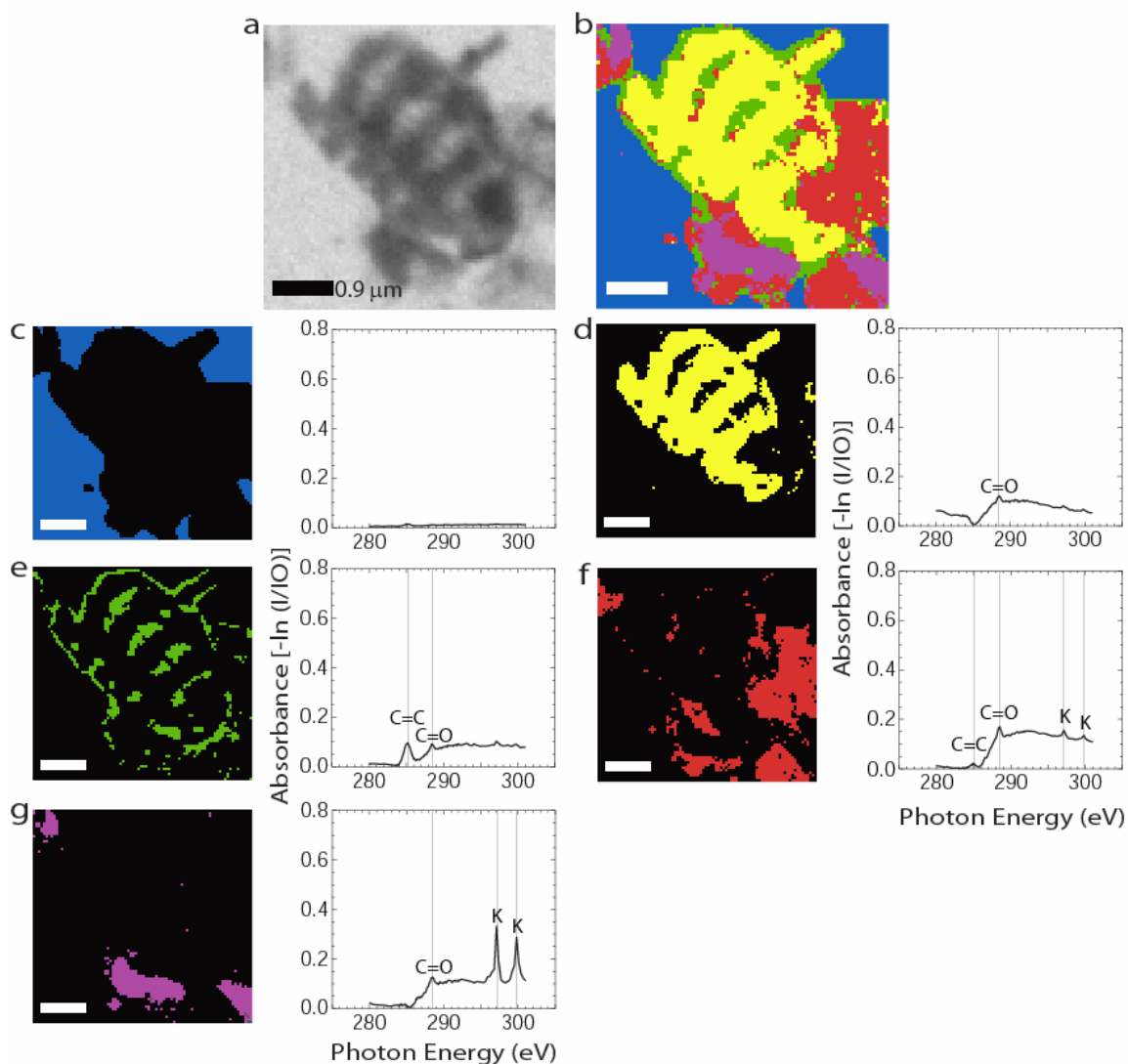


Figure 2.4. Results of cluster analysis on fragment of *C. closterium* frustule. Sample was freeze-lysed and cleaned with 2:1(CH₂)₂Cl₂:MeOH followed by 30% H₂O₂. The top left panel (a) is an image of the sample observed under STXM. The top right panel (b) depicts the clusters detected by cluster analysis. Five clusters were apparent. Images of each cluster are provided (c-g) with XANES spectra to right. The background (c) contained no carbon. The thick, solid regions of the frustule (d) contained carbonyl material (denoted by C=O). The thin, highly patterned regions (e) contained unsaturated or aromatic carbon (denoted by C=C) as well as carbonyl material. An additional cluster was present containing organic material, possibly with a small amount of potassium (f). A fifth cluster was present containing organic material and a larger amount of potassium (g). The x-axis is X-ray energy (eV) and the y-axis is $-\ln$ of the ratio in absorbance of the sample (I) and background (IO).

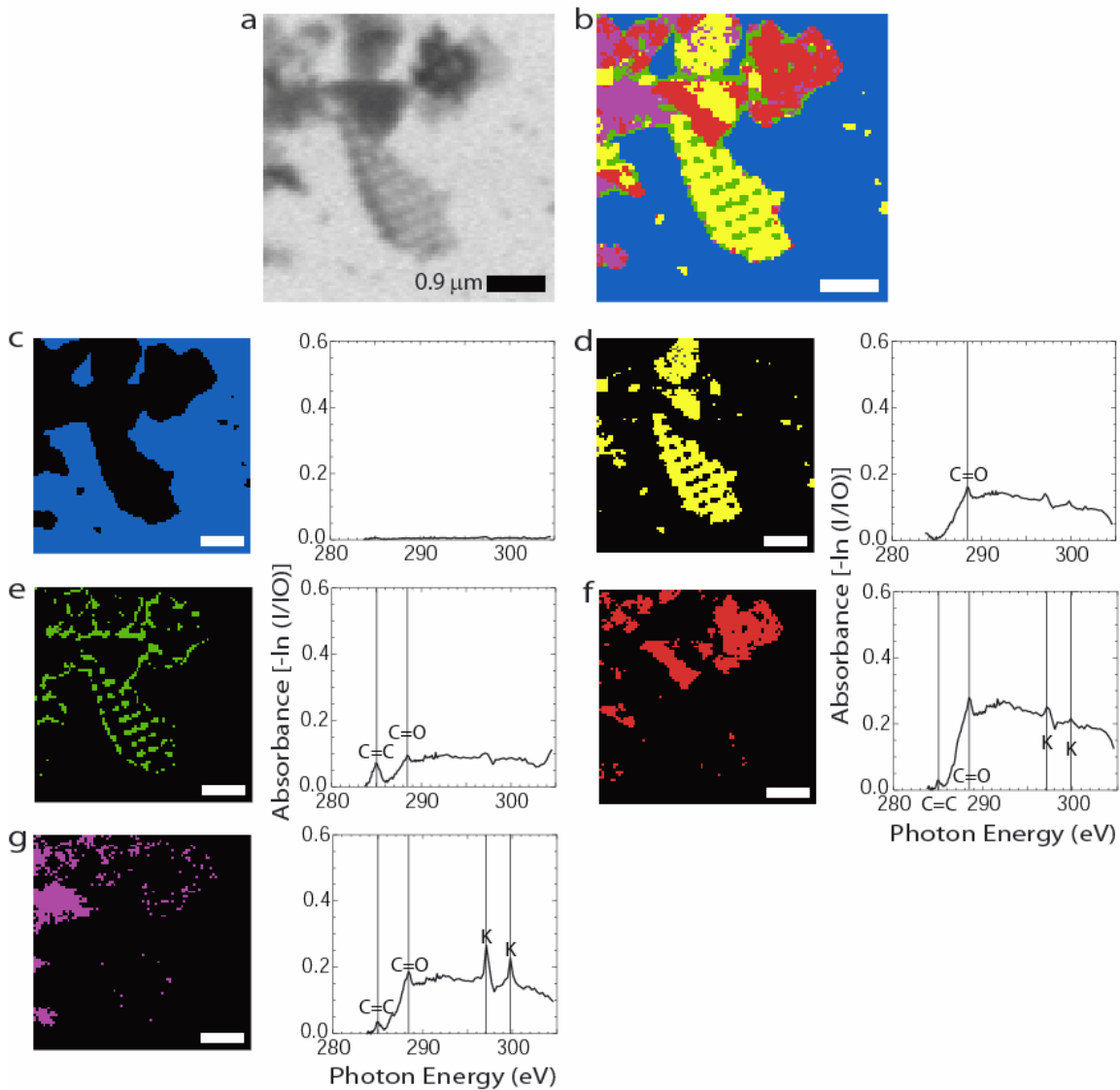


Figure 2.5. Results of cluster analysis on fragments of *C. closterium* frustule. The flat appearance of the fragments suggest that they may have originally part of one of the valves of the frustule (see box in Fig. 2.1). Sample was freeze-lysed, cleaned with 2:1(CH₂)₂Cl₂:MeOH, with 30% H₂O₂, and finally, hydrolyzed in 6N HCl at 110°C for 20 h. Panels (a-g) are as described in Fig. 2.4.

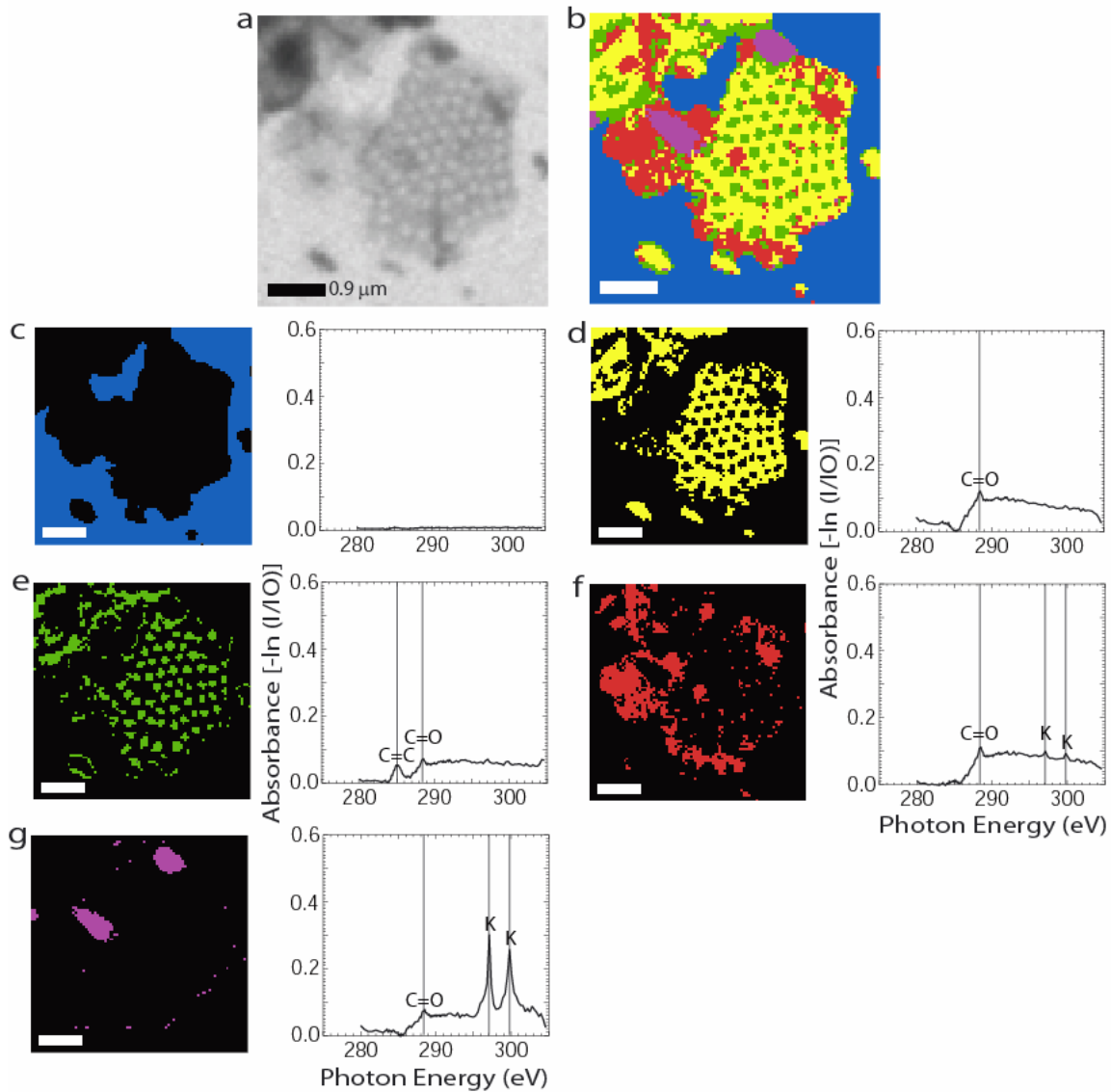


Figure 2.6. Results of cluster analysis on fragments of *C. closterium* frustule. Sample was freeze-lysed, cleaned with 2:1(CH₂)₂Cl₂:MeOH, with 30% H₂O₂, and finally, hydrolyzed in 6N HCl at 110°C for 20 h. Panels (a-g) are as described in Fig. 2.4.

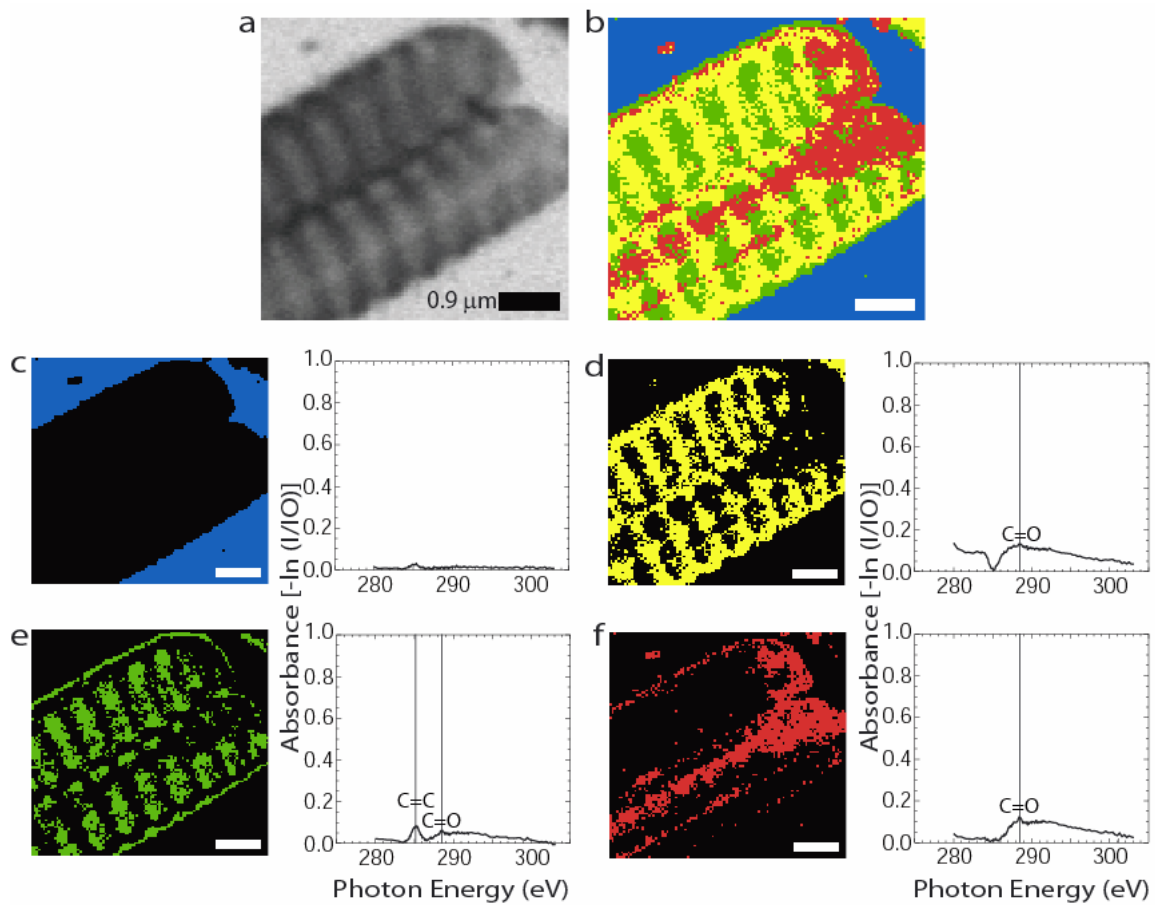
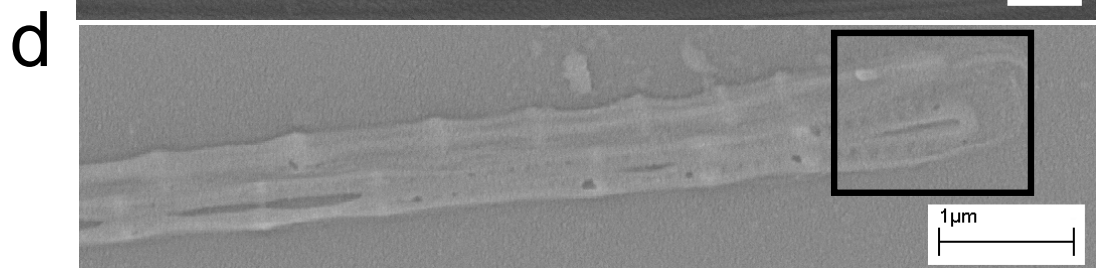
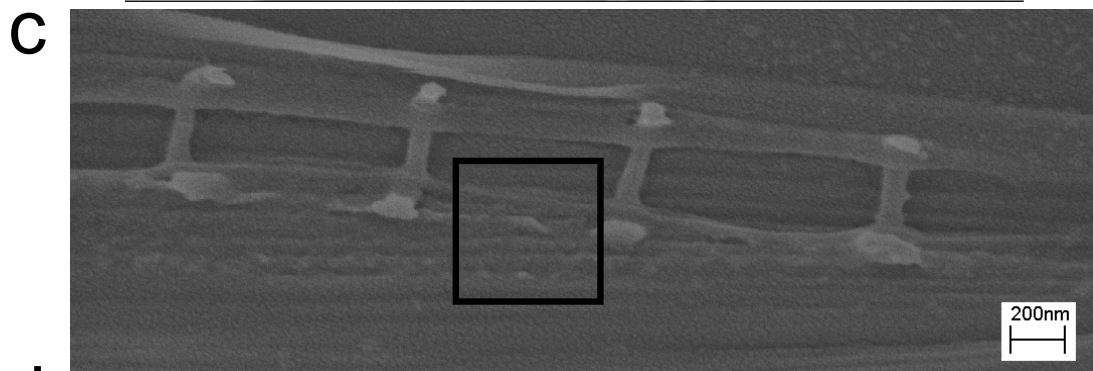
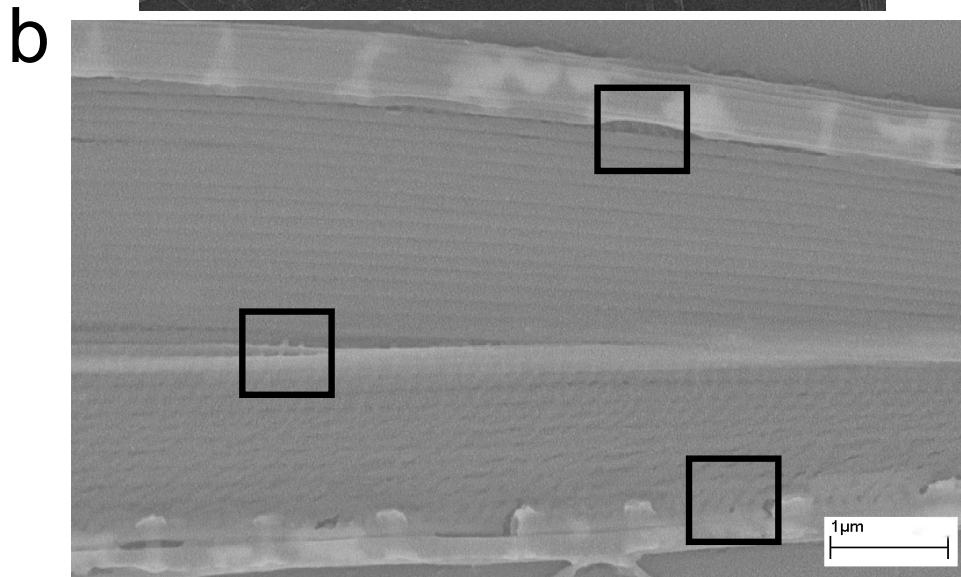
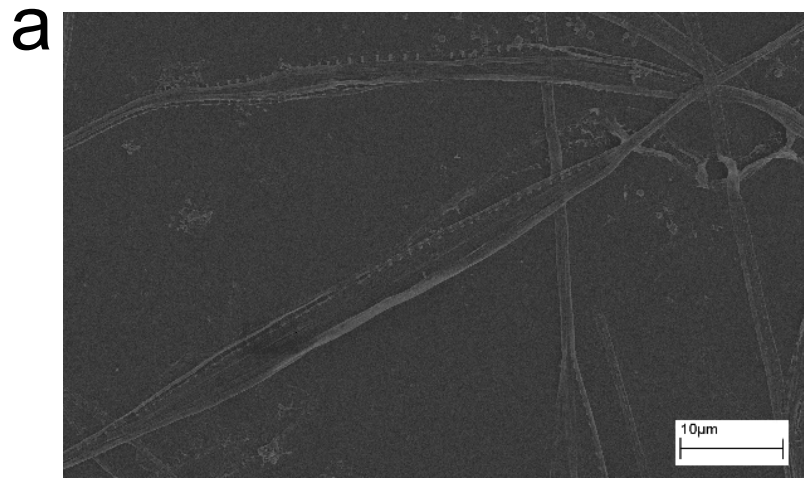


Figure 2.7. Results of cluster analysis on fragment of *C. closterium* frustule. Sample was freeze-lysed, cleaned with 2:1(CH₂)₂Cl₂:MeOH, with 30% H₂O₂, and finally, hydrolyzed in 6N HCl at 110°C for 20 h. Panels (a-f) are as described in Fig. 2.4.

Figure 2.8. SEM images of *C. closterium*. a) Overview of a cell taken at 5000x magnification. b) Image taken at 50,000x magnification showing small pores located along fibrulae (heavy silicified “buttons” at top and bottom of image and raphe (slit in center of frustule), indicated with boxes. Criss-cross pattern throughout the lower portion of the frustule may also be due to presence of pores. c) Image taken at 100,000x magnification showing pores along raphe. d) Image taken at 50,000x showing pores at the end of the spine. Pores were present throughout both spines.



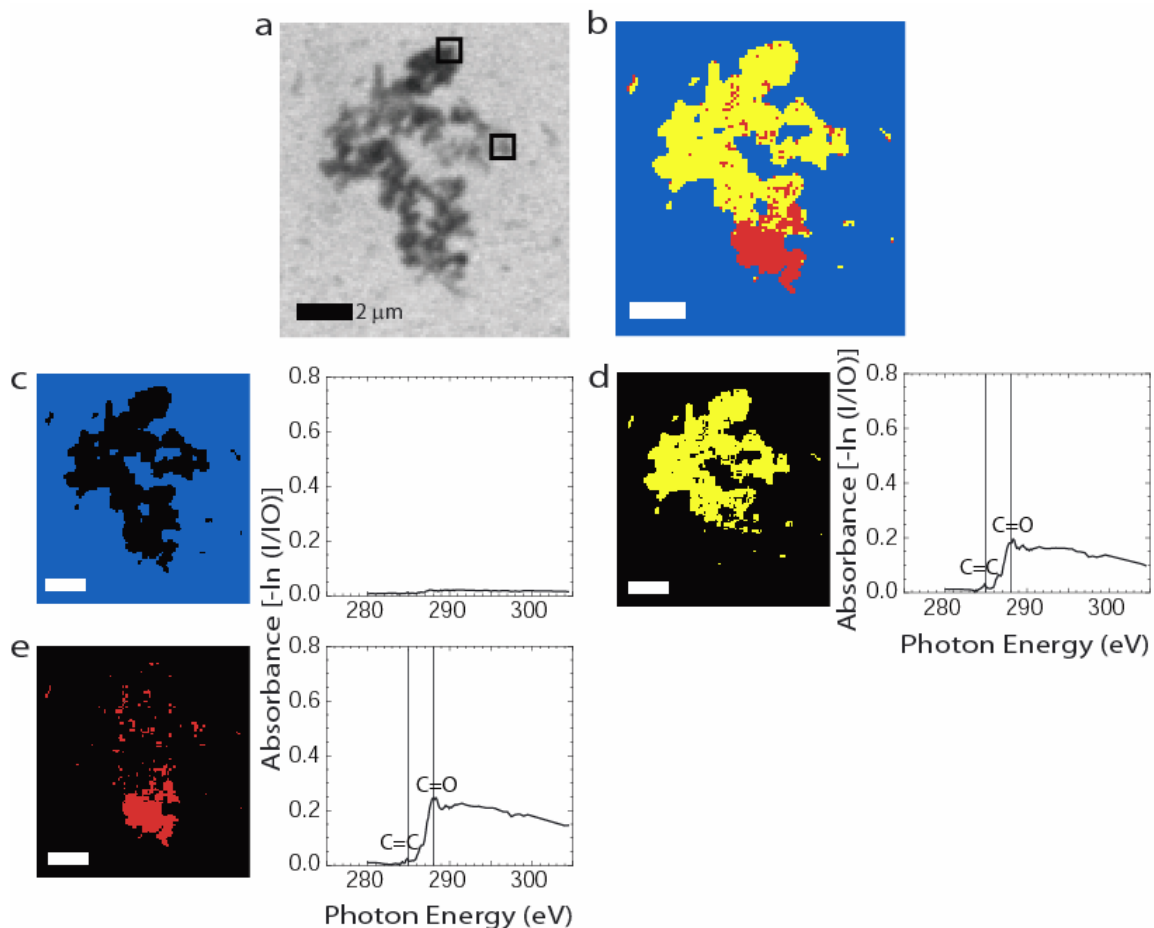


Figure 2.9. Beam damage test on fragment of *C. closterium* frustules. Sample was freeze-lysed and then cleaned with 2:1(CH)₂Cl₂:MeOH followed by 30% H₂O₂. Top left panel (a) depicts an image of the sample observed under STXM. Boxes indicate regions subjected to beam damage (area where shutter was opened, allowing full exposure to beam). Top right panel (b) depicts clusters detected by cluster analysis. Three clusters were apparent. Images of each cluster are provided (c-f) with XANES spectra to right. The background (c) contained no carbon. Two clusters (d and e) were very similar, primarily containing carbonyl carbon with some unsaturated or aromatic carbon. X-axis depicts X-ray energy (eV) and y-axis depicts $-\ln$ of the ratio in absorbance of the image (I) and background (IO).

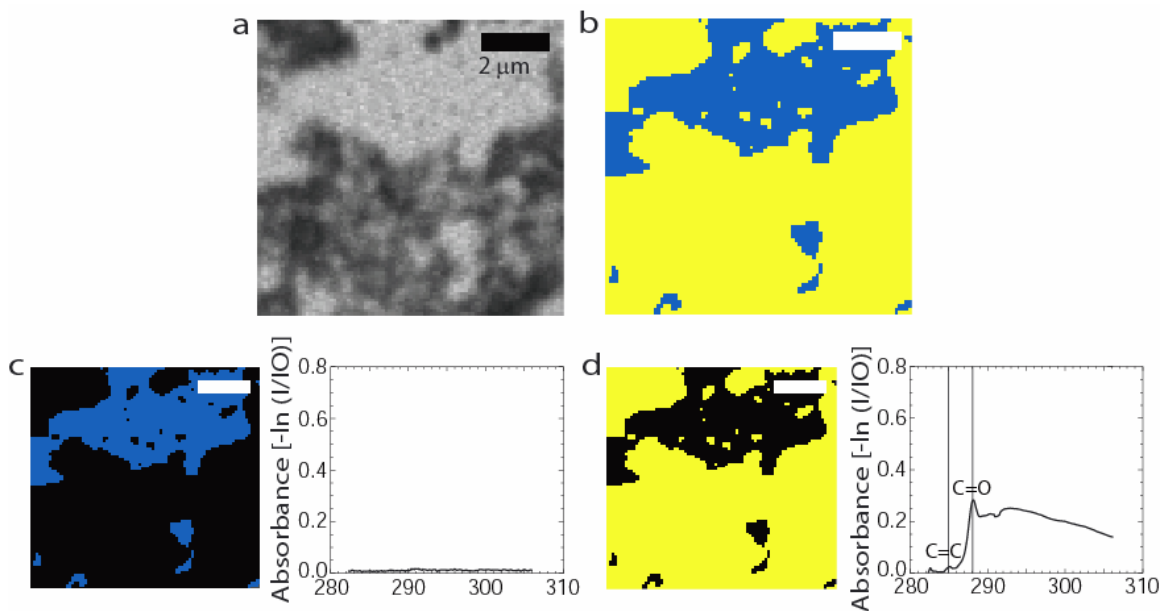


Figure 2.10. Results of cluster analysis on synthetic silica gel prepared by adding polylysine to a buffered solution of silicic acid. Following preparation, the sample was cleaned with 30% H_2O_2 and then hydrolyzed in 6N HCl. The top left panel (a) is an image of the sample observed under STXM and the top right (b) depicts the clusters detected by cluster analysis. Two clusters were apparent. Images of each cluster are provided (c-d) with XANES spectra to right. The background (c) contained no carbon. The gel (d) contained carbonyl material and possibly a small amount of unsaturated or aromatic carbon. The x-axis is X-ray energy (eV) and the y-axis is $-\ln$ of the ratio in absorbance of the sample (I) and background (IO).

CHAPTER 3

Organic Composition of *In Situ* Pump and Sediment Trap Samples: Implications for the Exchange of Material between Suspended and Sinking Particles

Abstract

The extent to which sinking particles disaggregate and exchange with surrounding material affects the efficiency of POC export to the deep sea. In 2003 and 2005, as part of the MedFlux project, we compared the pigment and amino acid compositions of sediment trap and *in situ* pump samples collected in the northwest Mediterranean Sea to assess exchange between sinking and suspended particles. The organic compound compositions of these two sample types were very different and remained consistently so with depth, suggesting exchange was limited at this site. Sinking particles appeared to be largely made up of fecal pellets and some phytoplankton aggregates, and were enriched in biogenic silica indicators. Suspended particles appeared to be more enriched in fresh phytoplankton containing biogenic calcium carbonate indicators. During the summer of 2003, the contribution of fecal pellet indicators to sinking particles was lower, and the contribution of microbial degradation products to both suspended and sinking particles was higher, indicating greater exchange during periods of low flux, when fecal pellets are not abundant. Spring particle fluxes at this site appear to be characterized by the unidirectional transfer of suspended algae into sinking fecal pellets; once this occurs, particles are rapidly exported to depth without undergoing appreciable disaggregation and exchange with the suspended pool. Decomposition certainly must occur within sinking particles, but would likely be far more extensive without this efficient export process. The lack of exchange between fecal pellets and suspended particles indicates that fecal pellet production is very important in POC fluxes at this location, contributing to the drawdown of atmospheric CO₂ and supply of energy to the benthos.

1. Introduction

The export of organic carbon from the surface ocean to the deep sea is largely mediated by the flux of sinking particles, which accounts for 50-80% of the vertical flux of carbon through the mesopelagic zone (Gardner, 2000; Baliño et al., 2001; Fasham et al., 2001). Heterotrophic remineralization of this particulate organic carbon (POC) in the open ocean is usually very efficient, as >90% of the POC produced in surface waters is returned to inorganic form in the euphotic zone or during transit through the water column. However, a small fraction of the organic matter produced in surface waters survives transit to the deep ocean or seafloor (Lee and Wakeham, 1988; Wakeham et al., 1997, Hedges et al., 2001), driving the sequestration of carbon dioxide from the atmosphere and supplying energy to the benthos.

The composition of particulate organic matter that reaches the deep sea depends on its original source and any alteration that occurs during transit. Exchange with suspended particles and dissolved organic matter via aggregation and disaggregation can also influence composition. Previous research in organic chemistry, radiochemistry, and microbiology has suggested that exchange among these pools may be extensive. For example, the continuous adsorption and desorption of radioisotopes onto particulate organic matter (Bacon and Anderson, 1982) suggests that material is extensively exchanged between the dissolved and particulate pools. Also, the proportion of free-living (as opposed to particle-associated) bacteria increases with depth (Cho and Azam, 1988; Knauer, 1988), while microbial and zooplankton alteration products accumulate in the suspended phase (Wakeham and Lee, 1993) suggesting that sinking particles disaggregate and are degraded by microbes at depth. Settling velocity measurements also suggest extensive disaggregation and re-aggregation of sinking particles. According to Stokes' Law, settling velocity is proportional to radius squared and a particle's excess density over seawater (McCave, 1975); therefore, as particles become larger or accumulate more minerals, they should sink increasingly faster. Hill (1998) concluded that the consistency of settling velocity measurements in the ocean implies that particles undergo continual aggregation and disaggregation to adjust to changes in size and density. As aggregates become larger or denser due to the continued accumulation of organic and inorganic material, shear eventually increases to a point where it causes disruption. In addition, inertial drag also increases with size, resulting in a large Reynolds number, so that Stokes Law may no longer apply (Khelifa and Hill, 2006).

The extent of particle disaggregation and exchange, and resulting changes in settling velocity, would affect the residence time of organic matter in the water column, and therefore the efficiency of remineralization during transit. Evaluating the extent of particle disaggregation and exchange in various marine ecosystems is therefore important in predicting organic matter fluxes. Particle source and microbial or zooplankton alteration can often be revealed using biomarkers (e.g., Wakeham et al., 1997; Sheridan et al., 2002). Here we use a biomarker approach to evaluate exchange, by comparing compositional differences among particles separated by size and settling velocity. Only a few studies have compared the organic compositions of suspended and sinking particles collected at approximately the same depths (Lee and Cronin 1982; 1984; Repeta and Gagosian, 1984; Wakeham and Canuel, 1988; Sheridan et al., 2002). These studies have found that suspended material often differs in composition from sinking particles, implying that disaggregation of sinking particles may not be a large source of suspended material.

We evaluated exchange by comparing the organic compositions of suspended and sinking particles collected by *in situ* pumps and sediment traps. Both of these sampling tools have been used widely to assess particle composition and flux in the ocean (Bishop et al. 1980; Buesseler et al. 1992; Wakeham and Lee, 1993; Honjo 1996), but more rarely in combination. Sediment traps collect sinking particles, while *in situ* pumps filter both the suspended and sinking pools. This distinction can be very informative, potentially revealing differences in the composition of suspended and sinking particles and the extent to which material is exchanged between these two pools (Anderson et al., 1983; Wakeham and Canuel, 1988; Sheridan et al., 2002). As part of the MedFlux project, we collected particles by *in situ* pumps and sediment traps in 2003 and 2005 at the DYFAMED site, a French JGOFS time-series site in the northwest Mediterranean Sea. We evaluated the extent of exchange by determining whether or not the pigment and amino acid compositions of these particles grew more similar with depth. In 2005, we also compared the compositions of the 1-70 μm pump fraction, assumed to represent suspended or very slowly settling particles, with those of the >70 μm fraction, assumed to represent sinking particles. Sediment trap samples were collected in both time-series mode, which enabled comparison of the pump samples with trap material collected during the same periods, and in settling-velocity mode (Peterson et al., 2005, submitted), which enabled comparison of the pumps with particles of different settling velocities.

As part of the MedFlux project, Armstrong et al. (submitted) found that the distribution of particle settling velocities at the DYFAMED site was remarkably constant over the range of seasons and depths sampled. In addition, Lee et al. (submitted) found that the composition of mineral ballast at this site did not vary much with settling velocity for particles with <40% organic matter. This lack of variation in settling velocity measurements and ballast composition may support the idea of extensive exchange between particles (i.e., rapid disaggregation and reaggregation, creating homogeneity), or simply indicate similar mineral sources to each settling velocity class.

On the other hand, Wakeham et al. (submitted) observed differences in organic matter composition with settling velocity in sinking particles at DYFAMED, indicating incomplete exchange. Biomarkers indicative of diatoms (e.g., chlorophyll *a*, serine, glycine, phytol, 16:1 and 20:5 fatty acids, 24-methylcholesta-5,22-dien-3 β -ol, and 24-methylcholesta-5,24(28)-dien-3 β -ol) and algal material that had been egested in zooplankton fecal pellets (e.g., cholesterol, pheophorbide, and pyropheophorbide) were enriched in faster sinking particles (49-979 m d⁻¹). In contrast, biomarkers of bacteria (pheophytin, γ -aminobutyric acid, and branched C15 and C17 fatty acids), cyanobacteria (chlorophyll-*b*), and other zooplankton products (cholesta-5,22-dien-3 β , cholest-5-en-3 β , hexadecanol, oleic acid) were enriched in smaller, more slowly settling particles (0.7-49 m d⁻¹). Organic matter associated with particles of different settling velocities therefore appears to be derived from different sources. This suggests exchange is incomplete, or all particles would have a similar organic composition.

By incorporating both small, suspended particles and larger, sinking particles in one study, we find further evidence for compositional differences with settling velocity and particle morphology. Sinking particles collected in sediment traps and on the >70 μm *in situ* pump screens appeared to be largely made up of fecal pellets, whereas suspended particles collected on the 1-70 μm *in situ* pump filters appeared to be more enriched in fresh phytoplankton and bacterial degradation products. These results suggest that exchange between sinking and suspended particles (i.e., via disaggregation and reaggregation processes) is limited. Fecal pellets may be a particularly robust type of sinking particle, and therefore resistant to disaggregation. The enrichment of fresh plankton indicators in the suspended phase, however, suggests that sinking phytoplankton aggregates may undergo greater exchange with other particles. At sites such as DYFAMED, where zooplankton

fecal pellets contribute substantially to the particle flux (Fowler et al., 1991; Carroll et al., 1998), particle export may be more efficient (i.e., a greater portion of surface production may escape decomposition) than at sites where phytoplankton aggregates dominate the sinking particle flux.

2. Methods

2.1. Sampling Location

Suspended and sinking particles were collected at the DYFAMED site (43°20'N, 7°40'E), a French JGOFS time-series site ~52 km off the coast of Nice in the Ligurian Sea (northwest Mediterranean). This location has been studied extensively for over a decade (Marty, 2002) and has many characteristics typical of open-ocean sites. It is ~2300 m deep, and despite being close to shore, is partly cut off from coastal runoff by a cross-coastal Ligurian current which circles the basin, producing a central gyre (Marty, 2002). Most terrestrial input at the site is derived from atmospheric deposition, and biominerals dominate over lithogenic material (Price et al., 1999).

Seasonal patterns in phytoplankton productivity at DYFAMED are typical for the mid-latitudes in the northern hemisphere. The spring bloom occurs in March through April and is characterized by maximum concentrations of chl *a* (0.02 to 0.12 $\mu\text{mol C l}^{-1}$) from the surface to ~50 m, and new production values reaching 80% (Marty et al., 2002). Coccolithophorids typically dominate phytoplankton community structure at this location, though diatoms are usually responsible for the spring bloom (Claustre et al., 1994; Barlow et al., 1997; Vidussi et al., 2000; Marty et al., 2002). In the summer, the chl *a* maximum decreases and shoals, and new production declines to an average of 15%. Destratification in the fall results in a second, smaller bloom, followed by intense vertical mixing in January-February. Since this seasonal cycle in production is fairly typical, biological factors affecting fluxes at DYFAMED may apply to a range of similar environments.

2.2. Sediment Trap Sampling

Sinking particles were collected using sediment traps fitted with an indented rotating sphere to exclude swimmers (Peterson et al., 1993). The base of each trap contained a rotating carousel that could be operated in time-series (TS) or settling-velocity (SV) modes (Peterson et al., 2005; submitted). In both modes, material was allowed to collect on top of

the sphere for one day, and then the sphere was rotated, depositing the material into a cup in the carousel poisoned with HgCl_2 . In TS mode, the carousel at the bottom was rotated once every few days, so that each cup would collect several days' worth of material. TS mode therefore provided a record of the temporal variability of particulate matter fluxes over the trap deployment. In SV mode, the carousel at the bottom underwent a full rotation every day, with each cup collecting material for a given period of time each day (with time intervals ranging from 1 min. to 12 h). This provided a record of the flux of particles of different settling velocities integrated over the entire time of deployment. A “dimpled sphere” was used in the TS traps, whereas a “saddle-and-ridge” sphere was used in SV traps (Peterson et al., submitted). The settling velocity calculations assume that the sphere does not alter particle size or settling velocity, which we have recently begun testing using lab and field-based experiments. Additional description of the sampling schemes used in this study is provided by Peterson et al. (submitted).

In 2003, the SV intervals sampled were 0.68-1.4, 1.4-2.7, 2.7-5.4, 5.4-11, 11-22, 22-49, 49-98, 98-196, 196-490, 490-980, and >980 m d^{-1} , respectively. In 2005, the SV spectrum was divided into more intervals at the high range (98-140, 140-196, 196-490, 196-326, 326-490 m d^{-1}), and the 3 slowest classes were combined into a single interval (0.68-5.4 m d^{-1}). Since the length of each settling velocity interval was not the same (i.e., material was collected over a longer period of time in some cups than in others), we normalized the mass collected in each cup to the length of these sampling intervals, assuming an otherwise steady supply within size classes. This normalization is described by Armstrong et al. (submitted) and will not be discussed here since we only compared the compositions, and not fluxes, of material in settling velocity traps.

In 2003, TS and SV trap arrays were deployed on March 6 and recovered May 6, then redeployed on May 14 and recovered again on June 30 (see sampling scheme in Table 3.1). During both periods, TS traps were deployed at approximately 200 m (actual sampling depths were 238 m during period 1 and 117 m during period 2) to collect the vertical flux associated with new or export production (Miquel et al., 1994). Additional TS traps were recovered from 771 m during period 1 and 1918 m during period 2 to determine changes in particle fluxes and composition with depth. SV traps were deployed at 238 m during period 1 (in duplicate) and at 117 m during period 2. In 2005, all traps were deployed during a

single period from March 4 to May 1. TS traps were deployed at 313 m and 924 m, and duplicate SV traps at 313 m, 524 m, and 1918 m.

Upon recovery, samples were split for multiple chemical analyses using a McLane™ WSD splitter. Samples for organic analyses were filtered onto combusted 0.7- μm glass fiber filters (GF/F) and frozen until analysis. Samples for mass, inorganic, and radionuclide analyses were filtered onto 0.4- μm (in 2003) or 0.6- μm (in 2005) Nuclepore filters and dried. Data on pigment and amino acid compositions are presented in this paper. Data on particulate mass, biogenic and lithogenic minerals, radionuclides, and additional organic composition of some of the samples are discussed elsewhere (Armstrong et al., submitted; Cochran et al., submitted; Lee et al., submitted; Szlosek et al., submitted; Wakeham et al., submitted).

2.3. *In Situ* Pump Sampling

Particles were also collected using Challenger Oceanic battery-operated *in situ* pumps (Cochran et al., submitted). Pumps were outfitted with 142 or 293 mm diameter, 70- μm Teflon or Nitex mesh screens as a prefilter followed by 142-mm diameter, 1- μm quartz microfiber or GF/F filters. These pumps had different inlet designs. The 142-mm pumps were fitted with either a baffled opening alone, or a baffled opening with a 30-cm PVC cylinder on top. The 293-mm pumps were fitted with either a 5-cm diameter, L-shaped tube on top of a sealed filter, or a filter holder with a solid top but many lateral openings (Liu et al., submitted). Material was sampled repeatedly at the same depths using these different pump designs, and we have averaged all of these measurements.

The material collected on the pre-filter (the $>70 \mu\text{m}$ fraction) of the pump is typically thought to represent the sinking fraction of particulate matter, whereas the material collected on the second filter (the 1-70 μm fraction) is typically thought to represent the suspended, or more accurately, very slowly settling fraction of particulate matter (Cochran and Masqué, 2003). To put this cutoff in perspective, it is similar to the 63 μm cutoff used to divide silt and sand. During each pump cast, approximately 500 – 1000 l of water were filtered over the course of 2 hours. CTD data were obtained shortly before or after the pump casts for determination of hydrographic conditions.

In 2003, pump casts were collected between March 4-10, May 7-12, and on June 30 (Table 3.1). In 2005, pump casts were collected March 2, March 9-14, and April 29-30. For

both years, the 1- μm filters were frozen immediately upon recovery, and later 20-mm diameter punches were taken for pigment and amino acid analyses. In 2005, material was also collected for these analyses from the 70- μm screen. The screen was rinsed with filtered seawater through a 25-mm diameter quartz microfiber (QM/A) filter, which was then dried, stored in the dark for ~ 100 d, and beta-counted for Th activity prior to taking 4-8 mm diameter punches for pigments and amino acids. Punches from both fractions were then frozen prior to organic analyses.

There was some concern that drying of the >70 μm pump filters could have caused degradation of the pigments on these filters. To test for this possible artifact, we later collected seawater from Long Island Sound, added fresh *Rhodomonas salina* culture to provide a strong chlorophyll *a* signal (in the ratio 1 ml culture: 3 ml seawater), incubated the mixture for 1 day to allow zooplankton to start grazing, and then filtered 4 10 ml aliquots. Two samples were frozen immediately, and two were dried overnight at 60°C and then frozen. Pigment concentrations and compositions in the frozen and dried samples differed by less than 0.7%.

2.4 Organic Analyses

Chloropigments and fucoxanthin were determined by high performance liquid chromatography (HPLC) after extraction in acetone (Mantoura and Llewellyn, 1983; Bidigare et al., 1985; Sun et al., 1991). Briefly, filters were sonicated twice in 1-5 ml HPLC-grade acetone, after which extracts were filtered through a 0.2- μm Phenomenex membrane and combined into one vial. Within 24 hours of extraction, samples were analyzed by HPLC after 20% dilution with Milli-Q water (to make them more miscible in the buffer used). Pigments were separated with a 5- μm Adsorbosphere or Alltech Altima C-18 HPLC column equipped with a guard column. Chloropigments were detected by fluorescence (excitation $\lambda = 410$ nm, emission $\lambda = 660$ nm) and fucoxanthin by UV absorbance (excitation $\lambda = 446$ nm). Retention times and concentrations were determined using authentic standards (Chl *a*: Turner Design; fucoxanthin: DHI Water and Environment; pheophytin-*a*, pheophorbide-*a*, and pyropheophorbide-*a*: synthesized from purified chl *a* and analyzed spectrophotometrically after King, 1993).

Total hydrolyzable amino acids were analyzed by fluorescence HPLC using pre-column o-phthaldialdehyde (OPA) derivatization after acid hydrolysis (Lee and Cronin, 1982,

1984; Lee et al., 2000; Ingalls et al. 2003). Filters were sealed under N₂ in glass vials containing 6N HCl with 0.25 wt% phenol and hydrolyzed at 110°C for 20h. Hydrolyzates were filtered through 0.2- μ m cellulose acetate filters, evaporated under N₂, and dissolved in Milli-Q water. Amino acids were analyzed by HPLC using a 5- μ m Alltech Altima column as described by Lindroth and Mopper (1979) or 4- μ m Waters Novapak column as described in Fabres et al. (submitted). The Waters column was eluted using a binary gradient at a flow rate of 1 ml/min., ramping from 100% eluant A (0.04 M sodium acetate at pH 7.0, 2% THF, and 10% methanol) to 44% eluant B (90% methanol and 10% 0.04 M sodium acetate) over 16 min., then to 55% B over the next 12 min., and finally to 73% B over the next 5 min. OPA-derivatized amino acids were detected by fluorescence and identified by comparison to the retention times of amino acids in a standard mixture (Pierce Chemical Standard H with the non-protein amino acids β -alanine and γ -aminobutyric acid added).

For pigments, duplicate analyses of the same samples differed by 2-30% (typically less than 10%), calculated as the standard deviation of the measurements divided by the average. For amino acids, duplicate analyses differed by 5-35% (typically less than 10%). For the pumps, replicate samples (i.e., replicate punches taken from the same filter), differed within 50% (typically less than 20% for amino acids and 30% for pigments), calculated by propagation of error (adding the variances squared of duplicate measurements for each replicate punch and then taking the standard deviation). For the traps, error for duplicate samples was often higher (most samples were within 30% for the amino acids and 50% for pigments, but a few were as high as 100%) since these samples were from duplicate traps deployed at the same depth, and therefore subject to some spatial heterogeneity.

Some pump data reported in the Appendix tables show >30-35% variation; however, this variation is not for replicate samples from the same pump cast, but rather averages of several days' pump measurements (to facilitate comparison with the traps). Therefore, the variation in these samples largely reflects temporal variability rather than sampling error.

2.5 Statistical Analyses

All pump and TS trap data for each year were compared using principal component analysis (PCA), a multivariate regression analysis which can reveal compositional differences among samples in a data matrix. PCA normally reduces the number of variables (i.e., 5 pigments and 21 amino acids) into principal components, or regression lines passing through

the center (mean) of the data along its maximum gradients. Principal component 1 (PC1) is the axis which explains the most variance in the data matrix, PC2 explains the next greatest amount of variance, etc. Sample site scores are the relative positions (i.e., coordinates) of each sample along these principal component axes, revealing the extent to which each sample differs from the origin (i.e., mean sample). Variable loadings, or eigenvectors, indicate each variable's contribution to the data variability along the principal component axes. The data matrix of amino acid and pigment composition (in mole %) used in the PCA was first standardized for each compound by subtracting the mean and dividing by the standard deviation. PCA analysis was performed on the standardized data using Sirius v. 7 (Pattern Recognition Systems).

Compositions of the 1-70 and >70 μm pump samples collected in 2005 were also compared using t-tests assuming unequal variances. This comparison was not possible between the pumps and traps since typically only 1-2 data points were available for each season from the exact same depths and dates of sampling.

Compositional variations with depth (in the case of the pumps) or settling velocity (in the case of the traps) were also assessed using Pearson's product-moment correlation. According to Cohen (1988), a correlation coefficient (r) of 0.30 to 0.49 or -0.30 to -0.49 is considered a moderate positive or negative correlation, and a coefficient of 0.50 to 1.00 or -0.50 to -1.00 is considered a strong positive or negative correlation.

3. Results

3.1. Comparison of Suspended (1-70 μm Pump) and Sinking (TS Trap) Particles: 2003

3.1.1. Quantity

During March 6-11, 2003, pigment and amino acid fluxes in the 238 m TS trap reached their maximum values of 33 and 1685 $\mu\text{mol C m}^{-2}\text{d}^{-1}$ (Fig. 3.3 a), respectively. At about this time (March 4-10), maximum pigment and amino acid concentrations in the 1-70 μm pump samples were 0.11 and 1.7 $\mu\text{mol C l}^{-1}$, respectively (Fig. 3.1 a). Chlorophyll *a* (chl *a*) was the only pigment detected in the 1-70 μm particles (Fig. 3.4). It is possible that pheopigments and/or fucoxanthin were present as well, but were not detected due to the low concentration of pigments in these samples. Using detection limits of $\sim 2\text{-}10 \times 10^{-5}$ μg for each pigment (resulting in a measurable concentration of $\sim 8 \times 10^{-6}$ $\mu\text{mol C l}^{-1}$ based on the sampling and extraction procedures used) as the maximum contributions of these pigments

to the samples, then they could together contribute at most 30% of the total pigments (and <1% in the upper 200 m)

3.1.2. Composition

As mentioned above, pigments in the suspended pump samples were at least 70% chl *a* (or >99% in the upper 200 m). By comparison, pigments in the TS trap samples at 238 and 771 m were only 10-11% chl *a* (Fig. 3.4). These samples were greatly enriched in pheophorbide (phide; 25-50%) and pyropheophorbide (pyrophide; 45-50%), which are produced by zooplankton enzymatic degradation of chl *a* (Currie, 1962; Mantoura and Llewellyn, 1983; Welschmeyer and Lorenzen, 1985). The traps also contained pheophytin (phytin; 5-9%), thought to be produced primarily by chl *a* alteration by bacteria and protozoans (Sun et al., 1993; Bianchi et al., 1988). Fucoxanthin (fuco; 7-10%), an accessory pigment produced by diatoms (Jeffrey and Vesk, 1981), was also present in the traps.

During this March period, the non-protein amino acids β -alanine (BALA) and γ -aminobutyric acid (GABA), which are produced by bacterial degradation of ASP and GLU, were enriched in the TS trap samples (0.5% BALA, 0.6% GABA) compared with the 1-70 μ m pump samples (0% BALA, 0-0.3% GABA). GABA increased with depth in the pumps ($r=0.85$ using the Pearson product-moment correlation test; see Table 3.2 for all correlation coefficients). We could not statistically compare changes in the trap composition with depth due to the insufficient number of depths sampled ($n=2$).

Aspartic acid (ASP) and glutamic acid (GLU), which are enriched in the tests of calcareous plankton (King, 1974; Weiner and Erez, 1984) contributed more to the 1-70 μ m pump samples (9-11% ASP and 9-14% GLU) compared with the traps (7-12% ASP and 8-12% GLU). The contribution of GLU decreased with depth in the 1-70 μ m pump samples ($r=-0.59$).

Serine (SER), threonine (THR), and glycine (GLY), which are enriched in the tests of siliceous plankton (Swift and Wheeler, 1991; Ingalls et al., 2003), contributed more to the traps (9-10% SER, 8% THR, and 17-18% GLY) compared with the 1-70 μ m pump samples (5-6% SER, 6-7% THR, and 9-15% GLY). GLY increased with depth in the pump samples ($r=0.50$).

At the next near-concurrent trap and pump sampling period (April 30-May 6 for the traps, May 7-12 for the pumps), there was a second, but much smaller peak in pigment and

amino acid fluxes of ~ 11 and $652 \mu\text{mol C m}^{-2}\text{d}^{-1}$, respectively, (Fig. 3.3 a). Concentrations in the 1-70 μm pump samples were higher than in March, reaching 0.31 and $4.0 \mu\text{mol C l}^{-1}$, respectively, at their maxima (Fig. 3.1 a). The 1-70 μm particle compositions ranged between 0-98% chl *a*, 2-100% phytin, 0-22% phide, 0-12% pyrophide, and 0-15% fuco with depth (Fig. 3.4). Contributions of phytin and pyrophide increased with depth ($r=0.93$ and 0.32 , respectively; Table 3.2), whereas chl *a* decreased ($r=-0.85$), consistent with microbial and zooplankton alteration. The diatom indicator fuco was most concentrated around 65-100 m (the mixed layer was <100 m, but a deep chl *a* maximum is often observed in the Mediterranean; see Faugeras et al. (2003). Fuco also exhibited a moderate negative correlation with depth ($r=-0.42$). The TS trap samples were again depleted in chl *a* (10-16%) and enriched in fuco (4-7%) and pyrophide (30-37%) compared with 1-70 μm pump samples from similar depths (Fig. 3.4). At this time, however, the trap samples contained similar or even lesser contributions of phytin (35-45%) and phide (6-10%) compared with the 1-70 μm pump samples.

As observed earlier in the spring, GABA was enriched in the TS trap samples (0.7-0.8% GABA) compared with the 1-70 μm pump samples (0-0.2%). BALA and GABA increased with depth in the pumps ($r=0.71$ and 0.37 , respectively). ASP was comparable in the 1-70 μm pump and TS trap samples (9-12%) but GLU was slightly higher in the pumps than traps (11-13% and 10-12%, respectively). The contributions of ASP and GLU decreased with depth in the 1-70 μm pump samples ($r=-0.58$ and -0.51 , respectively). SER, THR, and GLY again contributed more to the traps (7-9% SER, 7-8% THR, and 14-15% GLY) compared with the 1-70 μm pump samples (4-7% SER, 6-7% THR, and 9-11% GLY). SER increased with depth in the pump samples ($r=0.33$).

During the June 25-30 TS trap sampling, pigment and amino acid fluxes were substantially lower than in May (0.107 and $16 \mu\text{mol C m}^{-2}\text{d}^{-1}$, respectively), as were concentrations measured on June 30 in the 1-70 μm pump samples (0.07 and $1.9 \mu\text{mol C l}^{-1}$, respectively). The TS traps at 117 m again contained less chl *a* (0%) and more pyrophide (22-30%) compared with the 1-70 μm pump samples (23-95% and 0-13%, respectively), but both types of samples contained similar proportions of phytin, phide, and fuco (49-73%, 4-9%, and 0-11%, respectively, in the traps; 1-64%, 1-35%, and 0-16%, respectively, in the pumps) (Fig. 3.4). Chl *a* decreased with depth in the pump samples ($r=-0.65$) and phytin increased ($r=0.83$) (Table 3.2).

As observed during the two spring sampling periods, GABA was enriched in the TS trap samples (0.5-0.7% GABA) compared with the 1-70 μm pump samples (0-0.2%). BALA and GABA increased with depth in the pumps ($r=0.42$ and 0.33 , respectively). ASP and GLU were higher in the 1-70 μm pump samples (9-11%) compared with the traps (7-8%). The contributions of ASP and GLU decreased with depth in the 1-70 μm pump samples ($r=-0.62$ and -0.87 , respectively). SER and THR contributed about 6-7% to both the pumps and traps, but GLY were more enriched in the traps (15-17%) compared with the 1-70 μm pump samples (11-14%). The contribution of SER decreased with depth in the pump samples ($r=-0.65$).

3.1.3. Principal Component Analysis

Figure 3.6 shows a principal component analysis performed on all pump and TS trap samples for 2003. PC1 explained 37.8% of the variance in the data set, and PC2 explained 13.8%. The separation of the data along PC1 appeared to be partly related to the extent of contribution from bacteria and zooplankton alteration products since chl *a* plotted on the left side and its alteration products phide, pyrophide, and phytin (as well as the bacterial amino acids BALA and GABA) plotted on the right (for a similar approach, see Goutx et al., 2007; Engel et al. submitted b; Wakeham et al., submitted). PC2 also appeared to be related to source and alteration, since the fresh algae indicators chl *a*, ASP, GLU, SER, THR, GLY, and fuco plotted on the lower half of PC2, and the microbial and zooplankton alteration indicators phytin, BALA, GABA, phide, and pyrophide plotted on the upper half.

The 1-70 μm pump samples plotted on the left side of the PCA, near chl *a* and the amino acids ASP and GLU, which tend to be enriched in calcifying algae. The TS trap samples plotted on the right side of the PCA, near the alteration products phide, pyrophide, phytin, BALA, and GABA and the biogenic silica indicators SER, THR, and GLY. As the season progressed from early spring into summer, both the pump and trap samples moved towards the right and upwards, in the direction of the alteration products.

3.2. Comparison of Suspended (1-70 μm Pump) and Sinking (>70 μm Pump and TS Trap) Particles: 2005

3.2.1. Quantity

In 2005, maximum pigment and amino acid fluxes at 313 m (17 and 438 $\mu\text{mol C m}^{-2}\text{d}^{-1}$, respectively) occurred at the end of March and minimum fluxes (0.4 and 53 $\mu\text{mol C m}^{-2}\text{d}^{-1}$, respectively) at the end of April (Fig. 3.3 b). Additional smaller peaks occurred in early March and May (both \sim 6-7 and 237-315 $\mu\text{mol C m}^{-2}\text{d}^{-1}$, respectively). Concentrations in the 1-70 μm pump samples increased between early March and late April (from 0.003 and 1.0 $\mu\text{mol C l}^{-1}$ on March 2 to 0.03 and 4.8 $\mu\text{mol C l}^{-1}$ on April 29-30) (Fig. 3.1 b). A similar increase occurred in the >70 μm pump samples (from 0.002 nmol C l^{-1} and 0.002 $\mu\text{mol C l}^{-1}$, respectively on March 2 to 0.024 nmol C l^{-1} and 0.029 $\mu\text{mol C l}^{-1}$, respectively on April 29-30) (Fig. 3.2).

3.2.2. Composition

As depicted in Fig. 3.6 (and the Appendix, Tables 3.A3-3.A4), particle composition was similar to 2003 values, with sinking particles generally enriched in fecal pellet and bacterial degradation indicators. On March 2, all pigments were present at very low concentrations in the 1-70 μm pump samples, but mostly consisted of fuco (42-70%) and chl *a* (22-48%). Very little phytin (2-6%), phide (1-6%), or pyrophide (1-2%) were present in these samples. In contrast, large particles (LP) collected on the 70 μm mesh pump screens contained less chl *a* (14-38%) and fuco (19-21%), and more phytin (26-37%), phide (4-23%), and pyrophide (6-11%) (Fig. 3.6). On March 4-9, the TS trap samples at 313 and 924 m also contained less chl *a* (12-14%) and fuco (0-5%), more phytin (10-12%), and substantially more phide and pyrophide (23-25% and 49%, respectively) compared with the 1-70 μm pump samples. Chl *a*, phide, and pyrophide increased with depth in the 1-70 μm pump samples ($r=0.64$, 0.80 , and 0.85 , respectively; Table 3.2), whereas phytin and fuco decreased ($r=-0.042$ and -0.81 , respectively). We could not statistically compare changes in the trap or >70 μm pump sample composition with depth due to the insufficient number of depths sampled ($n=2$).

The amino acids ASP and GLU were enriched in the 1-70 μm pump samples (comprising 11-12% each) compared with most of the >70 μm pump samples (which ranged from 9-13% ASP and 8-14% GLU, but were usually on the lower end of this range). The 1-

70 μm pump samples were greatly enriched in ASP and GLU compared with the TS trap samples (1-9% ASP and 2-8% GLU). SER and THR were comparable in all samples, but GLY was enriched in the >70 μm pump (14-21%) and trap (15-43%) samples compared with the 1-70 μm pump samples (11-12%). BALA was also comparable in all samples (1-2%) but GABA was enriched in the traps (1-2%) compared with both pump fractions (0.1-0.2%). As in 2003, BALA increased with depth in the 1-70 μm pump samples ($r=0.56$). GLU, which with ASP can indicate the presence of biogenic carbonate, decreased with depth ($r=-0.50$) in these samples, whereas the biogenic silica indicators GLY and THR increased ($r=0.75$ and 0.41 , respectively).

On March 9-14, chl *a* again contributed substantially to the 1-70 μm pump samples throughout the water column (50-94%); fuco varied greatly (0-40%) (Fig. 3.6). The contributions of phytin, phide, and pyrophide (2-11%, 0.3-17%, and 1-10%, respectively) increased with depth in the water column as chl *a* decreased, consistent with bacterial and zooplankton alteration. The >70 μm pump samples, by comparison, contained much less chl *a* (2-20%) than the 1-70 μm fraction (Fig. 3.6). Fuco ranged from 0-91% and was greatest at about 100-150 m; which according to temperature profiles was often the approximate mixed layer depth during this time. Although this may appear to be very deep, the mixed layer depth has been observed to range from 40-150 m (D'Ortenzio et al., 2005). These samples again contained more phytin (1-65%), phide (2-37%), and pyrophide (2-22%) compared with the 1-70 μm particles. TS trap samples also contained less chl *a* (12-14%) and fuco (5-7%), and more phytin (10-14%), phide (22-25%), and pyrophide (40-50%) compared with the 1-70 μm pump samples (Fig. 3.6). Chl *a* decreased with depth in the 1-70 μm pump samples ($r=-0.84$; Table 3.2) and increased in the >70 μm pump samples ($r=0.61$). Pyro increased with depth in both pump fractions ($r=0.83$ and 0.38 , respectively). Phide, phytin, and fuco also increased with depth in the 1-70 μm pump fraction ($r=0.74$, 0.52 , and 0.58 , respectively).

Differences in amino acid compositions were not very pronounced among the different types of particles. BALA increased with depth in both the 1-70 and >70 μm pump fractions ($r=0.53$ and 0.95 , respectively), and GABA also increased in the 1-70 μm samples ($r=0.82$). These amino acids were relatively enriched in the deeper pump samples (0.2-4% BALA and 0.2-1% GABA in the 1-70 μm pumps; 0.1-8% BALA and 0.2-1% GABA in the >70 μm pump samples) compared with the traps (1-2% BALA and 0.6-0.7% GABA). GLU

decreased with depth in the 1-70 μm fraction ($r=-0.61$) and increased in the >70 μm fraction ($r=0.30$). GLY increased in both pump fractions ($r=0.74$ and 0.35 , respectively); SER also increased in the 1-70 μm fraction ($r=0.75$).

On April 29-30, the 1-70 μm pump samples contained less chl *a* (21-47%) than in March (Fig. 3.6). Fuco (0-49%) was present at the surface and decreased with depth ($r=-0.61$). Phytin was present throughout the water column (16-52%), and phide and pyrophide were present at depth (0-27% and 1-24%, respectively). The >70 μm pump samples contained less chl *a* (2-12%) and phytin (1-34%), and more fuco (0-73%), phide (7-51%), and pyrophide (7-35%) (Fig. 3.6). TS trap samples collected on April 23-38 were similar in composition to the >70 μm pump samples, with 11-14% chl *a*, 0% fuco, 6-15% phytin, 26% phide, and 48-54% pyrophide (Fig. 3.6). Phide and pyrophide increased and fuco decreased with depth in both pump fractions (phide: $r=0.75$ and 0.63 , respectively; pyrophide: $r=0.87$ for both; fuco: $r=-0.61$ and -0.75 , respectively; Table 3.2). Chl *a* also increased with depth in the >70 μm pump samples ($r=0.48$).

ASP and GLU were again enriched in the 1-70 μm pumps (10-13% ASP and 8-14% GLU) compared with the >70 μm pumps (7-12% ASP and 7-13% GLU) and TS traps (6-7% ASP and 5-8% GLU). ASP increased with depth in both pump fractions ($r=0.79$ and 0.70 , respectively), and GLU also increased in the >70 μm fraction ($r=0.79$). SER and THR were fairly comparable in all samples but GLY was more enriched in the >70 μm fractions (16-22%) and TS traps (14-20%) compared with the 1-70 μm fractions (10-20%). SER and GLY both increased with depth in the 1-70 μm pump samples ($r=0.90$ and 0.84), and SER decreased in the >70 μm pump fraction ($r=-0.73$). BALA also increased with depth in both pump fractions ($r=0.83$ and 0.62) and was enriched in these samples (0.3-3% in the 1-70 μm fractions; 0.2-2% in the >70 μm fractions) compared with the TS traps (0.4-0.9%). GABA followed the opposite pattern, decreasing with depth in the >70 μm pump fraction ($r=-0.72$).

Using t-tests assuming unequal variances, we statistically compared the 1-70 and >70 μm pump samples collected during all three sampling periods in 2005. The 1-70 μm samples were significantly enriched in ASP ($p=0.04$), GLU ($p=0.03$), and chl *a* ($p<0.001$) compared with the >70 μm fraction. The >70 μm samples were significantly enriched in GLY ($p<0.001$), phide ($p=0.001$), and pyrophide ($p<0.001$).

3.2.3. Principal Component Analysis

The principal component analysis for 2005 (Fig. 3.7) includes all TS trap data but only selected depths from each pump sampling. When all pump depths were included, the patterns were the same but were more difficult to distinguish visually. PC1 explained 28.1% of the variance in the data set, and PC2 explained 17.7%. As in 2003, PC1 appeared to be related to source and alteration since chl *a*, ASP, and GLU plotted on the left side of this axis and the zooplankton alteration products phytin, phide, and pyrophide, bacterial amino acid GABA, and biogenic silica indicators SER, GLY, and THR plotted on the right side. PC2 also appeared to be related to alteration since the fresh algae indicators plotted towards the top half of this axis and alteration products plotted towards the bottom half.

The 1-70 μm pump samples were located on the left side of the PCA (near chl *a* and the biogenic carbonate indicators), the TS trap samples fell on the right side (near the zooplankton alteration products and biogenic silica indicators), and the >70 μm pump samples fell between the 1-70 μm pump fraction and traps, overlapping with both (with shallower samples closer to the traps, and deeper samples closer to the pumps). Unlike in 2003, the bacterial indicators phytin and BALA did not plot near the fecal pellet indicators and trap samples, but were closer to the deeper 1-70 μm and >70 μm pump samples. As the season progressed from early spring into summer, all samples moved towards the right, closer to the alteration products. In addition, the deeper pump and trap samples, as well as the trap samples collected at later dates, moved towards the bottom of PC2, near the alteration products BALA, phytin, and phide.

3.3. Comparison of Suspended (1-70 μm Pump) and Sinking (SV Trap) Particles: 2003

Changes in composition with settling velocity for 2003 are shown in Fig. 3.8 (as well as the Appendix, Tables 3.A5-3.A6). In March-May, the composition of the 1-70 μm pump samples at 200 m was quite distinct from that of the trap samples at 238 m. Pigments in the 1-70 μm pump samples were composed primarily of chl *a* (64%) and the microbial degradation indicator phytin (23%), with lesser amounts of the fecal pellet indicators phide and pyrophide (5 and 7%, respectively) and no fuco. The slowest settling velocity class (0.7-1.4 m d^{-1}) contained much less chl *a* (7%) and more fuco (8%), phytin (29%), phide (6%), and pyrophide (50%) than the pumps. The SV classes between 1.4 and 979 m d^{-1} contained

13-17% chl *a*, 10-13% fuco, 6-15% phytin, 10-17% phide, and 49-57% pyrophide. The fastest-sinking particles ($>979 \text{ m d}^{-1}$) were distinct from the intermediate settling velocity classes, with lower chl *a* (6%), fuco (6%), and phide (7%), and more phytin (17%) and pyrophide (63%). Pearson product-moment correlation comparing organic composition with the minimum settling velocity for each interval in the SV trap revealed that pyrophide and phytin were moderately correlated with settling velocity ($r=0.49$ and 0.31 , respectively), and fuco, chl *a*, and phide exhibited moderate to strong negative correlations with settling velocity ($r= -0.63$, -0.46 and -0.42 , respectively; Table 3.2).

The biogenic calcite indicators ASP and GLU were abundant in the 1-70 μm pump samples ($\sim 11\%$ each). The biogenic silica indicators SER, THR, and GLY comprised 5%, 7%, and 11% of total amino acids, respectively. The degradation indicators BALA and GABA comprised 0.03% and 0.2% of the total, respectively. Compared with the 1-70 μm pump samples, most of the SV trap samples were slightly depleted in ASP (8-10%) and GLU (9-10%). The trap samples were also enriched in SER (6-10%) and GLY (13-17%) but not THR (7%). BALA (0.3-0.7%) and GABA (0.5-0.6%) were also enriched in the SV trap samples compared with the pumps. GLU and THR were strongly correlated with settling velocity ($r=0.61$ and 0.97 , respectively), and BALA and GABA were strongly negatively correlated with settling velocity ($r=-0.74$ and -0.79).

From May-June, 2003, the 1-70 μm pump samples at 100 m contained 17% chl *a*, 7% fuco, 43% phytin, 7% phide, and 26% pyrophide. As in the earlier season, chl *a* was again enriched in the 1-70 μm pumps compared with the SV trap. In the 117 m SV trap, most SV classes ($0.7\text{-}979 \text{ m d}^{-1}$) contained less chl *a* (12-25%), and more fuco (16-23%), pyrophide (11-34%), and phytin (27-51%) Phide was similar to the pumps (4-12%). The fastest sinking particles ($>979 \text{ m d}^{-1}$) had more phide (17%) and no fuco, but were otherwise comparable. Chl *a* and fuco were negatively correlated with settling velocity ($r=-0.32$ and -0.85 , respectively; Table 3.2), and phide and phytin were correlated with settling velocity ($r=0.57$ and 0.69 , respectively). The correlation between phytin and settling velocity may have been driven strongly by the $>979 \text{ m d}^{-1}$ interval. Amino acids in the trap and pump samples ranged from 11-14% ASP, 10-16% GLU, 5-7% SER, 0.4-13% GLY, 5-8% THR, 0-0.5% BALA, and 0-0.7% GABA. ASP (one of the biogenic carbonate indicators) increased with settling velocity ($r=0.54$), and GLY (one of the biogenic silica indicators) was negatively

correlated with settling velocity ($r=-0.43$). BALA and GABA were also negatively correlated with settling velocity ($r= -0.86$ and -0.63 , respectively).

3.4. Comparison of Suspended (1-70 μm Pump) and Sinking (SV Trap) Particles: 2005

Data for 2005 are shown in Fig. 3.9 (and the Appendix, Tables 3.A7-3.A8). At 300 m, the 1-70 μm pump (SP) samples contained far more chl *a* (52%) and fuco (23%) than the >70 μm pump (LP) samples (13% and 9%, respectively) and 313 m SV trap samples (6-10% and 4-10%, respectively). The 1-70 μm pump samples also contained 10% phytin, 8% phide, and 8% pyrophide. The >70 μm pump samples contained more phytin (33%), phide (24%), and pyrophide (21%), and less fuco (9%). Pyrophide was higher in the 313 m SV trap samples than in both pump fractions, comprising 52-71%. Phytin and phide were strongly correlated with settling velocity ($r= 0.70$ and 0.90 , respectively; Table 3.2), and chl *a* was moderately correlated with settling velocity ($r=0.31$). Pyrophide and fuco were negatively correlated with settling velocity (-0.67).

ASP and GLU were higher in both pump fractions (12 and 13-14%, respectively) than in the SV trap samples (7-9%). SER, THR, and GLY were comparable in all three types of samples. BALA was higher in the >70 μm pump samples (3%) compared with the 1-70 μm fraction (0.8%) and SV traps (0.2-0.6%), though GABA was comparable in all three types of samples (0.2-0.7%). BALA and GABA were negatively correlated with settling velocity in the traps ($r=-0.34$ and -0.60 , respectively).

Compositional patterns in the 500 m pumps and 524 m trap were similar to those in the shallower samples. The 1-70 μm pump samples contained 58% chl *a*, 15% fuco, 9% phytin, 14% phide, and 5% pyrophide. The > 70 μm pump samples contained more phytin (21%), phide (28%), and pyrophide (42%), and less fuco. The SV traps contained 6-12% chl *a*, 4-8% phide, 48-65% pyrophide, and 5-18% fuco. Chl *a* and fuco were strongly correlated with settling velocity ($r=0.76$ and 0.84 ; Table 3.2), and pyro was negatively correlated with settling velocity ($r=-0.58$).

As observed higher in the water column, the contribution of ASP and GLU was greater in both pump fractions (10-12% each) than in most SV classes (7-12% ASP, 6-10% GLU). SER was lower in the >70 μm pump samples than in the 1-70 μm pump or SV trap samples (6%, compared with 9-12% in the other samples), and was negatively correlated with settling velocity in the traps ($r=-0.38$). GABA was also negatively correlated with

settling velocity ($r=-0.34$). BALA had no significant correlation with settling velocity, but was slightly higher in the slowest SV class ($0.7-5.4 \text{ m d}^{-1}$) and 1-70 μm pump samples ($>1\%$ each, compared with $<1\%$ for the other samples) compared with the other SV classes and $>70 \mu\text{m}$ pump samples.

In the 1800 m pumps and 1918 m SV trap, the pigment compositions of suspended and sinking particles were similar to those higher in the water column. The 1-70 and $>70 \mu\text{m}$ pump samples again contained more chl *a* (55% and 20%, respectively) than the SV trap samples (6-10%). The 1-70 μm pump samples were also more enriched in fuco (29%) than the $>70 \mu\text{m}$ pump samples (0%) and SV traps (0-12%). The $>70 \mu\text{m}$ pump samples had a higher contribution of phytin (31%) and phide (28%) than the 1-70 μm pump samples (4% and 6%, respectively) and SV trap samples (7-15% and 17-22%, respectively). The fastest-sinking particles ($>979 \text{ m d}^{-1}$) were also relatively enriched in phytin compared with the other SV classes. Chl *a*, fuco, and phytin were correlated with settling velocity in the trap samples ($r=0.73$, 0.47 , and 0.68 , respectively; Table 3.2), and pyrophide was negatively correlated with settling velocity ($r=-0.79$).

The contribution of ASP and GLU remained high in the $>70 \mu\text{m}$ pump samples (12% each) but decreased in the 1-70 μm fraction (10% ASP and 8% GLU) relative to the shallower depths. The SV trap samples ranged from 9-11% ASP and 7-10% GLU. SER, THR, and GLY were comparable in the trap and both pump samples, though GLY was slightly enriched in the $140-979 \text{ m d}^{-1}$ SV trap classes (21-22%) compared with the rest of the samples (15-19%). SER was negatively correlated with settling velocity in the trap samples ($r=-0.67$), while THR, another diatom indicator, was positively correlated with settling velocity ($r=0.78$). GABA was comparable in all samples, but BALA was greatly enriched in the $>70 \mu\text{m}$ pump samples (8%) compared with the SV traps (1-2%) and 1-70 μm pump samples (2%). BALA and GABA both exhibited strong negative correlations with settling velocity in the trap samples ($r=-0.91$ and -0.68).

3.5. Comparison of All Suspended and Sinking Particles

3.5.1. Composition (Mole %) of All Samples below the Mixed Layer

Figure 3.10 depicts the average composition (in mol % of total pigments or amino acids) of all 1-70 μm pump (SP), $>70 \mu\text{m}$ pump (LP), TS trap (TS), and SV trap (SV) samples collected below the mixed layer in 2003 and 2005 (i.e., all trap samples, and all ≥ 200

m pump samples). Range bars indicate the maximum and minimum values observed for each of these classes of particles, and are not error bars. The compositions of each particle type varied with depth and season; however, differences in mean composition are still apparent between suspended and sinking particles. 1-70 μm pump samples were greatly enriched in chl *a* (mean= 66%) compared with all sinking particles (mean= 8-18%). The >70 μm pump samples, TS trap, and SV trap samples were enriched in phide (18-24%) and pyrophide (116, 28, and 40%, respectively) compared with the 1-70 μm pump samples (4%). On average, phytin was slightly higher in the sinking particles (15-30%) compared with the suspended particles (11%), but as discussed previously, this was not the case for the summer of 2003 (as shown by the overlapping range bars). Fuco was substantially higher in the >70 μm pump samples (36%) compared with the other samples (<11%), but this is biased by the fact that data for these samples was only available in 2005, when we observed a large fuco contribution in both pump fractions (up to 48% in the 1-70 μm fraction, and up to 91% in the >70 μm fraction).

Differences in amino acid compositions were less pronounced and showed greater overlap in the range bars. On average, both pump fractions were slightly enriched in ASP and GLU (10-11%) compared with the traps (9%). The >70 μm pump, TS trap, and SV trap samples were slightly enriched in SER (7%) and substantially enriched in GLY (16%) compared with the 1-70 μm pump (6% and 13%, respectively). The range for BALA was much greater for the >70 μm pump samples (up to 9%) than the other samples (<3%) but this was biased by just one large value (9% in the 1800 m sample from Mar. 9-14, 2005).

3.5.2. Pigment Ratios for All Pump and TS Trap Samples

Another way to examine compositional differences among samples is using compound ratios (e.g., pheopigments/ chl *a*). Fig. 3.11 depicts the relationship between chl *a* and its microbial degradation product phytin (a) or zooplankton alteration products phide + pyrophide (b) for all 1-70 μm pump (SP), >70 μm pump (LP), and TS trap samples (TS). These compounds are normalized to total pigments (i.e., as in the mol % calculations) to eliminate differences in total pigment concentrations. Data from all depths and time periods during these years are shown to illustrate the spread in the data.

The ratio of phytin/chl *a* ranged widely for all samples, but was greater on average for the TS trap and LP samples compared with the SP samples (Fig. 3.11 a). In 2003, values

of phytin/ chl *a* ranged from 0 to 11 (average= 0.6) for SP and from 0 to 21 (average= 3) for TS traps. In 2005, phytin/ chl *a* ranged from 0.03 to 4 (average= 0.4) for SP, from 0.2 to 25 (average 5) for LP, and from 0.4 to 2 (average= 1) for TS traps. The ratio of (phide + pyrophide)/ chl *a* did not range as widely among samples, and was almost always >1 for the TS trap and LP samples and <1 for the SP samples (Fig. 3.11 b). In 2003, values of (phide + pyrophide)/ chl *a* ranged from 0 to 6 (average= 0.3) for SP and 0.2 to 17 (average=4) for TS traps. In 2005, (phide + pyrophide)/ chl *a* ranged from 0.01 to 1 for SP (average= 0.2), from 0.2 to 13 (average= 5) for LP, and from 3 to 32 (average= 6) for TS traps.

4. Discussion

4.1. Sources and Alteration of Suspended and Sinking Particles

4.1.1. Sinking Particles

In 2003, the trap samples contained a large contribution of the pigments pheophorbide (phide) and pyropheophorbide (pyrophide), which together comprised 25-74% of total pigments (Fig. 3.10). Since these pigments are produced by zooplankton enzymatic degradation of chlorophyll *a* (Currie, 1962; Daley, 1973; Shuman and Lorenzen, 1975; Hendry et al., 1987), this indicates sinking particles contained a large contribution of zooplankton fecal material. Lipids in the traps (Wakeham et al., submitted) were also dominated by zooplankton-reworked algal material (e.g., zooplankton sterols such as cholesterol (27 Δ^5), stearic (18:0) and oleic (18:1 ω 9) acids). Sinking particles collected in 2005 also contained large contributions of fecal pellet indicators; phide + pyrophide generally comprised 65-80% of the pigments in the trap samples and 15-87% in the >70 μ m pump samples. At ~100-150 m, the >70 μ m pump particles were about 90% fucoxanthin, suggesting a large diatom contribution; however, the chloropigment composition was similar to that at other depths, with a large contribution of phide and pyrophide (combined, these were ~50% of total chloropigments).

During periods of high flux (i.e., March-May, 2003 and March, 2005), sinking particles were more enriched than suspended particles in the microbial degradation indicators pheophytin (phytin), β -alanine (BALA), and γ -aminobutyric acid (GABA). These microbial degradation products could have been present in fecal pellets or phytoplankton aggregates. In periods of lower flux (i.e., June, 2003 and April, 2005) this difference was not

as pronounced or the pattern was even reversed, with 1-70 μm pump samples becoming more enriched in bacterial degradation products.

Chlorophyll *a* (chl *a*) comprised 0-16% of total pigments in the 2003 trap samples, 11-14% in the 2005 trap samples, and 2-38% in the 2005 >70 μm pump samples, indicating some fresh, unaltered algal material was also present either in fecal pellets or in phytoplankton aggregates/ marine snow. Results from Tamburini et al. (submitted) suggest that the latter particle type was responsible; we collected numerous fecal pellets at 200 m depth in 2006 and found that they were 98% phide + pyrophide. The amount of chl *a* egested in fecal pellets could vary with the extent of zooplankton assimilation, but we have assumed that zooplankton assimilation efficiency in the spring of 2003 and 2005 was comparable to that in 2006.

Therefore, in both years, sinking particles appeared to be composed of zooplankton fecal material as well as algal material present in phytoplankton aggregates or marine snow. We cannot determine the precise contributions of these particle types to total fluxes, but can approximate these contributions based on the pigment composition of sinking particles. In these calculations, we assume that the contribution of phide + pyrophide to total pigments is representative of the contribution of fecal pellets to total POC fluxes, and that chl *a* + phytin is representative of the contribution of fresh and microbially degraded phytoplankton aggregates/ marine snow. Fecal pellets should also contain microbially degraded material, but we cannot determine the partitioning of phytin between fecal pellets and aggregates. Fucoxanthin was excluded from these calculations since it was generally a small component of total pigments, and it is difficult to determine whether it would be representative of aggregates of fecal pellets, since diatom-derived material may have been preferentially incorporated into fecal pellets (this is explained in section 4.1.3.).

Performing these calculations for the TS traps and >70 μm pump particles, approximate contributions of phytoplankton aggregates (aggs) and fecal pellets (FP) to total POC fluxes appear to be as follows: ~16-18% aggs and 74-75% FP in March, 2003; 46-61% aggs and 36-46% FP in April-May, 2003; 29-73% aggs (all phytin, no chl *a*) and 27-39% FP in June, 2003; 23-64% aggs and 15-74% FP in early March, 2005; 22-68% aggs and 33-53% FP in mid-March, 2005; and 8-42% aggs and 18-87% FP in April, 2005.

It is not surprising that fecal pellets were enriched in the sinking phase, since they typically have high settling velocities. Values previously reported for fecal pellets range from 60-200 m d⁻¹ (Honjo and Roman, 1978; Pilskaln and Honjo, 1987), although MedFlux results suggest particle settling rates may average at least 300-400 m d⁻¹ (Armstrong et al., submitted; Xue and Armstrong, submitted). However, it is surprising that fecal pellets apparently comprised such a large portion of sinking particle fluxes. Zooplankton fecal pellets are generally thought to be a relatively small component of organic particle fluxes. Pilskaln and Honjo (1987) found that in the open ocean, they account for only 5%, 1-10%, 0.5-4%, and 1-3% of the fluxes of mass, organic carbon, calcium carbonate, and silica, respectively (though they accounted for as much as 66% of the energy requirements of benthic biota). However, fecal pellets contribute more extensively to fluxes in sites where zooplankton grazing is tightly coupled with production; Fowler et al. (1991) and Carroll et al. (1998) previously reported fecal pellet contributions greater than 30% to POC fluxes in the northwest Mediterranean, the location of this study. This indicates that one particular site may not be representative of all similar environments; different factors (e.g., aggregation processes versus production/ grazing dynamics) may govern fluxes at different locations. Zooplankton species composition (e.g., microzooplankton versus macrozooplankton) may also be important. In the northwest Mediterranean, the dominant zooplankton species responsible for fecal pellet production are herbivorous copepods and euphausiids, though carnivorous species become more abundant as spring progresses into summer (Nival et al., 1975; Andersen et al., 2001a,b).

The composition of sinking particles remained remarkably consistent with depth. Fluxes decreased by 20-80% between the shallower and deeper traps in each season, so clearly some material dissolved or decomposed; however, the remaining material was not extensively altered in composition. This is particularly evident in examining the 2005 >70 µm pump particles, which were sampled over a greater range of depths than the traps. Although indicators of fresh algae (chl *a* and fuco) were often abundant in the upper water column, samples below 300 m were dominated by fecal pellet indicators and remained consistent in composition throughout the remainder of the water column.

4.1.2. *Suspended Particles*

The 1-70 μm pump samples, thought to represent suspended or very slowly settling particles, were generally enriched in chlorophyll *a* or pheophytin (Fig. 3.10), indicating they were largely composed of fresh plankton (particularly at the surface) and microbial degradation products (more commonly at depth). This is surprising, since one would normally expect the most slowly-sinking particles to be extensively altered; however, other studies (e.g., Lee et al., 2000; Sheridan et al., 2002) have observed this phenomenon as well. Possible sources of these particles include the slow settling of individual phytoplankton cells, which have sinking rates of about 0.1-1 m d^{-1} (Burns and Rosa, 1980; Bienfang, 1981), disaggregation of larger sinking particles, or horizontal advection of particles from other locations. Chl *a* often remained a surprisingly dominant component of these particles even below 1000 m. However, examination of the vertical profiles of pigment and amino acid concentrations (Fig. 3.1), demonstrates that most material in the 1-70 μm pool was rapidly lost with depth. Although the contribution of chl *a* to these samples remained high, the actual concentration of chl *a* decreased substantially. Suspended particles enriched in chl *a* below the euphotic zone have been observed in other locations, including up to 1000 m deep in the equatorial Pacific (Lee et al., 2000; Sheridan et al., 2002) and NE subarctic Pacific (Thibault et al., 1999), and up to 3000 m deep around Antarctica (Fileman et al., 1998). Also, even though pigments did not appear to be more degraded with depth, the bacterial amino acids BALA and GABA were consistently correlated with depth in the 1-70 μm pump samples. Sheridan et al. (2002) observed this as well in the equatorial Pacific.

Chl *a* decomposition can occur without substantial pheopigment production, since some processes such as photooxidation and grazing by microzooplankton can cleave the macrocyclic structure of chl *a*, converting it into colorless residues undetectable by fluorescence HPLC (Klein et al., 1986; Hendry et al., 1987). Furthermore, microzooplankton fecal pellets are small ($<35 \mu\text{m}$) and can therefore remain suspended and be subjected to extensive photooxidation (SooHoo and Kiefer, 1982; Welshmeyer and Lorenzen, 1985; Hendry et al., 1987).

Despite the extensive net loss of chl *a*, a small amount often remained at depth, leading to asymptotic background concentrations of 0.1-2 nmol C l^{-1} (Figs. 3.3 and 3.4). This phenomenon has often been observed in sediments (e.g., Sun et al., 1991; Sun et al., 1994)

and laboratory incubations (e.g., Shuman and Lorenzen, 1975; Ingalls et al., 2000); preservation of fresh algal material may be due to matrix effects such as interactions with minerals or complex organic polymers. Additionally, some chl *a* could have been supplied at depth if a small number of cells remained viable below the euphotic zone with an elevated chl *a* content due to light starvation. C: chl *a* ratios ranging from 25-50 are common in coastal environments, so high chl *a* levels do not always reflect a large number of particles (Lorenzen, 1968; Jamart et al., 1977; Welschmeyer and Lorenzen, 1985). Physical advection of fresh algal cells out of the euphotic zone could also account for this observation, but evidence of such vigorous deep mixing is not apparent from temperature/ salinity diagrams. Additionally, relatively fresh suspended particles may have been carried to the DYFAMED site by currents, or sinking particles from another location may have undergone some lateral transport to the site and then disaggregated. The possibility of disaggregation and exchange with sinking particles is discussed further in section 4.2.

4.1.3. Mechanisms of Sinking Particle Formation

As discussed above, sinking particles were more enriched in fecal pellets while suspended particles were more enriched in fresh algal cells. In addition, there is some evidence that the sources of algal material to these particles were different. Aspartic and glutamic acid (ASP and GLU), which are enriched in biogenic calcite (King, 1974; Weiner and Erez, 1984), typically contributed more to suspended (1-70 μm pump) than sinking (trap and >70 μm pump) particles (Fig. 3.10). This difference was statistically significant in comparing the 1-70 μm and >70 μm pump samples collected at the same depths and times in 2005. Sinking particles also contained a large contribution of ASP and GLU, and calcium carbonate was the dominant mineral present (Lee et al., submitted). However, relative to the suspended particles, the traps were enriched in the biogenic silica indicators SER, THR, and particularly GLY (Fig. 3.10). Lee et al. (2000) and Sheridan et al. (2002) observed similar compositional differences in the equatorial Pacific; sinking particles were enriched in fecal pellet indicators and GLY (but not SER and THR), while suspended particles were enriched in chl *a* and GLU (but not ASP).

Sinking particles were often enriched in the diatom pigment fucoxanthin (fuco) compared with the suspended particles; this was the case at least for March 4- May 2, 2003

and March 7-April 30, 2005. Serine (SER), threonine (THR), and glycine (GLY), which are enriched in the tests of siliceous plankton (Hecky et al., 1973; Swift and Wheeler, 1991), also contributed more to the sinking particles, even at times when fuco was not enriched in these samples (e.g., March 4-14, 2005). Differences in the preservation of these biomarkers within fecal pellets may explain why the amino acid markers were sometimes present but fuco was not. Zooplankton grazers degrade fucoxanthin to fucaxanthinol (Repeta and Gagosian, 1984), which we did not measure. SER, THR, and GLY, on the other hand, are bound within the silica frustule of diatoms, and therefore protected against decomposition to some extent (Ingalls et al., 2003; also see Chapter 1). Cowie and Hedges (1996) found that these diatom frustule components are enriched in fecal pellets, since zooplankton do not digest the frustule. GLY was particularly enriched in the sinking particles (this difference was statistically significant between the 1-70 and >70 μm particles), and has been experimentally shown to be preferentially preserved relative SER and THR during diatom decomposition, indicating that it is particularly well-protected within the frustule (Cowie and Hedges, 1996). It is important to note that the method used to analyze particulate amino acids cannot access the amino acids remaining inside biogenic silica; this could be accomplished only by dissolution of the silica in hydrofluoric acid (Ingalls et al., 2003). However, these compounds are abundant in phytoplankton-derived material that has not been treated with HF (Lee et al., 2000; Sheridan et al., 2002), indicating that some fraction of these biomineral-bound amino acids becomes accessible to analysis. The removal of organic surface coatings on the frustule can accelerate silica dissolution (Bidle and Azam, 1999; Bidle et al., 2002; also see carbon maps in Chapter 1 for evidence of changes in organic matter distribution with chemical treatment), so acid hydrolysis may result in some silica dissolution and release of SER, THR, and GLY for analysis. Silica data is available for the traps, but not pumps, so we must rely on the biomarkers instead.

Small prymnesiophytes typically dominate phytoplankton community structure at the DYFAMED site, though diatoms are usually responsible for the spring bloom (Claustre et al., 1994; Barlow et al., 1997; Vidussi et al., 2000; Marty et al., 2002). Grazing by large copepods may have preferentially incorporated diatoms into sinking fecal pellets, leaving smaller, calcifying algae enriched in the suspended pool. Vernet (1991) found a greater abundance of zooplankton alteration products of chl *a* when diatoms dominated the phytoplankton than when prymnesiophytes dominated, indicating that diatom material is

indeed more likely than coccolithophorid material to be incorporated into fecal pellets. Pymnesiophytes may have instead been grazed by microzooplankton or small macrozooplankton, producing smaller pellets that remained in the euphotic zone.

Alternatively, coccolithophorids may have been grazed as extensively as diatoms, but dissolved in the acidic guts of zooplankton or in acidic fecal pellets or aggregates. Since silica is undersaturated in the ocean we would expect faster dissolution of silica than calcium carbonate in sinking particles; the lack of calcium carbonate indicators may suggest preferential dissolution under the low-pH conditions present in zooplankton guts or fecal pellets.

The co-occurrence of diatom and fecal pellet indicators in sinking particles, and of fresh plankton and calcium carbonate indicators in the suspended particles, therefore suggests the selective incorporation or preservation of diatom material in zooplankton fecal pellets. We did not perform microscopic observation of the pump and trap samples, so we cannot determine conclusively whether they contained different abundances of silicifying and calcifying algae. Some qualitative information about plankton community structure is available from plankton tows. Numerous diatoms were visible in 2003 but not 2005 (though radiolarians were present) (J.C. Miquel and S.W. Fowler, personal communication). However, many large copepods were present at both times, indicating that intensive grazing may have kept diatom populations low (S.W. Fowler, personal communication). Since the cruise was only a week long, we may have missed earlier diatom productivity. The observation of diatom grazers but not diatoms in 2005 suggests that diatoms were originally present, but were efficiently removed from the surface by zooplankton grazing and incorporation into fecal pellets.

Fecal pellets have also been shown to be an important conduit for the transport and preservation of coccolithophorid material in the ocean (Honjo, 1976, 1978; Roth et al., 1975; Honjo and Roman, 1978; Pilskaln and Honjo, 1987), and the trap samples we collected clearly contained either prymnesiophytes or foraminifera, as evidenced by high concentrations of ASP, GLU, and calcium carbonate (Lee et al., submitted; Wakeham et al., submitted). However, preferential grazing on diatoms or selective preservation of biogenic silica over calcium carbonate in fecal pellets might have caused the compositional differences we observed between sinking and suspended particles.

Lee et al. (submitted) observed that in all near-surface (~200 m) trap samples for 2003 and 2005, as the % organic carbon increased, the contribution of calcium carbonate to total ballast also increased, whereas the contribution of biogenic silica remained relatively constant. This may indicate that diatom-derived material was primarily incorporated into sinking particles via zooplankton grazing and fecal pellet production, whereas aggregation was more important for calcifying algae. The reason why the amount of diatom material in sinking particles was unrelated to %OC may be that zooplankton assimilated some algal material as they grazed, so their fecal pellets were relatively depleted in organic carbon. Wakeham et al. (submitted) observed that the traps contained low abundances of the most labile diatom-derived fatty acids [e.g., hexadecenoic acid (16:1), octadecatetraenoic acid (18:4), and eicosapentaenoic acid (20:5)], even though other compounds indicative of diatoms (e.g., fuco, SER, GLY, THR, 16:1 and 20:5 fatty acids, 24-methylcholesta-5,22-dien-3 β -ol, and 24-methylcholesta-5,24(28)-dien-3 β -ol) were abundant, suggesting effective zooplankton assimilation of the most labile OC in diatoms. The incorporation of calcifying algae into sinking particles, on the other hand, may have been controlled by the amount of organic material available for aggregation, or may have reflected simultaneous OC decomposition and CaCO₃ dissolution, hence the strong relationship between %OC and CaCO₃.

Calcium carbonate is often enriched in sinking particles (Klaas and Archer, 2002; François et al., 2002) and has been shown to promote aggregation (Engel et al., submitted a, b). The incorporation of minerals into aggregates may result in the formation of numerous small, dense aggregates, rather than large flocs (Passow and de la Rocha, 2006; Engel et al., submitted a, b). These compact coccolithophorid aggregates can have settling velocities that are twice as high as comparably-sized diatom aggregates (Engel et al., submitted a). Therefore, if all sinking particles were formed by aggregation, we would expect sinking rather than suspended particles to be enriched in ASP and GLU. The fact that we observed the opposite again points to the importance of fecal pellets, rather than aggregates, in driving sinking particle fluxes at this site.

Alternatively, since ASP and GLU are degraded by bacteria to BALA and GABA, the differences in ASP and GLU between suspended and sinking particles may simply reflect the relative freshness of these particles. However, the small contributions of BALA and GABA (frequently <1%) seem insufficient to explain these differences. Inorganic carbon

data is not available for the pump samples, so the relative influences of freshness and biogenic calcite on the contribution of ASP and GLU cannot be determined conclusively.

4.2. Exchange between Suspended and Sinking Particles

4.2.1. Possible Differences between Sinking Fecal Pellets and Phytoplankton Aggregates

Rapid exchange between suspended and sinking particles would lead to increasing similarity in composition with depth; this was not observed at this site. Rather, both particle types maintained distinct compositions from the surface to 1900 m. Since the sinking particles were up to 75% phide + pyrophide, disaggregation of these particles would produce suspended particles enriched in these fecal pellet indicators, rather than chl *a* and phytin, as we observed. It appears that if sinking particles do disaggregate, it is the fresher, chl-rich portion of these particles (which amounted to 6-17% chl *a* in the spring) that disaggregates, rather than the fecal pellets. This suggests that phytoplankton aggregates may be more susceptible to disaggregation than fecal pellets. We cannot distinguish between fecal pellets and phytoplankton aggregates in our comparison of particle types since we only have bulk chemical measurements. However, as discussed above, the relative abundances of phide + pyrophide and chl *a* may be indicative of the relative contributions of fecal pellets and phytoplankton aggregates in our samples.

Crustacean fecal pellets have been shown to be extremely robust. Numerous intact fecal pellets have been found in sediment traps at depths greater than 3500 m, indicating that pellets produced in surface waters can survive transit to the seafloor (Pilskaln and Honjo, 1987). Many are enclosed in a chitin-like membrane or pellicle, which helps protect the organic and inorganic contents from dissolution and remineralization (Forster, 1953; Reeve, 1963; Johannes and Satomi, 1966). Honjo and Roman (1978) demonstrated that fecal pellet membranes can remain intact for at least 20 days at low temperatures characteristic of the deep sea ($\sim 5^{\circ}\text{C}$), and even once the membrane degrades, the contents and shape of the fecal pellet itself can be preserved for at least 2 months. Pilskaln and Honjo (1987) found that very few fecal pellets in sediment trap material contained fully intact membranes, but were nonetheless intact themselves, retaining their morphology and chemical composition during transit through the water column. Since we did not perform microscopic examination on the trap samples, we unfortunately do not have data on the physical characteristics of the fecal pellets collected. However, we visually observed that macroscopic fecal pellets

survived extensive laboratory sample splitting and filtration procedures, as also found by Pilskaln and Honjo (1987). Therefore, these compact, often membrane-protected fecal pellets can be a highly efficient means of transport of organic and inorganic materials to the seafloor.

In the summer of 2003, fluxes were lower than in spring and we observed a greater similarity between the 1-70 μm pump and trap samples (Fig. 3.4, 3), possibly indicating more exchange between these particles. The trap samples had a lower contribution of the fecal pellet indicators than in the spring (26-40% phide + pyrophide, as opposed to 75% in March), and a greater contribution of the microbial degradation product phytin (50-73%, as opposed to 5-8% in March). Bacterial lipids were also greater during this time (Wakeham et al, submitted). The 1-70 μm pump samples also contained more phytin, phide, and pyrophide than in the spring (~23-77% phytin and 0-45% phide + pyrophide below 200 m, as opposed to 0% in March). Since fluxes were an order of magnitude lower in the summer than in the spring, zooplankton grazing was probably lower due to lower phytoplankton biomass. Particles were likely processed more by bacteria or smaller zooplankton whose fecal pellets were retained in the suspended phase. The greater similarity between suspended and sinking particles in the summer suggests that exchange between these two pools is more extensive during periods of lower flux. This appears to be driven by the transition from zooplankton alteration of algal matter to microbial alteration, indicating again that fecal pellets may undergo less exchange with suspended particles than other types of aggregates.

Compositional differences among the settling velocity trap classes were not as substantial as the differences between the traps and 1-70 μm pumps. All settling velocity classes contained 45-85% phide + pyrophide in the spring of 2003 and 2005, or 15-40% in the summer of 2003. This may indicate that sinking particles undergo some incomplete disaggregation and exchange, but remain in the sinking phase. Alternatively, this may simply indicate that all sinking particles were largely composed of fecal pellets; therefore, phide and pyrophide dominated this material.

4.2.2. Mass-Balance Calculations: Phytoplankton-Derived Material

The idea that exchange between sinking and suspended particles was greater for phytoplankton aggregates than fecal pellets can be more quantitatively assessed using mass balance calculations. Assuming that chl *a*, phytin, and phide + pyrophide reflect the

contributions of phytoplankton-derived, microbially-degraded, and fecal pellet material, respectively, we can separately evaluate exchange for each of these particle types.

The inventory of chl *a* in the suspended or sinking phases within the mesopelagic can be described by a box model where the input term (the flux of chl *a* entering the mesopelagic) is balanced by the output terms (decay and the flux of chl *a* exiting into the deep ocean and sediments), as well as an exchange function, which could be either an input or output term. The change in the chl *a* concentration within this box over time ($\partial C/\partial t$) would be described by the reaction:

$$(\partial C/\partial t) = (\partial J/\partial z) - kC \pm E$$

where $\partial J/\partial z$ = change in flux with depth (in $\mu\text{mol C m}^{-2}\text{d}^{-1}$), $-kC$ = decay described by the decay constant (d^{-1}) multiplied by concentration (in $\mu\text{mol C m}^{-3}$), and E = the addition or subtraction of material due to exchange with the other particulate phase (in $\mu\text{mol C m}^{-3}\text{d}^{-1}$). For the suspended phase, E would be a positive term (indicating the addition of chl *a* due to disaggregation of sinking particles), and for the sinking phase, E would be a negative term (indicating the loss of chl *a* due to disaggregation). Assuming steady state ($\partial C/\partial t=0$) and that E is constant:

$$0 = (\partial J/\partial z) - kC \pm E$$

$$0 = -\omega(\partial C/\partial z) - kC \pm E$$

where ω = settling velocity (in m d^{-1}). It is possible that neither the steady state nor constant exchange assumption is met. The concentration of chl *a* does change with season, but the steady state assumption is probably a valid approximation if the flux and exchange processes are rapid relative to this seasonal change. Also, the exchange function may vary in proportion to concentration. Integrating over the depth interval z to z^* to obtain the depth-dependent decay function:

$$C(z^*) = [C(z) \pm (E/k)] e^{-(k/\omega)\Delta z} \pm (E/k)$$

Using the equation for the suspended phase, we can solve for E by entering the following boundary conditions:

$$C_{\text{susp}}(z^*) = [C_{\text{susp}}(z) - (E/k)] e^{-(k/\omega_{\text{susp}})z} + (E/k)$$

$$\text{as } z^* \rightarrow \infty, C_{\text{susp}}(z^*) \rightarrow (E/k)$$

$$\therefore E = k C_{\text{susp}}(z^*)$$

We approximated $C_{\text{susp}}(z^*)$ as $z^* \rightarrow \infty$ by calculating the asymptotic chl *a* concentration in the suspended phase from the depth profile. Of course z^* does not have to actually reach infinity; the requirement is only that the exponential term becomes sufficiently small that it can be ignored relative to E/k . The above approximation ($E = k C_{\text{susp}}(z^*)$) also applies as $\omega \rightarrow 0$, which may be an accurate assumption for $<70 \mu\text{m}$ -diameter phytoplankton. Using zero as a lower limit for excess density (common for many phytoplankton according to Smayda, 1970), and 0.08 g cm^{-3} as an upper limit for nutrient-starved phytoplankton (Eppley et al., 1967), Stokes' law predicts settling velocities of $0\text{-}0.5 \text{ m d}^{-1}$ for $<70 \mu\text{m}$ -diameter particles.

First-order decay constants for chl *a* (k) reported in the literature range from $0\text{-}0.20 \text{ d}^{-1}$ in various water column and sedimentary environments (Leavitt and Carpenter, 1990; Bianchi and Findlay, 1991; Sun et al., 1991; Ingalls et al., 2000, 2004). A value of 0.03 d^{-1} for k is frequently applied, and was reported by Welschmeyer and Lorenzen (1985) for a site where conditions were similar to those at DYFAMED (deep, coastal marine ecosystem, where suspended particles would have a long residence time in the water column). We used $0.03\text{-}0.2 \text{ d}^{-1}$ as an approximate range for k to obtain a range of possible values for E .

Having solved for E , we can then estimate the minimum change in sinking particle fluxes with depth required to support the decay of chl *a* in the suspended phase:

$$0 = (\partial J_{\text{sink}} / \partial z) - k C_{\text{sink}} - E$$

$$\text{If } -k C_{\text{sink}} = 0$$

$$\partial J_{\text{sink}} / \partial z = E$$

At a minimum, the change in sinking particle fluxes with depth must balance the exchange parameter (we could also take the opposite approach, and set $E=0$, in which case $\partial J_{\text{sink}} / \partial z$

would need to balance decay). If chl *a* in the sinking fraction is lost due to both decay and exchange (as is most likely the case), $\partial J_{\text{sink}}/\partial z$ would need to be even higher. To see how this estimate compares to the actual change in flux, we can use the following values to approximate each parameter: z = the base of the mixed layer (defined as the depth of the shallower sediment trap, i.e., 238 m in March-May, 2003, 117 m in May-June, 2003, or 313 m in March-April, 2005), z^* = the base of the mesopelagic (defined as the depth of the deeper sediment trap, i.e., 771 m in March-May, 2003, 1918 m in May-June, 2003, or 924 m in March-April, 2005), and $\partial J_{\text{sink}}/\partial z$ = the decrease in fluxes between depths z and z^* .

In addition to solving for the required change in sinking particle flux with depth, we can also solve for the minimum settling velocity as follows:

$$\begin{aligned}\partial J_{\text{sink}}/\partial z &= E \\ -\omega_{\text{sink}} (\partial C_{\text{sink}}/\partial z) &= E \\ -\omega_{\text{sink}} &= E \partial z/\partial C_{\text{sink}}\end{aligned}$$

We only have flux measurements in the traps, not concentration. However, we can use the chl *a* concentration in the large (>70 μm) pump particles to estimate sinking particle concentrations. Assuming that as $z^* \rightarrow 2200$ m, $C_{\text{sink}} \rightarrow 0$ (i.e., all chl *a* in sinking particles decays by the time the particles reach the sediment-water interface):

$$\partial C_{\text{sink}} = C_{\text{sink}}(z_0) - 0$$

where $C_{\text{sink}}(z_0)$ = the chl *a* concentration in the large pump fraction at the depth closest to z_0 (the shallower trap depth), and $\partial z = 2200$ m (the base of the water column) – z_0 . We can only perform this calculation for the 2005 samples, since we did not perform organic analyses on the large pump fraction in 2003.

Table 3.3 shows the estimates for E , minimum $\partial J/\partial z$, (minimum $\partial J/\partial z$)/(actual minimum $\partial J/\partial z$), and ω_{sink} calculated for each season. In each case (except for the April, 2005 samples, when chl *a* fluxes actually increased slightly between the two trap depths), the minimum $\partial J/\partial z$ required is greater than that actually measured. The required change in fluxes with depth ranges from 7x to 210x greater than that actually measured between traps.

The required settling velocities calculated based on the initial large pump particle concentrations are also much larger (by a factor of 3x to 832x) than the modal settling velocities typically measured in the SV traps ($\sim 300\text{-}400\text{ m d}^{-1}$). These results indicate that the asymptotic chl *a* concentrations measured in suspended particles below the mixed layer cannot be supported by measured fluxes or settling velocities. Either the traps did not collect the entire flux of chl-rich material (i.e., the flux measurements are an underestimate) or some of the sinking particles have extremely high settling velocities (10^3 to 10^5 m d^{-1}), rapidly transporting rare chl-rich particles to the mesopelagic, where they then disaggregate and become part of the suspended pool.

One possible source of this rapidly-sinking, fragile, chl-rich material may be large, rapidly sinking phytoplankton aggregates or marine snow. Engel et al. (submitted, a) observed that even fairly normal-sized aggregates ($<200\text{ }\mu\text{m}$ diameter) of *Emiliani huxleyii* incubated in rotating tanks had settling velocities of up to 2200 m d^{-1} , consistent with the lower range of settling velocities estimated in the above calculation. This suggests that field observations of the settling velocities of phytoplankton aggregates may be an underestimate, perhaps because these rapidly-sinking aggregates disintegrate easily and are not sampled in sediment traps. Large mucosal fecal pellets such as those produced by salps are another possible source of rapidly-sinking material. Salps produce very large (1-10 mm) fecal pellets with settling velocities ranging from 70 to 2700 m d^{-1} (Madin, 1982; Fortier et al., 1994). We observed many salps in plankton tows collected from early to mid-March in 2003 and 2005 (S.W. Fowler and J.C. Miquel, personal communication), so they may have been important contributors to the formation of sinking particles. In order for salp fecal pellets to be a source of the deep chl *a* observed in the suspended phase, however, they must not only have high settling velocities but also contain large amounts of undigested chl *a* and disaggregate easily. It is unclear whether they can meet these latter two requirements. In laboratory grazing experiments, Nelson (1989) found more extensive pigment alteration by salps than copepods, suggesting that their fecal pellets should not be a large source of undigested chl *a*. However, other studies have observed that salp fecal pellets can be a very rich green color (Iseki, 1981) and contain high concentrations of organic carbon (13-37 weight%), suggesting that under some conditions they can contain large amounts of undigested organic matter. Differences in the sizes of prey available to salps versus crustaceans may affect the extent to which these grazers assimilate organic matter. Salps are non-selective filter feeders and can

consume much smaller particles (as low as 0.7 μm , but typically 1-2 μm) than copepods or euphasiids (several μm to tens of μm) (Fortier et al., 1994). Perhaps when large amounts of small, chl-rich particles are available as a food source (as indicated by the high suspended particle concentrations in this study), salps have a low assimilation efficiency during grazing and their fecal pellets contain large amounts of chl *a*. Finally, the requirement that salp fecal pellets disaggregate extensively seems unlikely. Large, almost fully intact salp fecal pellets are often recovered from sediment traps (Iseki, 1981; Fortier, 1994), indicating that salp fecal pellets should not be a significant source of suspended chl *a*. In addition to forming fecal pellets, however, salps produce copious mucus which may entrain organic and inorganic material, forming very large, rapidly sinking aggregates (Morris et al., 1988). Perhaps these large marine snow particles produced by salps are more susceptible to disaggregation than their fecal pellets.

4.2.3. Mass Balance Calculations: Microbially-Degraded Material and Fecal Pellets

We can perform similar calculations to estimate the extent of pheopigment exchange between suspended and sinking particles. For pheopigments, we must also include a production term due to the decay of chl *a* ($k_{\text{chl}}C_{\text{chl}}$):

$$(\partial C/\partial t)=0= (\partial J/\partial z) - kC + (k_{\text{chl}}C_{\text{chl}}) \pm E$$

In addition, the microbial degradation product phytin and fecal pellet indicators phide and pyrophide may have different rates of exchange, so we need to include a term describing the fraction of decaying chl *a* that is converted to each pheopigment:

$$0= (\partial J_{\text{phytin}}/\partial z) - kC_{\text{phytin}} + f_{\text{phytin}}(k_{\text{chl}}C_{\text{chl}}) \pm E_{\text{phytin}}$$

$$0= (\partial J_{\text{phide} + \text{pyrophide}}/\partial z) - kC_{\text{phide} + \text{pyrophide}} + (1-f_{\text{phytin}}) (k_{\text{chl}}C_{\text{chl}}) \pm E_{\text{phide} + \text{pyrophide}}$$

where f_{phytin} = the fraction of decaying chl *a* that is converted into phytin. Without knowing more about the rates of microbial and zooplankton respiration during these time periods, we cannot estimate a reasonable value for f_{phytin} ; therefore, we have used 0.5 (i.e., equal production of microbial and zooplankton products) as a rough approximation. Values for

k_{phytin} , k_{phide} , and $k_{\text{pyrophide}}$ also range widely and have not been investigated as extensively as those for chl *a*. However, studies that measured decomposition rates for both pheopigments and chl *a* (e.g., Bianchi and Findlay, 1991; Sun et al., 1994; Ingalls et al., 2004) reported rate constants for phytin, phide, and pyrophide that were on average 58%, 100%, and 75%, respectively of those measured for chl *a*. Decay constants are somewhat temperature-dependent (Sun et al., 1993); however, both chl *a* and the pheopigments would have been subjected to the same temperature range as chl *a* in the water column. Based on our k_{chl} of 0.03 to 0.2 d⁻¹ we have estimated $k_{\text{phytin}} = 0.017$ to 0.116 d⁻¹ and $k_{\text{phide}} = 0.026$ to 0.175 d⁻¹ (an average of the values calculated for phide and pyrophide).

Table 3.4 shows the estimates for E , minimum $\partial J/\partial z$, and (minimum $\partial J/\partial z$)/(actual minimum $\partial J/\partial z$) calculated for each season. For phytin, the minimum $\partial J/\partial z$ varies greatly with season. In March of 2003 and 2005, the exchange parameter and required change in fluxes with depth are negative, indicating either that decay of phytin (which we ignored) is very large, or that there is a net transfer of suspended phytin from the suspended to sinking phase. The minimum $\partial J/\partial z$ is -4x to -160x less than that actually measured between the two trap depths. In June, 2003 and April, 2005, the opposite pattern is observed. The exchange parameter and required change in fluxes with depth are positive, indicating transfer of phytin from the sinking to suspended phase via disaggregation. In June, 2003, the required $\partial J/\partial z$ is much larger (by 54x to 891x) than measured $\partial J/\partial z$. In April, 2005, the difference between the required and measured change in fluxes is small (0.03x to 0.2x). The precise values obtained by these calculations are highly dependent on f_{phytin} , the fraction of decaying chl *a* that is converted into phytin, so they may be an over- or underestimate. The value for f_{phytin} may also change seasonally as there is a shift from zooplankton to microbial breakdown of organic matter. However, the relative differences among seasons should remain the same for any value of f_{phytin} . The results of these mass balance calculations indicate that the transfer of microbially-degraded material from the sinking to suspended phase is lowest in the spring and increases as the season progresses to summer. In June, 2003, we did not detect any chl *a* in the traps; this is also when the apparent transfer of phytin from the sinking to suspended phase was greatest, indicating that this transfer was due to the disaggregation of microbially degraded phytoplankton aggregates or marine snow.

For phide + pyrophide, the exchange parameter and minimum $\partial J/\partial z$ were consistently negative, suggesting a net transfer of phide and pyrophide from the suspended to sinking phase. Again, these values are determined by the precise value used for f , but even if an f of 0 is used (i.e., assuming all decaying chl a is converted into phide + pyrophide), E and $\partial J/\partial z$ remain negative for all seasons if $k=0.03 \text{ d}^{-1}$, and for March of 2003 and 2005 assuming $k=0.2 \text{ d}^{-1}$.

The mass balance calculations suggest that the transfer of material from fecal pellets to the suspended phase via disaggregation was probably insignificant. Instead, the reverse may have occurred. It appears that there may have been a net transfer of phide and pyrophide from the suspended to sinking phase (i.e., as suspended material was altered by zooplankton and incorporated into fecal pellets, it became part of the sinking phase). In addition, there was an apparent transfer of phytin from the suspended to sinking phase during the spring, possibly due to senescent or microbially degraded algal cells aggregating due to increased production of transparent exopolymer particles (Alldredge et al., 1993; Engel et al., 2004). These calculations demonstrate that the processes associated with the alteration of phytoplankton can also result in sinking particle formation. This may be particularly true in sites such as DYFAMED, where fecal pellet production is evidently so important.

As mentioned previously, chl a concentrations decreased rapidly with depth in the 1-70 μm pool (Fig. 3.1), indicating that suspended particles underwent extensive decomposition. Nevertheless, pheopigment concentrations remained low, and pheopigment/ chl a ratios were nearly always <1 (Fig. 3.11). Conversely, there was a consistent excess of pheopigments over chl a in the sinking phase and pheopigment/ chl a ratios were usually much >1 , suggesting an external source of pheopigments in the sinking phase (Fig. 3.11). These observations support our argument that material may be transferred from the suspended to sinking phase during alteration. Zooplankton grazing could remove chl a from the suspended phase and transfer it, in the form of phide and pyrophide, to the sinking phase. Microbial degradation and production of flocculation-inducing exudates could transfer suspended algal material into sinking aggregates.

Radiocarbon analyses on DOC and POC samples from the Sargasso Sea and off the California coast (Hwang and Druffel, 2003; Hwang et al. 2006) indicate that old DOC ($\Delta^{14}\text{C}$

of ~400‰) is incorporated into particles sinking through the water column, resulting in a decrease in radiocarbon age with depth (from 40-70‰ at the surface to -40‰ by 3450 m). This DOC incorporation appears to result from biological aggregation processes (e.g., production of phytoplankton or microbial exudates, which then scavenge DOC), since it is minimal in poisoned samples (Hwang and Druffel, 2003). This supports our argument that suspended particles are incorporated into the sinking phase by biologically mediated processes, such as microbial degradation and zooplankton fecal pellet production.

Other evidence for the transfer of material from the suspended to sinking phase includes the observation that ASP and GLU often decreased with depth in the 1-70 μm particles (demonstrated by the correlation analyses for 5 of the 6 sets of 1-70 μm pump samples; Table 3.2) and increased in the sinking particles (particularly evident in the correlation analyses for the >70 μm pump samples in 2005). To assess whether this was possible on a mass basis, we calculated the change in the concentrations of ASP and GLU in the 1-70 μm particles between every depth measured in the pump profiles ($\Delta C/\Delta d$), and compared this with the concentration of ASP and GLU present within >70 μm particles in that depth range. The results indicate that at all depths where a loss of ASP and GLU from suspended particles was observed, this loss could account for >100% of the ASP and GLU measured in the >70 μm particles. This was because the concentration of amino acids was always at least an order of magnitude greater in the 1-70 μm particles than in the >70 μm particles. On a mass basis, therefore, the incorporation of calcifying algae from the suspended phase into aggregates or fecal pellets could account for the observed decrease in the suspended phase.

4.2.4. Summary of Mass Balance Calculations: Differences between Phytoplankton Aggregates and Fecal Pellets

Extensive disaggregation of phytoplankton aggregates is required to explain the high concentrations of chl *a* in suspended particles below the mixed layer. For values of k_{chl} ranging from 0.03 to 0.2 d^{-1} and Stokes settling velocities <0.5 m d^{-1} , all chl *a* in the suspended phase should have degraded within 2.5 to 17 m of the mixed layer. Inputs of rapidly-sinking chl-rich particles are required to explain the presence of chl *a* as deep as 1800

m. Conversely, extensive disaggregation of fecal pellets is unlikely, or it would lead to greater enrichment of fecal pellet indicators in the suspended phase.

There are several sources of uncertainty in these calculations, including the possibility that the system was not in steady state as we have assumed (i.e., $\partial C/\partial t \neq 0$). However, if exchange, decay, and vertical transport are fast relative to temporal changes in concentration, this may be a valid approximation. Measurement error and uncertainties in parameters such as k and f_{phytin} also contribute to uncertainties in the calculations. It is also possible that there were additional chl *a* degradation products (e.g., colorless residues) or loss terms for pheopigments (e.g., photodegradation) we have neglected. In addition, we have neglected lateral advection and both vertical and lateral diffusion in this model. This is probably acceptable with respect to vertical processes since we are integrating over most of the water column. Lateral advection was most likely minimal at this location. The northwest Mediterranean is enclosed by a gyre (Marty, 2002) that limits lateral advection into and out of the site, and the region has small tidal excursions (<20 cm) (Misic and Fabiano, 2005). In addition, Anderson and Prier (2000) conducted a one-month study (May, 1995) of current speeds at DYFAMED and observed that current speeds at 200 and 1000 m were usually below the minimum detectable speed (3 cm s^{-1}) and never above 10 cm s^{-1} . If significant lateral advection does occur, we would expect it to be greater for aggregates, whereas the compact, cylindrical shape of fecal pellets should cause them to sink more vertically. Differences in lateral advection of aggregates and fecal pellets could have contributed to differences in their collection efficiency in traps. If rare, large phytoplankton aggregates are transported laterally and then disaggregate, this could contribute to the excess suspended chl *a* below the mixed layer.

Knowing the precise residence time (i.e., age) of the suspended particles in the water column would help us constrain the magnitude of sinking particle dissolution. The age of suspended particles could be determined by radioisotope analyses. We do not have ^{14}C measurements, but in the future, we are planning to compare ^{228}Th and ^{234}Th in the suspended and sinking particles collected during these years to determine the relative ages of both types of material. We would normally expect the residence time, and therefore the age, of smaller organic particles to be greater than that of larger organic particles. In many regions, dissolved organic carbon, which is even smaller than suspended POC, has a ^{14}C age that is hundreds of years greater than that of sinking particles (e.g., Hwang and Druffel,

2003; Hwang et al. 2006), consistent with this expectation. However, the presence of large amounts of chl *a* in the suspended phase indicates suspended particles are actually relatively young, indicating rapid exchange with chl-rich sinking particles.

5. Conclusions

The results of this study suggest that zooplankton fecal pellets at DYFAMED undergo little disaggregation and exchange with suspended particles during transit through the water column. It is possible that fecal pellets partially disaggregate but continued to sink (as suggested by the similarity in composition of the SV trap samples); however, complete disaggregation to the suspended phase seems unlikely based on the large compositional differences between suspended and sinking particles. Particle exchange at locations where production and zooplankton grazing are closely coupled may therefore be characterized by a net transfer of material from the suspended to sinking phase, followed by eventual decomposition or deposition at the sediment-water interface. This transfer of material to the sinking phase should be particularly important during the spring, when phytoplankton and zooplankton biomass are high. Fecal pellets sinking out of the mixed layer contain material that is already substantially altered by zooplankton at the surface, but apparently do not undergo much subsequent alteration with depth. Although microbial decomposition and dissolution undoubtedly occur in fecal pellets, these processes are likely much less extensive than they would be if particles underwent extensive disaggregation, which would result in longer residence times in the water column. Therefore, fecal pellets provide a relatively efficient mechanism for the export of sinking particles to the deep sea, reducing the extent of further degradation. This is important both for the drawdown of CO₂ from the atmosphere, as well as the use of biomarkers in the deep sea to reconstruct processes occurring higher in the water column.

The relative compositions of organic biomarkers (this study and Wakeham et al., submitted) as well as minerals (Lee et al., submitted) in sinking particles remained largely unchanged with depth, and appear to have been determined in the mixed layer. This indicates that mechanisms of sinking particle formation at DYFAMED, such as biological packaging into egested material and abiotic aggregation, are mainly controlled by the availability of organic material at the surface. The flux of material to the deep sea therefore reflects the history of processes occurring at the surface (i.e., production, grazing,

rem mineralization, and photodegradation) rather than new particle formation within the mesopelagic. Other studies of particle fluxes support this assertion, finding little evidence for substantial fecal pellet production in the mesopelagic (Bacon et al., 1984; Pilskaln and Honjo, 1987; Silver and Gowing, 1991).

The transport of phytoplankton aggregates through the water column does not appear to have been as efficient as for fecal pellets (i.e., transport may be slower relative to decomposition). Unlike robust fecal pellets, fractal phytoplankton flocs may be much more susceptible to disaggregation. We could not precisely distinguish between fecal pellets and phytoplankton aggregates in our mass balance calculations, since we only have bulk chemical measurements. However, if we assume that most chl *a* was present in sinking phytoplankton aggregates rather than fecal pellets, then the preferential disaggregation of phytoplankton aggregates could result in the transfer of fresh, chl-rich material from the sinking to suspended phase, explaining the fresh composition of suspended particles below the euphotic zone. Incubation experiments performed on DYFAMED particles in 2006 (see Chapter 4) support this hypothesis; phytoplankton aggregates incubated in rotating tanks appear to have undergone more extensive exchange with surrounding particles than fecal pellets.

Furthermore, our findings have significant implications for the use of the $>70 \mu\text{m}$ cutoff in the literature to represent export production (Cochran and Masqué, 2003). The similarity in composition between the $>70 \mu\text{m}$ pump and trap samples in 2005 indicate that both sampling mechanisms do indeed collect a similar pool of material, presumably sinking particles. It also suggests that the differences we observed between the 1-70 μm pump samples and traps were not due to sampling artifacts, but rather to actual differences in the particles present in each pool. Our subsequent drying experiments suggest that the $>70 \mu\text{m}$ pump samples were not extensively altered by drying prior to organic analyses.

The results of this study highlight that biological community structure is a critical factor controlling POC export from the surface to deep ocean. Future studies simultaneously measuring particle fluxes as well as phytoplankton and zooplankton community dynamics in a range of environments would allow for better understanding of POC export under different environmental conditions.

References

- Anderson, R.F., Bacon, M.P., Brewer, P.G., 1983. Removal of ^{230}Th and ^{231}Pa from the open ocean. *Earth and Planetary Science Letters* 62, 7-23.
- Andersen, V., Nival, P., Caparroya, C. P., Gubanova, A., 2001a. Zooplankton community during the transition from spring bloom to oligotrophy in the open NW Mediterranean and effects of wind events. 1 - Abundance and specific composition. *Journal of Plankton Research* 23, 227-242.
- Andersen, V., Gubanova, A., Nival, P., Ruellet, T., 2001b. Zooplankton community during the transition from spring bloom to oligotrophy in the open NW Mediterranean and effects of wind events. 2 - Vertical distributions and migrations. *Journal of Plankton Research* 23. 243-261.
- Armstrong, R.A., Peterson, M.L., Lee, C., Wakeham, S.G. Settling velocity spectra and the ballast ratio hypothesis. Submitted to *Deep-Sea Research II*.
- Bacon, M.P., Anderson, R.F., 1982. Distribution of thorium isotopes between dissolved and particulate forms in the deep sea, *Journal of Geophysical Research- Oceans* 87, 2045–2056.
- Bacon, M.P., Huh, C., Fleer, A.P., Deuser, W.G., 1985. Seasonality in the flux of natural radionuclides and plutonium in the deep Sargasso Sea. *Deep-Sea Research Part A* 3, 273-286.
- Baliño, B.M., Fasham, M. J. R., Bowles, M.C. (eds.), 2001. *Ocean biogeochemistry and global change. International Geosphere-Biosphere Programme (IGBP): A study of global change of the international council of Science (ICSU)*, Stockholm, Sweden.
- Barlow, R. G., Mantoura, R. F. C., Cummings, D. G., Fileman, T. W., 1997. Pigment chemotaxonomic distributions of phytoplankton during summer in the western Mediterranean. *Deep-Sea Research II* 44, 833-850.
- Bianchi, T.S., Dawson, R., Sawangwong, P., 1988. The effects of macrobenthic deposit-feeding on the degradation of chloropigments in sandy sediments. *Journal of Experimental Marine Biology and Ecology* 122 (3), 243-255.
- Bianchi, T.S., Findlay, S. 1991. Decomposition of Hudson estuary macrophytes: photosynthesis pigment transformation and decay constants. *Estuaries* 14, 65-73.
- Bidle, K., Azam, F., 1999. Accelerated silica dissolution by marine bacterial assemblages. *Nature* 397, 508-512.
- Bidle, K., Manganelli, M., Azam, F., 2002. Regulation of ocean silicon and carbon preservation by temperature control on bacteria. *Science* 298, 1980-1984.

- Bidigare, R.R., Kennicutt, M.C., Brooks, J.M., 1985. Rapid determination of chlorophylls and their degradation products by high-performance liquid chromatography. *Limnology and Oceanography* 30, 432-435.
- Bienfang, P.K., 1981. Phytoplankton sinking rates in oligotrophic waters off Hawaii. *Marine Biology* 61, 69-77.
- Bishop, J.K.B., Collier, R.W., Ketten D.R., Edmond, J.M., 1980. The chemistry, biology, and vertical flux of particulate matter from the upper 1500 m of the Panama Basin. *Deep-Sea Research Part A* 27, 615-640.
- Buesseler K.O., Bacon, M.P., Cochran, J.K., Livingston, H.D., 1992. Carbon and nitrogen export during the JGOFS North Atlantic Bloom Experiment estimated from ^{234}Th : ^{238}U disequilibrium. *Deep-Sea Research* 39, 1115-1137.
- Burns, N.M., Rosa, F., 1980. *In situ* measurement of the settling velocity of organic carbon particles and 10 species of phytoplankton. *Limnology and Oceanography* 25, 855-864.
- Carroll, M.L., Miquel, J.C., Fowler, S.W., 1998. Seasonal patterns and depth-specific trends of zooplankton fecal pellet fluxes in the Northwestern Mediterranean Sea. *Deep-Sea Research I* 45, 1303-1318.
- Cho, B.C., Azam, F., 1988. Major role of bacteria in biogeochemical fluxes in the ocean's interior. *Nature* 332, 336-338.
- Claustre, H., Kerhervé, P., Marty, J.-C., Prieur, L., Videau, C., Hecq, J.-H., 1994. Phytoplankton dynamics associated with a geostrophic front: ecological and biogeochemical implications. *Journal of Marine Research* 52, 711-742.
- Currie, R., 1962. Pigments in zooplankton faeces. *Nature* 193, 956-957.
- Cochran, J.K., Masqué, P. 2003. Short-lived U/Th series radionuclides in the ocean: Tracers for scavenging rates, export fluxes, and particle dynamics. p. 461-487. In: Bourdon, B., Henderson, G.M., Lundstrom, C.C., and Turner, S.P. (eds) *Reviews in Mineralogy and Geochemistry* 52.
- Cochran, J.K., Miquel, J.-C., Fowler, S., Gasser, B., Hirschberg, D., Szlosek, J., Rodriguez y Baena, A.M., Armstrong, R., Stewart, G., and Masqué, P.(eds) Time-series measurements of ^{234}Th in water column and sediment trap samples from the Northwestern Mediterranean. Submitted to *Deep-Sea Research II*.
- Cohen, J., 1988. *Statistical power analysis for the behavioral sciences* (2nd ed.). Lawrence Erlbaum Associates, Hillsdale, NJ.
- Cowie, G.L., Hedges, J.I., 1996. Digestion and alteration of the biochemical constituents of a diatom (*Thalassiosira weissflogii*) ingested by an herbivorous zooplankton (*Calanus pacificus*). *Limnology and Oceanography* 41, 581-594.

- Daley, R.J. 1973. Experimental characterization of lacustrine chlorophyll diagenesis. II. Bacterial, viral and herbivore grazing effects. *Archiv für Hydrobiologie* 72, 409-439.
- D'Ortenzio, F., Iudicone, D., de Boyer Montegut, Clement, Testor, P., Antoine, D., Marullo, S., Santoleri, R., Madec, G., 2005. Seasonal variability of the mixed layer depth in the Mediterranean Sea as derived from in situ profiles. *Geophysical Research Letters* 32, L12605, doi:10.1029/2005GL022463.
- Engel, A., Szlosek, J., Abramson, L., Liu, Z., Lee, C. Decomposition of calcifying and non-calcifying *Emiliana huxleyi* (Prymnesiophyceae): II. Formation, settling velocities and physical properties of aggregates. Submitted to *Deep-Sea Research II* (a).
- Engel, A., Abramson, L., Szlosek, J., Liu, Z., Stewart, G., Hirschberg, D., Lee, C. Investigating the effect of ballasting by CaCO₃ in *Emiliana huxleyi*: II. Decomposition of particulate organic matter. Submitted to *Deep-Sea Research II* (b).
- Eppley, R.W., Holmes, R.W., Strickland, J.D., 1967. Sinking rates of marine phytoplankton measured with a fluorometer. *Journal of Experimental Marine Biology and Ecology* I, 191-208.
- Fabres, J. Tesi, T., Velez, J., Batista, F., Lee, C., Calafat, A., Heussner, S., Miserocchi, S., Palanques, A. Seasonal and event controlled export of fresh organic matter from the shelf towards the Gulf of Lions continental slope. Submitted to *Continental Shelf Research*.
- Faugeras, B., Lévy, M., Mémery, L., Verron, J., Blum, J., Charpentier, I., 2003. Can biogeochemical fluxes be recovered from nitrate and chlorophyll data? A case study assimilating data in the Northwestern Mediterranean Sea at the JGOFS-DYFAMED station. *Journal of Marine Systems* 40-41, 99-125.
- Fasham, M.J.R., Baliño, B. M., Bowles, M. C. (eds). 2001. A new vision of ocean biogeochemistry after a decade of the Joint global Ocean flux study (JGOFS). *Ambio Special Report* 10.
- Forster, G.R. 1953. Peritrophic membranes in the *Carida* (Crustacea Decapoda). *Journal of the Marine Biological Association of the United Kingdom* 32, 315-318.
- Fortier, L., Le Fèvre, J., Legendre, L., 1994. Export of biogenic carbon to fish and to the deep ocean: the role of large planktonic microphages. *Journal of Plankton Research* 16, 809-839.
- François, R., Honjo, S., Krishfield, R., Manganini, S., 2002. Factors controlling the flux of organic carbon to the bathypelagic zone of the ocean. *Global Biogeochemical Cycles* 16, 1087.
- Fowler, S. W., Small, L. F., La Rosa, J., 1991. Seasonal particulate carbon flux in the coastal northwestern Mediterranean Sea, and the role of zooplankton fecal matter. *Oceanologica Acta* 14, 77-85.

- Gardener, W.D., 2000. Sediment trap sampling in surface waters. P. 240-281. In Hanson, R.B., Ducklow, H.W., and Fields, J.G. (Eds). The changing ocean carbon cycle: A midterm synthesis of the Joint Ocean Flux Study. Cambridge University Press.
- Goutx, M., Wakeham, S.G., Lee, C., Duflos, M., Guigue, C., Liu, Z., Moriceau, B., Sempéré, R., Tedetti, M., Xue, J., 2007. *Limnology and Oceanography* 52, 1645-1664.
- Hecky, R.E., Mopper, K., Kilham, P., Degens, E.T., 1973. The amino acid and sugar composition of diatom cell-walls. *Marine Biology* 19, 323-331.
- Hedges, J.I., Baldock, J.A., Gélinas, Y., Lee, C., Peterson, M. and Wakeham, S. 2001. Evidence for the non-selective preservation of organic matter in sinking marine particles. *Nature* 409, 801-804.
- Hendry, G.A.F., Houghton, J.D., and Brown, S.B. 1987. The degradation of chlorophyll – A biological enigma. *New Phytologist* 107, 255-302.
- Hill, P.S., 1998. Controls on floc size in the sea. *Oceanography* 11, 13-18.
- Honjo, S., 1976. Coccoliths: Production, transportation and sedimentation. *Marine Micropaleontology* 1, 65-79.
- Honjo, S., 1978. Sedimentation of materials in the Sargasso Sea at a 5867-m deep station. *Journal of Marine Research* 36, 469-492.
- Honjo, S., 1996. Fluxes of particles to the interior of the open oceans. In: Ittekkot, V., Schäfer, P., Honjo, S., Depetris, P.J. (eds.) *Particle Flux in the Ocean, SCOPE Vol. 57*. John Wiley & Sons, New York, p. 91-154.
- Honjo, S., Roman, M.R., 1978. Marine copepod fecal pellets: production, preservation and sedimentation. *Journal of Marine Research* 36, 45-57.
- Hwang, J., Druffel, E.R.M., 2003. Lipid-like material as the source of the uncharacterized organic carbon in the ocean? *Science* 299, 881-884.
- Hwang, J.S., Druffel, E.R.M., Bauer, J.E., 2006. Incorporation of aged dissolved organic carbon (DOC) by oceanic particulate organic carbon (POC): An experimental approach using natural carbon isotopes. *Marine Chemistry* 98: 315-322.
- Ingalls, A.E., Aller, R.C., Lee, C., Sun, M.Y., 2000. The influence of deposit-feeding on chlorophyll-*a* degradation in coastal marine sediments. *Journal of Marine Research* 58, 631-651.
- Ingalls, A.E., Lee, C., Wakeham, S.G., Hedges, J.I., 2003. The role of biominerals in the sinking flux and preservation of amino acids in the Southern Ocean along 170°W. *Deep-Sea Research II* 50:709-734.

- Iseki, K., 1981. Particulate organic matter transport to the deep sea by salp fecal pellets. *Marine Ecology Progress Series* 5, 55-60.
- Jamart, B.M., Winterg, D.F., Anderson, C., Lam, R.K., 1977. A theoretical study of phytoplankton growth and nutrient distribution in the Pacific Ocean off the northwestern U.S. coast. *Deep-Sea Research* 24: 753-773.
- Jeffrey, S.W., Vesk, M., 1981. The phytoplankton – systematics, morphology and ultrastructure. In: Clayton, M.N., King, R.J. (eds.), *Marine botany – an Australian perspective*. Longman-Cheshire, Melbourne, Australia. pp. 138-179.
- Johannes, R.E., Satomi, M. 1966. Composition and nutritive value of fecal pellets of a marine crustacean. *Limnology and Oceanography* 11, 91-197.
- Karl, D.M., Knauer, G.A., Martin, J.H., 1988. Downward flux of particulate organic matter in the ocean: a particle decomposition paradox. *Nature* 332, 438-441.
- Khelifa, A., Hill, P.S., 2006. Models for effective density and settling velocity of flocs. *Journal of Hydraulic Research* 44, 390–401.
- King, K., Jr., 1974. Preserved amino acids from silicified protein in fossil radiolaria. *Nature* 252, 690-692.
- King L.L., 1993 Chlorophyll diagenesis in the water column and sediment of the Black Sea. Dissertation, Massachusetts Institute of Technology.
- Klaas, C., Archer, D.E., 2002. Association of sinking organic matter with various types of mineral ballast in the deep sea: Implications for the rain ratio. *Global Biogeochemical Cycles* 16, 1116.
- Klein, B.W., Gieskes, W.C., Kraay, G.G., 1986. Digestion of chlorophylls and carotenoids by the marine protozoan *Oxyrrhis marina* studied by H.P.L.C. analysis of algal pigments. *Journal of Plankton Research* 8, 827-836.
- Leavitt, P.R., Carpenter, S.R., 1990. Aphotic pigment degradation in the hypolimnion: implications for sedimentation studies and paleolimnology. *Limnology and Oceanography* 35, 520-534.
- Lee C., Cronin, C., 1982. The vertical flux of particulate nitrogen in the sea: Decomposition of amino acids in the Peru upwelling area and the equatorial Atlantic. *Journal of Marine Research* 40, 227-251.
- Lee, C., Cronin, C., 1984. Particulate amino acids in the sea: Effects of primary productivity and biological decomposition. *Journal of Marine Research* 42, 1075-1097.
- Lee, C., Wakeham, S.G., 1988. Organic matter in seawater: Biogeochemical processes. In: Riley, J.P. (ed.), *Chemical Oceanography* 9, Academic Press. pp. 1-51.

- Lee, C., Wakeham, S.G., Hedges, J.I., 2000. Composition and flux of particulate amino acids and chloropigments in equatorial Pacific seawater and sediments. *Deep-Sea Research I* 47, 1535–1568.
- Lee, C., Peterson, M.L, Wakeham, S.G., Armstrong, Cochran, J.K., Miquel, J.C., Armstrong, R.A., Fowler, S., Hirschberg, D., Beck, A., Xue, J. Particulate organic matter and ballast fluxes measured using Time-Series and Settling Velocity sediment traps in the northwestern Mediterranean Sea. Submitted to *Deep-Sea Research II*.
- Liu, Z., Cochran, J.K., Lee, C., Gasser, B., Miquel, J.C., Wakeham, S.G. Further investigations on why POC concentrations differ in samples collected by Niskin bottle and *in situ* pump. Submitted to *Deep-Sea Research II*.
- Lorenzen, C.J., 1967. Vertical distribution of chlorophyll and phaeopigments: Baja California. *Deep-Sea Research* 14, 735-745.
- Lorenzen, 1968. Carbon/ chlorophyll relationships in an upwelling area. *Limnology and Oceanography* 13, 202-204.
- Lorenzen, C.J., Welschmeyer, N.A., 1983. The *in situ* sinking rates of herbivore fecal pellets. *Journal of Plankton Research* 5, 929-933.
- Lorenzen, C.J., Welschmeyer, N.A., Copping, A.E., Vernet, M., 1984. Sinking rates of organic particles. *Limnology and Oceanography* 28, 766-769.
- Madin, L.P., 1982. Production, composition and sedimentation of salp fecal pellets in oceanic waters. *Marine Biology* 67, 39-45.
- Mantoura, R.F.C., Llewellyn, C. A., 1984. Trace enrichment of marine algal pigments for use with HPLC-diode array spectroscopy. *Journal of High Resolution Gas Chromatography and Chromatography Communications* 7, 632- 635.
- Marty, J.C. 2002. The DYFAMED time-series program (French JGOFS). *Deep-Sea Research II* 49, 1963-1964.
- Marty, J.C., Chiavérini, J., Pizay, M. D., Avril, B., 2002. Seasonal and interannual dynamics of nutrients and phytoplankton pigments in the western Mediterranean sea at the DYFAMED time-series station (1991-1999) *Deep-Sea Research* 49, 1965-1985.
- McCave, I.N., 1984. Size spectra and aggregation of suspended particles in the deep ocean. *Deep-Sea Research* 31, 329-252.
- Misic, C., Fabiano, M., 2005. Enzymatic activity on sandy beaches of the Ligurian Sea (NW Mediterranean). *Microbial Ecology* 49 (4), 513-522.
- Miquel J.C., Fowler, S. W., La Rosa, J., Buat-Menard, P., 1994. Dynamics of the downward flux of particles and carbon in the open northwestern Mediterranean Sea. *Deep-Sea Research* 41, 243-261.

- Miquel, J.C., La Rosa, J., 1999. Suivi à long term des flux particulaires au site DYFAMED (mer Ligure, Méditerranée occidentale). *Océanis* 25, 303-318.
- Morris, R.J., Bone, Q., Head, R., Braconnot, J.C., Nival, P., 1988. Role of salps in the flux of organic matter to the bottom of the Ligurian Sea. *Marine Biology* 97, 237-241.
- Nelson, J.R., 1989. Phytoplankton pigments in macrozooplankton feces: variability in carotenoid alterations. *Marine Ecology Progress Series* 52, 129-144.
- Nival, P., Nival, S., Thiriot, A., 1975. Influences des conditions hivernales sur les productions phyto- et zooplanctoniques en Méditerranée nord-occidentale. V. Biomasse et production zooplanctonique Relations phyto-zooplancton. *Marine Biology* 31, 249-270.
- Passow, U., De La Rocha, C., 2006. The accumulation of mineral ballast on organic aggregates. *Global Biogeochemical Cycles* 20, GB1013, doi:10.1029/2005GB002579.
- Peterson, M.L., Fabres, J., Wakeham, S.G., Lee, C., Miquel, J.C. Sampling the vertical particle flux in the upper water column using a large diameter free-drifting NetTrap adapted to an Indented Rotating Sphere sediment trap. Submitted to *Deep-Sea Research II*.
- Peterson, M.L., Hernes, P.J., Thoreson, D.S., Hedges, J. I., Lee, C., Wakeham, S.G., 1993. Field evaluation of a valved sediment trap. *Limnology and Oceanography* 38, 1741-1761.
- Peterson, M.L., Wakeham, S. G., Lee, C., Askea, M., Miquel, J.C., 2005. Novel techniques for collection of sinking particles in the ocean and determining their settling rates. *Limnology and Oceanography Methods* 3, 520-532.
- Pilskaln, C.H., Honjo, S., 1987. The fecal pellet fraction of biogeochemical particle fluxes to the deep sea. *Global Biogeochemical Cycles*, 1, 31-48.
- Price, N.B., Brand, T., Pates, J.M., Mowbray, S., Theocharis, A., Civitarese, G., Misericchi, S., Heussner, S., Lindsay, F., 1999. Horizontal distributions of biogenic and lithogenic elements of suspended particulate matter in the Mediterranean Sea. *Progress in Oceanography* 44, 191-218.
- Reeve, M.R. 1963. The filter-feeding of *Artemia*. III. Faecal pellets and their associated membranes. *Journal of Experimental Biology* 40, 215-221.
- Repeta, D.J., Gagosian, R.B., 1984. Transformation reactions and recycling of carotenoids and chlorines in the Peru upwelling region (15°S, 75°W). *Geochimica et Cosmochimica Acta* 48, 1265-1277.
- Roth, P.H., Mullinand, M.M., Berger, W.H., 1975. Coccolith sedimentation by fecal pellets: laboratory experiments and field observations. *Geological Society of America Bulletin* 86, 1079-1084.

- Sheridan, C.C., Lee, C., Wakeham, S.G., Bishop, J.K.B., 2002. Suspended particle organic composition and cycling in surface and midwaters of the equatorial Pacific Ocean. *Deep-Sea Research I* 49, 1983-2008.
- Shuman, F.K., Lorenzen, C.J., 1975. Quantitative degradation of chlorophyll by a marine herbivore. *Limnology and Oceanography* 20, 580-286.
- Silver, M.W., Gowing, M.M., 1991. The "particle" flux: origins and biological components. *Progress in Oceanography* 26 (1), 75-113.
- Smayda, T.J., 1970. The suspension and sinking of phytoplankton in the sea. *Oceanography and Marine Biology Annual Review* 8, 353-414.
- SooHoo, J.B., Kiefer, D.A., 1982. Vertical distribution of phaeopigments. I. A simple grazing and photooxidative scheme for small particles. *Deep-Sea Research* 29, 1539-1551.
- Sun, M., Aller, R.C., Lee, C., 1991. Early diagenesis of chlorophyll-a in Long Island Sound sediments: a measure of carbon flux and particle reworking. *Journal of Marine Research* 49, 379-401.
- Sun, M., Aller, R.C., Lee, C., 1993. Laboratory studies of oxic and anoxic degradation of chlorophyll-*a* in Long Island Sound sediments. *Geochimica Cosmochimica Acta* 57, 147-157.
- Sun, M., Aller, R.C., and Lee, C. 1994. Spatial and temporal distributions of sedimentary chloropigments as indicators of benthic processes in Long Island Sound. *Journal of Marine Research* 52, 149-176.
- Szlosek, J.E., Cochran, J.K. Miquel, J.C., Masqué, P., Armstrong, R.A., Fowler, S.W.. Particulate Organic Carbon-²³⁴Th relationships in particles separated by settling velocity in the Northwest Mediterranean. Submitted to *Deep-Sea Research II*.
- Swift, D.M., Wheeler, P., 1991. Evidence of an organic matrix from diatom biosilica. *Journal of Phycology* 28, 202-209.
- Tamburini, C., Goutx, M., Guigue, C., Garel, M., Lefèvre, D., Charrière, B., Sempéré, R., Pepa, S., Peterson, M.L., Wakeham, S.G., Lee, C., Novel technique to simulate particles falling through the water column: Evaluation of pressure effects on organic matter mineralization by prokaryotes. Submitted to *Deep-Sea Research II*.
- Vernet, M., 1991. Phytoplankton dynamics in the Barents Sea estimated from chlorophyll budget models. *Polar Research* 10, 129-145.
- Vidussi, F., Marty, J.-C., Chiavérini, J., 2000. Phytoplankton pigment variations during the transition from spring bloom to oligotrophy in the northwestern Mediterranean Sea. *Deep-Sea Research I* 47, 423-445.
- Wakeham, S.G., Canuel, E.A., 1988. Organic geochemistry of particulate matter in the

- eastern tropical North Pacific Ocean: implications for particle dynamics. *Journal of Marine Research* 46, 183–213.
- Wakeham, S.G., Hedges, J.I., Lee, C., Peterson, M.L., Hernes, P.J., 1997. Composition and transport of lipid biomarkers through the water column and surficial sediments of the equatorial Pacific Ocean. *Deep-Sea Research II* 44, 2131-2162.
- Wakeham, S.G., Lee, C., 1993. Production, transport, and alteration of particulate organic matter in the marine water column. In: Engel, M.H., Macko, S.A. (eds.) *Organic Geochemistry*, Plenum Press. pp. 145-169.
- Wakeham, S.G., Lee, C., Peterson, M.L., Liu, Z., Szlosek, J., Putnam, I., Xue, J. Organic compound composition and fluxes in the Twilight Zone - time series and settling velocity sediment traps during MEDFLUX. Submitted to *Deep-Sea Research II*.
- Weiner, S. and Erez, J., 1984. Organic matrix of the shell of the foraminifer, *Heterostegina depressa*. *Journal of Foraminiferal Research* 14, 206-212.
- Welschmeyer, N.A., Lorenzen, C.J., 1985. Chlorophyll budgets: Zooplankton grazing and phytoplankton growth in a temperate fjord and the Central Pacific Gyres. *Limnology and Oceanography* 30, 1-21.
- Xue, J., Armstrong, R.A. An improved “benchmark” method for estimating particle settling velocities from time-series sediment trap fluxes. Submitted to *Deep-Sea Research II*.

Table 3.1. Dates and Depths of Sample Collection in 2003 and 2005				
Abbreviations: TS= time-series sediment trap, SV= settling velocity sediment trap, LP= >70 μ m pumps, SP= 1-70 μ m pumps				
2003				
March	April	May	June	
TS: 238 m and 771 m (Mar. 6-May 6)		TS: 117 m and 1918 m (May 14- Jun. 30)		
SV (x2): 238 m (Mar. 6-May 6)		SV: 117 m (May 14- Jun. 30)		
SP: 0-800 m (Mar.4-10)		SP: 2-1400 m May 7-12	SP: 2-1800 m Jun. 30	
2005				
March	April	May	June	
TS: 313 m and 924 m (Mar. 4- May 1)				
SV (x2): 313 m, 524 m, and 1918 m (Mar. 4-May 1)				
LP: 5-500 m (Mar. 2)	LP: 2-1800 m (Mar. 9-14)	LP: 0-750 m (Apr. 29-30)		
SP: 5-500 m (Mar. 2)	SP: 2-1800 m (Mar. 9-14)	SP: 0-750 m (Apr. 29-30)		

Table 3.1. Dates and depths at which time-series trap (TS), settling velocity trap (SV), >70 μ m pump (LP), and 1-70 μ m pump (SP) samples were collected.

Table 3.2. Pearson's Correlation Coefficients for Changes in Composition with Settling Velocity (SV Traps) and Depth (Pumps)												
Correlations with Settling Velocity (SV Traps)												
Sample	fuco	chl a	phytin	phide	pyrophide	ASP	GLU	SER	THR	GLY	BALA	GABA
2003												
Mar. 6-May 6 (238 m)	-0.64	-0.46	0.31	-0.42	0.49	ns	0.61	ns	0.97	ns	-0.74	-0.79
May 14-June 30 (117 m)	-0.85	-0.32	0.69	0.57	ns	0.54	ns	ns	ns	-0.43	-0.86	-0.63
2005												
Mar. 4-May 1 (313 m)	-0.67	0.31	0.90	0.70	-0.80	ns	ns	ns	ns	ns	-0.34	-0.60
Mar. 4-May 1 (524 m)	0.84	0.76	ns	ns	-0.58	ns	ns	-0.38	ns	ns	ns	-0.34
Mar. 4-May 1 (1918 m)	0.47	0.73	0.68	ns	-0.80	ns	ns	-0.67	0.78	ns	-0.91	-0.68
Correlations with Depth (1-70 µm Pumps)												
Sample	fuco	chl a	phytin	phide	pyrophide	ASP	GLU	SER	THR	GLY	BALA	GABA
2003												
Mar. 4-10 (0-800 m)	ns	ns	ns	ns	ns	ns	-0.59	ns	0.78	0.50	ns	0.85
May 7-12 (2-1400 m)	-0.42	-0.85	0.93	ns	0.32	-0.58	-0.51	0.33	ns	ns	0.71	0.37
Jun. 30 (2-1800 m)	ns	-0.65	0.83	ns	ns	-0.62	-0.87	-0.65	ns	ns	0.42	0.33
2005												
Mar. 2 (5-500 m)	-0.81	0.85	-0.42	0.64	0.80	ns	-0.50	ns	0.41	0.75	0.56	ns
Mar. 9-14 (2-1800 m)	0.58	-0.84	0.52	0.74	0.83	-0.24	-0.61	0.75	ns	0.74	0.53	0.82
Apr. 29-30 (0-750 m)	-0.61	nsns	ns	0.75	0.87	0.79	ns	0.90	-0.59	0.84	0.83	ns
Correlations with Depth (>70 µm Pumps)												
Sample	fuco	chl a	phytin	phide	pyrophide	ASP	GLU	SER	THR	GLY	BALA	GABA
2005												
Mar. 2 (5-500 m)	indeterminable due to the small # of samples above detection limits (n=2)											
Mar. 9-14 (2-1800 m)	ns	0.61	ns	ns	0.38	ns	0.30	ns	-0.76	0.35	0.95	ns
Apr. 29-30 (0-750 m)	-0.75	0.48	ns	0.63	0.87	0.70	0.79	-0.73	ns	-0.37	0.62	-0.72

Table 3.2. Pearson's correlation coefficients for changes in composition with settling velocity (for SV traps) and depth (for pumps) for all seasons in 2003 and 2005. Strong positive or negative correlations ($r=0.50$ to 1.00 or -0.50 to -1.00) are shown in bold, moderate positive or negative correlations ($r=0.30$ to 0.49 or -0.30 to -0.49) in regular text, and results that were not significant are labeled 'ns.'

Table 3.3. Exchange or Settling Velocities of Sinking Particles Required to Explain Suspended Chlorophyll <i>a</i> below the Mixed Layer								
Date	Asymptote in Suspended Phase [C _{susp} (z*) as z*→∞] (μmol C m ⁻³)	Exchange Required to Balance Decay [E=kC _{susp} (z*)] (μmol C m ⁻³ d ⁻¹)	Minimum Loss from Sinking Phase to Balance Exchange [∂J _{sink} /∂z=E, assuming kC _{sink} (z*)=0] (μmol C m ⁻² d ⁻¹)	Measured Loss from Shallow to Deep Trap [∂J _{sink} /∂z] (μmol C m ⁻² d ⁻¹)	Difference between Required & Measured Loss from Sinking Phase	[chl <i>a</i>] in Large Particles Near Shallow Trap [C _{sink} (z)] (μmol C m ⁻³)	Settling Velocity Required to Achieve Calculated Exchange [-ω _{sink} = E ∂z/C _{sink} (z)] (m d ⁻¹)	Difference between Required & Measured Settling Velocities (≈ 350 m d ⁻¹)
chl <i>a</i> (assuming k=0.03 to 0.2 d⁻¹):								
2003								
Mar. 4-10 Pumps, Mar. 6-11 Traps	0.15	4.4 x10 ⁻³ to 2.9 x10 ⁻²	8.8 to 59	1.3	7x to 44x	large pump data not available for 2003		
May 7-12 Pumps, Apr. 30- May 6 Traps	0.19	5.7 x10 ⁻³ to 3.8 x10 ⁻²	4.6 to 31	1.1	4x to 28x			
Jun. 30 Pumps, Jun. 25-30 Traps	0.22	6.6 x10 ⁻³ to 4.4 x10 ⁻²	9.9 to 66	nd in either trap				
2005								
Mar. 2 Pumps, Mar. 4-9 Traps	0.65	2.0 x10 ⁻² to 1.3 x10 ⁻¹	3.9 to 65	0.4	9x to 148x	8.6 x10 ⁻⁷	4.4 x10 ⁴ to 2.9 x10 ⁵	125x to 832x
Mar. 9-14 Pumps, Mar. 9-14 Traps	0.54	1.6 x10 ⁻² to 1.1 x10 ⁻¹	25 to 163	0.8	31x to 210x	1.3 x10 ⁻⁶	2.3 x10 ⁴ to 1.5 x10 ⁵	66x to 440x
Apr. 29-30 Pumps, Apr. 23-29 Traps	0.02	6.2 x10 ⁻⁴ to 4.1 x10 ⁻³	0.3 to 1.9	-0.2 (flux increased)	-2x to -11x	9.7 x10 ⁻⁷	1.2 x10 ³ to 8.1 x10 ³	3x to 23x

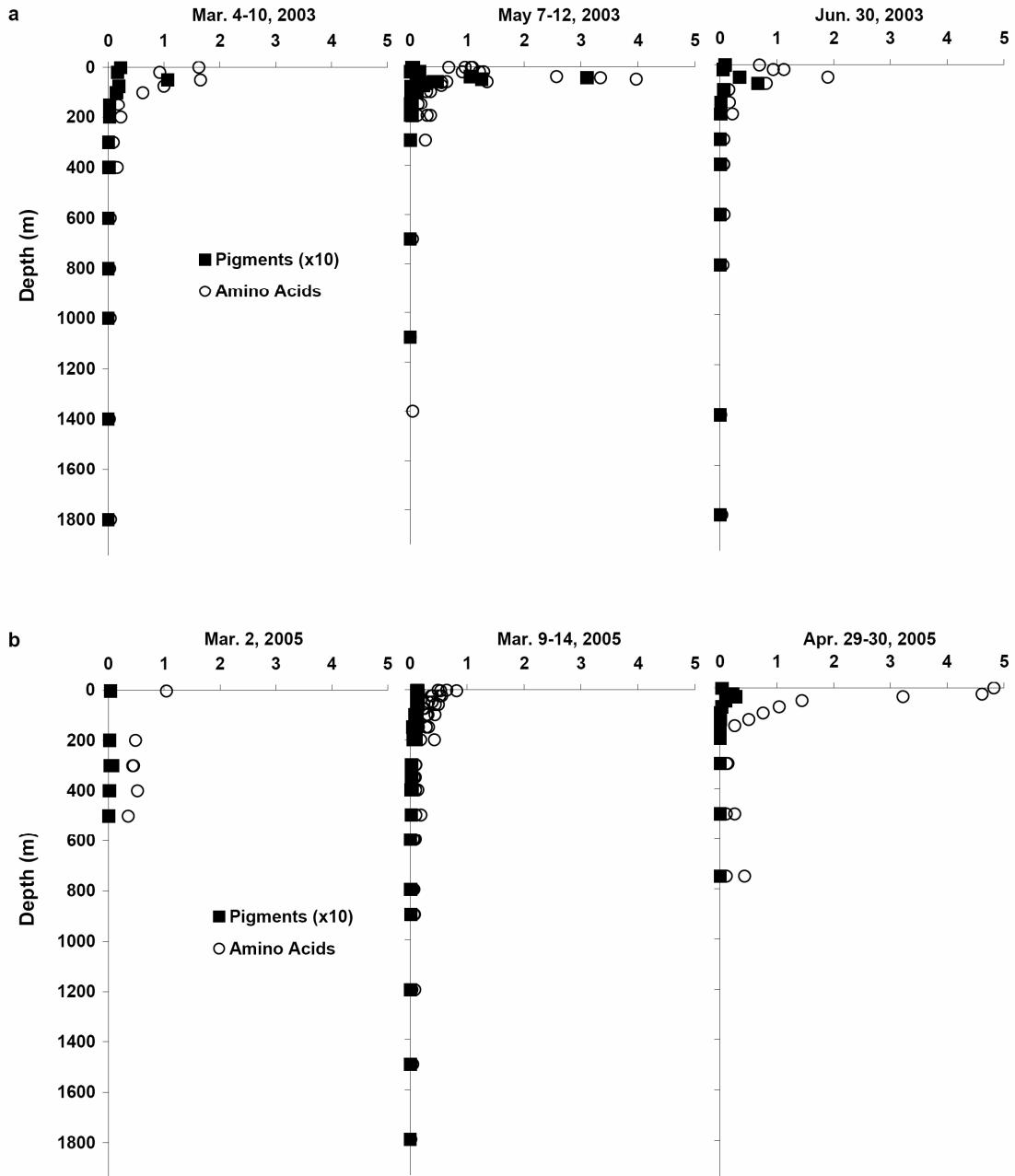
Table 3.3. Minimum change in sinking particle fluxes with depth ($\partial J_{\text{sink}}/\partial z$) and settling velocities (ω) required to balance the decay of chl *a* in the suspended phase.

Table 3.4. Exchange with Sinking Particles Required to Explain Suspended Pheopigments below the Mixed Layer					
Date	Asymptote in Suspended Phase [C _{susp} (z*) as z* → ∞] (μmol C m ⁻³)	Exchange Required to Balance Decay and Production [E=kC _{susp} (z*)-fk _(chl) C _{susp(chl)} (z*)] (μmol C m ⁻³ d ⁻¹)	Minimum Loss from Sinking Phase to Balance Exchange [∂J _{sink} /∂z=E, assuming kC _{sink} (z*)=0] (μmol C m ⁻² d ⁻¹)	Measured Loss from Shallow to Deep Trap [∂J _{sink} /∂z] (μmol C m ⁻² d ⁻¹)	Difference between Required & Measured Loss from Sinking Phase
phytin (assuming k=0.017 to 0.116 d⁻¹, f=0.5):					
2003					
Mar. 4-10 Pumps, Mar. 6-11 Traps	nd	-2.2 x10 ⁻³	-1.8	0.1	-16x
May 7-12 Pumps, Apr. 30- May 6 Traps	0.41	4.1 x10 ⁻³ to 4.5 x10 ⁻²	3.3 to 36	3.0	1.1x to 12x
Jun. 30 Pumps, Jun. 25-30 Traps	0.31	2.0 x10 ⁻³ to 3.3 x10 ⁻²	3.3 to 54	0.06	54x to 891x
2005					
Mar. 2 Pumps, Mar. 4-9 Traps	0.07	-8.6 x10 ⁻³ to -5.7 x10 ⁻²	-1.7 to -11	0.5	-4x to -25x
Mar. 9-14 Pumps, Mar. 9-14 Traps	0.05	-7.3 x10 ⁻³ to -4.9 x10 ⁻²	-11 to -74	0.5	-24x to -160x
Apr. 29-30 Pumps, Apr. 23-29 Traps	0.02	6.5 x10 ⁻⁵ to 4.9 x10 ⁻⁴	-0.01 to -0.1	-0.3	0.03x to 0.2x
phide + pyrophide (assuming k=0.026 to 0.175 d⁻¹, f=1-f_{phytin}=0.5):					
2003					
Mar. 4-10 Pumps, Mar. 6-11 Traps	nd	-2.2 x10 ⁻³	-1.8	4.7	-0.4x
May 7-12 Pumps, Apr. 30- May 6 Traps	0.41	-5.2 x10 ⁻⁴ to 1.3 x10 ⁻²	-0.4 to 10	1.2	-0.3x to 8x
Jun. 30 Pumps, Jun. 25-30 Traps	0.31	5.1 x10 ⁻⁴ to 2.2 x10 ⁻²	0.2 to 9	0.05	4x to 171x
2005					
Mar. 2 Pumps, Mar. 4-9 Traps	0.07	-8.4 x10 ⁻³ to -5.6 x10 ⁻²	-1.7 to -11	1.3	-1.3x to -9x
Mar. 9-14 Pumps, Mar. 9-14 Traps	0.05	-5.6 x10 ⁻³ to -3.7 x10 ⁻²	-8 to -56	0.8	-11x to -74x
Apr. 29-30 Pumps, Apr. 23-29 Traps	0.02	3.3 x10 ⁻⁴ to 2.2 x10 ⁻³	-0.04 to -0.3	-0.8	0.1x to 0.4x

Table 3.4. Minimum change in sinking particle fluxes with depth ($\partial J_{\text{sink}}/\partial z$) and settling velocities (ω) required to balance the decay and production of phytin and phide+pyrophide in the suspended phase.

Figure 3.1. Vertical profiles of pigments and amino acids in the 1-70 μm particulate fraction (collected on the 1 μm filter of in situ pumps) for three sampling periods in spring and summer of 2003 and 2005. Samples collected at the same depth within about a week were averaged for comparison with corresponding time series trap samples. a) During all sampling periods in 2003, pigments and amino acids reached a subsurface maximum at about 25-75 m and then decreased to nearly 0 $\mu\text{mol C l}^{-1}$ within the upper 200-400 m. As of March 4-10, 2003, the pigment and amino acid maxima occurred at 50 m depth, where concentrations were 0.11 and 1.7 $\mu\text{mol C l}^{-1}$, respectively. From May 7-12, the maxima remained at 50 m depth, where concentrations increased to 0.31 and 4.0 $\mu\text{mol C l}^{-1}$, respectively. By June 30, the pigment maximum was at 75 m and had decreased in concentration to 0.07 $\mu\text{mol C l}^{-1}$; the amino acid maximum remained at 50 m and had decreased to 1.9 $\mu\text{mol C l}^{-1}$. b) On March 2, 2005, pigments were about 0.003 $\mu\text{mol C l}^{-1}$ throughout the upper 300 m, thereafter decreasing to about 0.001 $\mu\text{mol C l}^{-1}$. The amino acid maximum occurred at the surface (1.0 $\mu\text{mol C l}^{-1}$). As of March 9-14, 2005, the pigment and amino acid maxima again occurred at the surface, where concentrations were 0.01 and 0.82 $\mu\text{mol C l}^{-1}$, respectively. By April 29-30, maximum concentrations had increased to 0.03 $\mu\text{mol C l}^{-1}$ pigments at 35 m and 4.8 $\mu\text{mol C l}^{-1}$ amino acids at the surface.

Pigment and Amino Acid Concentrations, 1-70 μm Particles ($\mu\text{mol C l}^{-1}$)



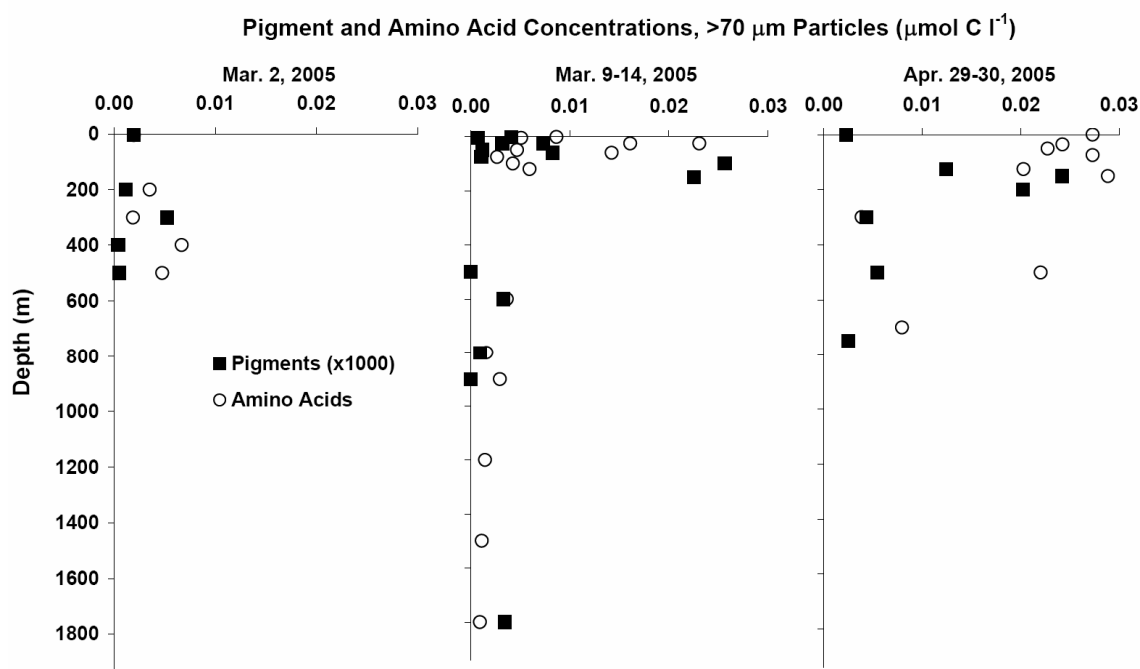


Figure 3.2. Vertical profiles of pigments and amino acids in the $>70 \mu\text{m}$ particulate fraction (collected on the $70 \mu\text{m}$ Teflon screen of in situ pumps) for three sampling periods in the spring of 2005. On Mar. 2, data markers for amino acids and pigments overlap at surface, so amino acid point is not visible. Concentrations were several orders of magnitude lower in this size class than in the $1-70 \mu\text{m}$ fraction, possibly because larger particles are generally rarer than smaller particles. Many samples were below detection limits, partly due to these low concentrations as well as the small size of the punches and possible artifacts from drying the samples. Pigment and amino acid maxima were generally deeper in the $> 70 \mu\text{m}$ fraction, probably since they represent organic matter export, rather than production. On March 2, concentrations of pigments and amino acids at the surface were about $0.002 \text{ nmol C l}^{-1}$ and $0.002 \mu\text{mol C l}^{-1}$, respectively (data markers overlap on figure), and increased to $0.005 \text{ nmol C l}^{-1}$ and $0.007 \mu\text{mol C l}^{-1}$ by 300-400 m depth. Since no data were available between 0-200 m depth, it is possible the actual maxima occurred higher in the water column. As of March 9-14, the amino acid maximum occurred at about 25 m depth ($0.023 \mu\text{mol C l}^{-1}$) and the pigment maximum at 100 m depth ($0.026 \text{ nmol C l}^{-1}$). On April 29-30, the pigment and amino acid maxima occurred at 150 m depth ($0.024 \text{ nmol C l}^{-1}$ and $0.029 \mu\text{mol C l}^{-1}$, respectively).

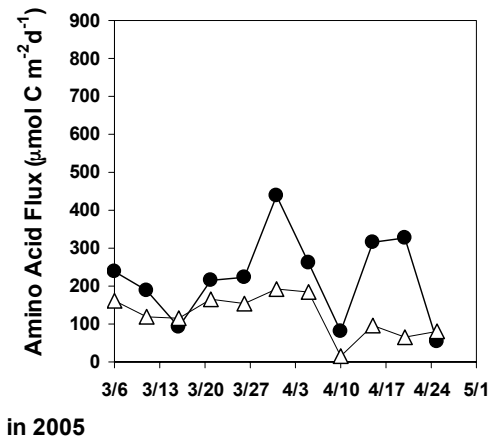
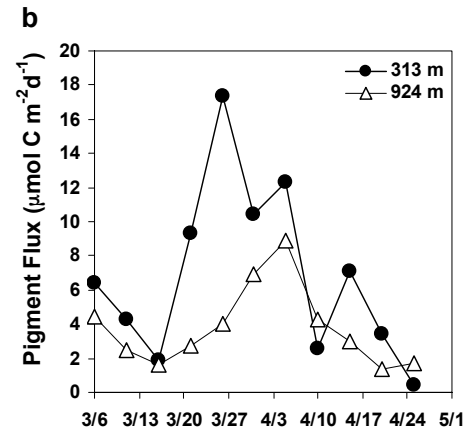
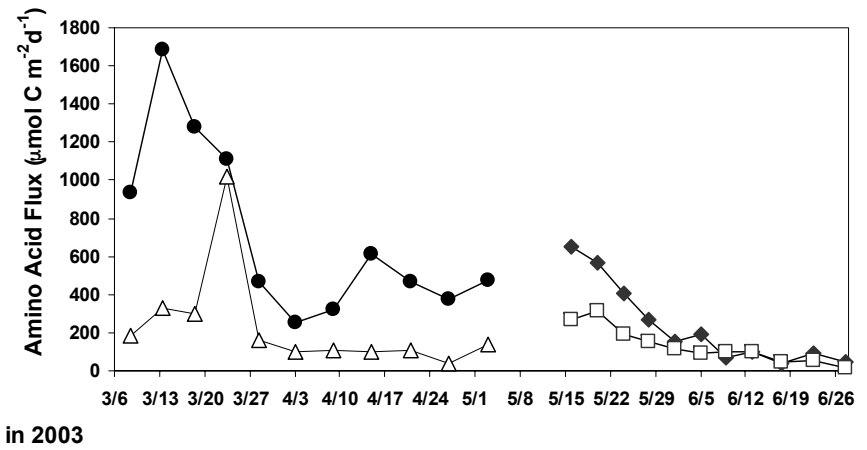
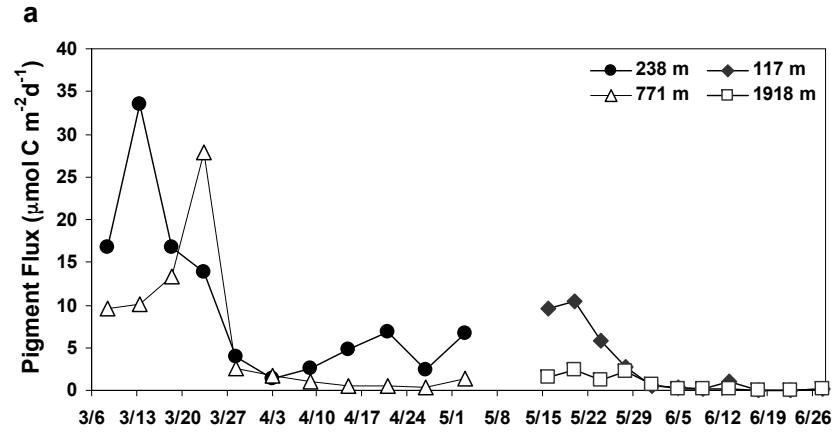
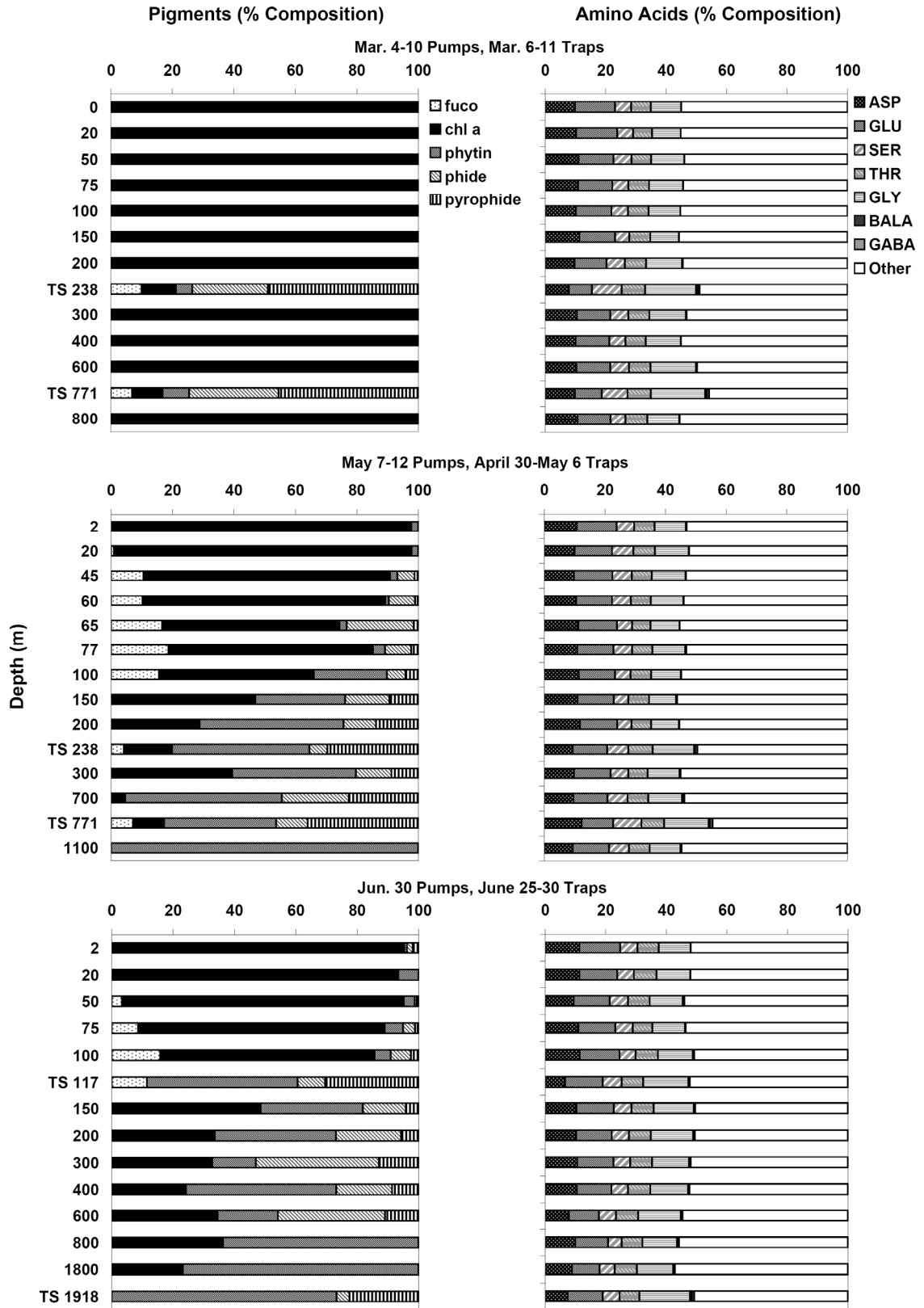
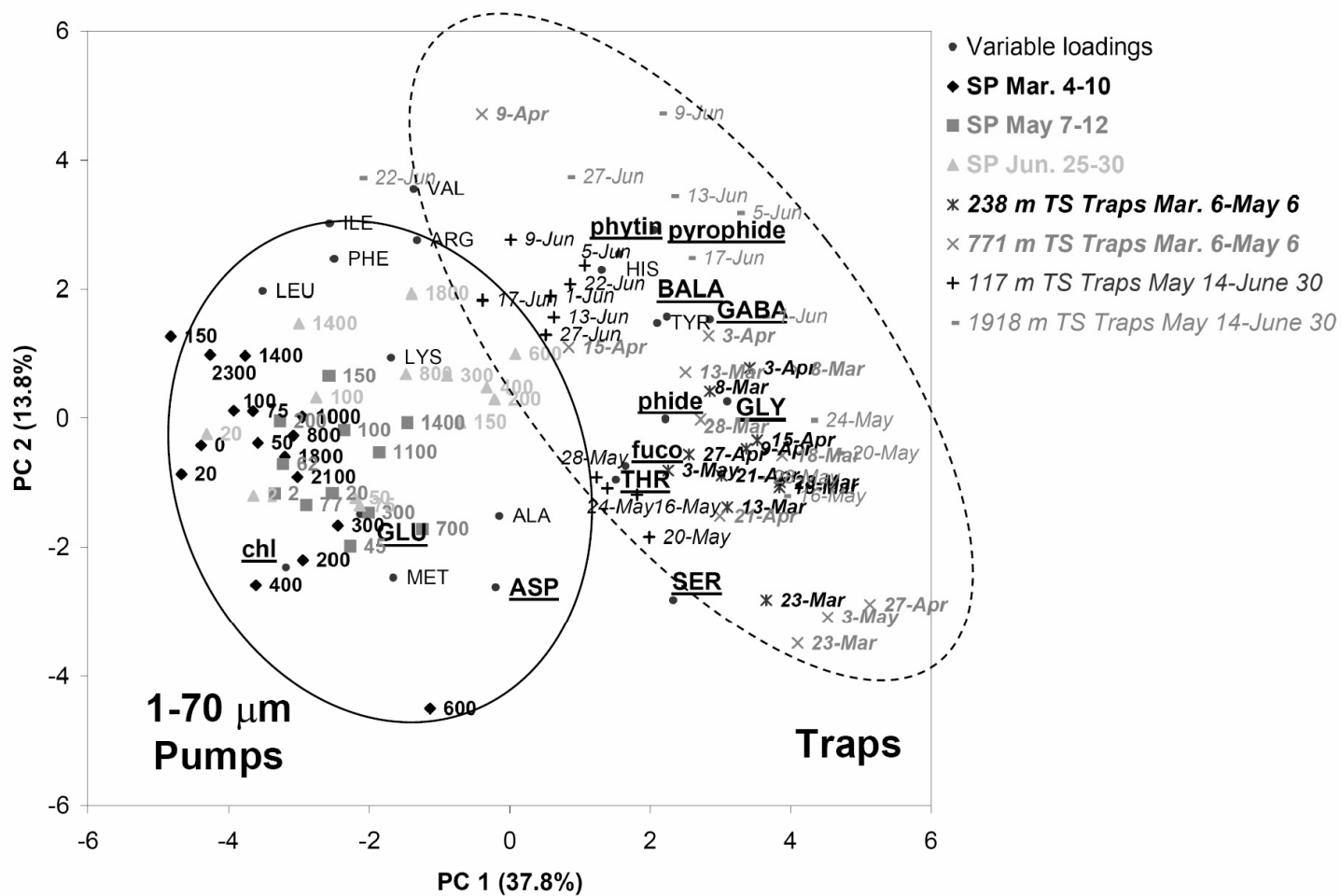


Figure 3.3. Temporal changes in pigment and amino acid fluxes from March 6-June 30, 2003 (a) and March 4-April 28, 2005 (b) measured using IRS sediment traps operated in time series mode. Each data point represents the median of a 5-7 day sampling interval. a) Time series data for 2003 are described by Lee et al. (submitted) and Wakeham et al. (submitted); data for pigments and amino acids are presented again here after conversion to $\mu\text{mol C m}^{-2}\text{d}^{-1}$ to facilitate comparison with the pumps. Fluxes of pigments and amino acids at 238 m peaked around March 13, reaching 33 and 1685 $\mu\text{mol C m}^{-2}\text{d}^{-1}$, respectively (synchronous with elevated satellite chlorophyll), then decreasing substantially to 4 and 255 $\mu\text{mol C m}^{-2}\text{d}^{-1}$, respectively, by the beginning of April. A small, secondary bloom occurred in early May, with fluxes increasing again to 11 and 652 $\mu\text{mol C m}^{-2}\text{d}^{-1}$, respectively, by about May 20, then decreasing to below 1 and 189 $\mu\text{mol C m}^{-2}\text{d}^{-1}$ throughout June. Fluxes at 771 and 1918 m were temporally offset by ~ 10 d and generally ranged from 20-80% of those at 238 or 117 m. Fluxes of total mass and organic carbon (Lee et al., submitted; Wakeham et al., submitted) followed similar temporal patterns (peaking at 910 and 71 $\text{mg m}^{-2}\text{d}^{-1}$, respectively, in early March, then decreasing to 138 and 11 $\text{mg m}^{-2}\text{d}^{-1}$ by early April, increasing again slightly to 165 and 16 $\text{mg m}^{-2}\text{d}^{-1}$ in the first two weeks of May, and finally decreasing to below 25 and 5 $\text{mg m}^{-2}\text{d}^{-1}$ throughout June). B) In 2005, maximum fluxes of pigments and amino acids at 313 m occurred around March 25, peaking at 17 and 438 $\mu\text{mol C m}^{-2}\text{d}^{-1}$, respectively. Smaller peaks occurred earlier in March and again around April 15, reaching 6-7 and 237-315 $\mu\text{mol C m}^{-2}\text{d}^{-1}$, respectively. By the end of April, pigment and amino acid fluxes decreased to 0.4 and 53 $\mu\text{mol C m}^{-2}\text{d}^{-1}$, respectively. Fluxes at 924 m were temporally offset by ~ 10 d and generally ranged from 20-90% of those at 313 m. Fluxes of total mass and organic carbon followed similar temporal variations, which appeared to be related to dust events (Lee et al., submitted), reaching 906 and 26 $\text{mg m}^{-2}\text{d}^{-1}$, respectively, in early March and 880 and 25 $\text{mg m}^{-2}\text{d}^{-1}$, respectively, at the end of March, then declining by the end of April to about 26 and 4 $\text{mg m}^{-2}\text{d}^{-1}$, respectively.

Figure 3.4. Depth profiles of pigment and amino acid composition of particles during three sampling periods in spring-summer, 2003. Most data shown are for 1-70 μm particles collected by in situ pump, thought to represent suspended or very slowly sinking particles. Data for time series trap (TR) samples, assumed to represent sinking particles, are shown where available. The time series trap data shown are for those cups which most closely overlapped with the pump casts. The March 4-10 pump casts are compared with the March 6-11 trap sample (1st deployment, 1st cup), the May 7-12 pump casts with the April 30 – May 6 trap sample (1st deployment, last cup), and the June 30 pump cast with the June 25-30 trap sample (2nd deployment, last cup).

2003





*variable loadings scaled up 10x to fit axes

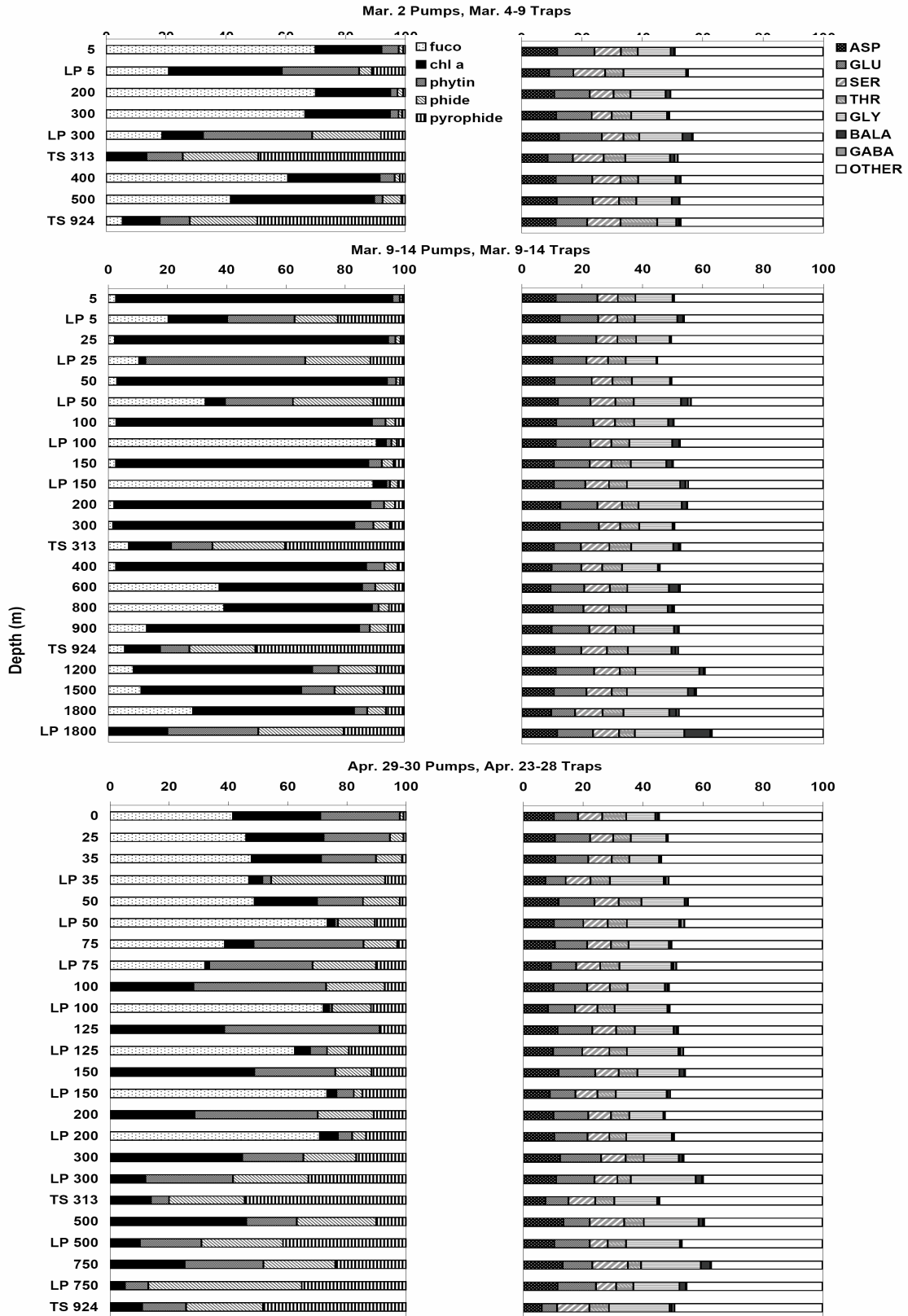
Figure 3.5. Principal component analysis on the 2003 pump and TS trap data. Variable loadings are scaled up 10X and plotted on the same axes as sample site scores. Numbers represent depth (in m) for the 1-70 μm pump samples and the date of the midpoint of each sampling interval for the TS samples.

Figure 3.6. Depth profiles of pigment and amino acid composition of particles during three sampling periods in the spring of 2005. Most data shown are for 1-70 μm particles collected by in situ pump, thought to represent suspended or very slowly sinking particles. Data for larger ($>70 \mu\text{m}$) pump (LP) and time series trap (TS) samples, assumed to represent sinking particles, are shown where available. The time series trap data shown are for those cups which most closely overlapped with the pump casts. The March 2 pump cast is compared with the March 4-9 trap sample (1st cup), the March 9-14 pump casts with the March 9-14 trap sample (2nd cup), and the April 29-30 pump cast with the April 23-28 trap sample (last cup).

2005

Pigments (% Composition)

Amino Acids (% Composition)



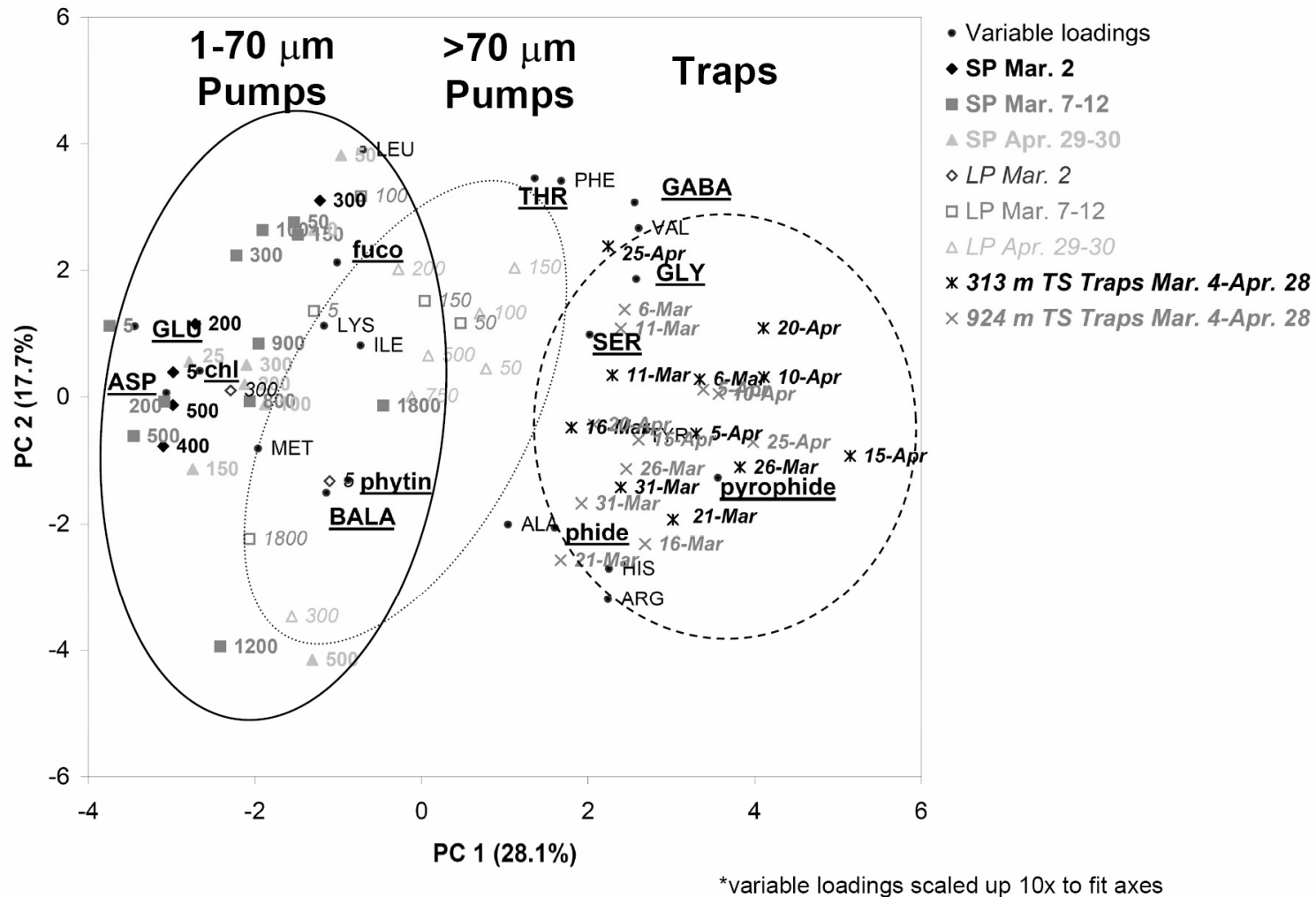


Figure 3.7. Principal component analysis on the 2005 pump and TS trap data. Variable loadings are scaled up 10X and plotted on the same axes as sample site scores. Numbers represent depth (in m) for the 1-70 μm pump samples and >70 μm pump samples, and the date of the midpoint of each sampling interval for the TS samples.

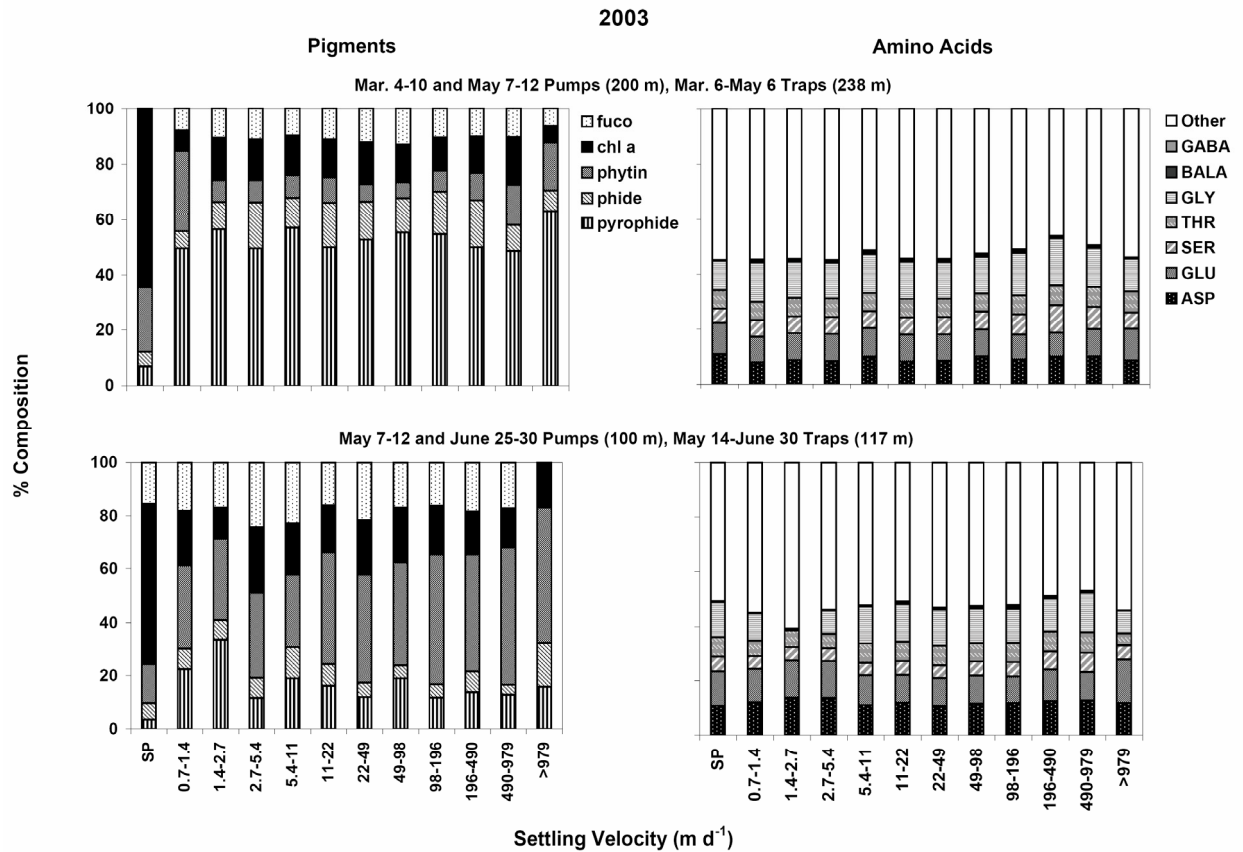


Figure 3.8. Changes in pigment and amino acid composition of particles with settling velocity for spring-summer, 2003. Most data shown are for the settling velocity trap (collected in duplicate and averaged). Also shown are data for the 1-70 μm pumps (small pump, or SP) collected at approximately the same depth. As the data for each settling velocity class are integrated over the entire deployment period, we have averaged the pump data collected at the beginning and end of each trap deployment for comparison. The 238 m SV trap deployment from March 6-May 6 is compared with the 200 m pump casts averaged over March 4-10 and May 7-12. The 117 m trap deployment from May 14-June 30 is compared with the 100 m pump casts averaged over May 7-12 and June 25-30.

2005

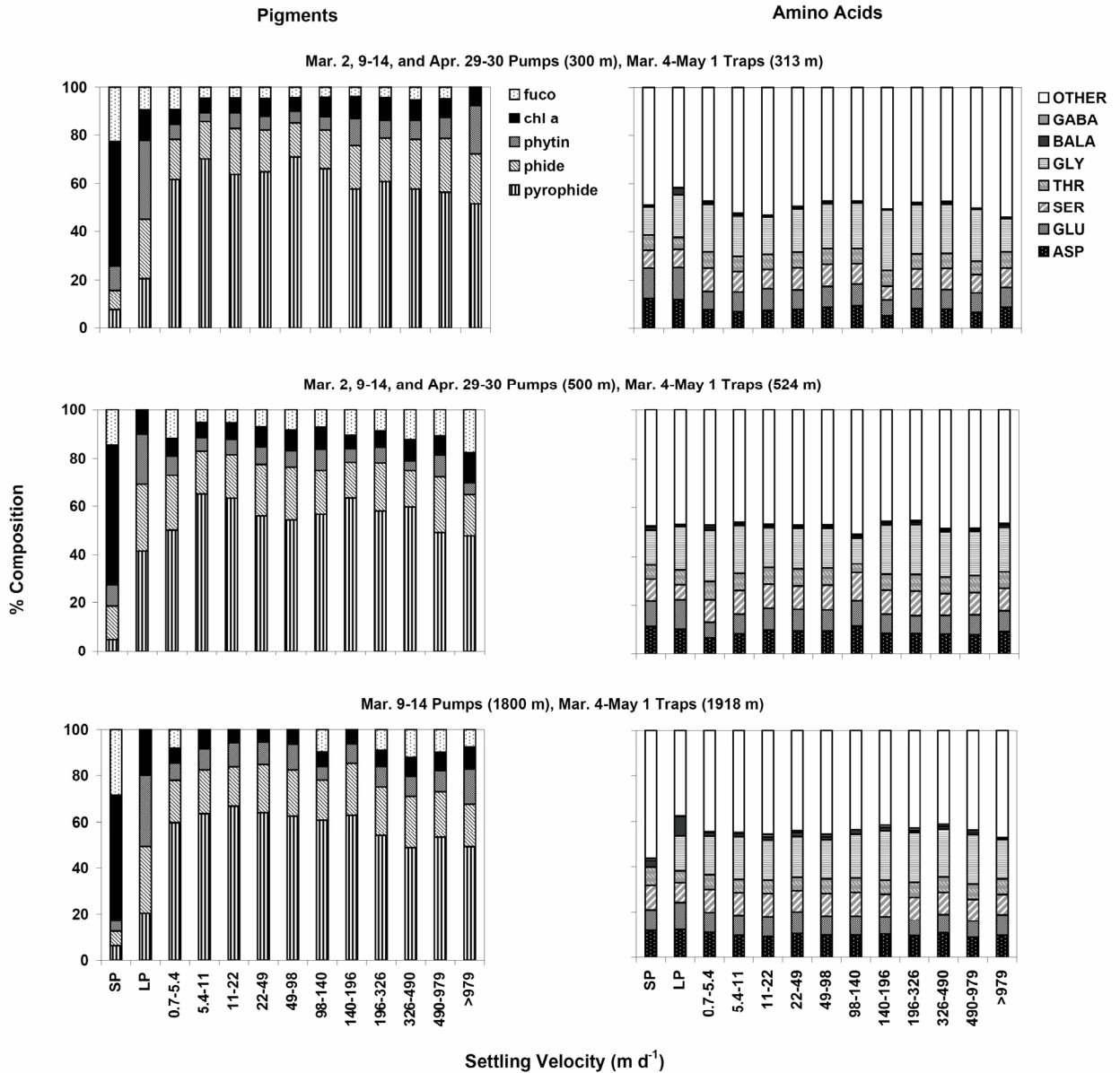


Figure 3.9. Changes in pigment and amino acid composition of particles with settling velocity for the spring of 2005. Most data shown are for the settling velocity traps (collected in duplicate and averaged) at 313, 524, and 1918 m. Also shown are data for the 1-70 μm pumps (small pump, or SP) and >70 μm pumps (large pump, or LP) collected at 300, 500, and 1800 m. As the data for each settling velocity class are integrated over the entire deployment period (March 4-May 1), wherever possible we have averaged the data from all three sets of pump casts (March 2, March 9-14, and April 29-30) for comparison. At 300 m, data for LP were available for March 2 and Apr. 29-30, but not March 9-14; data for SP were available for all 3 time periods. At 500 m, data for LP were available only from April 29-30; data for SP were available for all 3 time periods. At 1818 m, data for both LP and SP were available only from March 9-14.

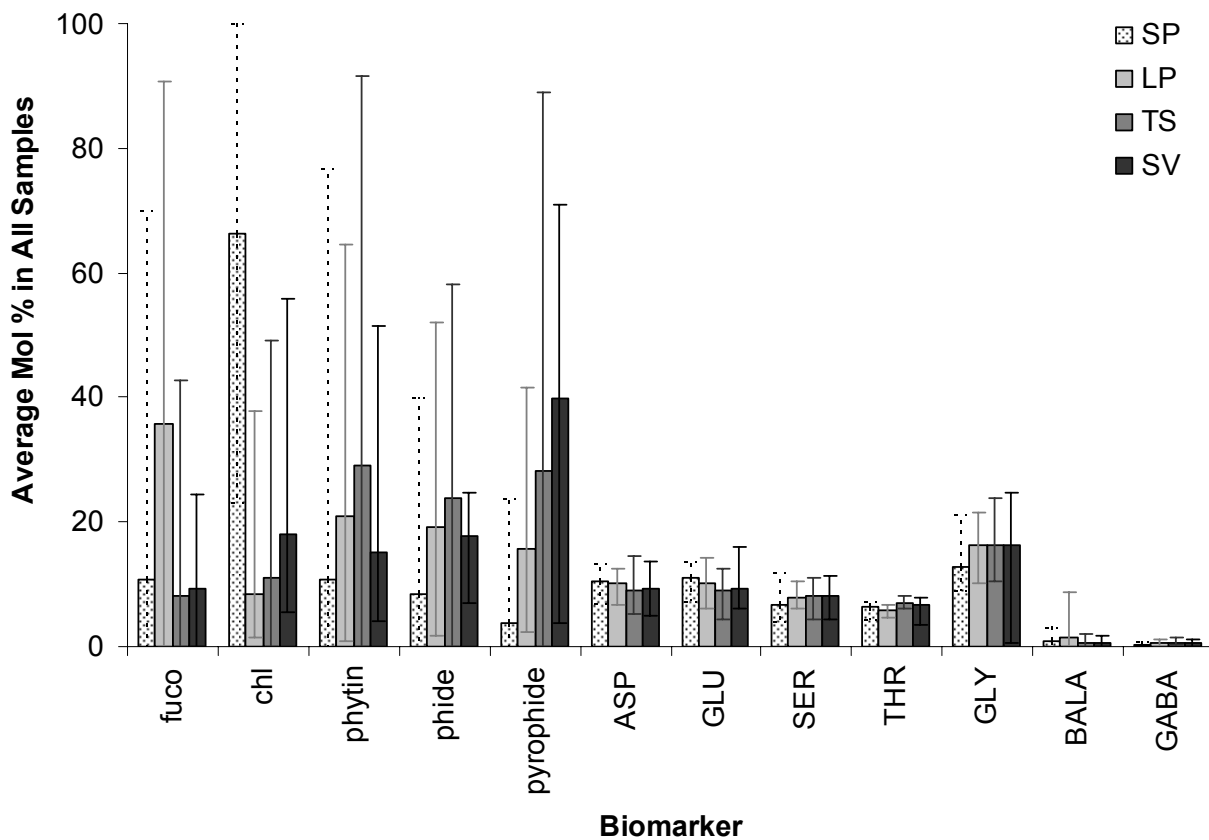


Figure 3.10. Average mole % of the pigment and amino acid biomarkers in all samples collected from > 200 m depth. Bar depicts the mean, and error bars the maximum and minimum contributions of each biomarker observed. SP: small particles (1-70 μm) collected by *in situ* pump in 2003 (200-800 m from March 5-10, 200-1100 m from May 7-12, and 200-1800 m on June 30) and 2005 (200-500 m on March 2, 200-1800 m from March 9-14, and 200-750 m from April 29-30). LP: large particles (>70 μm) collected by *in situ* pump in 2005 200-500 m on March 2, 200-1800 m from March 9-14, and 200-750 m from April 29-30). TS: time-series trap samples collected in 2003 (238 and 771 m from March 6-May 6; 117 and 1918 m from May 14-June 30) and 2005 (313 and 924 m from March 4-April 28). SV: settling-velocity trap samples collected in 2003 (238 m from March 6-May 6; 117 m from May 14-June 30) and 2005 (313, 524, and 1918 m from March 4-May 1).

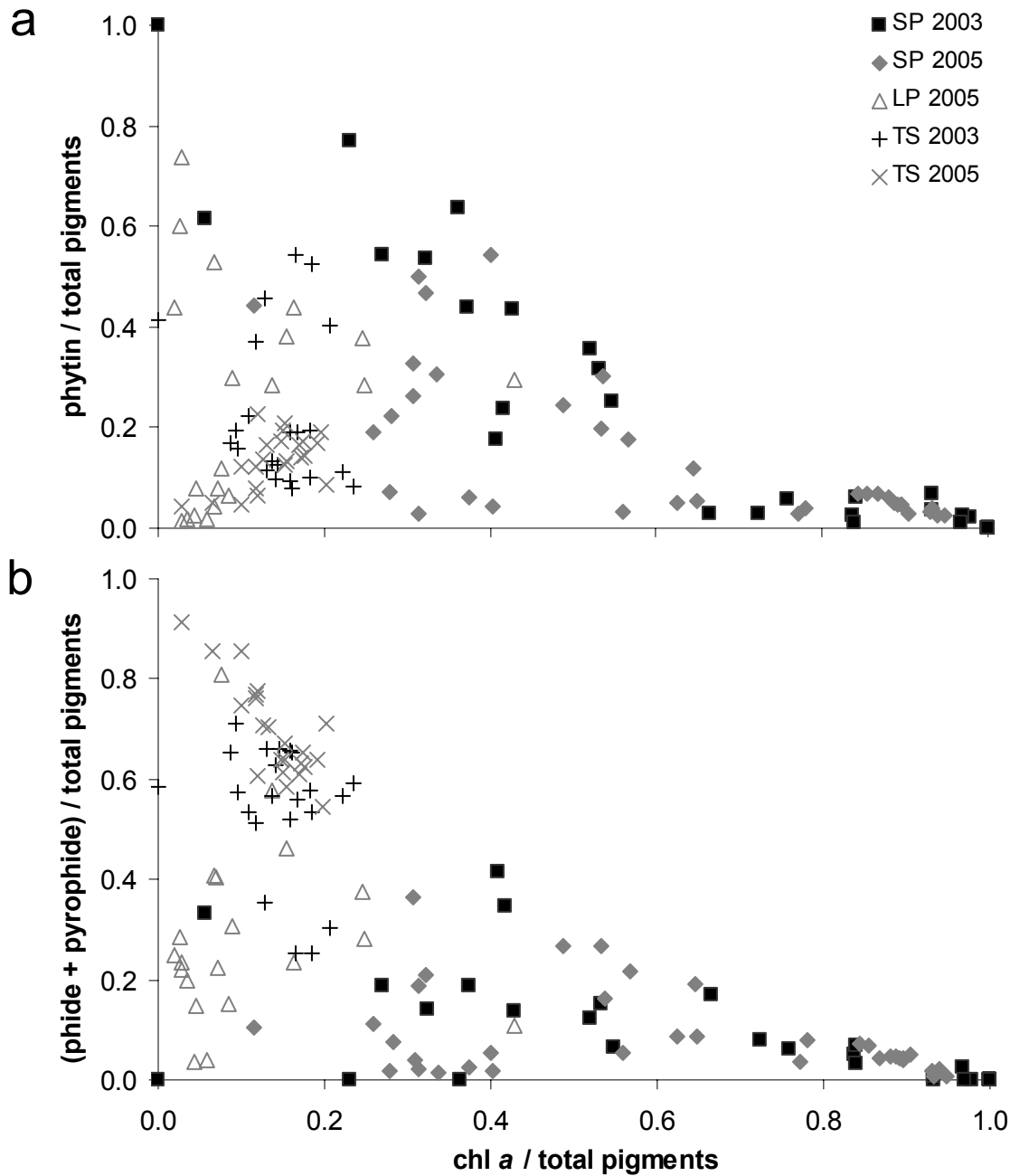


Figure 3.11. The relationship between chl *a* and its microbial degradation product phytin (a) or zooplankton alteration products phide + pyrophide (b) for all 1-70 μm pump (SP), >70 μm pump (LP), and TS trap samples (TS). Chl *a*, phytin, and phide + pyrophide are normalized to total pigments (i.e., as in the mol % calculations) to eliminate differences in total pigment concentrations. Data from all depths and time periods sampled are shown.

Appendix to Chapter 3

Table 3.A1. Concentration ($\mu\text{mol C l}^{-1}$) or flux ($\mu\text{mol C m}^{-2}\text{d}^{-1}$) and composition of pigments (mol %) during three sampling periods in spring-summer, 2003. Most data shown are for 1-70 μm particles collected by in situ pump, thought to represent suspended or very slowly sinking particles. Data for time series trap (TS) samples, assumed to represent sinking particles, are shown where available. The time series trap data shown are for those cups which most closely overlapped with the pump casts. Fig. 3.4 graphically depicts this data.

**Table 3.A1. Pigment Compositions of 2003
Pump and TS Trap Samples (mol %)**

March 4-10 Pumps, March 6-11 Traps:

Depth (m)	Pigment Concentration or Flux ($\mu\text{mol C l}^{-1}$ or $\mu\text{mol C m}^{-2} \text{d}^{-1}$)	%chl <i>a</i>	%phytin	%phide	%pyrophide	%fuco
0	2.29×10^{-2}	100	nd	nd	nd	nd
20	1.72×10^{-2}	100	nd	nd	nd	nd
50	0.11	100	nd	nd	nd	nd
75	1.94×10^{-2}	100	nd	nd	nd	nd
100	1.49×10^{-2}	100	nd	nd	nd	nd
150	3.08×10^{-3}	100	nd	nd	nd	nd
200	3.02×10^{-3}	100	nd	nd	nd	nd
TS 238	16.8	11.1	5.36	24.7	48.9	9.96
300	4.28×10^{-4}	100	nd	nd	nd	nd
400	2.08×10^{-3}	100	nd	nd	nd	nd
600	1.32×10^{-4}	100	nd	nd	nd	nd
TS 771	9.5	10.0	8.70	29.2	45.3	6.78
800	1.17×10^{-4}	100	nd	nd	nd	nd

May 7-12 Pumps, April 30-May 6 Traps

Depth (m)	Pigment Concentration or Flux ($\mu\text{mol C l}^{-1}$ or $\mu\text{mol C m}^{-2} \text{d}^{-1}$)	%chl <i>a</i>	%phytin	%phide	%pyrophide	%fuco
2	$4.76 \pm 1.19 \times 10^{-3}$	97.7 ± 1.4	2.27 ± 1.36	nd	nd	nd
20	$1.24 \pm 0.67 \times 10^{-2}$	97.0 ± 0.4	2.18 ± 1.63	nd	nd	0.86 ± 1.21
45	$1.81 \pm 1.13 \times 10^{-1}$	80.3 ± 6.8	2.34 ± 0.48	5.66 ± 4.66	1.18 ± 0.43	10.5 ± 2.2
60	$4.45 \pm 0.48 \times 10^{-2}$	79.1 ± 11.2	1.15 ± 1.28	8.57 ± 8.63	0.97 ± 0.16	10.2 ± 3.7
65	$2.98 \pm 0.01 \times 10^{-2}$	57.9 ± 5.1	2.39 ± 1.18	21.8 ± 0.3	1.44 ± 0.40	16.5 ± 3.9
77	$1.23 \pm 1.13 \times 10^{-2}$	66.6 ± 6.4	3.97 ± 3.38	8.51 ± 4.64	2.29 ± 0.54	18.6 ± 4.0
100	$7.55 \pm 4.47 \times 10^{-3}$	50.5 ± 6.1	23.9 ± 3.0	5.98 ± 1.47	4.16 ± 2.52	15.5 ± 5.0
150	$8.44 \pm 4.40 \times 10^{-4}$	47.0 ± 7.1	29.2 ± 0.5	14.4 ± 2.7	9.38 ± 3.88	nd
200	$2.03 \pm 1.45 \times 10^{-3}$	28.8 ± 9.4	46.7 ± 13.5	10.5 ± 7.08	13.8 ± 2.1	nd
TS 238	6.7	15.8	44.8	5.84	29.6	4.07
300	8.66×10^{-4}	39.5	40.2	11.5	8.75	nd
700	1.81×10^{-4}	4.62	51.0	21.9	22.5	nd
TS 771	1.4	10.2	36.4	10.3	36.1	7.03
1100	5.91×10^{-5}	nd	100	nd	nd	nd

June 30 Pumps, June 25-30 Traps:

Depth (m)	Pigment Concentration or Flux ($\mu\text{mol C l}^{-1}$ or $\mu\text{mol C m}^{-2} \text{d}^{-1}$)	%chl <i>a</i>	%phytin	%phide	%pyrophide	%fuco
2	9.51×10^{-3}	95.3	0.91	1.89	1.87	nd
20	5.82×10^{-3}	93.3	6.67	0.00	0.00	nd
50	3.48×10^{-2}	91.9	3.60	0.74	0.56	3.22
75	6.70×10^{-2}	80.5	5.93	3.94	1.09	8.56
100	6.75×10^{-3}	70.0	5.21	6.65	2.46	15.7
TS 117	0.25	nd	49.2	9.06	30.4	11.4
150	1.96×10^{-3}	48.5	33.4	14.0	4.13	nd
200	1.64×10^{-3}	33.6	39.5	21.4	5.61	nd
300	5.85×10^{-4}	32.8	14.3	40.1	12.9	nd
400	7.75×10^{-4}	24.3	48.9	18.2	8.66	nd
600	6.41×10^{-4}	34.6	19.6	34.9	10.9	nd
800	5.74×10^{-4}	36.2	63.8	0.00	0.00	nd
1800	6.61×10^{-4}	23.1	76.9	0.00	0.00	nd
TS 1918	0.11	nd	73.3	4.27	22.4	nd

nd= not detected

Table 3.A2. Amino Acid Compositions of 2003 Pump and TS Trap Samples (mol %)									
March 4-10 Pumps, March 6-11 Traps:									
Depth (m)	Amino Acid Concentration or Flux ($\mu\text{mol C l}^{-1}$ or $\mu\text{mol C m}^{-2} \text{ d}^{-1}$)	%ASP	%GLU	%SER	%THR	%GLY	%BALA	%GABA	%Other
0	1.63	9.81	13.3	5.35	6.47	10.1	nd	0.00	54.9
20	0.93	10.3	13.6	5.17	6.33	9.49	nd	0.00	55.2
50	1.66	11.0	11.7	5.85	6.59	10.9	nd	0.00	53.9
75	1.00	10.9	11.4	5.36	6.81	11.3	nd	0.00	54.3
100	0.63	10.2	11.8	5.48	6.73	10.6	nd	0.00	55.3
150	0.19	11.3	11.8	4.76	6.95	9.44	nd	0.00	55.7
200	0.23	9.80	10.5	6.04	6.97	12.0	nd	0.16	54.5
TS 238	932	7.86	7.58	9.87	7.73	16.9	0.52	0.56	49.0
300	9.38×10^{-2}	10.4	11.1	5.95	7.03	12.0	nd	0.17	53.3
400	0.16	10.1	11.1	5.32	6.74	11.6	nd	0.09	55.1
600	4.10×10^{-2}	10.3	11.2	6.22	7.18	15.0	nd	0.33	49.7
TS 771	186	9.86	8.81	8.56	7.69	18.1	0.47	0.72	45.8
800	3.16×10^{-2}	10.7	10.9	4.94	7.18	10.5	nd	0.22	55.5
May 7-12 Pumps, April 30-May 6 Traps:									
Depth (m)	Amino Acid Concentration or Flux ($\mu\text{mol C l}^{-1}$ or $\mu\text{mol C m}^{-2} \text{ d}^{-1}$)	%ASP	%GLU	%SER	%THR	%GLY	%BALA	%GABA	%Other
2	0.96 ± 0.19	10.8 ± 0.5	13.2 ± 0.8	5.80 ± 0.32	6.69 ± 0.36	10.4 ± 0.7	0.06 ± 0.12	0.08 ± 0.07	53.1 ± 1.5
20	1.14 ± 0.19	9.99 ± 0.93	12.41 ± 0.4	6.96 ± 0.74	7.10 ± 0.25	11.2 ± 1.0	nd	0.17 ± 0.02	52.2 ± 1.2
45	3.30 ± 0.70	9.80 ± 0.06	12.6 ± 1.4	6.45 ± 0.67	6.56 ± 0.35	11.2 ± 1.0	0.04 ± 0.06	0.09 ± 0.06	53.3 ± 1.8
60	1.00 ± 0.48	10.5 ± 0.4	11.8 ± 0.4	6.16 ± 0.71	6.69 ± 0.20	10.7 ± 0.3	nd	0.07 ± 0.03	54.1 ± 1.2
65	0.56	11.20	12.70	5.08	6.05	9.53	nd	0.10	55.35
77	0.33 ± 0.31	10.8 ± 0.7	12.0 ± 0.1	6.10 ± 1.09	6.76 ± 0.73	10.8 ± 1.8	0.21 ± 0.30	0.08 ± 0.11	53.2 ± 3.2
100	0.33 ± 0.05	11.4 ± 1.5	12.0 ± 0.3	5.17 ± 2.49	6.74 ± 0.74	9.9 ± 2.1	nd	0.10 ± 0.14	54.8 ± 4.0
150	0.17 ± 0.04	10.9 ± 2.1	12.0 ± 2.3	4.78 ± 1.78	6.78 ± 0.09	9.0 ± 1.9	0.07 ± 0.09	0.15 ± 0.05	56.3 ± 8.2
200	0.26 ± 0.10	11.7 ± 1.3	12.3 ± 0.2	4.72 ± 1.94	6.56 ± 0.63	9.1 ± 2.5	0.06 ± 0.10	0.13 ± 0.11	55.4 ± 4.2
TS 238	475	9.30	11.5	6.93	8.04	13.7	0.31	0.71	49.5
300	0.27	9.77	12.0	5.91	6.34	10.5	0.25	0.19	55.0
700	4.27×10^{-2}	9.61	11.2	6.63	6.78	11.2	0.48	0.21	53.8
TS 771	232	12.3	10.4	9.27	7.44	14.8	0.49	0.75	44.5
1400	4.85×10^{-2}	9.35	12.0	6.59	6.82	10.2	0.25	0.11	54.7
June 30 Pumps, June 25-30 Traps:									
Depth (m)	Amino Acid Concentration or Flux ($\mu\text{mol C l}^{-1}$ or $\mu\text{mol C m}^{-2} \text{ d}^{-1}$)	%ASP	%GLU	%SER	%THR	%GLY	%BALA	%GABA	%Other
2	0.70	11.3	13.5	5.72	7.04	10.5	nd	nd	51.9
20	1.13	11.2	13.0	5.51	7.77	11.7	nd	0.05	50.8
50	1.90	9.45	11.8	6.09	7.09	11.0	0.22	0.24	54.1
75	0.82	11.0	12.2	5.76	6.52	10.7	0.19	0.03	53.7
100	0.16	11.3	13.3	5.28	7.36	11.5	0.36	0.00	50.9
TS 117	42.6	6.50	12.4	6.35	7.15	14.9	nd	0.47	52.2
150	0.17	10.4	12.3	5.85	7.27	13.2	0.38	0.15	50.5
200	0.22	10.2	11.8	5.76	7.22	13.9	0.41	0.17	50.5
300	7.05×10^{-2}	10.6	12.0	5.47	7.20	12.3	0.37	0.09	52.0
400	6.97×10^{-2}	10.6	11.7	5.66	7.28	12.3	0.40	0.12	51.9
600	7.66×10^{-2}	7.79	9.96	5.64	7.35	14.0	0.43	0.21	54.6
800	5.53×10^{-2}	9.92	10.8	4.57	6.81	11.5	0.40	0.16	55.9
1800	3.60×10^{-2}	8.83	9.14	5.03	7.26	12.1	0.35	0.15	57.1
TS 1918	16.1	7.45	11.5	5.68	6.46	16.8	0.59	0.71	50.8

nd= not detected

Table 3.A2. Concentration ($\mu\text{mol C l}^{-1}$) or flux ($\mu\text{mol C m}^{-2} \text{ d}^{-1}$) and composition of amino acids (mol %) during three sampling periods in spring-summer, 2003. The caption for Table 3.A1 describes the samples in more detail.

Table 3.A3. Concentration ($\mu\text{mol C l}^{-1}$) or flux ($\mu\text{mol C m}^{-2}\text{d}^{-1}$) and composition of pigments (mol %) during three sampling periods in the spring of 2005. Most data shown are for 1-70 μm particles collected by in situ pump, thought to represent suspended or very slowly sinking particles. Data for larger ($>70 \mu\text{m}$) pump (LP) and time series trap (TS) samples, assumed to represent sinking particles, are shown where available. The time series trap data shown are for those cups which most closely overlapped with the pump casts. Fig. 3.5 graphically depicts this data.

**Table 3.A3. Pigment Compositions of 2005
Pump and TS Trap Samples (mol %)**

March 2 Pumps, March 4-9 Traps:

Depth (m)	Pigment Concentration or Flux ($\mu\text{mol C l}^{-1}$ or $\mu\text{mol C m}^{-2} \text{d}^{-1}$)	%chl a	%phytin	%phide	%pyropheide	%fuco
5	3.86×10^{-3}	22.3	5.72	1.50	0.66	69.8
LP 5	1.96×10^{-6}	37.8	25.9	4.24	11.2	20.8
200	2.59×10^{-3}	25.0	2.42	1.90	0.66	70.0
300	5.78×10^{-3}	28.5	2.82	1.16	1.06	66.5
LP 300	5.25×10^{-6}	13.6	36.6	23.0	8.08	18.7
TS 313	6.39	13.6	12.1	25.3	49.1	nd
400	1.79×10^{-3}	30.7	5.11	1.69	1.78	60.7
500	1.15×10^{-3}	48.1	2.86	6.18	1.34	41.5
TS 924	4.41	12.5	10.0	22.7	49.4	5.47

March 9-14 Pumps, March 9-14 Traps:

Depth (m)	Pigment Concentration or Flux ($\mu\text{mol C l}^{-1}$ or $\mu\text{mol C m}^{-2} \text{d}^{-1}$)	%chl a	%phytin	%phide	%pyropheide	%fuco
2	1.27×10^{-2}	86.3	4.68	4.04	2.53	2.48
LP 2	4.13×10^{-6}	5.52	42.6	36.0	15.9	0.00
5	1.38×10^{-2}	93.5	2.55	0.72	0.65	2.54
LP 5	7.47×10^{-3}	20.0	22.8	14.6	22.4	20.3
25	$1.33 \pm 0.11 \times 10^{-2}$	92.4 ± 4.5	2.41 ± 1.06	1.77 ± 1.84	1.24 ± 1.40	2.17 ± 0.24
LP 25	$2.26 \pm 2.94 \times 10^{-6}$	2.27 ± 0.06	54.1 ± 73.3	21.9 ± 9.5	11.4 ± 5.6	10.3 ± 1.6
50	1.30×10^{-2}	91.3	3.20	1.41	1.27	2.82
LP 50	1.16×10^{-6}	6.87	22.9	27.2	10.4	32.66
60	1.47×10^{-2}	87.3	2.70	5.03	2.60	2.34
LP 60	8.30×10^{-6}	2.54	64.6	20.2	12.7	0.00
75	1.33×10^{-2}	92.1	4.02	0.27	1.04	2.55
100	$1.10 \pm 0.20 \times 10^{-2}$	86.5 ± 4.2	4.6 ± 0.9	3.31 ± 1.24	3.00 ± 1.77	2.60 ± 0.26
LP 100	2.56×10^{-5}	3.21	1.92	1.81	2.47	90.6
150	$6.65 \pm 2.73 \times 10^{-3}$	85.4 ± 0.7	4.6 ± 2.1	4.0 ± 1.5	3.5 ± 0.1	2.5 ± 0.2
LP 150	2.25×10^{-5}	4.39	1.24	2.60	2.19	89.6
200	$8.31 \pm 3.49 \times 10^{-3}$	86.7 ± 0.1	4.61 ± 0.35	3.74 ± 0.03	3.07 ± 0.32	1.85 ± 0.11
300	$2.64 \pm 3.37 \times 10^{-3}$	81.7 ± 0.4	6.42 ± 0.05	5.55 ± 1.68	4.81 ± 1.90	1.57 ± 0.11
TS 313	4.26	14.4	13.8	24.7	40.1	6.93
350	$2.53 \pm 0.29 \times 10^{-3}$	85.5 ± 3.6	5.63 ± 2.42	4.56 ± 1.87	2.49 ± 0.52	1.84 ± 0.22
400	$3.05 \pm 1.22 \times 10^{-3}$	84.6 ± 3.9	6.22 ± 2.28	4.38 ± 1.86	2.29 ± 0.10	2.55 ± 0.11
500	2.58×10^{-3}	80.30	6.40	7.93	3.11	2.23
600	$7.86 \pm 5.50 \times 10^{-4}$	48.2 ± 28.7	4.49 ± 0.90	6.89 ± 5.79	2.92 ± 1.36	37.5 ± 36.8
800	$1.10 \pm 1.07 \times 10^{-3}$	50.1 ± 21.7	2.07 ± 1.40	3.60 ± 3.90	5.12 ± 1.86	39.1 ± 25.2
900	1.48×10^{-3}	71.8	3.57	6.25	5.46	12.9
TS 924	2.47	12.1	9.85	22.2	50.3	5.50
1200	7.89×10^{-4}	60.5	8.98	12.9	9.19	8.46
1500	3.32×10^{-4}	54.3	11.1	16.8	6.78	11.0
1800	8.90×10^{-5}	54.6	4.37	6.35	6.13	28.5
LP 1800	3.48×10^{-6}	20.0	30.8	28.8	20.4	0.00

April 29-30 Pumps, April 23-28 Traps:

Depth (m)	Pigment Concentration or Flux ($\mu\text{mol C l}^{-1}$ or $\mu\text{mol C m}^{-2} \text{d}^{-1}$)	%chl a	%phytin	%phide	%pyropheide	%fuco
0	3.79×10^{-3}	29.6	26.9	1.18	0.80	41.5
25	2.30×10^{-2}	26.3	22.5	4.46	0.87	45.9
35	2.77×10^{-2}	23.4	18.6	8.81	1.27	47.9
LP 35	4.65×10^{-5}	4.70	2.95	38.5	7.03	46.8
50	1.03×10^{-2}	21.1	15.6	12.4	2.08	48.8
LP 50	5.47×10^{-5}	2.47	1.23	12.5	10.4	73.3
75	3.51×10^{-3}	9.67	37.3	11.3	2.92	38.8
LP 75	6.17×10^{-5}	1.50	35.0	21.4	10.1	32.0
100	1.14×10^{-3}	28.2	44.9	19.8	7.12	nd
LP 100	3.51×10^{-5}	1.95	0.94	13.2	11.8	72.1
125	8.96×10^{-4}	38.6	52.4	nd	8.98	0.00
LP 125	1.24×10^{-5}	5.23	5.71	7.34	19.3	62.5
150	4.10×10^{-4}	48.8	27.3	12.3	11.6	nd
LP 150	2.42×10^{-5}	3.29	5.79	2.91	14.7	73.3
200	2.22×10^{-4}	28.5	41.6	19.1	10.8	nd
LP 200	2.02×10^{-5}	6.25	4.71	4.83	13.4	70.8
300	1.50×10^{-4}	44.7	20.8	17.8	16.8	nd
LP 300	4.36×10^{-6}	12.0	29.6	25.4	33.0	nd
TS 313	0.41	13.9	6.04	25.6	54.4	nd
500	1.59×10^{-4}	46.0	17.1	26.9	9.93	nd
LP 500	5.46×10^{-6}	10.1	20.9	27.6	41.5	nd
750	6.72×10^{-5}	25.3	26.6	24.2	23.9	nd
LP 750	2.49×10^{-6}	5.08	7.84	51.9	35.1	nd
TS 924	1.70	10.9	14.8	26.1	48.2	nd

nd= not detected

Table 3.A4. Concentration ($\mu\text{mol C l}^{-1}$) or flux ($\mu\text{mol C m}^{-2}\text{d}^{-1}$) and composition of amino acids (mol %) during three sampling periods in the spring of 2005. The caption for Table 3.A3 describes the samples in more detail.

Table 3.A4. Amino Acid Compositions of 2005 Pump and TS Trap Samples (mol %)

March 2 Pumps, March 4-9 Traps:

Depth (m)	Amino Acid Concentration or Flux								
	($\mu\text{mol C l}^{-1}$ or $\mu\text{mol C m}^{-2} \text{ d}^{-1}$)	%ASP	%GLU	%SER	%THR	%GLY	%BALA	%GABA	%Other
5	1.05	11.8	12.5	8.68	5.55	10.9	1.11	0.21	49.2
LP 5	1.96×10^{-3}	9.22	8.04	10.5	6.00	20.7	0.53	0.15	44.8
200	0.49	10.9	11.7	7.95	5.55	11.7	1.48	0.13	50.6
300	0.45	11.5	11.8	6.69	6.38	11.9	0.52	0.17	51.1
LP 300	1.86×10^{-3}	12.5	14.2	7.09	5.24	14.4	3.13	0.20	43.3
TS 313	237	8.76	8.31	10.3	7.06	14.8	1.55	1.08	48.2
400	0.53	11.5	12.1	9.29	5.91	12.4	1.58	0.16	47.2
500	0.36	11.7	12.0	8.69	5.78	11.7	2.37	0.20	47.6
TS 924	162	11.5	10.3	11.2	6.30	12.1	0.76	0.72	47.2

March 9-14 Pumps, March 9-14 Traps:

Depth (m)	Amino Acid Concentration or Flux								
	($\mu\text{mol C l}^{-1}$ or $\mu\text{mol C m}^{-2} \text{ d}^{-1}$)	%ASP	%GLU	%SER	%THR	%GLY	%BALA	%GABA	%Other
2	0.57	11.1	12.2	7.32	6.16	11.5	0.46	0.30	50.9
LP 2	8.65×10^{-3}	6.69	5.97	9.79	6.50	15.8	0.52	0.45	54.3
5	0.68	11.4	13.8	6.75	5.80	12.4	0.23	0.21	49.5
LP 5	5.12×10^{-3}	12.6	12.7	6.38	5.76	14.1	2.00	0.20	46.2
25	0.46 ± 0.11	11.0 ± 0.8	13.7 ± 1.0	6.99 ± 0.07	6.23 ± 0.01	11.1 ± 0.9	0.33 ± 0.004	0.20 ± 0.004	50.5 ± 1.0
LP 25	$1.96 \pm 0.49 \times 10^{-2}$	10.1 ± 0.5	11.4 ± 1.0	7.04 ± 0.15	5.88 ± 0.35	10.2 ± 0.01	0.10 ± 0.01	0.20 ± 0.01	55.0 ± 1.0
50	0.36	10.9	12.3	6.95	6.38	12.7	0.38	0.17	50.3
LP 50	4.68×10^{-3}	12.0	10.7	8.35	6.02	15.7	2.24	1.02	43.9
60	0.47	9.96	11.5	7.27	6.24	13.8	0.36	0.26	50.6
LP 60	1.42×10^{-2}	6.84	6.47	7.97	6.50	11.3	0.15	0.18	60.6
75	0.24	10.1	12.2	7.53	5.87	12.4	1.87	0.21	49.8
100	0.34 ± 0.04	11.4 ± 2.4	12.4 ± 1.3	7.07 ± 1.38	6.36 ± 0.32	11.3 ± 1.2	1.71 ± 0.02	0.20 ± 0.16	49.5 ± 0.7
LP 100	4.26×10^{-3}	11.4	11.3	7.03	5.99	14.2	2.27	0.39	47.4
150	0.23 ± 0.11	10.6 ± 2.2	12.0 ± 1.0	7.19 ± 1.06	6.36 ± 0.02	11.9 ± 1.0	1.93 ± 0.73	0.23 ± 0.05	49.8 ± 1.8
LP 150	5.93×10^{-3}	10.6	10.5	7.90	5.85	17.7	1.72	0.90	44.8
200	0.21 ± 0.21	12.9 ± 0.9	12.3 ± 0.8	8.06 ± 0.57	5.50 ± 0.94	14.4 ± 6.1	1.63 ± 0.47	0.12 ± 0.03	45.1 ± 6.3
300	0.10 ± 0.03	12.6 ± 0.4	12.9 ± 0.02	7.14 ± 1.30	6.29 ± 0.33	11.1 ± 0.9	0.47 ± 0.002	0.15 ± 0.04	49.4 ± 1.5
TS 313	189	10.6	8.95	9.47	7.21	14.1	1.74	0.57	47.4
350	$8.52 \pm 1.26 \times 10^{-2}$	8.88 ± 3.46	12.0 ± 0.8	6.61 ± 0.51	7.35 ± 0.97	12.5 ± 1.7	0.56 ± 0.14	0.23 ± 0.08	51.9 ± 0.7
400	0.12 ± 0.03	9.96 ± 0.25	9.75 ± 0.34	7.04 ± 0.86	6.56 ± 0.08	11.8 ± 0.5	0.49 ± 0.04	0.17 ± 0.05	54.2 ± 0.3
500	0.15	9.10	9.94	6.29	4.82	13.40	0.58	0.32	55.50
600	$7.31 \pm 1.80 \times 10^{-2}$	9.61 ± 1.23	11.1 ± 2.2	8.53 ± 2.06	5.76 ± 0.05	13.8 ± 0.7	3.25 ± 2.91	0.42 ± 0.03	47.5 ± 0.8
800	$4.89 \pm 2.04 \times 10^{-2}$	10.3 ± 1.9	10.2 ± 1.0	8.43 ± 0.71	5.70 ± 0.85	13.8 ± 1.6	1.49 ± 0.02	0.62 ± 0.08	49.4 ± 1.3
900	7.33×10^{-2}	9.97	12.4	8.67	6.10	13.3	1.33	0.32	47.8
TS 924	120	10.8	8.90	8.50	6.99	14.5	1.26	0.73	48.2
1200	6.09×10^{-2}	11.3	12.7	8.49	5.17	21.2	1.35	0.38	39.3
1500	3.55×10^{-2}	10.6	10.8	8.36	5.06	20.2	2.22	0.44	42.3
1800	1.62×10^{-2}	9.82	7.91	9.08	6.92	15.1	2.34	0.81	48.0
LP 1800	9.15×10^{-4}	11.8	12.0	8.59	5.17	16.5	8.63	0.38	37.0

April 29-30 Pumps, April 23-28 Traps:

Depth (m)	Amino Acid Concentration or Flux								
	($\mu\text{mol C l}^{-1}$ or $\mu\text{mol C m}^{-2} \text{ d}^{-1}$)	%ASP	%GLU	%SER	%THR	%GLY	%BALA	%GABA	%Other
0	4.83	10.2	8.12	8.18	7.93	9.75	0.82	0.33	54.7
25	4.62	10.6	11.7	7.83	5.90	11.8	0.34	0.14	51.7
35	3.23	10.7	11.1	7.91	5.80	9.97	0.56	0.18	53.9
LP 35	2.42×10^{-2}	7.35	6.91	8.18	6.60	18.0	0.51	1.01	51.4
50	1.45	11.9	12.0	8.05	7.57	14.5	0.79	0.33	44.9
LP 50	2.27×10^{-2}	10.2	9.89	8.13	6.44	17.4	0.67	1.16	46.2
75	1.05	10.6	10.8	7.95	5.89	13.3	0.76	0.24	50.4
LP 75	2.73×10^{-2}	9.30	8.45	7.99	6.46	17.4	0.54	0.96	48.9
100	0.76	10.1	11.2	7.63	5.89	12.5	0.87	0.36	51.4
LP 100	0.10	8.40	8.95	7.44	5.72	17.7	0.27	0.41	51.1
125	0.51	11.6	11.6	7.84	6.16	13.1	1.08	0.27	48.4
LP 125	2.02×10^{-2}	9.99	9.74	9.05	5.91	17.1	0.74	1.00	46.5
150	0.26	11.9	12.3	7.85	6.17	14.0	1.67	0.23	45.9
LP 150	2.89×10^{-2}	8.97	8.55	7.21	6.15	17.1	0.37	0.63	51.1
200	0.36	10.2	11.6	7.68	6.05	11.4	0.22	0.23	52.6
LP 200	4.14×10^{-2}	10.3	11.2	7.29	5.61	15.3	0.27	0.48	49.6
300	0.13	12.3	13.8	8.15	6.10	11.6	1.34	0.25	46.5
LP 300	3.85×10^{-3}	11.0	12.9	7.62	4.51	21.5	2.21	0.26	40.0
TS 313	53.2	7.35	7.86	8.85	6.37	14.3	0.44	0.30	54.5
500	0.19	13.4	8.82	11.51	6.49	18.4	1.37	0.43	39.6
LP 500	2.21×10^{-2}	10.3	11.8	6.06	6.03	18.1	0.53	0.14	47.0
750	0.28	13.1	10.0	11.93	4.28	20.0	3.20	0.21	37.3
LP 750	7.97×10^{-3}	11.5	12.9	6.62	5.73	15.5	2.01	0.31	45.4
TS 924	82.3	6.24	5.10	10.76	6.63	20.1	0.85	0.85	49.4

nd= not detected

Table 3.A5. Pigment Compositions of 2003 Pump and SV Trap Samples (mol %)					
March 4-10 and May 7-12 Pumps (200 m), March 6-May 6 Traps (238 m):					
SV (m d⁻¹)	%chl <i>a</i>	%phytin	%phide	%pyrophide	%fuco
>979	5.80 ± 8.21	17.3 ± 10.0	7.39 ± 10.45	63.2 ± 17.6	6.33 ± 8.95
490-979	16.9 ± 0.8	14.7 ± 1.9	9.53 ± 3.63	48.5 ± 1.2	10.4 ± 3.4
196-490	13.0 ± 1.3	9.87 ± 0.55	17.0 ± 0.03	50.0 ± 0.5	10.1 ± 1.4
98-196	11.8 ± 3.0	7.42 ± 0.56	15.5 ± 6.4	54.7 ± 9.3	10.6 ± 0.5
49-98	13.6 ± 1.8	5.63 ± 0.95	12.6 ± 10.6	55.3 ± 12.2	12.9 ± 1.3
22-49	15.0 ± 0.5	6.30 ± 0.26	13.9 ± 5.5	52.7 ± 7.7	12.1 ± 2.0
11-22	13.4 ± 0.8	9.31 ± 0.88	16.2 ± 0.3	50.0 ± 0.5	11.1 ± 0.7
5.4-11	14.2 ± 2.1	8.21 ± 1.97	10.9 ± 8.2	57.0 ± 5.6	9.7 ± 1.6
2.7-5.4	14.6 ± 1.7	7.96 ± 3.21	16.8 ± 0.6	49.5 ± 1.6	11.2 ± 0.7
1.4-2.7	15.1 ± 1.7	7.90 ± 0.06	9.82 ± 8.83	56.6 ± 6.5	10.6 ± 0.5
0.7-1.4	7.28 ± 1.12	29.1 ± 24.6	6.23 ± 4.68	49.6 ± 25.2	7.8 ± 3.0
SP	64.4 ± 50.3	23.4 ± 33.1	5.26 ± 7.45	6.90 ± 9.75	nd
May 7-12 and June 25-30 Pumps (100 m), May 14-June 30 Traps (117 m):					
SV (m d⁻¹)	%chl <i>a</i>	%phytin	%phide	%pyrophide	%fuco
>979	17.0	50.6	16.8	15.6	nd
490-979	14.9	51.3	3.76	12.7	17.2
196-490	16.5	43.8	7.79	13.6	18.4
98-196	18.5	48.7	4.98	11.6	16.2
49-98	20.8	38.6	4.85	18.9	17.0
22-49	20.5	40.7	5.44	11.8	21.6
11-22	18.0	41.9	7.96	16.1	16.0
5.4-11	19.5	27.2	11.7	18.8	22.8
2.7-5.4	24.7	32.0	7.58	11.4	24.3
1.4-2.7	12.0	30.2	7.14	33.7	16.9
0.7-1.4	20.6	31.3	7.63	22.3	18.1
SP	17.1 ± 16.5	43.2 ± 5.2	7.1 ± 4.9	25.8 ± 17.0	6.8 ± 9.6

nd= not detected

Table 3.A5. Composition of pigments (mol %) with settling velocity for spring-summer, 2003. Most data shown are for the settling velocity trap (collected in duplicate and averaged). Also shown are data for the 1-70 µm pumps (small pump, or SP) collected at approximately the same depth. As the data for each settling velocity class are integrated over the entire deployment period, we have averaged the pump data collected at the beginning and end of each trap deployment for comparison.

Table 3.A6. Amino Acid Compositions of 2003 Pump and SV Trap Samples (mol %)								
March 4-10 and May 7-12 Pumps (200 m), March 6-May 6 Traps (238 m):								
SV (m d ⁻¹)	%ASP	%GLU	%SER	%THR	%GLY	%BALA	%GABA	%Other
>979	8.48 ± 3.04	11.5 ± 0.6	6.01 ± 2.57	7.88 ± 0.24	12.0 ± 2.5	0.08 ± 0.11	0.13 ± 0.19	54.0 ± 7.5
490-979	10.1 ± 1.1	9.75 ± 0.29	8.23 ± 0.70	7.35 ± 0.17	14.1 ± 0.5	0.40 ± 0.33	0.53 ± 0.11	49.5 ± 1.3
196-490	9.93 ± 0.36	8.64 ± 0.28	10.2 ± 0.75	7.14 ± 0.17	17.3 ± 0.5	0.40 ± 0.09	0.35 ± 0.03	46.1 ± 1.4
98-196	8.94 ± 0.15	8.87 ± 0.40	7.61 ± 0.31	6.94 ± 0.03	15.4 ± 0.03	0.68 ± 0.07	0.56 ± 0.03	51.0 ± 0.02
49-98	10.0 ± 1.2	9.73 ± 0.70	6.68 ± 0.12	6.64 ± 0.02	13.2 ± 0.8	0.55 ± 0.05	0.61 ± 0.01	52.6 ± 1.4
22-49	8.31 ± 0.42	9.65 ± 0.45	6.41 ± 0.03	6.80 ± 0.09	13.4 ± 0.3	0.46 ± 0.08	0.50 ± 0.001	54.5 ± 0.5
11-22	8.01 ± 0.31	9.89 ± 0.22	6.41 ± 0.33	6.73 ± 0.31	13.5 ± 0.2	0.52 ± 0.06	0.48 ± 0.07	54.5 ± 0.5
5.4-11	9.88 ± 1.79	10.3 ± 0.5	6.27 ± 0.34	6.64 ± 0.05	14.3 ± 0.04	0.64 ± 0.13	0.60 ± 0.0006	51.4 ± 1.8
2.7-5.4	8.16 ± 0.42	9.91 ± 1.71	6.36 ± 0.28	6.82 ± 0.04	12.9 ± 0.3	0.42 ± 0.22	0.49 ± 0.10	54.9 ± 1.2
1.4-2.7	8.68 ± 0.78	9.60 ± 0.60	6.38 ± 0.47	6.75 ± 0.19	13.1 ± 0.5	0.44 ± 0.16	0.53 ± 0.01	54.5 ± 1.1
0.7-1.4	7.77 ± 1.00	9.29 ± 0.80	6.13 ± 1.29	6.66 ± 0.02	14.5 ± 1.1	0.34 ± 0.22	0.51 ± 0.01	54.8 ± 2.8
SP	10.8 ± 1.4	11.4 ± 1.3	5.38 ± 0.93	6.77 ± 0.29	10.6 ± 2.1	0.03 ± 0.04	0.15 ± 0.02	55.0 ± 0.7
May 7-12 and June 25-30 Pumps (100 m), May 14-June 30 Traps (117 m):								
SV (m d ⁻¹)	%ASP	%GLU	%SER	%THR	%GLY	%BALA	%GABA	%Other
>979	11.8	16.0	5.07	4.68	8.35	nd	nd	54.1
490-979	12.6	10.5	7.08	7.70	14.3	0.34	0.43	47.1
196-490	12.4	11.7	6.57	7.48	12.0	0.19	0.66	49.0
98-196	11.8	9.70	5.28	7.29	12.4	0.46	0.79	52.3
49-98	11.6	10.2	5.18	7.02	12.6	0.33	0.48	52.6
22-49	10.6	10.2	4.73	7.13	13.4	0.25	0.55	53.1
11-22	12.0	10.1	5.07	7.32	13.7	0.38	0.59	50.9
5.4-11	11.1	10.9	4.47	7.25	13.6	0.13	0.30	52.4
2.7-5.4	13.5	13.6	4.66	5.61	8.38	nd	0.27	53.9
1.4-2.7	13.6	13.7	4.82	6.34	0.44	nd	0.31	60.8
0.7-1.4	12.0	12.2	4.61	5.94	9.93	nd	0.20	55.0
SP	10.8 ± 0.8	12.5 ± 1.1	5.52 ± 0.34	7.29 ± 0.10	12.7 ± 1.7	0.39 ± 0.04	0.09 ± 0.12	50.7 ± 0.3

nd= not detected

Table 3.A6. Composition of amino acids (mol %) with settling velocity for spring-summer, 2003. The caption for Table 3.A5 describes the samples in more detail.

Table 3.A7. Pigment Compositions of 2005 Pump and SV Trap Samples (mol %)					
March 2, March 9-14, and April 29-30 Pumps (300 m), March 4-May 1 Traps (313 m):					
SV (m d ⁻¹)	%chl <i>a</i>	%phytin	%phide	%pyropheide	%fuco
>979	7.52 ± 1.41	20.3 ± 10.1	20.6 ± 11.0	51.6 ± 2.3	0.00
490-979	7.99 ± 2.87	8.65 ± 4.06	22.3 ± 3.7	56.3 ± 3.9	4.81 ± 6.80
326-490	8.54 ± 2.88	8.01 ± 2.88	20.4 ± 7.2	57.7 ± 5.4	5.33 ± 7.54
196-326	9.52 ± 5.53	7.50 ± 3.40	18.0 ± 6.7	60.7 ± 9.5	4.33 ± 6.12
140-196	9.32 ± 4.11	11.2 ± 8.5	17.8 ± 1.0	57.7 ± 8.1	3.92 ± 5.55
98-140	8.14 ± 0.12	5.66 ± 0.40	16.0 ± 0.5	66.0 ± 5.9	4.21 ± 5.95
49-98	5.52 ± 0.07	5.17 ± 0.35	14.1 ± 0.4	70.9 ± 6.2	4.34 ± 6.14
22-49	7.18 ± 0.16	6.11 ± 0.48	17.2 ± 0.3	64.8 ± 6.3	4.69 ± 6.63
11-22	6.07 ± 0.12	6.83 ± 0.52	19.0 ± 0.4	63.7 ± 6.0	4.41 ± 6.23
5.4-11	5.88 ± 0.24	3.98 ± 2.76	15.5 ± 0.3	70.1 ± 9.8	4.58 ± 6.47
0.7-5.4	6.39	6.25	16.5	61.7	9.24
LP	12.8 ± 1.1	33.1 ± 4.9	24.2 ± 1.7	20.5 ± 17.6	9.36 ± 13.24
SP	51.6 ± 27.3	10.0 ± 9.5	8.17 ± 8.62	7.54 ± 8.21	22.7 ± 38.0
March 2, March 9-14, and April 29-30 Pumps (500 m), March 4-May 1 Traps (524 m):					
SV (m d ⁻¹)	%chl <i>a</i>	%phytin	%phide	%pyropheide	%fuco
>979	12.6 ± 3.0	4.93 ± 5.95	17.0 ± 8.8	47.7 ± 6.5	17.7 ± 5.3
490-979	7.94	9.11	23.1	49.1	10.8
326-490	8.51 ± 2.88	4.14 ± 1.59	15.4 ± 6.0	59.7 ± 1.2	12.3 ± 3.6
196-326	6.77 ± 1.66	6.38 ± 1.09	20.1 ± 3.9	58.0 ± 5.2	8.74 ± 1.45
140-196	5.46 ± 0.03	5.59 ± 1.69	15.0 ± 1.2	63.5 ± 0.4	10.5 ± 0.9
98-140	8.91 ± 0.82	8.68 ± 1.34	18.5 ± 3.0	56.7 ± 12.7	7.27 ± 10.28
49-98	8.57 ± 0.92	6.72 ± 1.27	22.1 ± 1.8	54.4 ± 9.5	8.28 ± 11.71
22-49	8.30 ± 0.20	7.12 ± 0.69	21.6 ± 3.7	55.9 ± 6.8	7.06 ± 9.98
11-22	6.89 ± 0.44	6.24 ± 0.09	18.2 ± 0.7	63.3 ± 6.7	5.44 ± 7.69
5.4-11	6.19 ± 1.57	5.54 ± 0.15	18.0 ± 7.1	65.0 ± 1.1	5.27 ± 7.45
0.7-5.4	7.25 ± 0.37	8.12 ± 0.24	22.7 ± 2.1	50.1 ± 2.3	11.8 ± 0.02
LP	10.1	20.9	27.6	41.5	nd
SP	58.1 ± 19.2	8.79 ± 7.42	13.7 ± 11.5	4.8 ± 4.5	14.6 ± 23.4
March 9-14 Pumps (1800 m), March 4-May 1 Traps (1918 m):					
SV (m d ⁻¹)	%chl <i>a</i>	%phytin	%phide	%pyropheide	%fuco
>979	9.30 ± 4.01	15.1 ± 2.3	18.5 ± 10.4	49.1 ± 23.4	7.98 ± 11.3
490-979	7.72 ± 0.22	9.10 ± 1.04	19.6 ± 1.9	53.3 ± 0.8	10.2 ± 1.9
326-490	8.13 ± 0.49	8.59 ± 1.95	22.3 ± 1.9	48.7 ± 6.5	12.3 ± 2.2
196-326	7.01 ± 0.68	8.70 ± 2.60	21.1 ± 1.0	54.0 ± 4.2	9.2 ± 0.1
140-196	6.53 ± 1.80	8.29 ± 0.10	22.2 ± 1.0	63.0 ± 0.9	nd
98-140	6.08 ± 0.85	5.76 ± 0.14	17.2 ± 0.1	60.8 ± 0.6	10.1 ± 1.7
49-98	6.72 ± 0.65	11.0 ± 0.3	19.6 ± 2.7	62.6 ± 3.7	nd
22-49	5.86 ± 0.82	9.50 ± 3.09	20.7 ± 2.8	64.0 ± 1.2	nd
11-22	6.20 ± 0.19	10.2 ± 3.9	16.8 ± 2.5	66.9 ± 1.7	nd
5.4-11	8.57 ± 1.85	9.09 ± 3.05	18.7 ± 0.3	63.7 ± 0.9	nd
0.7-5.4	6.26 ± 0.09	7.44 ± 0.83	18.0 ± 3.0	59.8 ± 2.3	8.5 ± 0.1
LP	20.0	30.8	28.8	20.4	nd
SP	54.6	4.37	6.35	6.13	28.6

nd= not detected

Table 3.A7. Composition of pigments (mol %) with settling velocity for the spring of 2005. Most data shown are for the settling velocity traps (collected in duplicate and averaged). Also shown are data for the 1-70 μm pumps (small pump, or SP) and >70 μm pumps (large pump, or LP) collected at approximately the same depths. As the data for each settling velocity class are integrated over the entire deployment period, we have averaged the pump data from all three pump casts to the extent possible.

Table 3.A8. Amino Acid Compositions of 2005 Pump and SV Trap Samples (mol %)								
March 2, March 9-12, and April 29-30 Pumps (300 m), March 4-May 1 Traps (313 m):								
SV (m d ⁻¹)	%ASP	%GLU	%SER	%THR	%GLY	%BALA	%GABA	%Other
>979	8.50 ± 0.89	8.57 ± 0.47	8.02 ± 0.76	6.52 ± 0.38	13.6 ± 0.4	0.38 ± 0.28	0.19 ± 0.09	54.3 ± 0.6
490-979	6.48 ± 1.93	8.36 ± 0.33	7.54 ± 0.48	5.42 ± 1.11	21.1 ± 10.2	0.23 ± 0.12	0.32 ± 0.19	50.6 ± 10.6
326-490	7.76 ± 0.64	8.45 ± 0.85	8.67 ± 0.72	6.21 ± 0.67	20.3 ± 1.3	0.64 ± 0.39	0.54 ± 0.18	47.4 ± 0.5
196-326	7.94 ± 2.25	8.49 ± 0.51	8.22 ± 1.50	6.11 ± 0.80	20.5 ± 0.4	0.43 ± 0.23	0.51 ± 0.33	47.8 ± 4.6
140-196	5.09 ± 3.72	6.50 ± 6.68	5.96 ± 2.47	6.46 ± 0.32	24.7 ± 15.3	0.22 ± 0.04	0.20 ± 0.03	50.9 ± 2.1
98-140	9.22 ± 0.76	9.32 ± 1.44	8.22 ± 1.36	6.17 ± 0.23	18.9 ± 1.3	0.40 ± 0.37	0.51 ± 0.43	47.2 ± 3.0
49-98	8.55 ± 0.16	8.92 ± 1.39	9.08 ± 0.15	6.29 ± 0.05	18.8 ± 3.9	0.49 ± 0.15	0.62 ± 0.26	47.2 ± 3.3
22-49	7.57 ± 0.08	8.54 ± 1.74	1.26 ± 0.01	6.35 ± 0.43	17.8 ± 2.0	0.57 ± 0.49	0.59 ± 0.33	49.5 ± 2.8
11-22	7.27 ± 0.51	9.28 ± 1.75	7.88 ± 0.37	6.07 ± 0.23	15.4 ± 2.7	0.44 ± 0.06	0.35 ± 0.23	53.3 ± 0.8
5.4-11	6.74 ± 0.87	8.42 ± 1.16	8.39 ± 1.54	6.15 ± 0.35	16.7 ± 3.9	0.49 ± 0.36	0.46 ± 0.38	52.6 ± 6.3
0.7-5.4	7.53	7.98	9.48	6.67	19.7	0.60	0.72	47.3
LP	11.7 ± 1.0	13.5 ± 0.9	7.33 ± 0.41	4.85 ± 0.49	17.9 ± 5.1	2.67 ± 0.65	0.23 ± 0.04	41.5 ± 2.1
SP	12.2 ± 0.6	12.8 ± 1.0	7.33 ± 0.75	6.26 ± 0.14	11.5 ± 0.4	0.78 ± 0.49	0.19 ± 0.05	49.0 ± 2.3
March 2, March 9-12, and April 29-30 Pumps (500 m), March 4-May 1 Traps (524 m):								
SV (m d ⁻¹)	%ASP	%GLU	%SER	%THR	%GLY	%BALA	%GABA	%Other
>979	9.33 ± 0.25	8.40 ± 0.51	9.03 ± 0.54	6.62 ± 0.36	18.6 ± 1.0	0.95 ± 0.74	0.65 ± 0.29	46.5 ± 1.4
490-979	8.03 ± 0.15	8.07 ± 2.09	9.01 ± 0.64	6.82 ± 0.23	18.3 ± 3.1	0.70 ± 0.53	0.58 ± 0.36	48.4 ± 2.1
326-490	8.20 ± 0.49	7.64 ± 0.34	8.90 ± 0.56	6.67 ± 0.40	18.7 ± 1.5	0.71 ± 0.20	0.64 ± 0.04	48.5 ± 2.0
196-326	8.51 ± 0.09	7.27 ± 0.42	9.87 ± 0.34	6.71 ± 0.14	20.7 ± 0.3	0.91 ± 0.03	0.74 ± 0.14	45.3 ± 0.8
140-196	8.62 ± 1.81	7.69 ± 1.34	9.69 ± 0.91	6.46 ± 0.05	20.4 ± 2.2	0.82 ± 0.10	0.69 ± 0.01	45.6 ± 0.2
98-140	11.5 ± 1.0	10.3 ± 0.6	11.5 ± 2.5	3.56 ± 4.41	10.6 ± 5.5	0.91 ± 0.10	0.76 ± 0.22	50.9 ± 7.5
49-98	9.51 ± 1.42	8.57 ± 1.28	10.0 ± 0.6	6.92 ± 0.38	16.4 ± 4.9	0.81 ± 0.25	0.74 ± 0.05	47.1 ± 0.9
22-49	9.51 ± 1.38	8.73 ± 1.71	9.47 ± 0.30	6.93 ± 0.36	16.8 ± 5.6	0.67 ± 0.12	0.63 ± 0.07	47.3 ± 1.8
11-22	9.94 ± 0.16	8.85 ± 0.97	9.60 ± 0.05	6.78 ± 0.52	16.6 ± 4.9	0.71 ± 0.16	0.66 ± 0.06	46.8 ± 3.4
5.4-11	8.30 ± 1.52	8.07 ± 1.33	9.52 ± 0.32	6.92 ± 0.12	19.9 ± 0.9	0.61 ± 0.09	0.61 ± 0.01	46.1 ± 1.6
0.7-5.4	6.82 ± 1.02	6.23 ± 1.89	9.08 ± 0.56	7.40 ± 1.30	21.20 ± 0.9	1.24 ± 0.59	0.82 ± 0.06	47.2 ± 0.7
LP	10.3	11.8	6.06	6.03	18.1	0.53	0.14	47.0
SP	11.4 ± 2.2	10.2 ± 1.6	8.83 ± 2.61	5.69 ± 0.84	14.5 ± 3.5	1.44 ± 0.90	0.32 ± 0.12	47.6 ± 8.0
March 9-12 Pumps (1800 m), March 4-May 1 Traps (1918 m):								
SV (m d ⁻¹)	%ASP	%GLU	%SER	%THR	%GLY	%BALA	%GABA	%Other
>979	9.42 ± 1.30	9.16 ± 3.15	9.04 ± 1.04	6.93 ± 0.55	17.1 ± 6.0	0.48 ± 0.46	0.48 ± 0.46	47.4 ± 3.0
490-979	8.59 ± 1.80	7.17 ± 1.02	9.66 ± 0.003	6.79 ± 0.41	21.7 ± 0.2	1.29 ± 0.22	1.07 ± 0.16	43.8 ± 2.7
326-490	10.7 ± 0.9	8.04 ± 0.83	9.74 ± 0.11	6.84 ± 0.61	21.4 ± 1.8	1.20 ± 0.21	0.97 ± 0.15	41.2 ± 3.9
196-326	9.20 ± 0.65	6.99 ± 0.55	10.1 ± 0.2	6.62 ± 0.94	21.9 ± 0.7	1.34 ± 0.22	1.08 ± 0.07	42.9 ± 2.7
140-196	9.97 ± 1.14	7.89 ± 0.96	9.81 ± 0.43	6.35 ± 0.53	21.9 ± 0.1	1.48 ± 0.61	1.02 ± 0.09	41.6 ± 1.4
98-140	9.45 ± 0.52	8.69 ± 1.63	10.3 ± 0.004	6.37 ± 1.09	19.1 ± 3.1	1.50 ± 1.03	0.91 ± 0.32	43.6 ± 1.2
49-98	9.64 ± 0.10	8.44 ± 0.62	9.98 ± 0.50	6.40 ± 0.18	17.1 ± 2.7	1.49 ± 0.54	0.94 ± 0.03	46.0 ± 1.8
22-49	10.3 ± 0.8	9.58 ± 0.58	9.33 ± 1.11	5.91 ± 0.70	17.9 ± 5.9	1.81 ± 1.15	1.11 ± 0.17	44.0 ± 4.1
11-22	9.00 ± 2.23	8.84 ± 1.47	10.2 ± 0.04	6.03 ± 0.59	17.3 ± 5.3	1.51 ± 0.82	1.07 ± 0.01	46.0 ± 1.8
5.4-11	9.37 ± 3.58	9.02 ± 1.79	9.96 ± 0.43	5.88 ± 0.54	18.8 ± 4.7	1.45 ± 0.55	0.91 ± 0.14	44.6 ± 0.4
0.7-5.4	10.5 ± 1.5	8.72 ± 1.72	9.79 ± 0.29	6.37 ± 0.05	19.1 ± 3.5	1.38 ± 0.44	0.88 ± 0.18	43.3 ± 1.1
LP	11.8	12.0	8.59	5.17	16.5	8.63	0.38	37.0
SP	9.82	7.91	9.08	6.92	15.1	2.34	0.81	48.0

nd= not detected

Table 3.A8. Composition of amino acids (mol %) with settling velocity for the spring of 2005. The caption for Table 3.A7 describes the samples in more detail.

CHAPTER 4

Fecal Pellets and Phytoplankton Aggregates: Differences in the Extent of Exchange between Suspended and Sinking Particles

Abstract

The extent to which sinking particles disaggregate and exchange with surrounding material affects the efficiency of particulate organic carbon (POC) export to the deep sea. To assess the extent of exchange between different particle types, we collected suspended and sinking particles at depths of 20 m (50- μm mesh plankton tow) and 200 m (50- μm mesh, neutrally buoyant NetTrap) in the Mediterranean Sea in 2006, and incubated them (independently) for 54-72 h in rotating tanks. Particles collected at 20 m were primarily composed of phytoplankton, and particles collected at 200 m by NetTrap were composed of phytoplankton (~60-80% based on pigment compositions) and fecal pellets (~20-40%). Suspended and sinking phytoplankton material from 20 m underwent extensive exchange during the incubation, as evidenced by relative homogeneity in composition and repeated mass transfers. Material collected at 200 m underwent less exchange, with some transfer of suspended phytoplankton material into the sinking phase, but no apparent disaggregation. Fecal pellet indicators underwent the least exchange in both incubations. Unlike phytoplankton aggregates, fecal pellets appear to undergo little exchange with surrounding material during transit, likely reducing their residence times and decomposition in the water column.

1. Introduction

In the open ocean, the vast majority of individual particles produced in the water column are less than 2 μm in diameter, so their export to the deep ocean is largely controlled by aggregation processes such as abiotic flocculation or incorporation into fecal pellets (McCave, 1975; Pilskaln and Honjo, 1987; Alldredge and Silver, 1988). The aggregation of individual plankton cells or inorganic particles increases their settling velocities by 1-5 orders of magnitude, depending on the size and density of the resulting aggregates (Shanks and Trent, 1980; Alldredge and Gottschalk, 1988; Gibbs, 1985). Therefore, the extent to which

particles aggregate or disaggregate in the water column mediates the vertical flux of organic and inorganic material and greatly affects ocean geochemistry (Fowler and Knauer, 1986; Asper et al., 1992).

The vertical flux of particulate organic carbon (POC) is of particular importance in geochemical cycles, since it controls the drawdown of atmospheric CO₂ into the ocean in many locations. Attempts to quantitatively predict POC fluxes often relate export to primary or new production; however, recent studies suggest that fluxes and production can be decoupled, and that fluxes may be determined by other factors such as ballasting by minerals (Armstrong et al., 2002; Francois et al., 2002; Klaas and Archer, 2002). Obviously, the extent to which sinking particles disaggregate, resulting in lower settling velocities, also affects the efficiency of POC export. Therefore, we propose that the composition of aggregates and their resulting robustness is another critical factor determining POC fluxes.

We compared the pigment and amino acid compositions of sediment trap and *in situ* pump samples collected in 2003 and 2005 in the northwest Mediterranean Sea to assess the extent of exchange between sinking and suspended particles (Chapter 3). Sinking particles were enriched in fecal pellet indicators, whereas suspended particles were enriched in chlorophyll *a* and occasionally, bacterial degradation products. These compositions remained consistent with depth, suggesting that exchange was limited. Our findings suggest that fecal pellets remain largely intact during transit through the water column, undergoing very little disaggregation and reaggregation with surrounding material. However, we could not determine if the same was true for phytoplankton aggregates, and in fact found some indication that they may undergo more extensive exchange.

To experimentally confirm our field observations and examine differences in the extent to which fecal pellets and aggregates can exchange with surrounding material, in 2006 we performed shipboard incubations of phytoplankton and sinking fecal pellets. To mimic the continual aggregation and disaggregation that might occur in the water column, we incubated particles in cylindrical rotating tanks on roller tables. Shanks and Edmondson (1989) demonstrated that the particle collisions generated by this rotation are capable of inducing flocculation. The extent of particle aggregation and disaggregation was investigated by determining the exchange of mass, organic matter, and inorganic material between the suspended and sinking fractions.

2. Methods

2.1. Particle Collection and Incubation

Particles were collected in April, 2006 at the DYFAMED site (43°20'N, 7°40'E), a French JGOFS time-series site ~52 km off the coast of Nice in the Ligurian Sea (northwest Mediterranean). Plankton were collected from the mixed layer using a 50 μm mesh plankton net deployed at 20 m depth on April 11. Particles sinking out of the mixed layer were collected using a 50 μm mesh NetTrap deployed at 200 m for 15 h overnight on April 9-10. The NetTrap is a large (2 m diameter), conical particle collection apparatus based on the design of a closing plankton trap, but is neutrally buoyant so it can be deployed at depth in an upright position to collect sinking particles (Peterson et al., 2005, submitted). During recovery of this sample, the trap failed to close completely, so it likely contained some material from higher in the water column.

Upon recovery of the plankton net and NetTrap, the composition of the material collected was determined by microscopy. The plankton tow contained almost entirely diatoms, with occasional coccolithophorids, copepods, or euphausiids. The main species observed were *Thalassionema nitzschioides*, *Thalassiothrix frauenfeldi*, *Ditylum brightwellii*, *Chaetoceros atlanticum*, and *Skeletonema costatum* (identified by S.W. Fowler). The NetTrap contained individual phytoplankton, phytoplankton aggregates, amorphous organic matter, and numerous fecal pellets distributed across a range of particle sizes.

Approximate settling velocities of the particles were estimated by timing the settling of visibly sinking particles in a graduated cylinder. For the plankton tow samples, sinking rates ranged from several m d^{-1} to $\sim 100 \text{ m d}^{-1}$. For the NetTrap samples, sinking rates ranged from several m d^{-1} to $\sim 900 \text{ m d}^{-1}$ for large fecal pellets. Both types of samples also contained suspended material that did not sink appreciably within 30 min. This material was largely composed of individual phytoplankton cells and amorphous organic matter. Although the NetTrap is designed to collect sinking particles, we have collected particles with settling velocities as low as 0.7 m d^{-1} (Peterson et al., 2005). Also, as mentioned previously, the NetTrap failed to close completely during recovery, so material from higher in the water column was entrained in the trap. Finally, some phytoplankton aggregates were disrupted during handling and splitting (described below) of the material, providing another source of initial suspended material in this incubation.

Samples were then split using a McLane™ WSD splitter to produce five homogeneous portions for incubation. Two ml of each split were filtered onto a 0.6- μm pre-weighed Nuclepore filter and later re-weighed to determine the success of homogenization. The 20 m plankton tow mass splits agreed within 4%, and the 200 m NetTrap splits within 7%.

Each of the 5 splits was rinsed into a 1.2-l cylindrical tank (7.39 cm radius and 7 cm deep) and diluted with 0.7- μm filtered seawater collected from the same depth (20 or 200 m) until the tanks were full. All visible zooplankton were removed from the tanks so that they would not graze extensively on the remaining material. The tanks were sealed and placed on a roller table rotating at 2.07 rpm (the minimum speed required to prevent collision of the fastest sinking NetTrap particles with the tank walls). The same rotational velocity was used for the plankton tow and NetTrap samples so that shear would be similar in both tanks. Also, most particles in the plankton tow were present as individual particles, so we expected settling velocities to increase as the particles aggregated. Tanks were incubated in the dark for 54-72 h at $\sim 18^\circ\text{C}$. Due to the limited number of tanks available, brevity of the cruise, and limited material collected (in the case of the NetTrap), the tank incubations could not be replicated either in series or in parallel (though at every time point, replicate samples were removed from each tank for all analyses). However, homogenization ensured that similar amounts of material were placed in each tank, as revealed by close agreement of the initial masses of each split (5-7%). Since all five tanks appeared to be the same initially, changes over the course of the experiment were not likely an artifact of differences in the amount of material in each tank. Also, the experiment was repeated with material collected at two depths, providing verification of some results that were similar in both incubations.

2.2. Sampling of Incubation Chambers

Suspended and sinking particles were sampled separately to assess the extent of exchange between these two pools. Samples were collected from the plankton tow incubation at 0, 6, 18, 36, and 54 h, and from the NetTrap incubation at 0, 6, 16, 36, and 72 h. At each time point, one of the 5 tanks was placed on its side for 20 min. to allow sinking particles to settle. Since the tank was 7 cm deep, this resulted in the separation of particles with settling velocities less than and greater than 5.1 m d^{-1} , operationally defined here as “suspended” and “sinking” particles. Visible particles (generally $\geq 1 \text{ mm}$) that had settled to

the bottom were counted and their approximate diameters were measured with a millimeter-scale ruler prior to sampling.

The plankton tow incubation contained a large amount of material ($\sim 108 \text{ mg l}^{-1}$), so for the last time point, a sample was taken for dissolved oxygen to assess whether or not the tanks had become anoxic. A 20-ml scintillation vial was gently submerged in the tank as soon as it was opened, filled to the top, poisoned with HgCl_2 , and sealed tightly with electrical tape and parafilm. This sample was analyzed upon return to shore with a dissolved oxygen meter, and contained $4.8 \text{ mg l}^{-1} \text{ O}_2$ (slightly lower than *in situ* concentrations during the time of collection, which were 7.3 mg l^{-1} at 20 m and 5.9 mg l^{-1} at 200 m).

After the sinking particles had settled to the bottom, the overlying water was gently siphoned off into a bottle until only 1 cm remained at the bottom, and then particles on the bottom were taken up with a transfer pipette. Sinking particles were diluted to 250-280 ml with $0.7\text{-}\mu\text{m}$ filtered seawater to provide a sufficient volume for filtration. The bottles containing each fraction were then vortexed to homogenize the material. Two-three ml subsamples of each fraction were immediately observed under a light microscope to determine the gross composition (i.e., phytoplankton, fecal pellets) of the samples. Each fraction was then gently filtered ($\sim 200 \text{ mbar}$) in duplicate onto combusted ($\geq 4\text{h}$ at 460°C) $0.7\text{-}\mu\text{m}$ glass fiber filters (GF/F) for organic analyses (organic carbon/nitrogen, inorganic carbon, pigments, and amino acids) and pre-weighed $0.6\text{-}\mu\text{m}$ nucleopore filters for mass and silica. Filters for organic analyses were rinsed with $\sim 10 \text{ ml}$ $0.7\text{-}\mu\text{m}$ filtered seawater, and mass filters were rinsed 5x with 2 ml aliquots of distilled water to remove salts. For the plankton tow incubation, 10-30 ml of material were filtered for each analysis. For the NetTrap incubation, 20-40 ml of the sinking particles and 30-80 ml of the suspended particles were filtered for each analysis. Filters were then stored frozen until analysis.

2.3. Chemical Analyses

Mass was determined by drying the material on the pre-weighed filters overnight at 60°C and re-weighing. Total particulate carbon (TPC), nitrogen (PN), and organic carbon (POC) samples were determined after a modification of Hedges and Stern (1984), by drying samples overnight at 60°C and measuring on a Carlo Erba EA-1100 CHN analyzer. POC samples were first fumed for 2h in HCl-saturated air to remove inorganic carbon (Hedges and Stern, 1984). Particulate inorganic carbon (PIC) was determined by subtracting POC

from TPC. Analytical error for these analyses was ~2% for C and 5% for N; total uncertainty for duplicate samples (including both sampling and analytical error) was within 40% for C and 60% for N (but generally less than 20% for both). The high error may have been due to incomplete homogenization prior to filtration. Since pigments and particulate amino acids (which tend to be present within cells) had lower error, it is possible that extracellular material such as transparent exopolymer particles exhibited greater heterogeneity. Also, in the NetTrap incubation, the small amount of sample available for each analysis may have contributed to some of the error.

Silica was measured by leaching samples in 0.2 N NaOH for 4h, removing a portion at 30 min., 1 h, 2.5 h, and 4 h, neutralizing with ¼ volume of 1 N HCl, and analyzing spectrophotometrically using the molybdate method (Strickland and Parsons, 1972; Fanning and Pilson, 1973). Biogenic silica was determined from the intercept (at time zero) of leaching time v. concentration, and lithogenic silica as the final amount of silica remaining minus the intercept. For determining the contribution of silica to total mass, the mass of biogenic silica in samples was calculated using the molecular weight of anhydrous opal (SiO_2 , 60 g mol^{-1}). For simplicity, H_2O was not included since the extent of hydration in opal can vary substantially. Since we did not determine the mineral form of the lithogenic silica, we converted Si to the mass of lithogenic material using the crustal ratio in aluminosilicates (59.71 weight% SiO_2). Total error for duplicate samples (sampling and analytical error) was typically <20% for biogenic silica and <50% for lithogenic silica (though a few points had ~100% error). There is some uncertainty in the partitioning between biogenic and lithogenic silica, since determination of the two fractions is interdependent. The lithogenic silica data has particularly high error since it includes the variance in the total silica measurements as well as the biogenic silica determinations.

Chloropigments and fucoxanthin were determined by high performance liquid chromatography (HPLC) as described in Chapter 3. Analytical error (duplicate analyses of the same samples) was ~5-10% for both analyses. Total sample error was generally within 30% for more concentrated pigments and amino acids (i.e., those that comprised >10% of total pigments, or >5% of total amino acids) and within 60% for more dilute compounds.

2.4. Statistical Analyses

To compare the % composition of individual compounds or compound classes between particles, we performed t-tests assuming unequal variances. The 95% confidence level was used to determine statistical significance, though some samples that fell just outside this range are reported. Correlations between composition and time were assessed using Pearson's product-moment correlations. Correlation coefficients (r) greater than 0.30 or less than -0.30 were considered indicative of a significant positive or negative correlation. A single-factor ANOVA was also performed to assess differences in pheopigment composition among all four particle types (suspended and sinking particles at 20 and 200 m).

In addition, the compositions of suspended and sinking particles were compared by principal component analysis (PCA) as described in Chapter 3. Amino acid and pigment composition were standardized prior to PCA by subtracting the mean mole % (out of total pigments or amino acids) for each compound and dividing by its standard deviation. Carbon, nitrogen, and silica composition were standardized by subtracting the mean weight % (out of total mass) for each component and dividing by its standard deviation.

3. Results and Discussion

3.1. Exchange between Suspended and Sinking Particles in the 20 m Plankton Tow Incubation

3.1.1. *Visual and Microscopic Observations*

After turning the plankton tow incubation tanks on their sides, numerous 2-3 mm diameter aggregates and some larger, amorphous clouds of material settled to the bottom. Many particles disaggregated when collected for analysis. Microscopic observation confirmed that both the sinking and suspended pools were largely composed of individual plankton or aggregates.

3.1.2. *Particulate Mass, Organic Carbon, Nitrogen, Silica, and Inorganic Carbon*

Figure 4.1 depicts changes in particulate mass, organic carbon, inorganic carbon, nitrogen, biogenic silica, and lithogenic silica throughout the plankton tow experiment. While the total material in each tank remained fairly constant (or decreased slightly) over time, the partitioning of material in the suspended and sinking phases varied, suggesting transfers of mass between these two phases. There is some uncertainty in the precise

magnitude of these transfers, but the magnitudes of changes in both pools were usually greater than the measurement error. Over the first 6-18h of the incubation, 30-70% of the particulate mass, organic carbon (POC), biogenic silica (BSi), pigments, and amino acids in the suspended phase were transferred to the sinking phase (Fig. 4.1, 4.2). From 18 to 54 h, 30-50% of the mass, POC, BSi, pigments, and amino acids in the sinking phase were transferred back to suspended particles. The transfer of mass from suspended to sinking particles during the first 18 h probably resulted from aggregation induced by the rotation of the tanks (Shanks and Trent, 1980), and the subsequent transfer back to suspended particles was probably due to shear induced by the increased abundance of large, rapidly-sinking aggregates (Hill, 1988). It is also possible that part of the observed increases and decreases in material in the two phases resulted from exchange with dissolved inorganic and organic material (i.e., precipitation, dissolution, adsorption, and desorption), but the simultaneous changes in the suspended and sinking phases suggests that exchange between these particle types was at least partly responsible.

Total mass in the tank may have decreased by ~24% over the course of the 54 h incubation (from 157 ± 23 mg to 119 ± 15 mg), though we cannot determine this with certainty since the change was within the range of error. The proportion of mass in sinking and suspended particles varied substantially over time (by ~30%), indicating the transfer of material between the two pools. Initially, mass in the suspended phase (119 ± 15 mg) was 3x higher than that in the sinking phase (39 ± 2 mg), but within 6 h of rotation 29% of this mass (35 ± 0.6 mg) was transferred to the sinking phase. This transfer of material reversed between 18-36 h, when 32% of the mass in sinking particles (25 ± 4 mg) was transferred back to the suspended phase.

Particulate organic carbon (POC) decreased by 21% over 54 h (from 19 ± 1 mg to 15 ± 2 mg). Initial POC in the suspended and sinking pools were about equal (9 ± 0.4 and 10 ± 1 mg), but between 18-36 h, 33% of the POC in the sinking phase (3 ± 3 mg) was transferred to the suspended phase. The large error in the 36 h suspended mass measurement (36%) creates uncertainty in the extent of POC exchange between pools; however, by 54 h, it was clear that the suspended particles contained 30% more POC (9 ± 1 mg) than the sinking particles (6 ± 0.2 mg). Particulate nitrogen (PN) was initially about equal in suspended (3 ± 0.1 mg) and sinking (4 ± 4 mg) particles. After 6 h, however, PN

was consistently ~2x higher in the suspended phase than in the sinking phase (~4 mg compared with ~ 2 mg).

Total biogenic and lithogenic silica may have decreased slightly over the course of the incubation, but this change was within the range of error for these measurements. Like total mass and organic carbon, biogenic silica underwent transfers between the suspended and sinking phase. Biogenic silica (BSi) was initially greater in the suspended phase ($291 \pm 139 \mu\text{mol}$) than in the sinking phase ($75 \pm 2 \mu\text{mol}$). By 18 h, 71% of the BSi in the suspended phase was transferred to the sinking phase ($216 \pm 6 \mu\text{mol}$), and by 36 h, 46% ($18 \pm 2 \mu\text{mol}$) of the BSi in sinking particles was transferred back to suspended particles. Molar BSi:OC ratios in all samples ranged from 0.01 to 0.11, but were mostly within 0.06-0.08, in good agreement for the average value for living diatoms, 0.09 (Brzezinski, 1985). Lithogenic silica (LSi) was comparable in suspended and sinking particles throughout the incubation ($18\text{-}39 \mu\text{mol}$).

Particulate inorganic carbon (PIC) did not exhibit the same pattern as total mass, organic carbon, and BSi, but was consistently a greater portion of the mass in suspended particles ($p=0.06$) (Fig. 4.5). PIC was initially 9x higher in the suspended phase ($9 \pm 0.4 \text{ mg}$) compared with the sinking phase (1 ± 1), and increased in both particle types over the course of the incubation (to $13 \pm 2 \text{ mg}$ in suspended particles and $7 \pm 5 \text{ mg}$ in sinking particles). This is consistent with field observations at DYFAMED in 2003 and 2005 showing that amino acids enriched in biogenic calcium carbonate contributed more to total amino acids in suspended particles than in sinking particles (Chapter 3). The total concentration of particulate inorganic carbon also increased by 2x over the course of the incubation, suggesting that dissolved inorganic carbon was added to the particulate phase by biological precipitation or by sorption onto particles. The precipitation of this much carbonate would require the removal of $1.8 \text{ mg l}^{-1} \text{ CO}_3^{2-}$ from the dissolved phase, which is plausible since it would only decrease alkalinity by ~3% (given typical seawater alkalinities of ~2.3-2.6 meq l^{-1} or 60-68 mg $\text{CO}_3^{2-} \text{ l}^{-1}$; Stumm and Morgan, 1996).

Despite the apparent transfers of mass between phases, the bulk organic and inorganic compositions of the suspended and sinking particles were somewhat different. Inorganic carbon was generally enriched in the suspended particles (10-28%) compared with the sinking particles (3-18%) ($p=0.06$). Organic carbon was slightly greater in the sinking

particles (12-26%) than suspended particles (10-17%), but this difference was not statistically significant. Biogenic silica (12-17% of the mass in the sinking particles, 9-19% in the suspended particles), lithogenic material (2-10% of sinking particles, 2-16% of suspended particles), and nitrogen (3-9% of the sinking particles, 3-13% of the suspended particles) were not statistically different between the two particle types.

3.1.3. *Pigments and Amino Acids*

Pigments were initially 147 ± 6 $\mu\text{mol C}$ in suspended particles and 42 ± 7 $\mu\text{mol C}$ in the sinking phase (Fig. 4.2). They subsequently underwent similar transfers between pools as mass, organic carbon, and biogenic silica. Within 6-18 h, 30% of pigments (28 ± 5 $\mu\text{mol C}$) were transferred from the suspended to sinking phase, and then 34% (39 ± 9 $\mu\text{mol C}$) were transferred back to the suspended phase. Changes in particulate amino acids (PAAs) within sinking particles were similar to those for total mass and pigments, but changes in suspended amino acids were less pronounced. Suspended amino acids increased slightly from 572 ± 17 $\mu\text{mol C}$ to 628 ± 21 $\mu\text{mol C}$ during the incubation. Sinking particles increased initially from 257 ± 23 $\mu\text{mol C}$ to 452 ± 6 , then decreased to 266 ± 36 $\mu\text{mol C}$. Part of this decrease (42%) appears to have been due to a transfer of material into the suspended phase; the remainder was a net loss. As for particulate nitrogen, amino acids were consistently 1.2-2.4x more concentrated in suspended than sinking particles ($p=0.002$) (Fig. 4.1 and 4.2). Whereas pigments are unique to primary producers, amino acids and nucleic acids (the dominant sources of PN) are ubiquitous in all organisms. Therefore, total amino acids may not have behaved in the same way as mass, organic carbon, BSi, and pigments because they partly reflected non-algal sources of organic matter, such as viral, bacterial, protozoan, and zooplankton biomass (or dead phytoplankton biomass in which pigments had been degraded to colorless residues). Bacterial cells in particular tend to be protein-rich and have a lower than Redfield C:N ratio (Vrede et al., 2002). However, based on typical bacterial masses of roughly 300-500 fg C cell⁻¹ (Loferer-Kröbber et al., 1998), the initial increase in amino acids over 0-18 h would have required the addition of about 5×10^{14} bacterial cells and is therefore too large to be explained exclusively by bacteria.

Amino acids comprised 67-86% of POC (11-16% of total mass) in the suspended particles, consistent with typical values in plankton (Wakeham et al., 1997). For the sinking particles, the contribution of amino acids to POC (30-60%, or 12-27% of total mass) was

more similar to that typically found in shallow sediment traps (Wakeham et al., 1997), suggesting the composition of sinking particles may be determined in the mixed layer. This difference was statistically significant ($p=0.001$). The contribution of pigments to POC was not significantly different for the two particle types (5-15% in sinking particles; 9-20% in suspended particles; ~2% of total mass in both). This is substantially higher than pigment concentrations measured in surface waters in the equatorial Pacific (<1%), which generally has high productivity (Wakeham et al., 1997). However, the pigment content of phytoplankton in coastal environments often ranges from 2-15% of carbon, and can be particularly high under light starvation (Lorenzen, 1968; Jamart et al., 1977; Welschmeyer and Lorenzen, 1985). Since our plankton tow was collected at night (11 pm) and then incubated in the dark, this might explain the high pigment concentrations. Both the amino acid and pigment contributions to POC increased in the sinking particles over the first 18 h (from 30 to 58% and 5 to 15%, respectively).

Over the course of the incubation, the contributions of amino acids and pigments increased in sinking particles ($r=0.75$ and 0.77 , respectively), becoming more similar to suspended particles and typical values for plankton (Wakeham et al., 1997). This also suggests that the aggregation and disaggregation of phytoplankton cells was responsible for the observed transfers of mass between pools.

3.1.4. Particular Pigment Biomarkers

Examining changes in particular biomarkers in more detail, both chlorophyll *a* (chl *a*) and fucoxanthin (fuco; a diatom pigment) exhibited changes over time that were similar to those for mass and total pigments (Fig. 4.3). On a molar basis, these pigments comprised 48-56% and 23-25%, respectively, of pigments in the suspended particles and 45-54% and 24-27%, respectively, of pigments in the sinking particles (Fig. 4.6). The fact that both particle types had high contributions of chl *a* and fuco, which tend to be enriched in fresh plankton (Lee et al., 2000; Sheridan, 2002), and the fact the transfers of mass between suspended and sinking particles were reflected particularly well by these compounds suggests that fresh algal material was responsible for the exchange of material between sinking and suspended pools. This supports our microscopic observation that the material in both pools was mainly composed of individual diatoms and diatom aggregates.

Pheophytin (phytin), which is produced by microbial degradation of chl *a*, and pheophorbide (phide) and pyropheophorbide (pyrophide), which are produced by zooplankton enzymatic degradation of chl *a* (Currie, 1962; Daley, 1973; Hendry et al., 1987), also followed similar patterns; 58-60% of the phide and pyrophide in the suspended phase was transferred to the sinking phase over 18 h, and then 40-44% of the material in sinking particles were transferred back to the suspended phase. The initial increase in these pigments within the sinking phase was 1.5x greater than the subsequent decrease. In addition to the transfer from the suspended phase, this was partly due to the fact that total concentrations increased, suggesting some production of fecal pellets.

Although we attempted to remove grazers prior to incubation, some were inevitably included, particularly since we collected the plankton tow at night when zooplankton migrate to the surface to feed. There was clearly some exchange of phide and pyrophide between suspended and sinking particles, but we cannot determine if this was due to disaggregation of fecal pellets or the incorporation of fecal pellets into phytoplankton aggregates, which then disaggregated. Theories about these two possibilities are discussed further in Section 3.3.

Since visible zooplankton were removed prior to the start of the incubation, fecal pellet production was lower than it would have been under natural conditions. The exchange between suspended and sinking particles might have been reduced if more grazers had been included. However, by reducing new fecal pellet production, we were able to examine how aggregation/ disaggregation dynamics would affect fecal pellets once they have already been produced.

Phide, pyrophide, and phytin comprised 12-14%, 7-13%, and 0.5-2%, respectively, of the total pigments in suspended particles, and 13-18%, 7-12%, and 0.4-1%, respectively in sinking particles. Phide was significantly enriched in sinking particles compared with suspended material ($p=0.04$). Suspended particles collected near the surface at this site in 2003 and 2005 (Chapter 3) generally contained lower contributions of phide and pyrophide (usually close to 0%), but deeper suspended particles contained up to 40%, so the contributions observed in this study are within the natural range observed in the water column. We did not see fecal pellets under the microscope in the plankton tow incubation; however, some amorphous material was present that could not be identified, and may have consisted in part of small fecal pellets or larger pellets that had been broken up by

coprophagy or mechanical disruption. Also, although we attempted to exclude visible grazers, complete removal was impossible and some smaller organisms were inevitably included.

The fact that phide was 20% more concentrated than pyrophide in the plankton tow incubation may be an indication of the source of this material. As explained in Hendry et al. (1987), chl *a* can be degraded to phide by two pathways. The removal of Mg converts chl *a* to phytin, which can then be converted to phide by hydrolysis and removal of the phytol side-chain. Alternatively, the phytol side chain can be removed first to form chlorophyllide, followed by Mg removal to form phide. The first pathway is more common in bacteria and microzooplankton, while the latter pathway is more common in zooplankton. Production of phide usually occurs via the chlorophyllide pathway (i.e., zooplankton alteration). This pathway seems more likely in the case of our samples, since phytin was <1% of pigments. Therefore, the phide in this incubation may have been indicative of partial zooplankton alteration of chl *a*.

3.1.5. Particular Amino Acid Biomarkers

The amino acids serine (SER), threonine (THR), and glycine (GLY), which are enriched in the tests of siliceous plankton (Hecky, 1973; Swift and Wheeler, 1991; Ingalls et al., 2003), and aspartic acid (ASP) and glutamic acid (GLU), which are enriched in the tests of calcareous plankton (King, 1974; Weiner and Erez, 1984), all exhibited a 70-87% increase in the sinking phase from 0-18 h, followed by a 24-93% decrease from 18-54 h (Fig. 4.4). For all but GLU, there was a corresponding decrease in the suspended phase from 0-18 h followed by an increase from 18-54 h, though these changes were 2-6x smaller. The amino acids β -alanine (BALA), and γ -aminobutyric acid (GABA), which are non-protein bacterial amino acids, did not show appreciable variations over time within the range of uncertainty for these amino acids, though BALA was 1.3-2x higher throughout the incubation in the suspended phase compared with the sinking particles.

On a molar basis, the contributions of most of these amino acids were similar between suspended and sinking particles, with 7-8% SER, 5-7% THR, 8-13% GLY, and 9-11% ASP (Fig. 4.6). Like inorganic carbon, however, glutamic acid (GLU) comprised a significantly greater portion of amino acids in suspended (13-15%) than sinking particles (11-12%) ($p=0.008$) (Fig. 4.6), suggesting that suspended particles were enriched in calcifying

algae. SER, in contrast, was significantly enriched in sinking particles ($p=0.01$), suggesting they were enriched in diatoms. These findings are consistent with field results from 2003 and 2005 showing that ASP and GLU were enriched in 1-70 μm pump particles, and SER, GLY, and THR were enriched in sediment trap samples (Chapter 3). The mechanism for the partitioning of these biomarkers is unclear. For the pump and trap samples (Chapter 3), we proposed that diatoms are preferentially incorporated into fecal pellets, leaving prymnesiophytes enriched in the suspended phase. Since the exchange of material in the 20 m plankton tow appeared to be largely due to aggregation/disaggregation processes, and we did not observe fecal pellets produced by large diatom grazers such as copepods, it is surprising that inorganic carbon was not enriched in sinking particles. Calcium carbonate usually promotes aggregation, forming small, dense aggregates with extremely high settling velocities (Passow and de la Rocha, 2006; Engel et al., submitted a, b). However, the organisms collected in the plankton tow were overwhelmingly diatoms, so even if coccolithophorids were incorporated into aggregates, the effect may have been greatly diluted by the large diatom presence.

In addition, the large number of diatoms present may have impeded self-aggregation of calcifying algae. Coccolithophorid aggregation is thought to be promoted partly by acidic polysaccharides on the surface of coccoliths that contain ester sulfate and uronic acid groups that bind Ca^{2+} (de Jong et al., 1976; van Emburg et al., 1986). Coccolithophorid aggregation may therefore be a relatively species-specific process requiring a predominance of calcifying algae in the plankton. This hypothesis is purely speculative, however, as it has not been previously tested.

3.1.6. Principal Component Analysis

When principal component analysis was performed on the 20 m plankton tow samples from each time point, principal component 1 (PC1) explained 27.8% of the variance in the data, and principal component 2 (PC2) explained 24.1% (Fig. 4.7). Chl *a* plotted in the lower left of the PCA and the alteration products phytin, phide, pyrophide, BALA, and GABA plotted towards the upper part or to the right. Suspended and sinking particles were separated along PC1. Suspended particles plotted closer to chl *a*, inorganic carbon (IC), the amino acids ASP and GLU (which are enriched in biogenic calcite), and biogenic silica (BSi). Nitrogen (N), phytin, pyrophide, and THR had very small loadings on PC1 and plotted

between the two particle groups but were slightly closer to suspended particles. Sinking particles plotted closer to the alteration products phide, BALA, and GABA, the diatom indicators SER, GLY, fuco, and biogenic silica (BSi), and organic carbon (OC). This supports the compositional data from Chapter 3 showing that suspended particles at DYFAMED were enriched in fresh plankton and calcifying algae indicators, whereas sinking particles were more enriched in fecal pellet indicators.

3.2. Exchange between Suspended and Sinking Particles in the 200 m NetTrap Incubation

3.2.1. Visual and Microscopic Observations

After turning the NetTrap incubation tanks on their sides, the material which settled to the bottom consisted of ~10-20 fecal pellets and 5-20 phytoplankton aggregates ranging from 0.25-1 cm in diameter. Aggregates often disaggregated upon sampling whereas the fecal pellets did not. Under microscopic observation, both pools were found to contain phytoplankton and amorphous material. Fecal pellets were observed in the sinking pool.

3.2.2. Particulate Mass, Organic Carbon, Nitrogen, Silica, and Inorganic Carbon

Figure 4.8 depicts changes in particulate mass, organic carbon, inorganic carbon, nitrogen, biogenic silica, and lithogenic silica during the NetTrap experiment. Total particulate mass, organic carbon, nitrogen, pigments, amino acids, and biogenic silica increased by 1.5-4.5x over the 72 h NetTrap incubation, possibly due to phytoplankton growth. In addition, there appeared to be some transfer from the suspended to sinking phase for most of these parameters, as evidenced by simultaneous decreases in the suspended phase and increases in the sinking phase. There is some uncertainty as to the sources of the observed changes, including measurement error and exchange with the dissolved phase. However, the simultaneous changes in both the suspended and sinking phases and fact that these changes were usually larger than the error suggests that some suspended material aggregated, forming sinking particles. Unlike in the 20 m plankton tow incubation, there was no apparent transfer of material back to the suspended phase, suggesting that sinking particles did not disaggregate once formed.

The observed increases in particulate organic carbon, nitrogen, biogenic silica, amino acids, and chl *a* in the 200 m NetTrap incubation (discussed in greater detail below) are

consistent with a phytoplankton growth rate of 0.23-0.71 doublings d^{-1} (0.23 for chl *a*, 0.36 for OC, 0.45 for PN, 0.59 for BSi, and 0.71 for amino acids). The carbon fixation rate required to explain the increase in POC is $7.8 \mu\text{g C l}^{-1} \text{h}^{-1}$; estimates derived using biogenic silica and chl *a* are 12.4 and $2.4 \mu\text{g C l}^{-1} \text{h}^{-1}$, respectively, assuming typical cellular ratios of 0.09 for BSi: OC (Brzezinski, 1985) and 0.04 for chl *a*: OC (Lorenzen, 1968; Jamart et al., 1977; Welschmeyer and Lorenzen, 1985). The lower range of these estimates is consistent with rates of primary production previously measured in incubations of near-surface (<30 m) water at DYFAMED, which ranged from 1.59 - $7.46 \mu\text{g C l}^{-1} \text{h}^{-1}$ (Marty and Chiavérini, 2002). Most of the apparent phytoplankton growth in the tanks occurred in the sinking phase, rather than the suspended phase. This suggests either that new cells were immediately transferred into aggregates as they grew, or that cells grew within pre-formed aggregates or fecal pellets. The observed increases could be due to factors other than phytoplankton growth, such as evaporative water loss from the tanks, but this explanation is highly unlikely as the tanks were sealed tightly with screws and rubber o-rings and we did not observe any decrease in water level over time.

Although the tanks were incubated in the dark, the initial exposure to light upon bringing the material to the surface, splitting it, and preparing the tanks for incubation may have stimulated the observed phytoplankton growth. Particularly for diatoms, a variety of algal resting stages such as vegetative cells, resting cells, and resting spores have been shown to survive throughout the water column and sediments and be re-activated by exposure to light (Smayda and Mitchell-Innes, 1974; Hargraves, 1976; French and Hargraves, 1980). Dark survival can last for at least 21-49 d in water column conditions (Peters, 1996), or 27-112 months in sediments (Lewis et al., 1999). Phytoplankton, particularly diatoms, can also remain viable in zooplankton fecal pellets (Fowler and Fisher, 1983). The reactivation of dormant cells may explain why we observed indications of phytoplankton growth in the 200 m NetTrap incubation, but not in the 20 m plankton tow incubation.

In addition, removing visible grazers most likely affected the balance of production and respiration in both incubations. Some of the algal growth observed in the 200 m NetTrap incubation may have been attributable to reduced grazing pressure. If grazers had been present, they might have prevented or compensated for the observed increase in organic matter.

Discussing each of these parameters in greater detail, total mass in the tank increased during the incubation from 3.4 ± 0.8 mg to 6.1 ± 0.1 mg over the course of the 72 h incubation. Mass was initially slightly higher in suspended (2.1 ± 0.8 mg) than sinking (1.3 ± 0.3 mg) particles. The mass in both particle fractions increased over the first 36 h (to 2.4 ± 0.03 mg in the sinking phase, an increase of 93%, and to 3.7 ± 0.9 mg in the sinking phase, an increase of 73%). Between 36 and 72 h, ~50% of the mass in the suspended phase (1.9 ± 0.09 mg) appears to have been transferred to the sinking phase.

Particulate organic carbon (POC) increased by 32% in sinking particles (from 0.41 ± 0.2 to 0.54 ± 0.01 mg), and by a factor of 3 in suspended particles (from 0.25 ± 0.02 to 0.86 ± 0.07 mg), mostly over the first 18 h. Since similar increases occurred in the sinking and suspended phases, we cannot determine what portion of the increase in the sinking phase was due to exchange as opposed to phytoplankton growth.

Particulate nitrogen (PN) was initially higher in the suspended phase (0.09 ± 0.01 mg) than in the sinking phase (0.02 ± 0.006 mg). Nitrogen increased by a factor of 4 in sinking particles (to 0.08 ± 0.008) within the first 6 h, synchronous with a 0.04 ± 0.007 mg decrease in the suspended phase. Between 6-18 h, nitrogen increased 2.4x in the suspended phase (to 0.22 ± 0.009 mg), and then consistently remained enriched in suspended particles over sinking particles. As a result of these increases, total particulate nitrogen increased by $\sim 0.17 \pm 0.02$ mg. This magnitude of uptake would have decreased dissolved nitrate concentrations by 10.2 ± 1.4 μ M, which is very high given that typical NO_3^- concentrations at 200 m depth at the DYFAMED site (the source of the water in this incubation) are only ~ 7 -8 μ M (Marty et al., 2002). These calculations suggest that initial PN was slightly underestimated or final PN was overestimated, possibly due to incomplete homogenization of the tanks prior to sampling at each time point.

Total biogenic silica (BSi) increased in the sinking phase from 1.5 ± 0.8 μ mol to 7.9 ± 1 μ mol over 72 h; a small increase (0.9 ± 0.7 μ mol) may have occurred in the suspended phase as well. This increase would require the uptake of 8.0 ± 1.9 μ mol (6.7 ± 1.6 μ M) dissolved Si(OH)_4 during the incubation, which also seems high given that Si(OH)_4 concentrations at 200 m depth at the DYFAMED site are typically only ~ 7 -8 μ M (Marty et al., 2002), and we measured ~ 6 μ M in 2003. However, particulate lithogenic silica decreased slightly (by 2.2 ± 1.0 μ mol) during the incubation, adding some Si(OH)_4 back to the dissolved phase. Based on these calculations, the net change in dissolved silicate

concentrations should have been $\sim 4.8 \pm 2.4 \mu\text{M}$, a more feasible estimate. Throughout the incubation, biogenic silica was significantly enriched in sinking particles compared with suspended material ($p=0.02$). Molar BSi:OC ratios ranged from 0.04 to 0.17, in good agreement with the average value for living diatoms, 0.09 (Brzezinski, 1985).

Total lithogenic silica (LSi) gradually decreased in the suspended phase from $3.3 \pm 0.3 \mu\text{mol}$ to $0.8 \pm 0.4 \mu\text{mol}$, while increasing in the sinking phase from $1.4 \pm 0.08 \mu\text{mol}$ to $2.2 \pm 0.8 \mu\text{mol}$. On a weight % basis, however, there was a net decrease in the contribution of LSi to both particle types over time ($r=-0.85$ and -0.60 , respectively), suggesting some dissolution of lithogenic material or that dust particles stuck to the walls of the tank.

Particulate inorganic carbon (PIC) aggregation occurred in the 200 m NetTrap incubation, unlike in the 20 m plankton tow incubation. PIC steadily decreased in suspended particles (from $1.14 \pm 0.21 \text{ mg}$ to $0.47 \pm 0.08 \text{ mg}$) and increased in sinking particles (from $0.08 \pm 0.23 \text{ mg}$ to $0.67 \pm 0.09 \text{ mg}$) over the course of the incubation, indicating that about 35% of the particulate inorganic carbon (PIC) initially present in the suspended phase was transferred to sinking particles. As a result, the contribution of PIC to total mass (weight %) decreased over time for suspended particles ($r=0.71$) while increasing in sinking particles ($r=0.69$) (Fig. 4.12). The decrease in BSi, LSi, and PIC in suspended particles and increase in sinking particles support previous studies which demonstrated that minerals catalyze organic matter aggregation and enhance sinking rates (Hamm, 2002).

Even more extensive differences in the bulk composition of the particles were apparent than for the 20 m plankton tow samples (Fig. 4.12). Biogenic silica (BSi) was slightly higher in the sinking particles (8-12% of total mass) compared with suspended material (3-9%) ($p=0.02$); however, lithogenic material was not significantly different (4-16% in sinking particles and 5-11% in suspended). Inorganic carbon (IC) was enriched in suspended particles (25-54%) compared with sinking particles (3-22%), though this was significant only at the 90% confidence level ($p=0.08$). Organic carbon (OC) decreased from 34% to 12% of particulate mass in sinking particles ($r=-0.99$) and increased from 14% to 47% in suspended particles ($r=0.94$) during the incubation. Particulate nitrogen ranged from 2-5% in sinking particles and 2-11% in suspended particles, also demonstrating a decrease in contribution to sinking particles ($r=-0.33$) and increase in contribution of suspended particles ($r=0.85$) over time. Most of these contributions are higher than those measured in 200-300 m deep sediment traps in 2005 (2-7% LSi, 10-42% BSi, 2-10% IC, 0-1.6% IC, 0-

1.6% N, and 3-17% OC), perhaps due to the entrainment of some surface material in the NetTrap during recovery or interannual variability in particle composition.

Surprisingly, a greater portion of mass was characterized by our analyses (POC, PN, PIC, BSi, and lithogenic material) than in the plankton tow incubation (compare Fig. 4.6 and 4.12), mostly due to greater contributions of organic and inorganic carbon (13-47% and 3-54% of total mass, respectively, compared with 10-27% and 3-28%, respectively in the plankton tow incubation). This may have been partly due to phytoplankton growth during the NetTrap sample incubation. Also, a deep chl maximum is often observed in this region of the Mediterranean (Faugeras et al., 2003), so the NetTrap material may have been nearly as fresh as the surface material. Alternatively, there may have been a systematic error in the mass measurements, such as mineral dissolution caused by the repeated rinsing of the mass filters with distilled water to remove salts. Since the material in the NetTrap incubation was relatively dilute (initially $\sim 1\%$ of that in the phytoplankton tow experiment), mineral dissolution could have contributed to a greater error in mass.

3.2.3. Pigments and Amino Acids

Pigments behaved similarly to total mass, organic carbon, biogenic silica, and lithogenic silica (Fig. 4.9), increasing in the sinking phase from $0.21 \pm 0.07 \mu\text{mol C}$ to $1.08 \pm 0.02 \mu\text{mol C}$ over 72 h, while decreasing in the suspended phase from $0.83 \pm 0.05 \mu\text{mol C}$ to $0.48 \pm 0.01 \mu\text{mol C}$. However, this exchange was more gradual over time, rather than the sudden aggregation apparent from 36-72 h in the other parameters. Total pigments increased by $0.52 \pm 0.18 \mu\text{mol C}$ over the course of the incubation. The contribution of pigments to POC also increased over time in the sinking phase ($r=0.93$) but decreased in the suspended phase ($r=-0.82$), suggesting that new algal cells were probably incorporated into the sinking phase.

Amino acids behaved in a similar manner as nitrogen, increasing in both fractions over 0 to 18 h (from $2 \pm 0.2 \mu\text{mol C}$ to $12 \pm 0.7 \mu\text{mol C}$ in sinking particles, $p=0.74$, and from $8 \pm 2.8 \mu\text{mol C}$ to $33 \pm 1.8 \mu\text{mol C}$ in suspended particles, $p=0.37$), consistent with algal growth. Amino acids were 2.7-4x higher in the suspended phase compared with sinking particles throughout the incubation.

The contribution of pigments to total POC decreased over time from 4 to 0.7% (or 0.5 to 0.3% of mass) in the suspended phase and increased from 0.6-2.4% (or 0.2 to 0.4% of

mass) in the sinking phase. Amino acids were 38-50% of POC (10-20% of mass) in suspended particles and 12-27% of POC (5-13% of mass) in sinking particles, representing a decrease of 60% and 40%, respectively, from amino acid contributions at 20 m.

3.2.4. Particular Pigment Biomarkers

Examining changes in the particular biomarkers in more detail, chl *a* and fuco both exhibited changes over time that were similar to those for mass and total pigments (Fig. 4.10), suggesting that these changes were at least partly due to diatom aggregation. Phide also increased in the sinking phase (by $0.047 \pm 0.01 \mu\text{mol C}$) and decreased in the suspended phase (by $0.018 \pm 0.006 \mu\text{mol C}$), possibly indicating the incorporation of small fecal pellets into larger aggregates (Fig. 4.10). However, this could only account for 1/3 of the observed increase in phide during the course of the incubation. Pyrophide also increased by 1.7x ($0.05 \pm 0.03 \mu\text{mol C}$) in the sinking phase, but this did not appear to be due to aggregation from the suspended phase, since this pigment was consistently 1-5x more concentrated in sinking particles. These results indicate that there may have been some new fecal pellet production during the incubation.

As in the plankton tow incubation, both sinking and suspended particles were highly enriched in pigments indicative of fresh phytoplankton (Lee et al., 2000; Sheridan, 2002), but compositional differences between these two phases were more pronounced. Suspended particles were significantly enriched in chl *a* (58-73%) compared with sinking particles (34-61%) ($p=0.02$), while sinking particles were significantly enriched in phide and pyrophide (6-9% and 12-26%, respectively) compared with suspended particles (4-6% each) ($p=0.009$ and 0.007) (Fig. 4.13). The relative abundances of phide and pyrophide were different than at 20 m as well. Compared with sinking particles in the 20 m plankton tow incubation, sinking particles in the 200 m NetTrap incubation had a 2-3x greater contribution (on a mole % basis) of pyrophide, and 2x lower contribution of phide, indicating more extensive alteration of chl *a*. Suspended particles, meanwhile, contained equal proportions of phide and pyrophide, similar to both particle types in the 20 m plankton tow. This suggests that differences in the relative abundances of phide and pyrophide may be indicative of different sources of material.

3.2.5. Particular Amino Acid Biomarkers

SER, THR, GLY, ASP, and GLU all increased by 4-5x in the suspended particles and by 3-4x in the sinking particles over 0 to 18 h., much like total amino acids (Fig. 4.11). ASP and GLU were slightly enriched in the suspended particles (9-10% and 16-19%, respectively) compared with the sinking particles (7-10% and 11-15%, respectively) ($p=0.09$ and 0.01 , respectively), much like PIC. Therefore, despite the role of PIC in promoting aggregation, it appears to remain relatively enriched in suspended particles. As mentioned previously, Cowie and Hedges (1996) suggested that diatom frustules are selectively preserved in fecal pellets, but the acidic guts of zooplankton may dissolve coccoliths. It is possible that PIC incorporated into fecal pellets, rather than aggregates, was partially dissolved.

BALA increased by 0.03 ± 0.009 $\mu\text{mol C}$ in both particle fractions during the incubation, but was slightly enriched in the sinking particles (0.1-0.3%) compared with the suspended particles (0.1-0.2%) ($p=0.02$). GABA increased by 0.04 ± 0.01 $\mu\text{mol C}$ in the sinking particles. In the suspended particles, GABA initially increased (0.05 ± 0.02 $\mu\text{mol C}$) until 18 h followed by a decrease (0.04 ± 0.03 $\mu\text{mol C}$) from 18 to 72 h. GABA was not significantly different between particle types (0.2-0.4% and 0.1-0.2%, respectively). The concentration of all 7 of these amino acids was 2-4x higher in the suspended particles, though GABA did become 1.4x more concentrated in the sinking particles at 72 h.

3.2.6. Principal Component Analysis

In the principal component analysis on the 200 m NetTrap samples (Fig. 4.14), PC1 explained 33.3% of the variance, and PC2 explained 17.6%. Suspended and sinking particles were again separated on PC1, with suspended particles plotting closer to chl *a*, inorganic carbon, ASP, GLU, biogenic silica, and nitrogen, and sinking particles closer to phide, pyrophide, BALA, and GABA. Organic carbon, SER, THR, GLY, and fuco had small loadings on PC1 and plotted between the two groups, though slightly closer to sinking particles. Phytin also plotted between the two groups but slightly closer to suspended particles. Again, the results of this study as well as those of Chapter 3 suggest that suspended particles at DYFAMED were enriched in fresh plankton, particularly calcifying algae, and sinking particles were enriched in fecal pellets.

3.3. Fecal Pellets and Phytoplankton Aggregates: Differences in the Extent of Exchange with Suspended Particles

For the plankton tow samples, we observed evidence of the aggregation and disaggregation of material, resulting in extensive exchange between suspended and sinking particles. For the NetTrap samples, new material was apparently added to the sinking phase, possibly via aggregation and phytoplankton growth. However, there was no appreciable loss of material, indicating disaggregation was limited.

Whether the observed increases in the 200 m NetTrap incubation were due to experimental artifacts or due to phytoplankton growth, the overall conclusions of the study are the same. Regardless of changes in the total amount of material over the course of the incubation, changes in the proportion of mass in the suspended and sinking pools reveal a great deal about exchange. It appears that repeated aggregation and disaggregation occurred in the 20 m plankton tow incubation, but there was only some initial aggregation and/or phytoplankton growth in the 200 m NetTrap incubation. It is possible that disaggregation of the NetTrap material would have occurred if the incubation were continued for longer, but it was at least not as rapid as that observed in the plankton tow incubation (where aggregation occurred within 18 h, and disaggregation over the next 18 h). This suggests that the material present in the NetTrap samples was more robust than that in the phytoplankton samples. This may be partly due to the age of the material (e.g., production of algal exudates by senescent plankton). However, as evidenced by the greater exchange of algal biomarkers relative to fecal pellet indicators, the robustness of the NetTrap samples may be particularly influenced by the high fecal pellet contribution to NetTrap samples.

Compositional differences between suspended and sinking particles were much greater for the 200 m NetTrap samples compared with the 20 m plankton tow samples, as illustrated particularly well by the principal component analyses (Fig. 4.7, 4.14, 4.15). PC1 explained slightly more variance in the NetTrap PCA than in the plankton tow PCA (33.3% v. 27.8%), indicating greater separation between suspended and sinking particles along this axis. In addition, when all samples were combined in one principal component analysis (Fig. 4.15), the separation between suspended and sinking particles was fairly small for the plankton tow samples, and much more pronounced for the NetTrap samples. When the 20 m and 200 m samples were combined into one principal component analysis (Fig. 4.15), the

separation between the 20 m suspended and sinking particles became far less pronounced. Suspended particles from both incubations plotted closer to chl *a*, inorganic carbon, GLU, ASP, nitrogen, and phytin (i.e., all had negative loadings on PC2), and sinking particles from both incubations plotted closer to phide, pyrophide, fuco, BSi, SER, THR, GLY, lithogenic material, organic carbon, BALA, and GABA (i.e., all had positive loadings on PC2). However, the suspended and sinking particles from 20 m plotted closer together whereas those from 200 m exhibited greater separation. These results suggest that particles at the surface may undergo exchange and be relatively homogeneous in composition, but by the time these particles sink out of the mixed layer, they have distinct compositions. At least at DYFAMED, the major mechanism for this fractionation of material appears to be fecal pellet formation.

In the NetTrap incubation, there was no evidence of the disaggregation apparent in the plankton tow incubation. This was probably due to the large number of robust fecal pellets in these samples. However, these samples were also quite rich in phytoplankton, suggesting that the phytoplankton aggregates at 200 m may also have been more robust. Aggregates exiting the euphotic zone may have contained more senescent phytoplankton than at the surface. Phytoplankton in the stationary growth phase often exude transparent exopolymer particles (Alldredge et al., 1993; Engel et al., 2004), which may make their aggregates more robust. However, since there appeared to be some phytoplankton growth during the incubation, many cells were likely in the exponential growth phase.

In both incubations, indicators of fresh plankton underwent greater transfer (i.e., aggregation and/or disaggregation) between pools than fecal pellet indicators. This was evidenced by changes in the concentration and contributions of chl *a* (mole %), fuco (mole %), amino acids (% OC), and nitrogen (weight %) in the different phases over time (Fig. 4.5, 4.6, 4.12, 4.13). Therefore, although phytoplankton aggregates do play a role in the export of organic matter to the deep sea, they may undergo extensive exchange with surrounding material in the process. Hill (1998) and Khelifa and Hill (2006) suggested that continual aggregation and disaggregation of sinking particles occurs in response to changes in size and density. As particles grow larger or denser, shear and inertial drag increase, causing disruption. These adjustments in size probably apply more to phytoplankton aggregates than fecal pellets, whose size is determined upon egestion from zooplankton, and not as much by abiotic flocculation mechanisms. Disruption of phytoplankton aggregates would

increase the residence time of this material in the water column, subjecting it to greater diagenetic alteration. By comparison, fecal pellets may export more intact POC, reducing its residence time and decomposition in the water column.

The results also suggest that not all fecal pellets are alike, since phide underwent greater transfer between suspended and sinking pools in both incubations, while material rich in pyrophide was especially resistant to exchange with suspended particles. It is not clear whether the exchange of phide between pools was due to disaggregation of small fecal pellets or due to the incorporation of fecal pellets into larger aggregates. Since the aggregates we measured were 0.25-3 mm in diameter, they were large enough to incorporate small fecal pellets.

Pyrophide was most enriched in sinking particles from 200 m depth, whereas phide was more enriched in sinking particles collected in surface waters (20 m) and suspended particles from 200 m (Fig. 4.6, 4.13, and 4.15). This may indicate different sources for phide and pyrophide. To more quantitatively assess this difference, we compared the ratio of pyrophide:phide in all four groups of samples (suspended and sinking particles at 20 m and 200 m) using a single-factor ANOVA. Differences in pyrophide: phide among samples were highly significant ($p= 6 \times 10^{-6}$), and decreased in the order: 200 m sinking particles (mean = 2.7) > 200 m suspended particles (0.99) > 20 m suspended particles (0.79) > 20 m sinking particles (0.56). This suggests that large fecal pellets (such as those observed in the NetTrap, which were ≥ 200 m) are enriched in pyrophide, possibly because algal material undergoes more extensive alteration when it passes through the guts of larger grazers. Coprophagy by large grazers could also subject algal material to repeated alteration. Therefore, material rich in phide relative to pyrophide (e.g., both types of particles in the plankton tow, and suspended particles in the NetTrap samples) may be a better indicator for smaller zooplankton, while material rich in pyrophide (e.g., sinking particles in the NetTrap samples) may be derived from larger zooplankton. This idea is purely speculative, since it has not been experimentally tested.

Microzooplankton fecal pellets (<35 μm) sink slowly and can remain suspended in the mixed layer (SooHoo and Kiefer, 1982; Welshmeyer and Lorenzen, 1985; Hendry et al., 1987). In addition, smaller fecal pellets may disaggregate more easily. Viitasalo et al. (1999) observed that the sedimentation of intact fecal pellets in the Baltic Sea was an order of magnitude higher when calanoid copepods were present, whereas the proportion of broken

fecal pellets was greater when smaller copepods were abundant (ranging from 27% in near-shore waters to 61% in the open sea).

4. Conclusions

Our results suggest that the source of sinking particles is very important in controlling the extent of exchange with suspended material, indicating that biological community structure is a critical factor controlling POC export from the surface to deep ocean. Large fecal pellets appeared to be the most robust type of material, whereas phytoplankton aggregates and possibly small fecal pellets underwent greater exchange with surrounding material. Therefore, in seasons (e.g., spring) or locations with abundant macrozooplankton, productivity and deep ocean fluxes may be more closely coupled. When abiotic flocculation mechanisms dominate the formation of sinking particles, there may be greater decoupling between observed productivity and measured fluxes at depth. The results of this study highlight the importance of understanding biological community structure in controlling POC export. A predictive understanding of POC fluxes requires further investigation of the factors controlling the robustness of different types of sinking particles.

References

- Allredge, A.L., Gotschalk, C.C., 1988. *In situ* settling behavior of marine snow. *Limnology and Oceanography* 33, 339-351.
- Allredge, A.L., Passow, U., Logan, B.E. 1993. The abundance and significance of a class of large, transparent organic particles in the ocean. *Deep-Sea Research* 40, 1131-1140.
- Allredge, A.L., Silver, M., 1988. Characteristics, dynamics and significance of marine snow. *Progress in Oceanography* 20, 41-82.
- Armstrong, R.A., Lee, C., Hedges, J.I., Honjo, S., Wakeham, S.G. 2002. A new, mechanistic model for organic carbon fluxes in the ocean based on the quantitative association of POC with ballast minerals. *Deep-Sea Research II* 49, 219-236.
- Asper, V.L., Deuser, W.G., Knauer, G.A., Lohrenz, S.E., 1992. Rapid coupling of sinking particle fluxes between surface and deep ocean waters. *Nature* 357, 670-672.
- Bidigare, R.R., Kennicutt, M.C., Brooks, J.M., 1985. Rapid determination of chlorophylls and their degradation products by high-performance liquid chromatography. *Limnology and Oceanography* 30, 432-435.
- Brzezinski, M.A., 1985. The Si:C:N ratio of marine diatoms: interspecific variability and the effect of some environmental variables. *Journal of Phycology* 21, 347-357.
- Cowie, G.L., Hedges, J.I., 1996. Digestion and alteration of the biochemical constituents of a diatom (*Thalassiosira weissflogii*) ingested by an herbivorous zooplankton (*Calanus pacificus*). *Limnology and Oceanography* 41, 581-594.
- Currie, R., 1962. Pigments in zooplankton faeces. *Nature* 193, 956-957.
- Daley, R.J., 1973. Experimental characterization of lacustrine chlorophyll diagenesis. II. Bacterial, viral and herbivore grazing effects. *Archiv für Hydrobiologie* 72, 409-439.
- de Jong, E.W., Bosch, L., Westbroek, P., 1976. Isolation and characterisation of a Ca²⁺-binding polysaccharide associated with coccoliths of *Emiliania huxleyi*. (Lohman) Kamptner. *European Journal of Biochemistry* 70, 611-621.
- Engel, A., Thoms, S., Riebesell, U., Rochelle-Newall, E., Zondervan, I. 2004. Polysaccharide aggregation as a potential sink of marine dissolved organic carbon. *Nature* 428, 929-932.
- Engel, A., Szlosek, J., Abramson, L., Liu, Z., Lee, C. Decomposition of calcifying and non-calcifying *Emiliania huxleyi* (Prymnesiophyceae): II. Formation, settling velocities and physical properties of aggregates. Submitted to *Deep-Sea Research II* (a).

- Engel, A., Abramson, L., Szlosek, J., Liu, Z., Stewart, G., Hirschberg, D., Lee, C.
Investigating the effect of ballasting by CaCO₃ in *Emiliana huxleyi*: II.
Decomposition of particulate organic matter. Submitted to Deep-Sea Research II (b).
- Fabres, J., Tesi, T., Velez, J., Batista, F., Lee, C., Calafat, A., Heussner, S., Miserocchi, S.,
Palanques, A. Seasonal and event controlled export of fresh organic matter from the
shelf towards the Gulf of Lions continental slope. Submitted to Continental Shelf
Research.
- Fanning, K.A., Pilson, M.E., 1973. On the spectrophotometric determination of dissolved
silica in natural waters. *Analytical Chemistry* 45, 136-140.
- Faugeras, B., Lévy, M., Mémery, L., Verron, J., Blum, J., Charpentier, I., 2003. Can
biogeochemical fluxes be recovered from nitrate and chlorophyll data? A case study
assimilating data in the Northwestern Mediterranean Sea at the JGOFS-DYFAMED
station. *Journal of Marine Systems* 40-41, 99-125.
- Fowler, S.W. and Fisher, N.S., 1983. Viability of marine phytoplankton in zooplankton
faecal pellets. *Deep-Sea Research* 30, 963-969.
- Fowler, S.W. and Knauer, G.A., 1986. Role of large particles in the transport of elements
and organic compounds through the oceanic water column. *Progress in
Oceanography* 16, 147-194.
- François, R., Honjo, S., Krishfield, R., Manganini, S., 2002. Factors controlling the flux of
organic carbon to the bathypelagic zone of the ocean. *Global Biogeochemical Cycles*
16, 1087.
- French, F.W., Hargraves, P.E., 1980. Physiological characteristics of plankton diatom resting
spores. *Marine Biology Letters* 1, 185-195.
- Gibbs, R.J., 1985. Estuarine flocs: Their size, settling velocity and density. *Journal of
Geophysical Research* 90, 3249-3251.
- Hamm, C.E., 2002. Interactive aggregation and sedimentation of diatoms and clay-sized
lithogenic material. *Limnology and Oceanography* 47, 1790-1795.
- Hargraves, P.E. 1976. Studies on marine plankton diatoms. II. Resting spore morphology.
Journal of Phycology 12, 119-128.
- Hecky, R.E., Mopper, K., Kilham, P., Degens, E.T., 1973. The amino acid and sugar
composition of diatom cell-walls. *Marine Biology* 19, 323-331.
- Hedges, J.I., Stern, J.H., 1984. Carbon and nitrogen determinations of carbonate-containing
solids. *Limnology and Oceanography* 29, 657-663.
- Hendry, G.A.F., Houghton, J.D., Brown, S.B. 1987. The degradation of chlorophyll – A
biological enigma. *New Phytologist* 107, 255-302.

- Hill, P.S., 1998. Controls on flocc size in the sea. *Oceanography* 11, 13-18.
- Ingalls, A.E., Lee, C., Wakeham, S.G., Hedges, J.I., 2003. The role of biominerals in the sinking flux and preservation of amino acids in the Southern Ocean along 170°W. *Deep-Sea Research II* 50:709-734.
- Jamart, B.M., Winterg, D.F., Anderson, C., Lam, R.K., 1977. A theoretical study of phytoplankton growth and nutrient distribution in the Pacific Ocean off the northwestern U.S. coast. *Deep-Sea Research* 24: 753-773.
- Khelifa, A., Hill, P.S., 2006. Models for effective density and settling velocity of flocs. *Journal of Hydraulic Research* 44, 390–401.
- King, K., Jr., 1974. Preserved amino acids from silicified protein in fossil radiolaria. *Nature* 252, 690-692.
- King L.L., 1993. Chlorophyll diagenesis in the water column and sediment of the Black Sea. Dissertation, Massachusetts Institute of Technology.
- Klaas, C., Archer, D.E., 2002. Association of sinking organic matter with various types of mineral ballast in the deep sea: Implications for the rain ratio. *Global Biogeochemical Cycles* 16, 1116.
- Lorenzen, 1968. Carbon/ chlorophyll relationships in an upwelling area. *Limnology and Oceanography* 13, 202-204.
- Lee C., Cronin, C., 1982. The vertical flux of particulate nitrogen in the sea: Decomposition of amino acids in the Peru upwelling area and the equatorial Atlantic. *Journal of Marine Research* 40, 227-251.
- Lee, C, Wakeham, S.G., Hedges, J.I., 2000. Composition and flux of particulate amino acids and chloropigments in equatorial Pacific seawater and sediments. *Deep-Sea Research I* 47, 1535–1568.
- Lewis, J., Harris, A.S.D., Jones, K.J., Edmonds, R.L., 1999. Long-term survival of marine planktonic diatoms and dinoflagellates in stored sediment samples. *Journal of Plankton Research* 21, 343-354.
- Loferer-Kröbächer, M., Klima, J., Psenner, R., 1998. Applied and Environmental Microbiology 63, 688-694.
- Lorenzen, 1968. Carbon/ chlorophyll relationships in an upwelling area. *Limnology and Oceanography* 13, 202-204.
- Marty, J.C., Chiavérini, J., Pizay, M.D., Avril, B., 2002. Seasonal and interannual dynamics of nutrients and phytoplankton pigments in the western Mediterranean Sea at the DYFAMED time-series station (1991-1999). *Deep-Sea Research II* 49, 1965-1985.

- Marty, J.C., Chiavérini, J., 2002. Seasonal and interannual variations in phytoplankton production at DYFAMED time-series station, northwestern Mediterranean Sea. *Deep-Sea Research II* 49, 2017-2030.
- McCave, I.N., 1984. Size spectra and aggregation of suspended particles in the deep ocean. *Deep-Sea Research* 31, 329-252.
- Passow, U., De La Rocha, C., 2006. The accumulation of mineral ballast on organic aggregates. *Global Biogeochemical Cycles* 20, GB1013, doi:10.1029/2005GB002579.
- Peters, E., 1996. Prolonged darkness and diatom mortality: II. Marine temperate species. *Journal of Experimental Marine Biology and Ecology* 207, 43-58.
- Peterson, M.L., Fabres, J., Wakeham, S.G., Lee, C., Miquel, J.C. Sampling the vertical particle flux in the upper water column using a large diameter free-drifting NetTrap adapted to an Indented Rotating Sphere sediment trap. Submitted to *Deep-Sea Research II*.
- Peterson, M.L., Wakeham, S. G., Lee, C., Askea, M., Miquel, J.C., 2005. Novel techniques for collection of sinking particles in the ocean and determining their settling rates. *Limnology and Oceanography Methods* 3, 520-532.
- Pilskaln, C.H., Honjo, S., 1987. The fecal pellet fraction of biogeochemical particle fluxes to the deep sea. *Global Biogeochemical Cycles*, 1, 31-48.
- Shanks, A.L., Edmondson, E.W., 1989. Laboratory-made artificial marine snow: A biological model of the real thing. *Marine Biology* 101, 463-470.
- Shanks A.L., Trent, J.D., 1980. Marine snow: sinking rates and potential role in vertical flux. *Deep-Sea Research* 27, 137-143.
- Smayda, T.J., Mitchell-Innes, B., 1974. Dark survival of autotrophic planktonic marine diatoms. *Marine Biology* 25, 195-202.
- SooHoo, J.B., Kiefer, D.A., 1982. Vertical distribution of phaeopigments. I. A simple grazing and photooxidative scheme for small particles. *Deep-Sea Research* 29, 1539-1551.
- Strickland, J.D.H., Parsons, T.R., 1972. A practical handbook of sea-water analysis. *Journal of the Fisheries Research Board of Canada*. 167, 311 pp.
- Stumm, W., Morgan, J.J., 1996. *Aquatic Chemistry: Chemical Equilibria and Rates in Natural Waters* (3rd ed.). John Wiley and Sons, New York, 1022 pp.
- Sun, M., Aller, R.C., Lee, C., 1991. Early diagenesis of chlorophyll-a in Long Island Sound sediments: a measure of carbon flux and particle reworking. *Journal of Marine Research* 49, 379-401.

- Sun, M., Aller, R.C., Lee, C., 1994. Spatial and temporal distributions of sedimentary chloropigments as indicators of benthic processes in Long Island Sound. *Journal of Marine Research* 52, 149-176.
- Swift, D.M., Wheeler, P., 1991. Evidence of an organic matrix from diatom biosilica. *Journal of Phycology* 28, 202-209.
- van Emburg, P.R., de Jong, E.W., Daems, W., 1986. Immunochemical localization of a polysaccharide from biomineral structures (coccoliths) of *Emiliania huxleyi*. *Journal of Ultrastructure and Molecular Structure Research* 94, 246-259.
- Vuittasalo, M., Rosenberg, M., Heiskanen, A.S., Kosi, M., 1999. Sedimentation of copepod fecal material in the coastal northern Baltic Sea: where did all the pellets go? *Limnology and Oceanography* 44, 1388-1399.
- Vrede, K., Heldal, M., Norland, S., Bratbak, G., 2002. Elemental composition (C, N, P) and cell volume of exponentially growing and nutrient-limited bacterioplankton. *Applied and Environmental Microbiology* 68, 2965-2971.
- Wakeham, S.G., Hedges, J.I., Lee, C., Peterson, M.L., Hernes, P.J., 1997. Compositions and transport of lipid biomarkers through the water column and surficial sediments of the equatorial Pacific Ocean. *Deep-Sea Research II* 44, 2131-2162.
- Weiner, S., Erez, J., 1984. Organic matrix of the shell of the foraminifer, *Heterostegina depressa*. *Journal of Foraminiferal Research* 14, 206-212.
- Welschmeyer, N.A., Lorenzen, C.J., 1985. Chlorophyll budgets: Zooplankton grazing and phytoplankton growth in a temperate fjord and the Central Pacific Gyres. *Limnology and Oceanography* 30, 1-21.

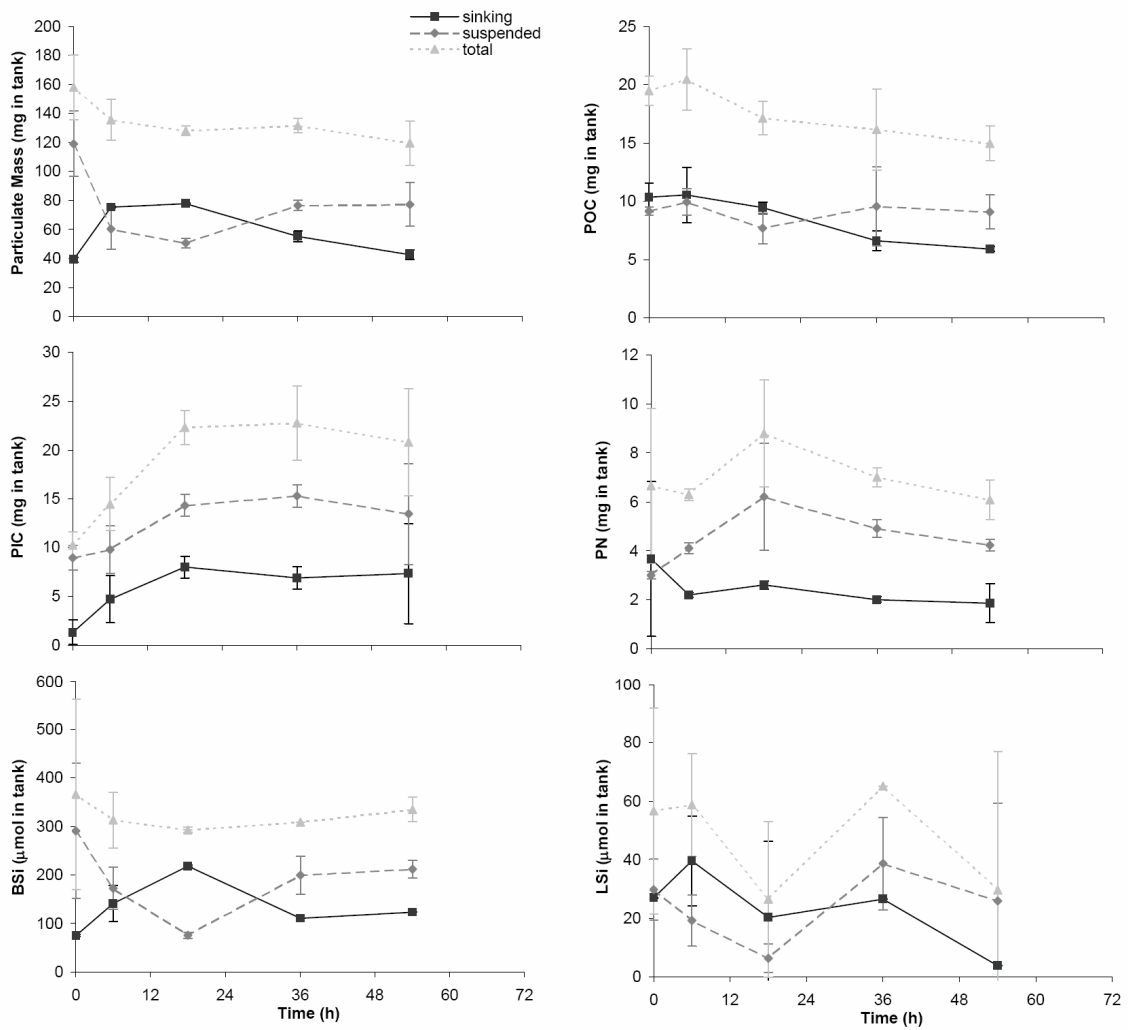


Figure 4.1. Changes in particulate mass, organic carbon (POC), inorganic carbon (PIC), nitrogen (PN), biogenic silica (BSi), and lithogenic silica (LSi) in suspended and sinking particles during incubation of the 20 m plankton tow material.

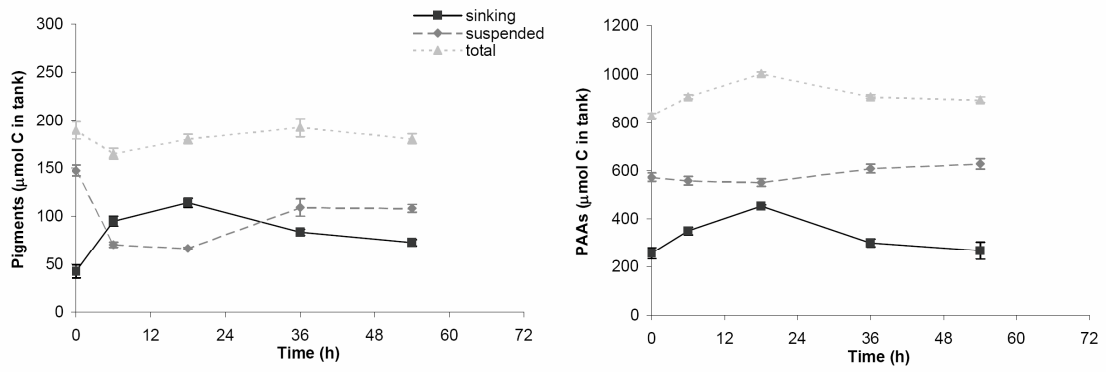


Figure 4.2. Changes in particulate pigments and amino acids (PAAs) in suspended and sinking particles during the 20 m plankton tow incubation.

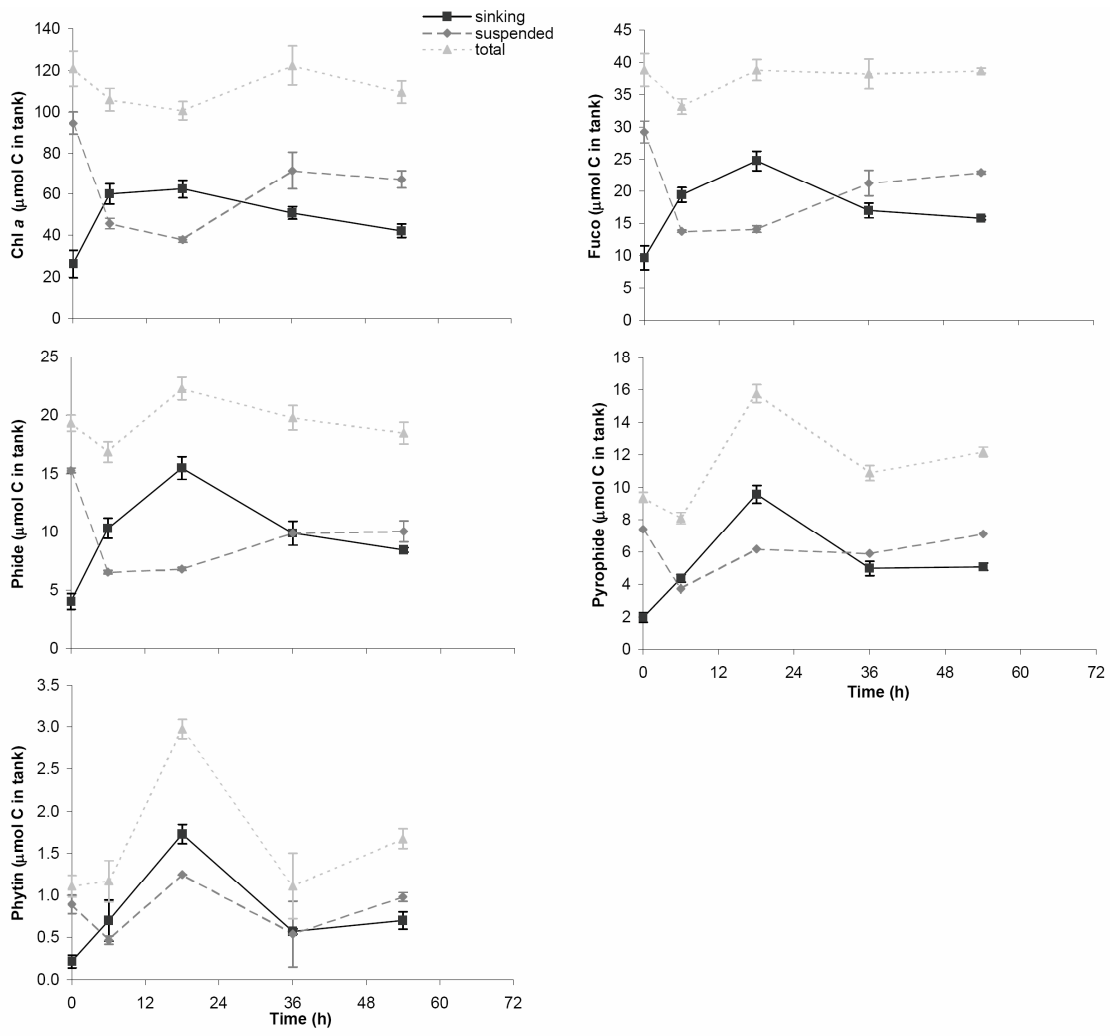


Figure 4.3. Changes in the pigments chlorophyll *a* (chl *a*), fucoxanthin (fuco), pheophorbide (phide), pyropheophorbide (pyrophide), and pheophytin (phytin) in suspended and sinking particles during the 20 m plankton tow incubation.

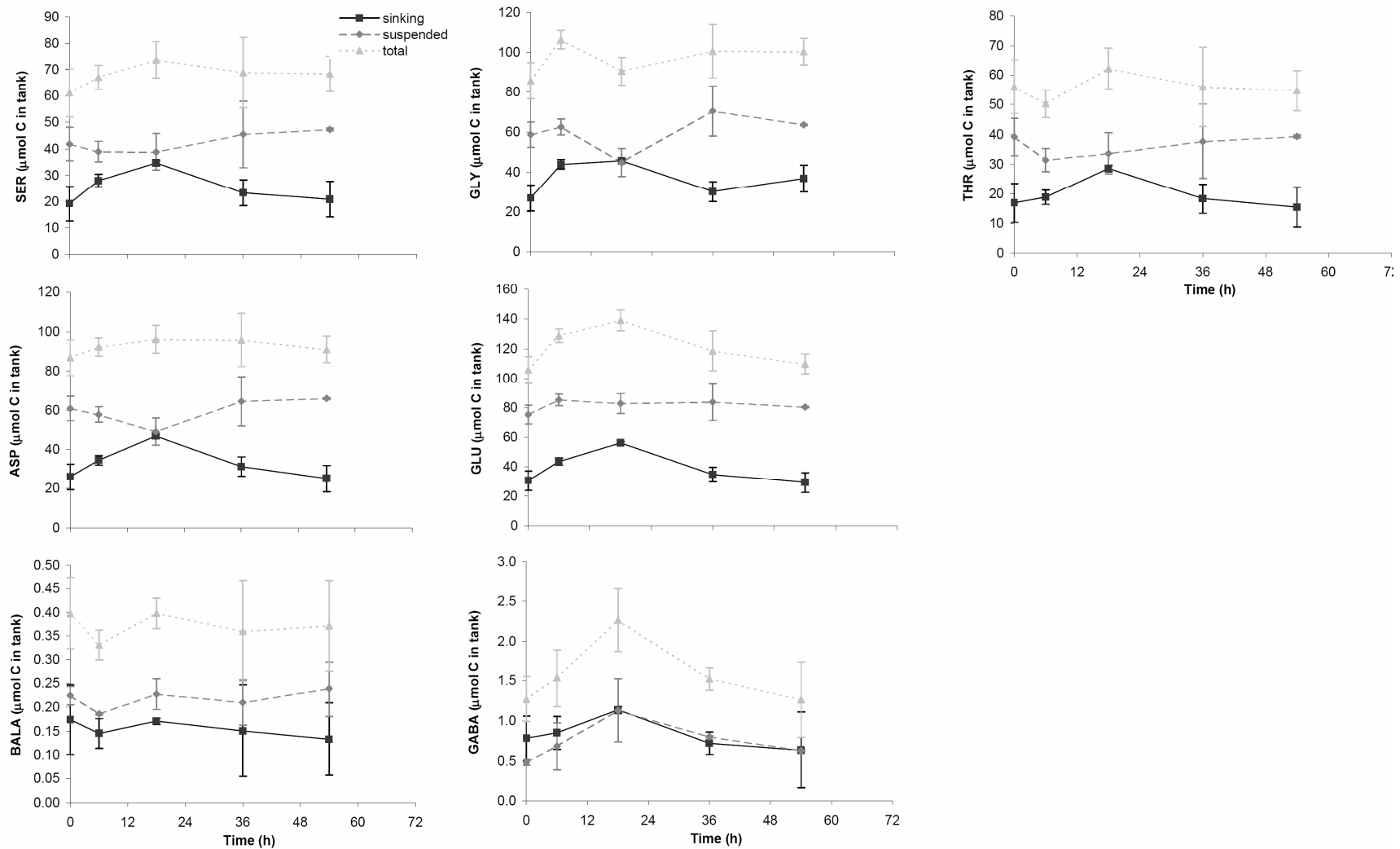


Figure 4.4. Changes in the amino acids serine (SER), threonine (THR), glycine (GLY), aspartic acid (ASP), glutamic acid (GLU), β -alanine (BALA), and γ -aminobutyric acid (GABA) in suspended and sinking particles during the 20 m plankton tow incubation.

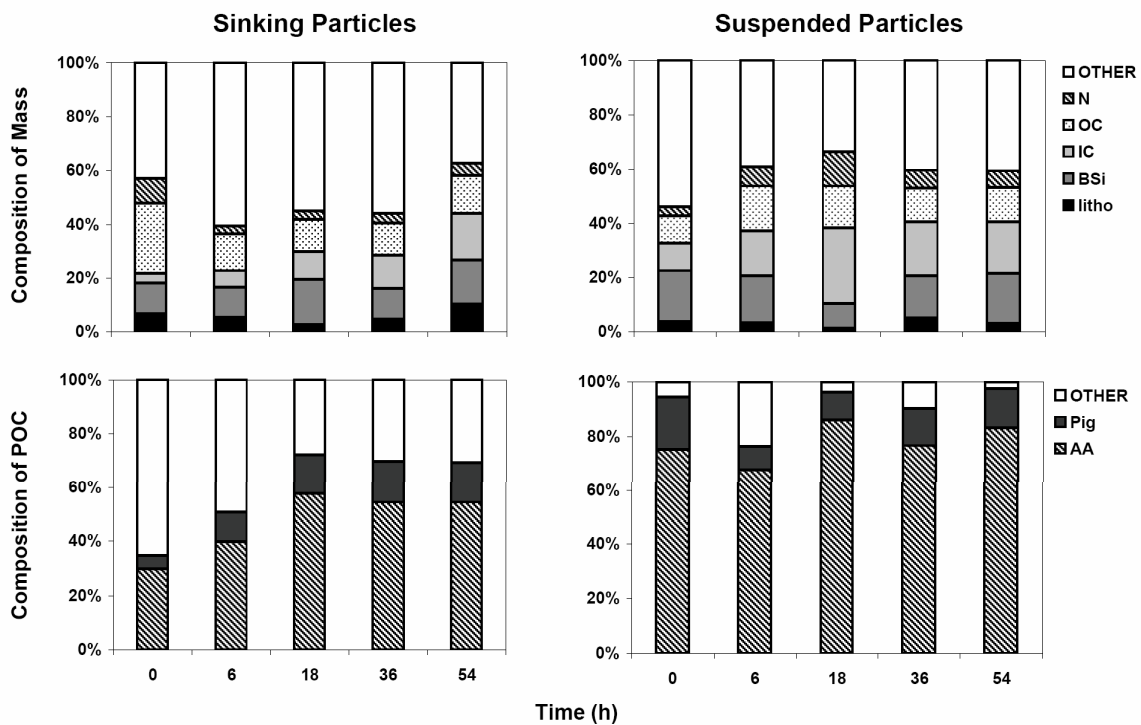


Figure 4.5. Composition of total particulate mass and organic carbon in suspended and sinking particles in the 200 m NetTrap incubation. Top panel shows the % contribution of particulate nitrogen (N), organic carbon (OC), inorganic carbon (IC), biogenic silica (BSi) as SiO_2 , lithogenic material (litho) calculated from lithogenic silica measurements assuming crustal ratios, and uncharacterized components (other) to total mass. Bottom panel shows the contribution of pigments (pig) and amino acids (AA), and uncharacterized components to particulate organic carbon.

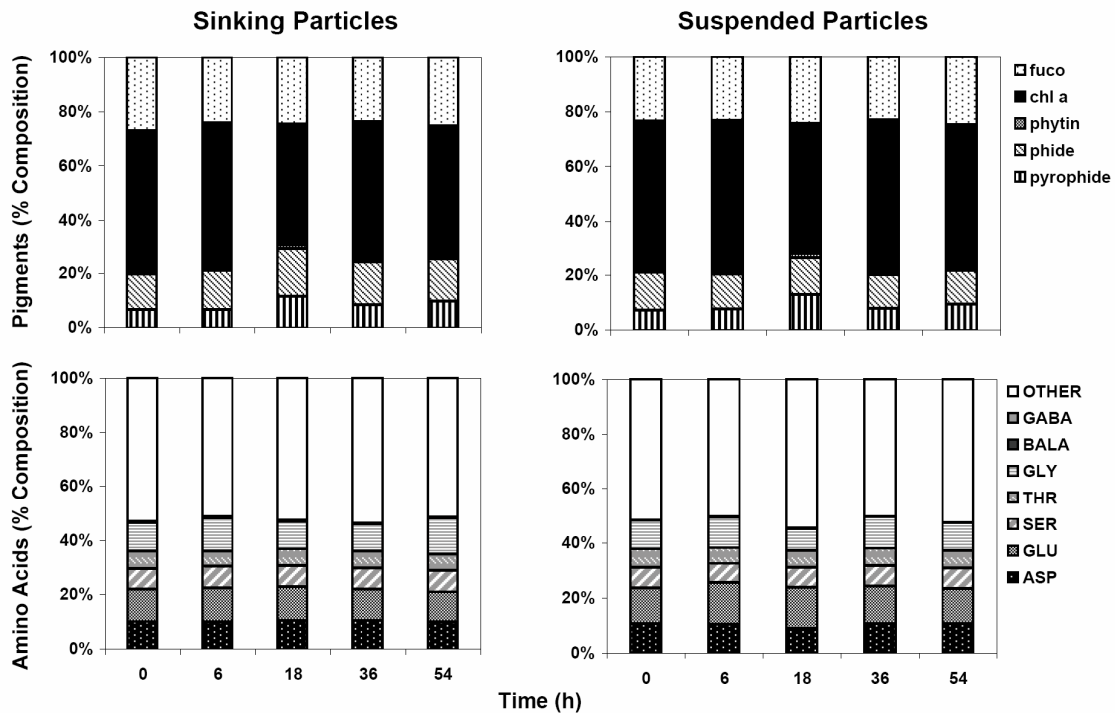


Figure 4.6. Percent composition (in mol % of total pigments and amino acids) of selected pigments and amino acids in suspended and sinking particles during the 20 m plankton tow incubation. Pigments shown are chlorophyll *a* (chl *a*), fucoxanthin (fuco), pheophorbide (phide), pyropheophorbide (pyrophide), and pheophytin (phytin). Amino acids shown are (SER), threonine (THR), glycine (GLY), aspartic acid (ASP), glutamic acid (GLU), β -alanine (BALA), and γ -aminobutyric acid (GABA).

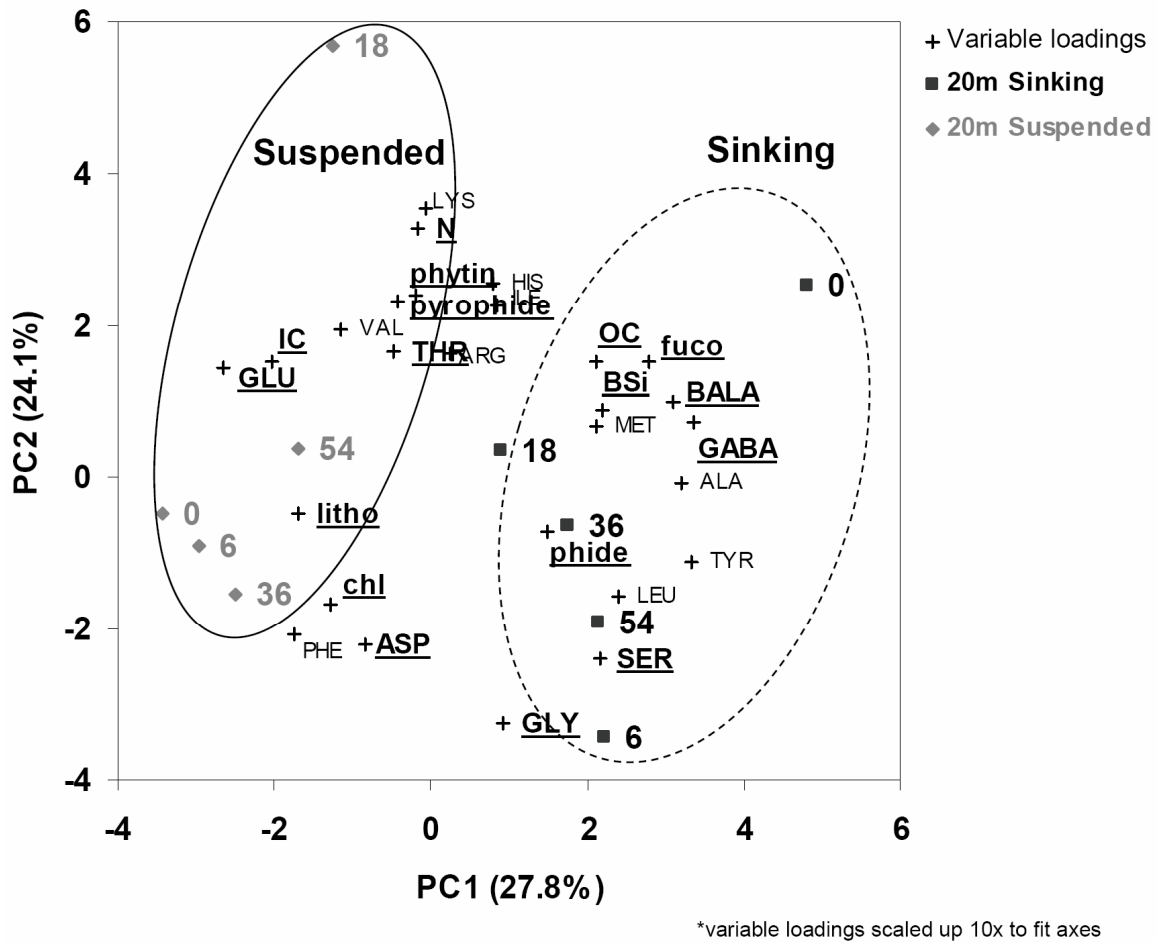


Figure 4.7. Principal component analysis performed on the data from the 20 m plankton tow incubation. Suspended and sinking particles are circled.

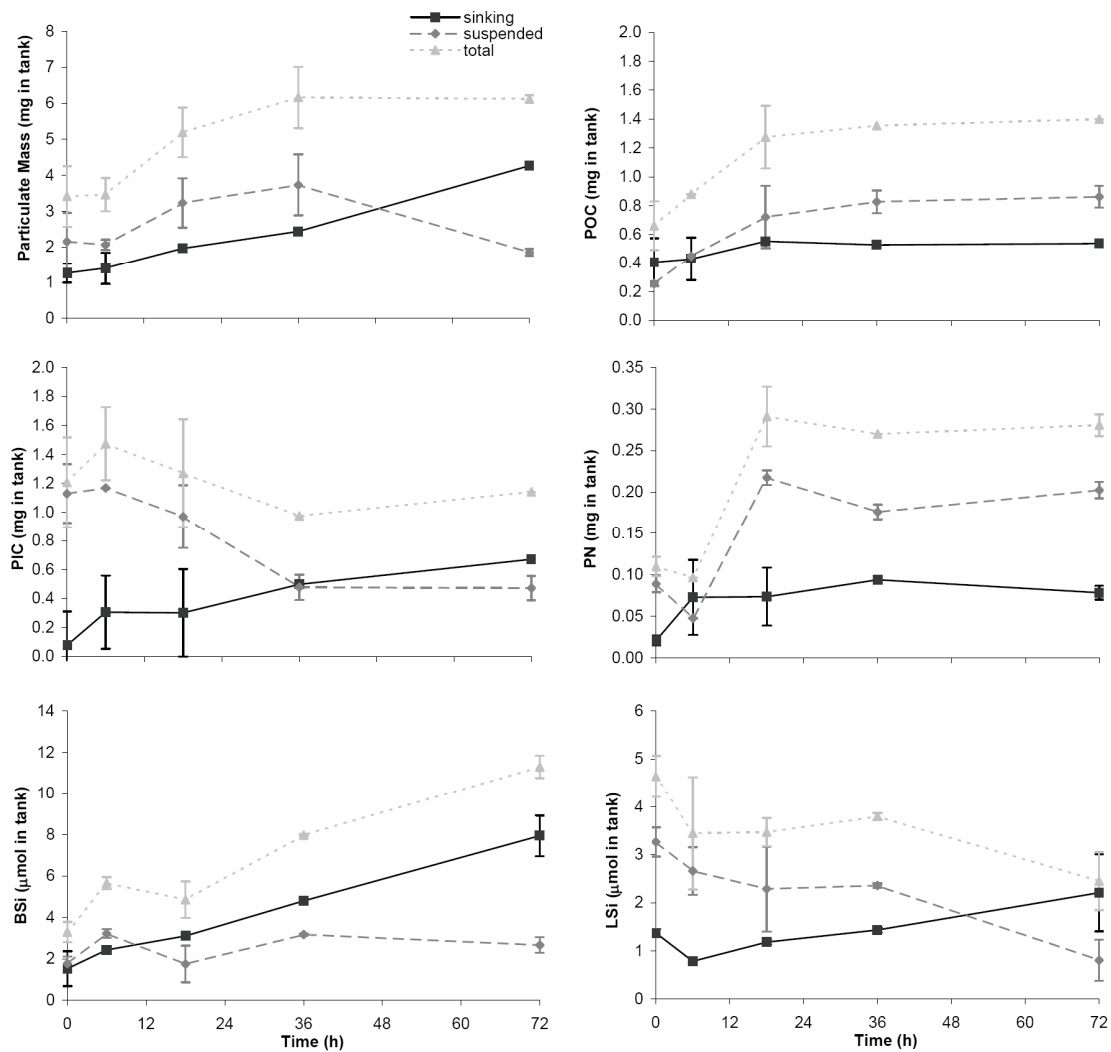


Figure 4.8. Changes in particulate mass, organic carbon (POC), inorganic carbon (PIC), nitrogen (PN), biogenic silica (BSi), and lithogenic silica (LSi) in suspended and sinking particles during the 200 m NetTrap incubation.

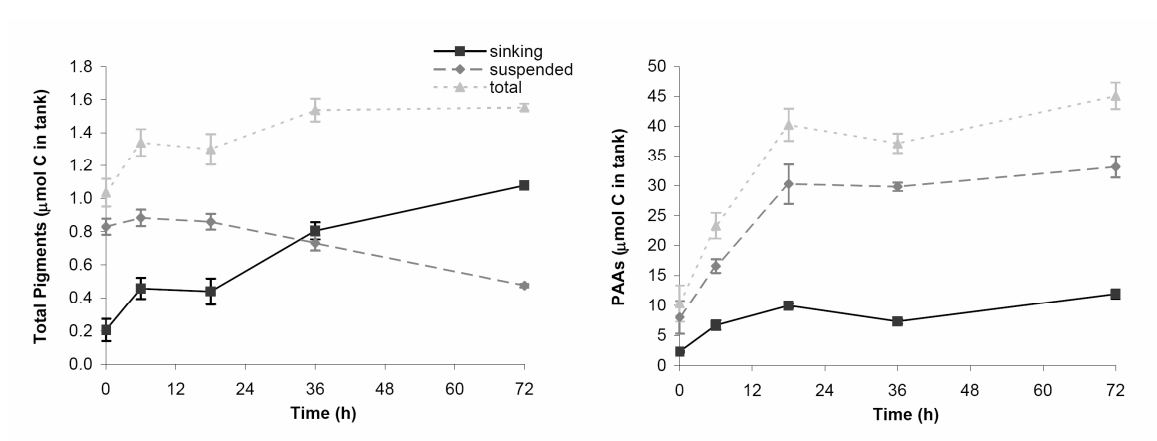


Figure 4.9. Changes in particulate pigments and amino acids (PAAs) in suspended and sinking particles during the 200 m NetTrap incubation.

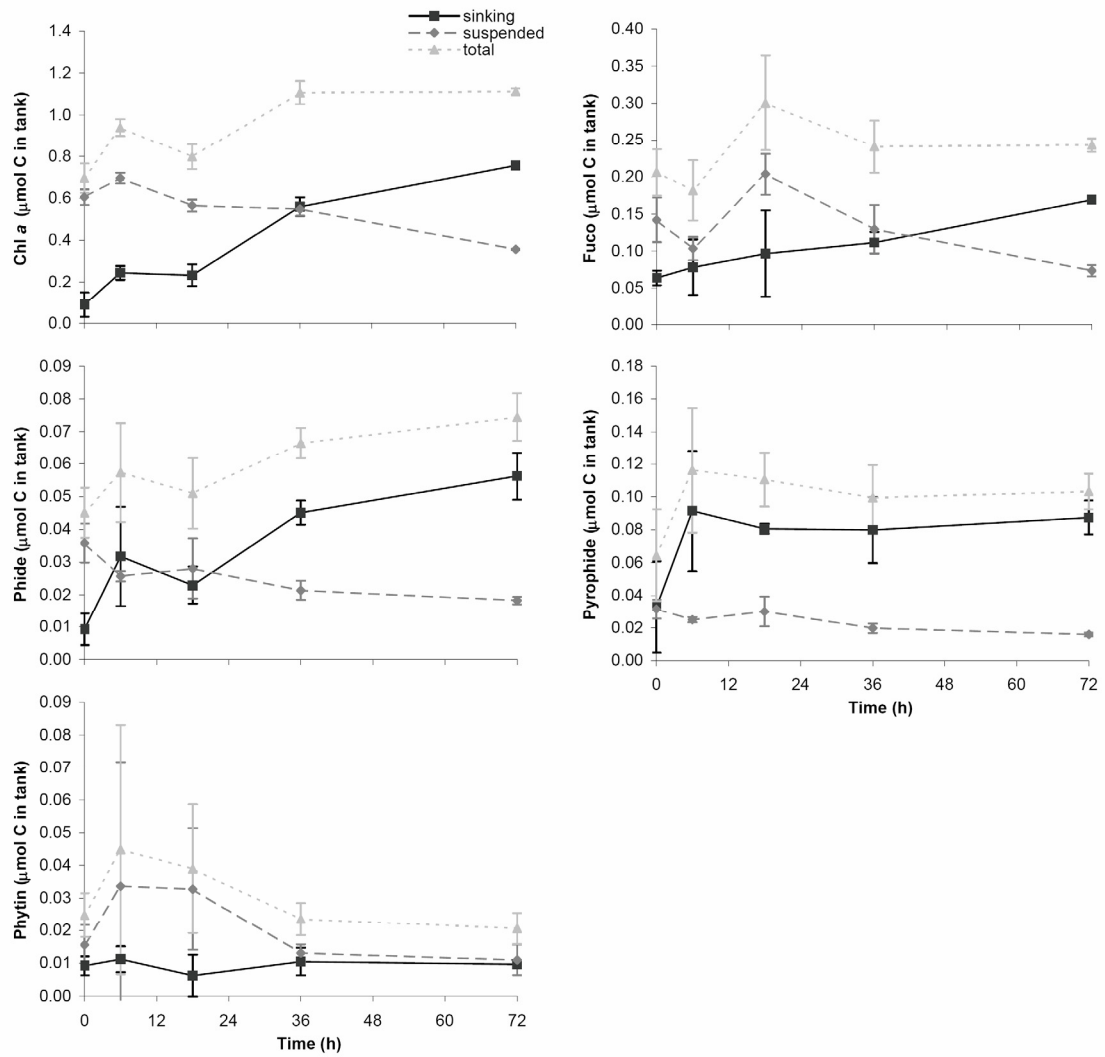


Figure 4.10. Changes in the pigments chlorophyll *a* (chl *a*), fucoxanthin (fuco), pheophorbide (phide), pyropheophorbide (pyrophephide), and pheophytin (phytin) in suspended and sinking particles during the 200 m NetTrap incubation.

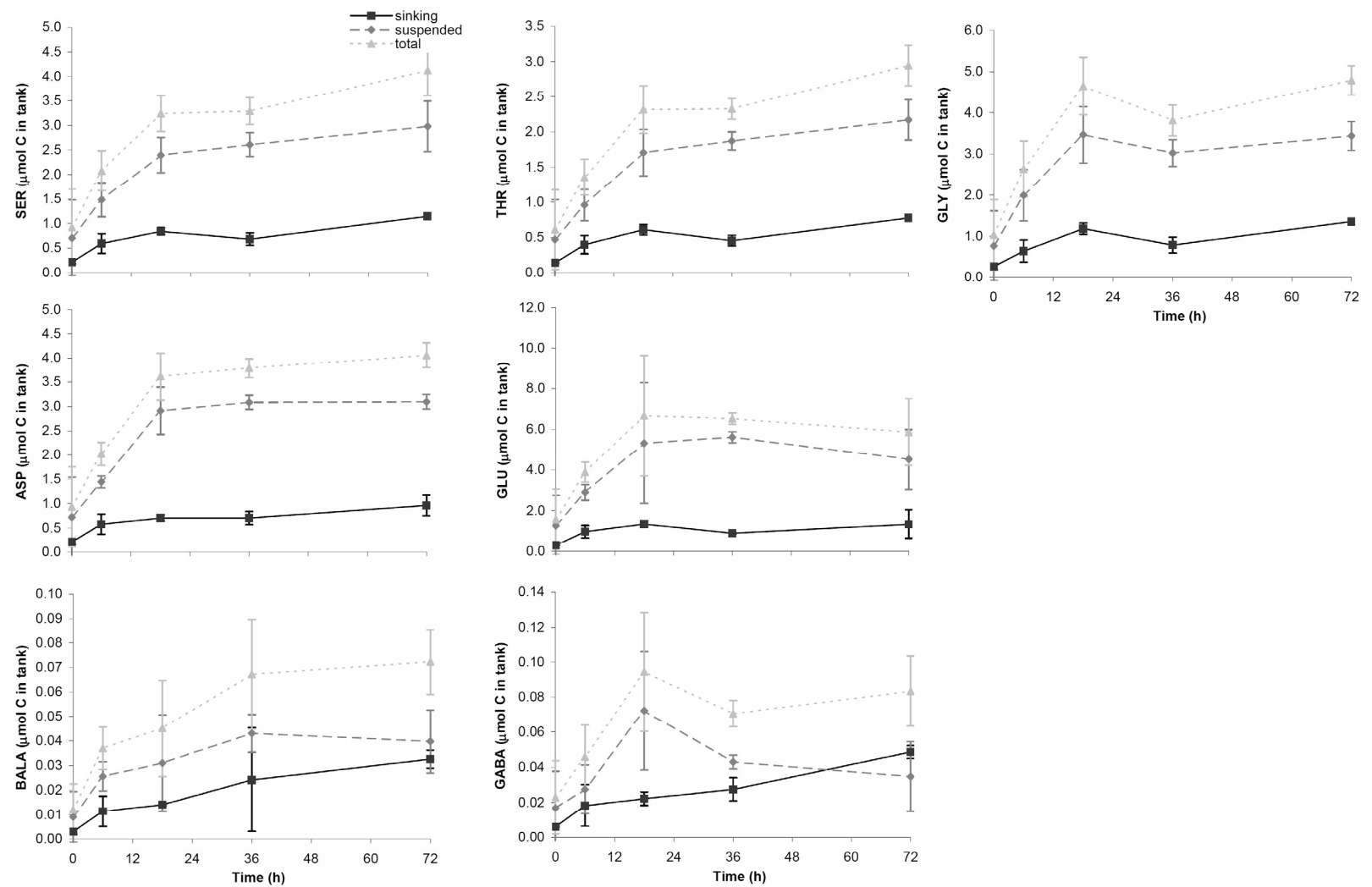


Figure 4.11. Changes in the amino acids serine (SER), threonine (THR), glycine (GLY), aspartic acid (ASP), glutamic acid (GLU), β -alanine (BALA), and γ -aminobutyric acid (GABA) in suspended and sinking particles during the 200 m NetTrap incubation.

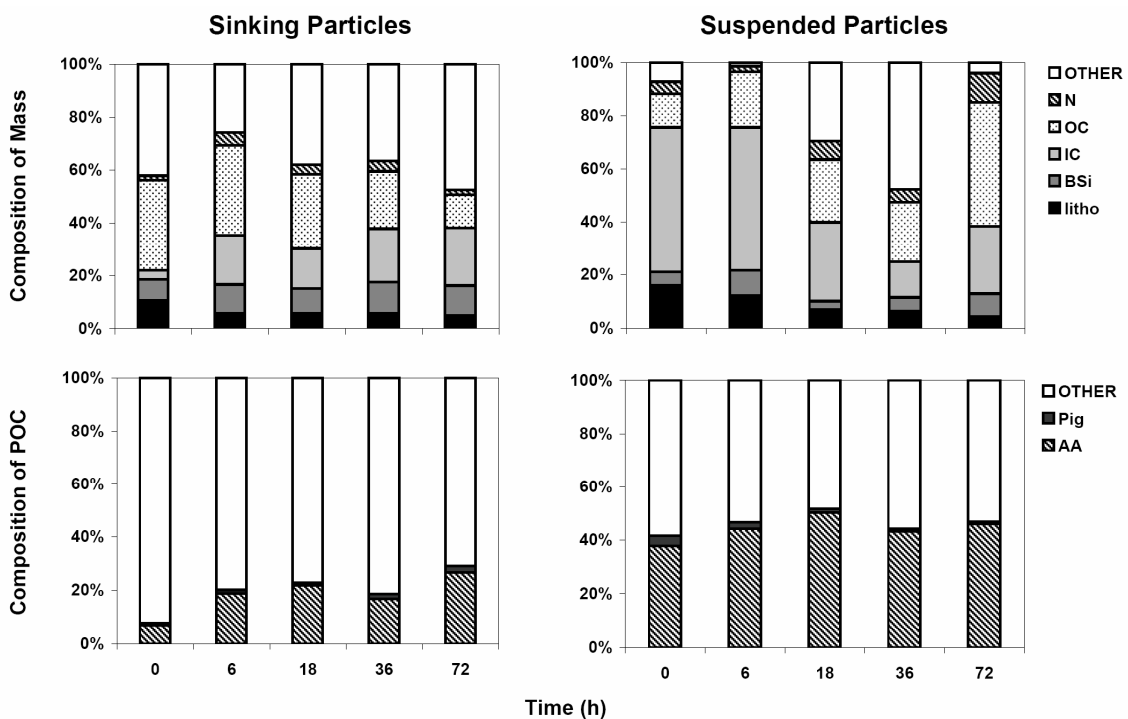


Figure 4.12. Composition of total particulate mass and organic carbon in suspended and sinking particles in the 200 m NetTrap incubation. Top panel shows the % contribution of particulate nitrogen (N), organic carbon (OC), inorganic carbon (IC), biogenic silica (BSi) as SiO_2 , lithogenic material (litho) calculated from lithogenic silica measurements assuming crustal ratios, and uncharacterized components (other) to total mass. Bottom panel shows the contribution of pigments (pig) and amino acids (AA), and uncharacterized components to total particulate organic carbon.

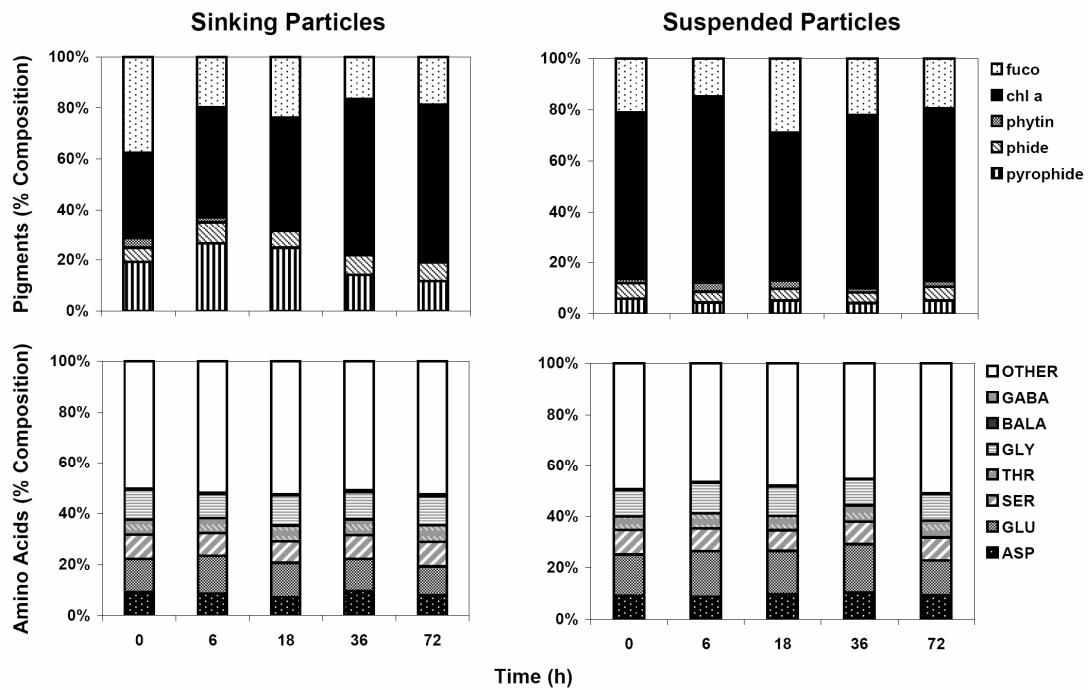


Figure 4.13. Percent composition (in mol % of total pigments and amino acids) of selected pigments and amino acids in suspended and sinking particles during the 200 m NetTrap incubation. Pigments shown are chlorophyll *a* (*chl a*), fucoxanthin (*fuco*), pheophorbide (*phide*), pyropheophorbide (*pyropheide*), and pheophytin (*phytin*). Amino acids shown are (SER), threonine (THR), glycine (GLY), aspartic acid (ASP), glutamic acid (GLU), β -alanine (BALA), and γ -aminobutyric acid (GABA).

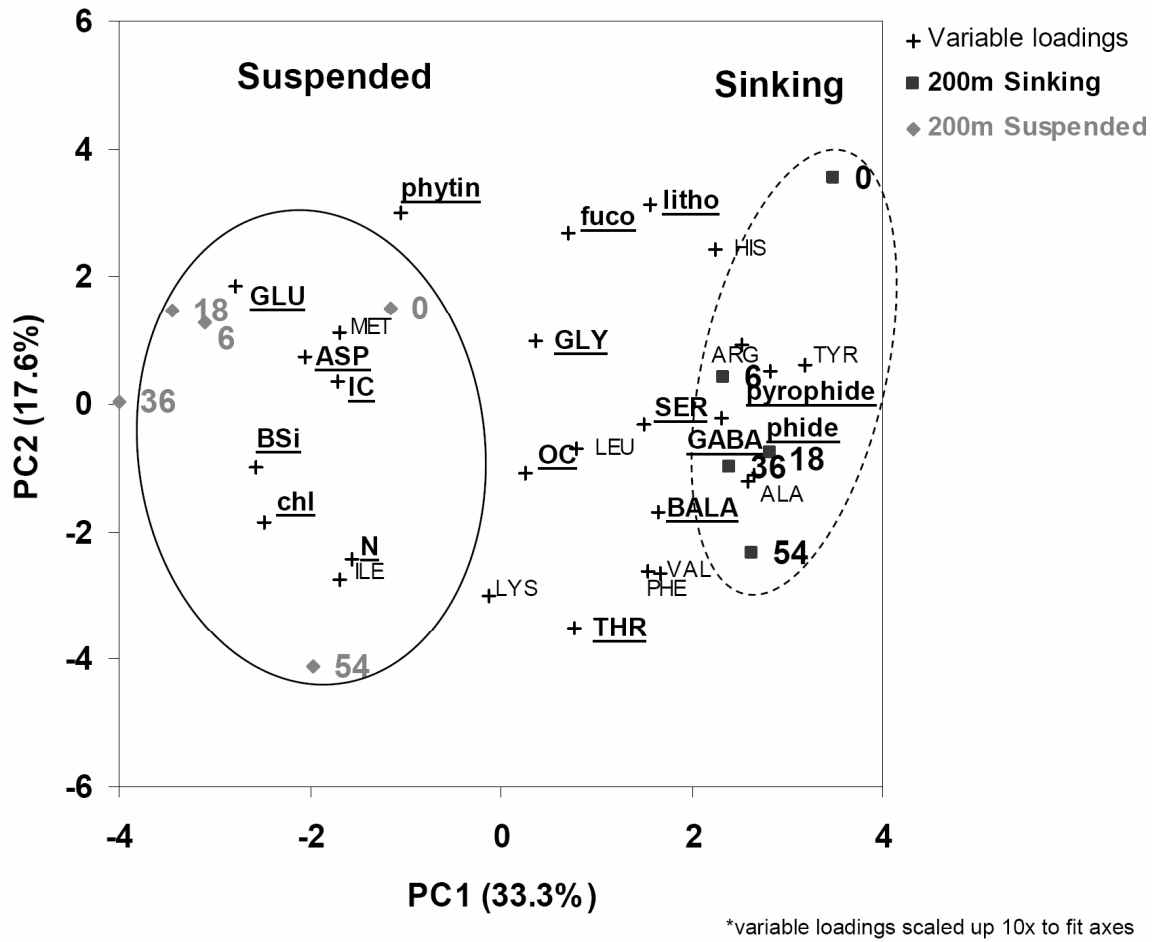
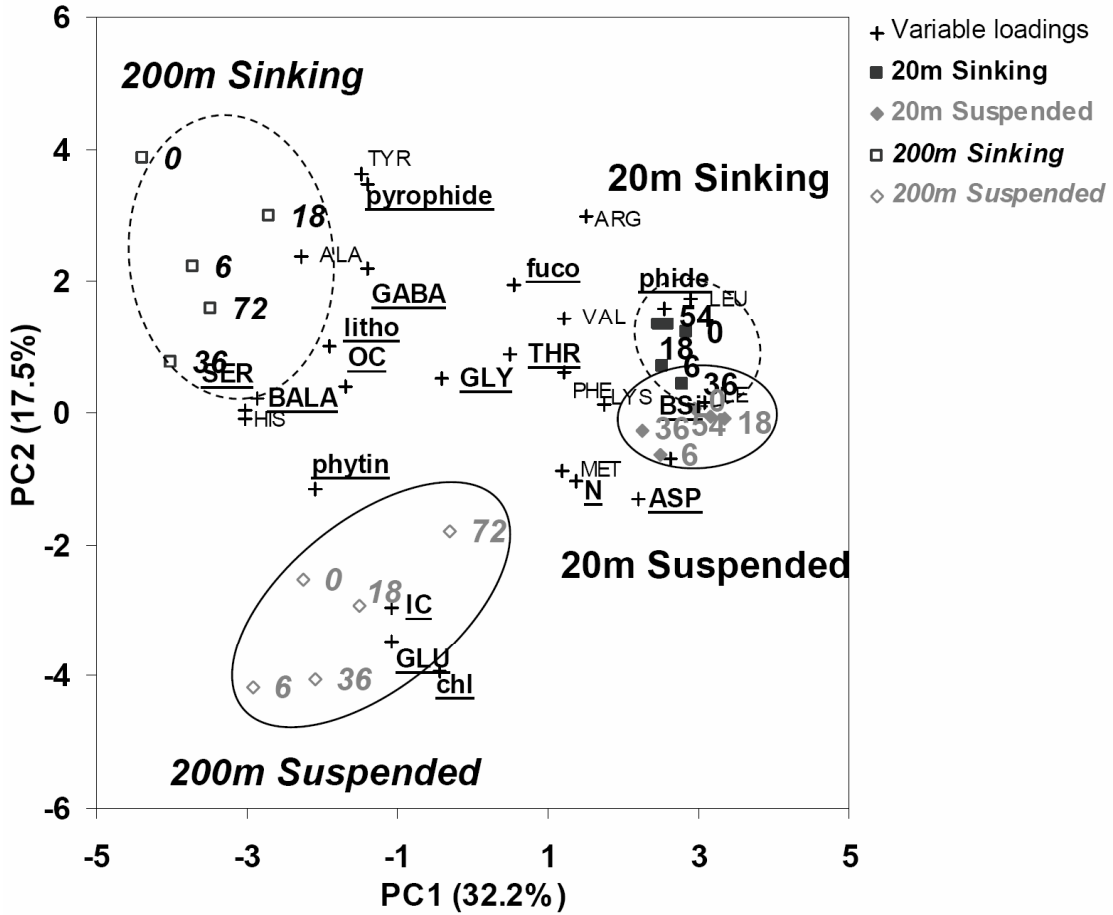


Figure 4.14. Principal component analysis performed on the data from the 200 m NetTrap incubation. Suspended and sinking particles are circled.



*variable loadings scaled up 10x to fit axes

Figure 4.15. Principal component analysis performed on the combined data from the 20 m plankton tow and 200 m NetTrap incubations. Suspended and sinking particles from both incubations are circled.

CHAPTER 5

Conclusions

1. Summary and Implications of Major Findings

This thesis provides information about two important mechanisms of particulate organic carbon (POC) export and preservation in the water column: physical or chemical protection by minerals, and aggregation processes.

In Chapter 2, we used a combination of scanning transmission X-ray microscopy (STXM) and carbon X-ray absorption near-edge structure (XANES) spectroscopy to characterize the distribution and composition of organic matter in frustules of the diatom *Cylindrotheca closterium* and a biomimetic silica gel. Organic carbon, most likely protein (as evidenced by a large carboxyl component), was distributed throughout the frustules and was not completely removed by 2:1 (CH)₂Cl₂:MeOH, 30% H₂O₂, or hydrolysis in 6N HCl, suggesting that frustule-bound organic carbon is protected from decomposition until the frustule dissolves. Previous studies have also found evidence for protection of organic matter within diatom frustules. Ingalls et al. (2003) observed that the contribution of the frustule-bound amino acids serine, threonine, and glycine to total particulate amino acids increased with depth in the water column and sediments in the Southern Ocean. Cowie and Hedges (1996) experimentally determined that frustules of *Thalassiosira weissflogii* were preserved in zooplankton fecal pellets while intracellular organic matter was digested, indicating selective preservation of frustule-bound organic matter. The results of this thesis support these observations, and provide new information as to the extent and mechanisms of this protection.

The distribution of organic matter in frustules changed slightly when exposed to increasingly stringent levels of treatment, suggesting different levels of association with silica (e.g., sorption onto the surface, binding to the cell wall, and complete protection within the biomineral structure). The physical structure of the frustules appeared to be related to the chemical composition of this organic matter, with aromatic or unsaturated carbon concentrated in the most intricately patterned regions of the frustule, possibly corresponding with the perforated roofs covering pores in the frustule. A similar physical and chemical

structure was observed in a biomimetic silica gel precipitated with poly-lysine. These results are consistent with the theory that organic constituents of diatom frustules direct silica precipitation, as suggested by previous researchers (Hecky et al., 1973; Sumper, 2002). The relationship between organic matter composition and silica morphology, the failure of harsh chemical treatments to remove this organic matter, and the spontaneous nature of the coprecipitation of silica and organic matter indicate some chemical interaction between the siliceous and organic components of diatom frustules. There is no evidence for molecular bonding between silica and organic matter (Kinrade et al., 2002; Sahai, 2004), suggesting that hydrogen bonding or condensation onto SER, THR, and GLY in the silicellemma is responsible for this chemical interaction (Hecky et al., 1973; Volcani, 1981). The results of this study suggest that physical occlusion and weak chemical interaction may both play a role in retarding the degradation of biomineral-bound organic matter.

Chapter 3 provides evidence that fecal pellets, an important component of POC fluxes in the Mediterranean Sea (Fowler et al., 1991; Carroll et al., 1998), undergo very little exchange with suspended particles via disaggregation and reaggregation during transit through the water column. Suspended and sinking particles collected in the Mediterranean Sea during the spring and summer of 2003 and 2005 differed greatly in composition. Suspended particles collected on the 1-70 μm *in situ* pump filters were generally enriched in chl *a* (the average for all 6 sampling periods was 66%) compared with sinking particles collected in sediment traps and on the >70 μm pump pre-filters (8-18%). Sinking particles were enriched in the fecal pellet indicators phide and pyrophide (18-24% and 16-40%, on average) compared with suspended particles (8 and 4% on average). Sinking particles do not appear to uniformly disaggregate and exchange with suspended material, or these two particle types would be more similar in composition. Mass balance calculations evaluating the potential supply of pigments to the suspended phase via disaggregation of sinking particles (determined as the decrease in fluxes between two trap depths integrated over the entire two-month trap deployment) indicate that the observed composition of suspended particles is more likely explained by preferential disaggregation of phytoplankton aggregates. Fecal pellets do not appear to undergo extensive disaggregation and exchange with suspended material, suggesting they are a more efficient mode of POC export to the deep sea than phytoplankton aggregates.

Differences in composition were less pronounced in the summer of 2003 than in the spring of both years, suggesting that exchange may be greater during periods of low flux, when phytoplankton aggregates are rarer and fecal pellets are smaller. Alternatively, since both particle types were more enriched in bacterial degradation indicators pheophytin, β -alanine, and γ -aminobutyric acid during the summer than in the spring, their similarity in composition may simply reflect more extensive microbial alteration during the summer.

Other studies (e.g., Repeta and Gagosian, 1984; Wakeham and Canuel, 1988; Sheridan et al., 2002) have shown that suspended and sinking particles differ greatly in composition. Our results provide a mechanistic explanation for this observation – that preferential disaggregation of phytoplankton aggregates is responsible for this difference.

This study also provided evidence that suspended and sinking particles are enriched in material derived from different algal sources. Aspartic acid (ASP) and glutamic acid (GLU), which are enriched in the tests of calcareous plankton (King, 1974; Weiner and Erez, 1984) generally contributed to a greater portion of total amino acids in suspended particles (11% on average, compared with 9-10% in sinking particles). The diatom pigment fucoxanthin and amino acids serine (SER), threonine (THR), and glycine (GLY), which are enriched in the tests of siliceous plankton (Hecky, 1974; Swift and Wheeler, 1991), generally contributed more to sinking particles (6-26% each, as compared with 6-12% in suspended particles). This may indicate selective grazing on diatoms by large zooplankton, leaving prymnesiophytes relatively enriched in the suspended phase. Alternatively, diatom frustules may be better preserved in fecal pellets than calcium carbonate, which may dissolve in acidic zooplankton guts (Cowie and Hedges, 1996).

Chapter 4 provided experimental evidence in support of the 2003 and 2005 field observations. Phytoplankton collected at 20 m and sinking fecal pellets collected at 200 m were incubated independently in rotating tanks to assess the extent to which they exchanged with suspended particles. Phytoplankton aggregates appeared to form within 18 h, as evidenced by the transfer of \sim 30% of mass, POC, biogenic silica, and pigments from the suspended to sinking phase. Aggregates then appeared to disaggregate between 18-54 h, resulting in an approximately equal transfer of mass back to the suspended phase. Sinking particles collected in the Net Trap at 200 m demonstrated a unidirectional transfer of \sim 30-90% of mass, particulate organic and inorganic carbon, biogenic silica, and pigments from the suspended to sinking phase over the course of 72 h. Unlike in the plankton tow

incubation, this was not followed by a return of mass to the suspended phase, indicating that disaggregation was minimal. Disaggregation may have occurred if the experiment had been continued for longer, but does not appear to have been as rapid as that observed in the plankton tow incubation. This suggests that material exiting the mixed layer is more robust than material in surface waters.

Suspended and sinking particles collected from 200 m also differed more greatly in composition than those at 20 m. Suspended particles were consistently enriched in chl *a* and biogenic calcite indicators, while sinking particles were enriched in fecal pellet and biogenic silica indicators, similar to field results from 2003 and 2005. These results support the conclusion that fecal pellets undergo less disaggregation and exchange with suspended particles than phytoplankton aggregates. In addition, the extent of exchange with suspended particles may differ for different types of fecal pellets. Pheophorbide was relatively enriched in sinking particles at 20 m and suspended particles at 200 m, and underwent greater transfers between the suspended and sinking pools compared with pyropheophorbide. Pyropheophorbide, which is indicative of more extensive alteration of chl *a*, consistently remained enriched in sinking particles at 200 m depth. This suggests that the source of fecal pellets (e.g., microzooplankton v. macrozooplankton, or fresher v. more heavily altered) may be an important factor influencing their transport to the deep sea. These findings emphasize the importance of phytoplankton and zooplankton community composition and population dynamics in determining POC export from the surface to deep ocean.

2. Directions for Future Research

The results of this thesis indicate that particle source is an extremely important factor controlling the magnitude of POC export from the surface ocean and its preservation during transit through the mesopelagic zone. The compositional differences observed between suspended and sinking particles in Chapters 3-4 suggest some interesting areas for further investigation. First, to quantitatively assess the extent of exchange between suspended and sinking particles, it is important to know their relative residence times in the water column. Synchronous analyses of radioisotopes and organic compounds in both particle types would provide information about the relative ages of these particles as well as their source and alteration. In the near future, when ^{228}Th analyses from the Med Flux project are complete, we plan to use the ratio of ^{228}Th to ^{234}Th to determine the relative ages of sinking and

suspended particles, enabling this comparison. Also, a more complete picture of particle disaggregation and remineralization would be obtained by including dissolved organic and inorganic material in similar chemical comparisons in the future.

The results of this thesis demonstrate that chemical characterization of particles separated by size and settling velocity can reveal a great deal about particle dynamics in the ocean. Further studies characterizing the compositions of different particle classes could be very informative. One type of analysis we intended to perform in 2005 was the separation of Net Trap particles into different density fractions, followed by chemical characterization. Unfortunately, we were unable to conduct as many Net Trap deployments as originally planned due to some damage to one of the traps, so this analysis was not performed. Density fractionations and chemical characterization in sediments (e.g., Bock and Mayer, 2000; Arnarson and Keil, 2001) have provided information about the association between organic matter and minerals in sedimentary aggregates. Performing these analyses on water column samples is a little more difficult due to the lower mass of material, but is possible. It would be interesting to collect sinking particles in settling velocity sediment traps, separate a portion by size (e.g., by filtration of splits through different size mesh or filters, perhaps of a similar mesh size as those in the pumps) and another portion by density (e.g., by suspension in sodium polytungstate solutions of different densities), and analyze the organic and inorganic chemical composition of these particles. This could reveal more about the extent to which specific minerals and organic compounds partition into different particle phases, or undergo exchange among these phases. In addition, having settling velocity, size, density, and chemical measurements on the same samples would be a more direct way of testing the hypothesis that sinking particles undergo continuous exchange to adjust to changes in size and density (Hill, 1988).

In addition, to better understand how surface primary productivity translates to deep carbon export, factors influencing the robustness of different sinking particle types should be more thoroughly investigated. Additional laboratory and field-based comparisons of the robustness of fecal pellets and phytoplankton aggregates would be useful in this regard. For example, fecal pellets and phytoplankton aggregates could be sonicated, examined under a microscope to evaluate the extent of disaggregation, and analyzed for organic composition to assess decomposition.

Aggregates derived from different species of phytoplankton, or plankton in different phases of growth might also differ in their extent of exchange with suspended particles. Coccolithophorid aggregates formed during the Engel et al. (submitted a, b) experiment appeared to be relatively robust, whereas diatom aggregates formed during the incubation of Mediterranean particles (Chapter 4) were not, indicating that the source of algal material may influence its transport to the deep sea. Monospecific algal cultures may aggregate more easily than mixed assemblages of phytoplankton such as those used in Chapter 4. Therefore, time periods (e.g., the spring bloom) or locations where phytoplankton biomass is dominated by a particular phytoplankton species may have greater POC export. Some previous research (e.g., Alldredge et al., 1993; Engel et al., 2004) has addressed the effects of species composition and aging on aggregate formation and robustness, but this topic warrants further investigation.

In addition, the relative enrichment of biogenic calcite indicators in suspended particles observed in Chapters 3-4 is surprising, since carbonate generally promotes aggregation (Klaas and Archer, 2002). Further investigation of the mechanisms contributing to the relative enrichment of diatoms and coccolithophorids in different particle types would enable better prediction of POC export, and clearer interpretation of what these biomarkers indicate. For example, causes of the enrichment of diatoms in fecal pellets could be investigated in experiments assessing zooplankton grazing on different species and resulting effects on decomposition and dissolution.

The findings of this research highlight the importance of biological community structure in controlling POC export from the surface to deep ocean. Future research simultaneously assessing biological community composition and population dynamics as well as particle fluxes and composition would allow for better predictive understanding of the factors controlling POC export under different conditions.

References

- Allredge, A.L., Passow, U., Logan, B.E., 1993. The abundance and significance of a class of large, transparent organic particles in the ocean. *Deep-Sea Research* 40, 1131-1140.
- Arnarson, T.S., Keil, R.G., 2001. Organic-mineral interactions in marine sediments studied using density fractionation and X-ray photoelectron spectroscopy. *Organic Geochemistry* 32 :1401-1415.
- Bock, M.J., Mayer, L.M., 2000. Mesodensity organo-clay associations in a near-shore sediment. *Marine Geology* 163 :65-75.
- Carroll, M.L., Miquel, J.C., Fowler, S.W., 1998. Seasonal patterns and depth-specific trends of zooplankton fecal pellet fluxes in the Northwestern Mediterranean Sea. *Deep-Sea Research I* 45, 1303-1318.
- Cowie, G.L., Hedges, J.I., 1996. Digestion and alteration of the biochemical constituents of a diatom (*Thalassiosira weissflogii*) ingested by an herbivorous zooplankton (*Calanus pacificus*). *Limnology and Oceanography* 41, 581-594.
- Engel, A., Thoms, S., Riebesell, U., Rochelle-Newall, E., Zondervan, I. 2004. Polysaccharide aggregation as a potential sink of marine dissolved organic carbon. *Nature* 428, 929-932.
- Engel, A., Szlosek, J., Abramson, L., Liu, Z., Lee, C. Decomposition of calcifying and non-calcifying *Emiliania huxleyi* (Prymnesiophyceae): II. Formation, settling velocities and physical properties of aggregates. Submitted to *Deep-Sea Research II* (a).
- Engel, A., Abramson, L., Szlosek, J., Liu, Z., Stewart, G., Hirschberg, D., and Lee, C. Investigating the effect of ballasting by CaCO₃ in *Emiliania huxleyi*: II. Decomposition of particulate organic matter. Submitted to *Deep-Sea Research II* (b).
- Fowler, S. W., Small, L. F., La Rosa, J., 1991. Seasonal particulate carbon flux in the coastal northwestern Mediterranean Sea, and the role of zooplankton fecal matter. *Oceanologica Acta* 14, 77-85.
- Hamm, C.E., 2002. Interactive aggregation and sedimentation of diatoms and clay-sized lithogenic material. *Limnology and Oceanography* 47, 1790-1795.
- Hecky, R.E., Mopper, K., Kilham, P., Degens, E.T., 1973. The amino acid and sugar composition of diatom cell-walls. *Marine Biology* 19, 323-331.
- Hill, P.S., 1998. Controls on floc size in the sea. *Oceanography* 11, 13-18.
- Ingalls, A.E., Lee, C., Wakeham, S.G. Hedges, J.I., 2003. The role of biominerals in the sinking flux and preservation of amino acids in the Southern Ocean along 170°W. *Deep-Sea Research II* 50, 709-734.

- King, K., Jr., 1974. Preserved amino acids from silicified protein in fossil radiolaria. *Nature* 252, 690-692.
- Kinrade, S.D., Gillson, A.M.E., Knight, C.T.G., 2002. Silicon-29 NMR evidence of a transient hexavalent silicon complex in the diatom *Navicula pelliculosa*. *Journal of the Chemical Society – Dalton Transactions* 3, 307-309.
- Klaas, C., Archer, D.E., 2002. Association of sinking organic matter with various types of mineral ballast in the deep sea: Implications for the rain ratio. *Global Biogeochemical Cycles* 16, 1116.
- Repeta, D.J., Gagosian, R.B., 1984. Transformation reactions and recycling of carotenoids and chlorines in the Peru upwelling region (15°S, 75°W). *Geochimica et Cosmochimica Acta* 48, 1265-1277.
- Sahai, N., 2004. Calculation of ²⁹Si shifts of silicate complexes with carbohydrates, amino acids, and MuHicarboxylic acids: potential role in biological silica utilization. *Geochimica et Cosmochimica Acta* 68, 227-234.
- Sheridan, C.C., Lee, C., Wakeham, S.G., Bishop, J.K.B., 2002. Suspended particle organic composition and cycling in surface and midwaters of the equatorial Pacific Ocean. *Deep-Sea Research I* 49, 1983-2008.
- Sumper, M., 2002. A phase separation model for the nanopatterning of diatom biosilica. *Science* 295, 2430-2433.
- Swift, D.M. and Wheeler, P. 1991. Evidence of an organic matrix from diatom biosilica. *Journal of Phycology* 28, 202-209.
- Wakeham, S.G., Canuel, E.A., 1988. Organic geochemistry of particulate matter in the eastern tropical North Pacific Ocean: implications for particle dynamics. *Journal of Marine Research* 46, 183–213.
- Weiner, S., Erez, J., 1984. Organic matrix of the shell of the foraminifer, *Heterostegina depressa*. *Journal of Foraminiferal Research* 14, 206-212.